UNIVERSITÀ DEGLI STUDI DI MILANO
Doctorate School in Chemical Sciences and Technologies
Doctorate in Industrial Chemistry – XXV Cycle

Biodiesel Production from Non-foodstuff: Chemistry, Catalysis and Engineering

SSD: CHIM/04 and ING-IND/25

Daria Camilla Boffito, R08782
Tutor: Prof. Claudia L. Bianchi
Co-Tutor: Dr. Carlo Pirola

Coordinator: Prof. Dominique Roberto

Doctorate Thesis - A.Y. 2011-2012

dedicated to
Stefano

You can't always get what you want, but if you try sometimes,
well you might find you get what you need

(the Rolling Stones, 1969)

Table of contents

List of abbreviations

ASTM: American Society for Testing and Materials
B100: 100% biodiesel fuel
B20: fuel containing 20% of biodiesel
BD: biodiesel
CFPP: cold filter plugging point
CN: cetane number
CRO: crude rapeseed oil
DMP: dimethyl pyridine
DVB: divinylbenzene
EN: European Normative
FAME: fatty acids methyl esters
FFA: free fatty acids
GC: gaschromatographic analysis
IV: iodine value
MW: microwaves
PN: peroxide number
POB: palm oil biodiesel
SN: saponification number
US: ultrasound
WCO: waste cooking oil
WSO: winterized sunflower oil

General abstract

1. Introduction

Biodiesel (BD) is a liquid biofuel that is defined as a fatty acid methyl ester fulfilling standards such as the ones set by European (EN 14214) and the American (ASTM 6751) regulations. BD is obtained by the transesterification (Scheme 1.1) or alcoholysis of natural triglycerides contained in vegetable oils, animal fats, waste fats and greases, waste cooking oils (WCO) or side-stream products of refined edible oil production with short-chain alcohols, usually methanol or ethanol and using an alkaline homogeneous catalyst (Perego and Ricci, 2012).

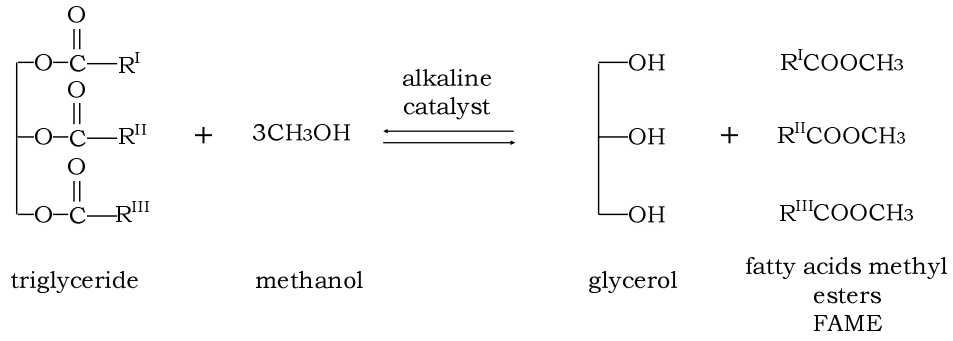

Scheme 1.1. Transesterification reaction.

BD presents several advantages over petroleum-based diesel such as: biodegradability, lower particulate and common air pollutants (CO, SO_x emissions, unburned hydrocarbons) emissions, absence of aromatics and a closed CO_2 cycle.

Refined, low acidity oilseeds (e.g. those derived from sunflower, soy, rapeseed, etc.) may be easily converted into BD, but their exploitation significantly raises the production costs, resulting in a

biofuel that is uncompetitive with the petroleum-based diesel (Santori et al., 2012; Lotero et al., 2005). Moreover, the use of the aforementioned oils generated a hot debate about a possible food vs. fuel conflict, i.e. about the risk of diverting farmland or crops at the expense of food supply. It is so highly desirable to produce BD from crops specifically selected for their high productivity and low water requirements (Bianchi et al., 2011; Pirola et al., 2011), or from low-cost feedstock such as used frying oils (Boffito et al., 2012a) and animal fats (Bianchi et al., 2010).

The value of these second generation biofuels, i.e. produced from crop and forest residues and from non-food energy crops, is acknowledged by the European Community, which states in its RED directive (European Union, RED Directive 2009/28/EC):

"For the purposes of demonstrating compliance with national renewable energy obligations [...], the contribution made by biofuels produced from wastes, residues, non-food cellulosic material, and ligno-cellulosic material shall be considered to be twice that made by other biofuels".

However, the presence of free fatty acids in the feedstock, occurring in particular in the case of not refined oils, causes the formation of soaps as a consequence of the reaction with the alkaline catalyst. This hinders the contact between reagents and the catalyst and makes difficult the products separation. Many methods have been proposed to eliminate FFA during or prior to transesterification (Pirola et al., 2011; Santori et al., 2012). Among

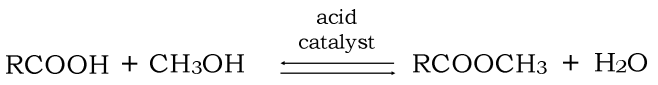

Scheme 1.2. Free fatty acids esterification reaction.

these the FFA pre-esterification method is a very interesting approach to lower the acidity since it allows to lower the acid value as well as to obtain methyl esters already in this preliminary step (Boffito et al., 2012a, 2012b; 2012c Bianchi et al., 2010, 2011; Pirola et al., 2010, 2011).

Aims of the work

The aims of this work are framed in the context of the entire biodiesel production chain, ranging from the choice of the raw material, through its standardization to the actual biodiesel production. The objectives can be therefore summarized as follows:

- Assessing the potential of some vegetable or waste oils for biodiesel production by their characterization, deacidification and final transformation into biodiesel;
- To test different ion exchange resins and sulphated inorganic systems as catalysts in the FFA esterification;
- To assess the use of ultrasound to assist the sol-gel synthesis of inorganic sulphated oxides to be used as catalysts in the FFA esterification reaction;
- To assess the use of sonochemical techniques such as ultrasound and microwave to promote both the FFA esterification and transesterification reaction.

2. Experimental details

2.1 Catalysts

In this work, three kinds of acid ion exchange resins were used as catalysts for the FFA esterification: Amberlyst®15 (A15),

Amberlyst®46 (A46) (Dow Chemical) and Purolite®D5081 (D5081). Their characteristic features are given in Tab. 2.1.

Various sulphated inorganic catalysts, namely sulphated zirconia, sulphated zirconia+titania and sulphated tin oxide were synthesized using different techniques. Further details will be given as the results inherent to these catalysts will be presented.

Catalyst	A15	A46	D5081
Physical form		opaque beads	
Type		Macroreticular	
Matrix		Styrene-DVB	
Cross-linking degree	medium	medium	high
Functional group		$-SO_3H$	
Functionalization	internal external	external	external
Form	dry	wet	wet
Surface area ($m^2\ g^{-1}$)	53	75	514[a]
Ave. D_p (Å)	300	235	37[a]
Total V_p (ccg^{-1})	0.40	0.15	0.47
Declared Acidity (meq H^+g^{-1})	4.7	0.43	0.90-1.1
Measured acidity (meq H^+g^{-1})	4.2	0.60	1.0
Moisture content ($\%_{wt}$)	1.6	26-36	55-59
Shipping weight ($g\ l^{-1}$)	610	600	1310[a]
Max. operating temp (K)	393	393	403

Tab. 2.1. Features of the ion exchange resins used as catalysts.

The acidity of all the catalysts was determined by ion exchange followed by pH determination as described elsewhere (López et al., 2007; Boffito et al., 2012a; 2012b). Specific surface areas were determined by BET (Brunauer, Emmett and Teller, 1938) and pores sizes distribution with BJH method (Barrett, Joyner and Halenda, 1951). XRD, XPS SEM-EDX and HR-TEM analyses were performed in the case of catalysts obtained with the use of ultrasound (Boffito et al. 2012a). Qualitative analyses of Lewis and Brønsted acid sites

by absorption of a basic probe followed by FTIR analyses was also carried out for this class of catalysts (Boffito et al, 2012a).

2.2 Characterization of the oils

Oils were characterized for what concerns acidity (by acid-base titrations) as reported by Boffito et al. (2012a, 2012b; 2012c), iodine value (Hannus method (EN 14111:2003)), saponification value (ASTM D5558), peroxide value and composition by GC analyses of the methyl ester yielded by the esterification and transesterification. Cetane number and theoretical values of the same properties were determined using equations already reported elsewhere (Winayanuwattikun et al., 2008).

2.3 Esterification and transesterification reactions

In Tab. 2.2, the conditions adopted in both the conventional and sonochemically-assisted esterification are reported. For all these experiments a temperature of 336 K was adopted. Vials were used to test the sulphated inorganic oxides, while Carberry reactor (confined catalyst) (Boffito et al., 201c) was used just for the FFA esterification of cooking oil.

Rector	oil (+ FFA) (g)	MeOH (g)	catalyst amount
vial	21	3.4	$5\%_{wt}/g_{FFA}$ sulphated inorganic catalysts
slurry	100	16	- 10 g ion exchange resins - $5\%_{wt}/g_{F\ FA}$ sulphated inorganic catalysts
Carberry	300	48	10 g (5 g in each basket)

Tab. 2.2. Free fatty acids esterification reaction conditions for conventional and sonochemically-assisted experiments.

All the sonochemically-assisted experiments were performed in a slurry reactor.

FFA conversions were determined by acid-base titrations of oil samples withdrawn from the reactors at pre-established times and calculated as follows:

$$FFA\ conversion\ (\%)=\frac{FFA_{t=0}-FFA_t}{FFA_{t=0}}\ \text{x}\ 100$$

In Tab. 2.3, the conditions of both the conventional and ultrasound (US)-assisted transesterification are reported. KOH and CH_3ONa were used for conventional experiments, while just KOH for the US-assisted experiments. The BD yield was determined by GC (FID) analysis of the methyl esters.

Method	Reactor	Step	g_{MeOH}/100 g_{oil}	g_{KOH}/100 g_{oil}	Temp. (K)	Time (min)
traditional	batch	step 1	20	1.0	333	90
		step 2	5.0	0.50		60
US-assisted	batch	step 1	20	1.0	313, 333	30
US-assisted	continuos	step 1	20	1.0	338	30

Tab. 2.3. Transesterification reaction conditions.

3. Results and Discussion

3.1 Characterization and deacidification of different oils by ion exchange resins: assessment of the potential for biodiesel production

In Tab. 3.1 the results of the characterization of the oils utilized in this work are displayed. The value in parentheses indicate the

theoretical value of the properties, calculated basing on the acidic composition. The acidity of all the oils exceeds 0.5%$_{wt}$ (~0.5 mg$_{KOH}$/g), i.e. the acidity limit recommended by both the European normative (EN 14214) and American standard ASTM 6751 on biodiesel (BD). The iodine value (IV) is regulated by the EN 14214, which poses an upper limit of 120 gI_2/100 g.

The number of saturated fatty chains in the fuel determines its behaviour at low temperatures, influencing parameters such as the cloud point, the CFPP (cold filter plugging point) and the freezing point (Winayanuwattikun et al., 2008). The IV are in most of the cases similar to the ones calculated theoretically. When the experimental IV differs from the theoretical one, it is in most of the cases underestimated. This can be explained considering the peroxide numbers (PN), which indicates the concentration of O_2 bound to the fatty alkyl chains and is therefore an index of the conservation state of oil. Oils with high IV usually have a high concentration of peroxides, whereas fats with low IV have a relatively low concentration of peroxides at the start of rancidity (King et al., 1933). Moreover, although PN is not specified in the current BD fuel standards, it may affect cetane number (CN), a parameter that is regulated by the standards concerning BD fuel. Increasing PN increases CN, altering the ignition delay time. Saponification number (SN) is an index of the number of the fatty alkyl chains that can be saponified. The long chain fatty acids have a low SN because they have a relatively fewer number of carboxylic functional groups per mass unit of fat compared to short chain fatty acids. In most of the cases the experimental SN are lower than the ones calculated theoretically. This can be explained always considering the PN, indicating a high concentration of oxygen bound to the fatty alkyl chains.

Oil	Acidity (%wt)	IV[1] (gI_2/ 100 g)	PN[2] ($meqO_2$ /kg)	SN[3] (mg KOH/g)	CN[4]	Fatty acids composition (%wt)
animal fat (lard)*	5.87	51	2.3	199	62.3	n.d.
soybean*	5.24	138	3.8	201	42.4	n.d.
tobacco1	1.68	143 (149)	21.9	199 (202)	41.6 (39.8)	C14:0 (2.0) C16:0 (8.3) C18:0 (1.5) C18:1 (12.0) C18:2 (75.3) C18:3 (0.6) C20:0 (0.1) C22:0 (0.2)
sunflower*	3.79	126	3.7	199	45.4	n.d.
WSO[5]	0.50	118 (129)	71.3	187 (200)	48.9 (44.6)	C16:0 (6.9) C18:0 (0.9) C18:1 (40.1) C18:2 (50.9) C18:3 (0,3) C20:0 (0.1) C20:1 (0.4) C22:0 (0.4)
palm	2.71	54.0 (53.0)	12.3	201 (208)	61.3 (60.6)	16:0 (43.9) 18:0 (5.6) 18:1 (40.5) 18:2 (8.6)
WCO[6]	2.10	53.9 (50.7)	11.0	212 (196)	59.9 (62.7)	C16:0 (38.8) C18:0 (4.1) C18:1 (47.9) C18:2 (4.2)
WCO:CRO =3:1	2.12	69.0 (75.5)	30.1	200 (212)	58.1 (55.1)	C16:0 (30.1) C18:0 (3.1) C18:1 (51.9) C18:2 (12.0) C18:3 (2.%) C20:0 (0.2) C22:0 (0.1)
WCO:CRO =1:1	2.19	76.8 (90.7)	51.3	188 (203)	58.1 (52.8)	C16:0 (21.5) C18:0 (2.1) C18:1 (55.8) C18:2 (14.7) C18:3 (5.1) C20:0 (0.8) C22:0 (0.1)
WCO:CRO =1:3	2.24	84.5 (104)	62.4	177 (202)	58.1 (49.9)	14:0 (0.1) 16:0 (14.7) 16:1 (0.7) 18:0 (6.85) 18:1 (40.0) 18:2 (37.0) 18:3 (0.25) 20:0 (0.25) 22:0 (0.15)
rapeseed (CRO[7])	2.20	118 (123)	71.6	165 (200)	52.8 (45.9)	C16:0 (4.1) C18:0 (0.1) C18:1 (63.7) C18:2 (20.2) C18:3 (10.2) C20:0 (1.5) C22:0 (0.2)
rapeseed*	4.17-5.12	108 (107)	3.5	203 (200)	48.9 (49.5)	C16:0 (7.6) C18:0 (1.3) C18:1 (64.5) C18:2 (23.7) C18:3 (2.4) C20:0 (0.5)
Brassica juncea	0.74	109 (110)		178 (185)	52.4 (51.1)	C16:0 (2.4) C18:0 (1.1) C18:1 (19.9) C18:2 (19.2) C18:3 (10.9) C20:0 (7.2) C20:1 (1.7) C22:0 (0.9) C22:1 (34.8) 24:0 (1.9)
safflower	1.75	139	48.9	170	47.1	n.d.
WCO: tobacco2 =1:1	4.34	119 (112)	56.0	191 (203)	48.1 (48.0)	C16:0 (22.5) C18:0 (3.2) C18:1 (32.0) C18:2 (42.1) C18:3 (0.2)
tobacco2	6.17	141 (151)	33.4	183 (201)	44.4 (39.5)	C16:0 (8.7) C18:0 (1.6) C18:1 (12.8) C18:2 (76.0) C18:3 (0.7) C20:0 (0.1) C22:0 (0.1)

[1]Iodine value; [2]Peroxide number; [3]Saponification number; [4]Cetane number; [5]Winterized sunflower oil, [6]Waste cooking oil; [7]Crude rapeseed oil; * refined, commercial oils acidified with pure oleic acid up to the indicated value.

Tab. 3.1. Results of the characterization of the oils.

The results of the FFA esterification performed on the different oils are given in Fig. 3.1.

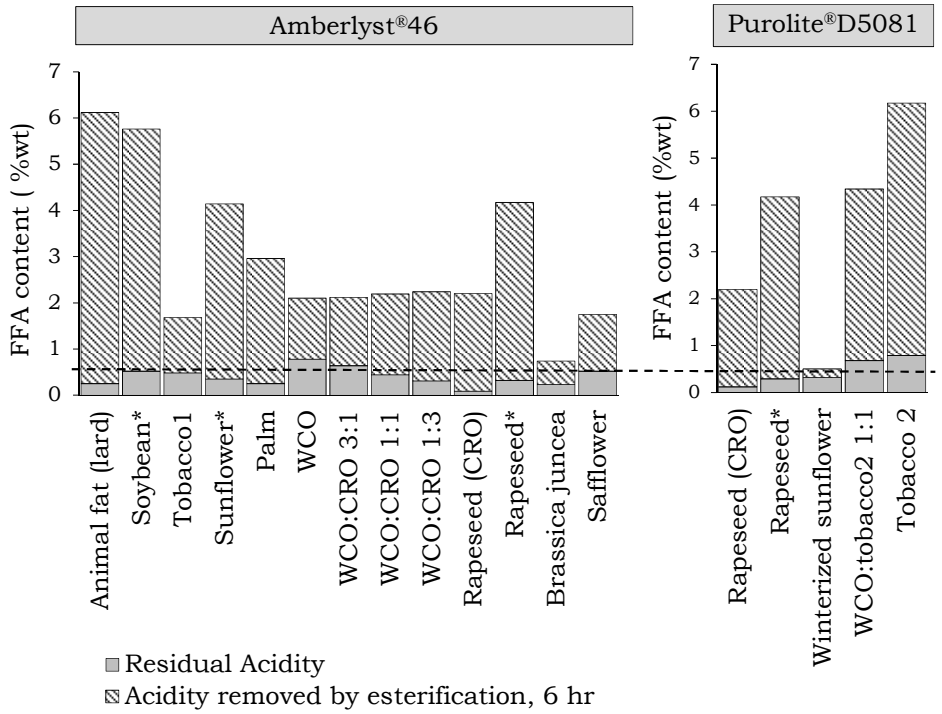

Fig. 3.1. Results of the FFA esterification reaction on different oils.

The dotted line represents a FFA concentration equal to 0.5%$_{wt}$, i.e. the limit required by both the European and American directives on BD fuel and to perform the transesterification reaction avoiding excessive soaps formation. The FFA esterification method is able to lower the acidity of most of the oils using the ion exchange resins A46 and D5081 as catalysts in the adopted reaction conditions. High conversion was obtained with A15 at the first use of the catalyst, but then its catalytic activity drastically drops after each cycle. The total loss of activity was estimated to be around 30% within the 5 cycles (results not shown for the sake of brevity). A

possible explanation concerning this loss of activity may be related to the adsorption of the H_2O yielded by the esterification on the internal active sites, which makes them unavailable for catalysis. When H_2O molecules are formed inside the pores, they are unable to give internal retro-diffusion due to their strong interaction with H^+ sites and form an aqueous phase inside the pores. The formation of this phase prevents FFA from reaching internal active sites due to repulsive effects.

What appears to influence the FFA conversion is the refinement degree of the oil. WCO is in fact harder to process in comparison to refined oils (Bianchi et al., 2010; Boffito et al., 2012c), probably due to its higher viscosity which results in limitations to the mass transfer of the reagents towards the catalyst. Indeed, the required acidity limit is not achieved within 6 hours of reaction. A FFA concentration lower than $0.5\%_{wt}$ is not achieved also in the case of WCO mixture 3:1 with CRO and 1:1 with tobacco oil and in the case of the second stock of tobacco oil (tobacco2). This is attributable to the very low quality of these feedstocks due to the waste nature of the oil itself, in the case of WCO, or to the poor conservation conditions in the case of tobacco oilseed. In this latter case, the low FFA conversion was also ascribed to the presence of phospholipids, responsible for the deactivation of the catalyst.

BD yields ranging from 90.0 to 95.0 and from 95.0 to 99.9% were obtained from deacidified raw oils using KOH and $NaOCH_3$ as a catalyst, respectively. In Fig. 3.2, the comparison between A46 and D5081 at different temperatures and in absence of drying pretreatment (wet catalyst) is displayed. As expected, D5081 performs better than A46 in all the adopted conditions. Nevertheless, the maximum conversion within a reaction time of 6

hours is not achieved by any of the catalysts both operating at 318 K and in the absence of drying pretreatment.

A more detailed study on the FFA esterification of WCO and its blends with rapeseed oil and gasoline was carried out. In Tab. 3.2 a list of all the experiments performed with WCO is reported together with the FFA conversion achieved in each case, while in Fig. 3.3 the influence of the viscosity of the blends of WCO is shown.

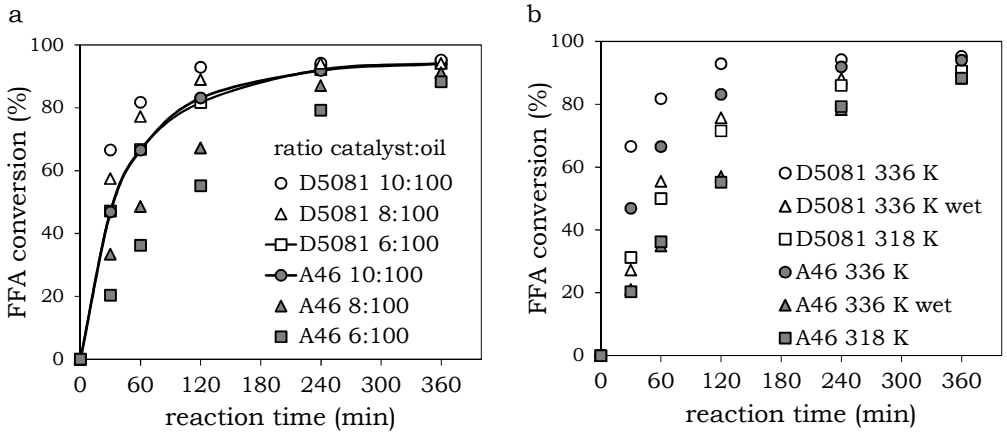

Fig. 3.2. Comparison between the catalysts. D5081 and A46 at a) different catalysts amounts and b) temperatures and treatments.

The results show that Carberry reactor is unsuitable for FFA esterification since a good contact between reagents and catalyst is not achieved due to its confinement. A15 deactivated very rapidly, while A46 and D5081 maintained their excellent performance during all the cycles of use due to the reasons already highlighted previously. The blends of WCO and CRO show an increase of the reaction rate proportional to the content of the CRO, that is attributable to the decreases viscosity (Fig. 3.3), being all the blend characterized by the same initial acidity. Also the use of diesel as a solvent resulted in a beneficial effect for the FFA esterification reaction, contributing to the higher reaction rate.

	Feedstock	$\%_{wt}FFA_{t=0}$	Reactor	Cat.	$g_{cat}/100\ g_{oil}$	$g_{cat}/100$ g feedstock	Number of cat. re-uses	FFA conv. (%), 1st use, 6 hr
1	WCO	2.10	Carberry	A15	3.3	3.3	6	15.4
2	WCO	2.10	slurry	A15	10	10	6	71.7
3	WCO	2.10	Carberry	A46	3.3	3.3	6	7.7
4	WCO	2.10	slurry	A46	10	10	6	62.0
5	WCO	2.10	slurry	D5081	10	10	6	63.7
6	CRO	2.20	slurry	A46	10	10	10	95.9
7	CRO	2.20	slurry	D5081	10	10	10	93.7
8	WCO	2.10	slurry	A46	10	10	0	62.0
9	WCO 75 CRO 25	2.12				7.5		71.3
10	WCO 50 CRO 50	2.19				5.0		79.9
11	WCO 25 CRO 75	2.24				2.5		86.1
12	CRO	2.20				10		95.9
13	WCO 75 DIESEL 25	1.74				7.5		76.8
14	WCO 50 DIESEL 50	1.17				5.0		58.7
15	WCO 25 DIESEL 75	0.65				2.5		40.4
16	WCO 25 DIESEL 75 (higher FFA input)	2.44				2.5		63.5

Tab. 3.2. Experiments performed with waste cooking oil.

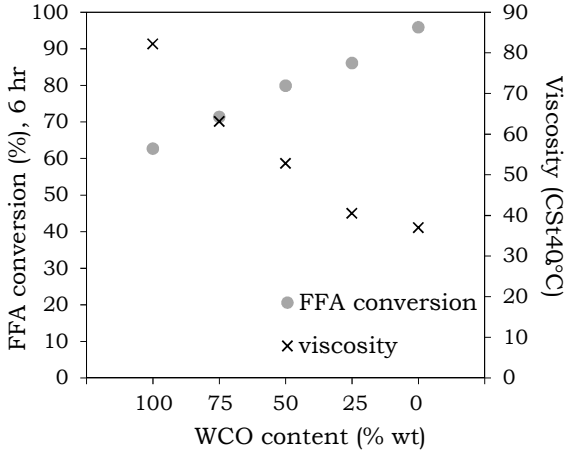

Fig. 3.3. FFA conversions and viscosities of the blend of WCO with rapeseed oil.

3.2. Sulphated inorganic oxides as catalysts for the free fatty acid esterification: conventional and ultrasound assisted synthesis

Conventional syntheses

In Tab. 3.3, the list of all the catalyst synthesized with conventional techniques is reported together with the results of the characterization.

	Catalyst	Composition	Prep. method	precursors	T calc.	SSA (m^2g^{-1})	V_p (cm^3g^{-1})	meq H^+g^{-1}
1	SZ1	SO_4^{2-}/ZrO_2	one-pot sol-gel	ZTNP[1], $(NH_4)_2SO_4$	893 K O_2	107	0.09	0.90
2a	SZ2a	SO_4^{2-}/ZrO_2	two-pots sol-gel	ZTNP, H_2SO_4	893 K	102	0.10	0.11
2b	SZ2b	SO_4^{2-}/ZrO_2	two-pots sol-gel	ZTNP, H_2SO_4	653 K	110	0.10	0.12
3	SZ3	SO_4^{2-}/ZrO_2	Physical mixing	$ZrOCl_2.8H_2O$ $(NH_4)_2SO_4$	873 K	81	0.11	1.3
4	SZ4	$Zr(SO_4)_2/SiO_2$	Impregnation	$Zr(SO_4)_2.4H_2O$ SiO_2	873 K	331	0.08	1.4
5	SZ5	$Zr(SO_4)_2/Al_2O_3$	Impregnation	$Zr(SO_4)_2.4H_2O$ Al_2O_3	873 K	151	0.09	0.67
6	ZS	$Zr(SO_4)_2.4H_2O$ (commercial)	-	-	-	13	0.12	9.6
7	STTO_0	SO_4^{2-}/SnO_2	Physical mixing + impregnation	SnO_2 TiO_2 P25 H_2SO_4	773 K	16.8	0.10	3.15
8	STTO_5	SO_4^{2-} /95%SnO_2-5%TiO_2			773 K	15.9	0.11	3.43
9	STTO_10	SO_4^{2-}/ 90%SnO_2-10%TiO_2			773 K	16.5	0.09	5.07
10	STTO_15	SO_4^{2-}/ 85%SnO_2-15%TiO_2			773 K	14.9	0.11	7.13
11	STTO_20	SO_4^{2-}/ 80%SnO_2-20%TiO_2			773 K	16.9	0.09	7.33

Tab. 3.3. Sulphated inorganic catalysts synthesized with conventional techniques.

The FFA conversions of the sulphated Zr-based systems are provided in Fig. 3.4a and show that Zr-based sulphated systems do not provide a satisfactory performance in the FFA esterification,

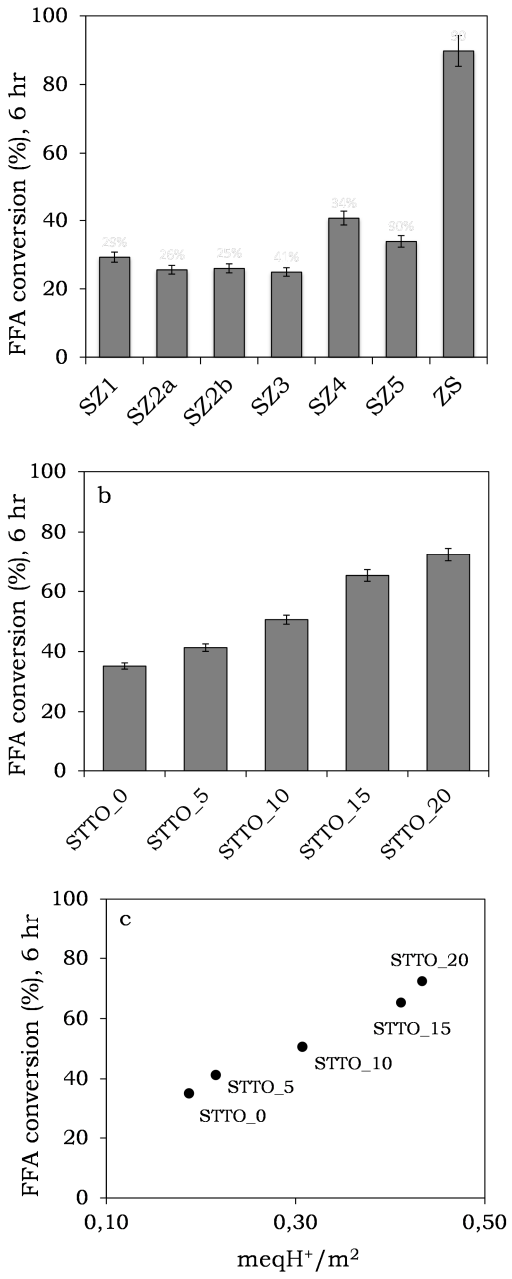

Fig. 3.4. FFA conversions of the a) sulphated Zr-based catalysts and b), c) sulphated Sn-Ti systems.

probably due to their low acid sites concentration related to their high SSA. Even if catalysts such as SZ3 and SZ4 exhibit higher acidity compared to other catalysts, it is essential that this acidity is located mainly on the catalyst surface to be effectively reached by the FFA molecules, as in the case of ZS.

In Figure 3.4b, the results of the FFA esterification tests of the sulphated Sn-Ti systems are shown. Other conditions being equal, these catalysts perform better than the sulphated Zr-based systems just described. This is more likely due to the higher acidity along with a lower surface area. With increasing the TiO_2 content, the acidity increases as well. This might be ascribable to the charge imbalance resulting from the heteroatoms linkage for the generation of acid centres, (Kataota and Dumesic, 1988). As a consequence, the activity increases with the TiO_2 content along with the acidity of the

samples. For the sake of clarity, in Fig. 3.4c the FFA esterification conversion is represented as a function of the number of active sites per unit of surface area of the samples.

Ultrasound- assisted synthesis

In Tab. 3.4, the list of all the catalyst synthesized with conventional techniques is reported together with the results of the characterization. Samples SZ and SZT refer to catalysts obtained with traditional sol-gel method, while samples termed USZT refer to US-obtained sulphated 80%ZrO_2-20%TiO_2. The name is followed by the US power, by the length of US pulses and by the molar ratio of water over precursors. For example, USZT_40_0.1_30 indicates a sample obtained with 40% of the maximum US power, on for 0.1 seconds (pulse length) and off for 0.9 seconds, using a water/ZTNP+TTIP molar ratio equal to 30. SZT was also calcined at 773 K for 6 hours, employing the same heating rate. This sample is reported as SZT_773_6h in entry 2a. Further details about the preparation can be found in a recent study (Boffito et al., 2012b).

Entry	Catalyst	Acid capacity (meq H^+/g)	SSA (m^2g^{-1})	V_p (cm^3g^{-1})	Ave. BJH D_p (nm)	Zr:Ti weight ratio	S/(Zr+Ti) atomic ratio
1	SZ	0.30	107	0.20	6.0	100	0.090
2	SZT	0.79	152	0.19	5.0	79:21	0.085
2a	SZT_773_6h	0.21	131	0.20	5.0	n.d.[1]	n.d
3	USZT_20_1_30	0.92	41.7	0.12	12.5	80:20	0.095
4	USZT_40_0.1_30	1.03	47.9	0.11	9.5	81:19	0.067
5	USZT_40_0.3_30	1.99	232	0.27	4.5	81:19	0.11
6	USZT_40_0.5_7.5	1.70	210	0.20	5.0	78:22	0.086
7	USZT_40_0.5_15	2.02	220	0.20	5.0	80:20	0.13
8	USZT_40_0.5_30	2.17	153	0.20	5.0	78:22	0.12
9	USZT_40_0.5_60	0.36	28.1	0.10	10	79:21	0.092
10	USZT_40_0.7_30	1.86	151	0.16	5.0	78:22	0.11
11	USZT_40_1_15	3.06	211	0.09	7.0	80:20	0.15
12	USZT_40_1_30	1.56	44.1	0.09	7.0	80:20	0.17

Tab. 3.4. Sulphated inorganic Zr-Ti systems synthesized with ultrasound-assisted sol-gel technique.

Some of the results of the characterizations are displayed in Tab. 3.4. The results of the catalytic tests are shown in Fig. 3.5 a, b and c. In Fig. 3.5a and 3.5b the FFA conversions are reported for the samples synthesized using the same or different H_2O/precursors ratio, respectively.

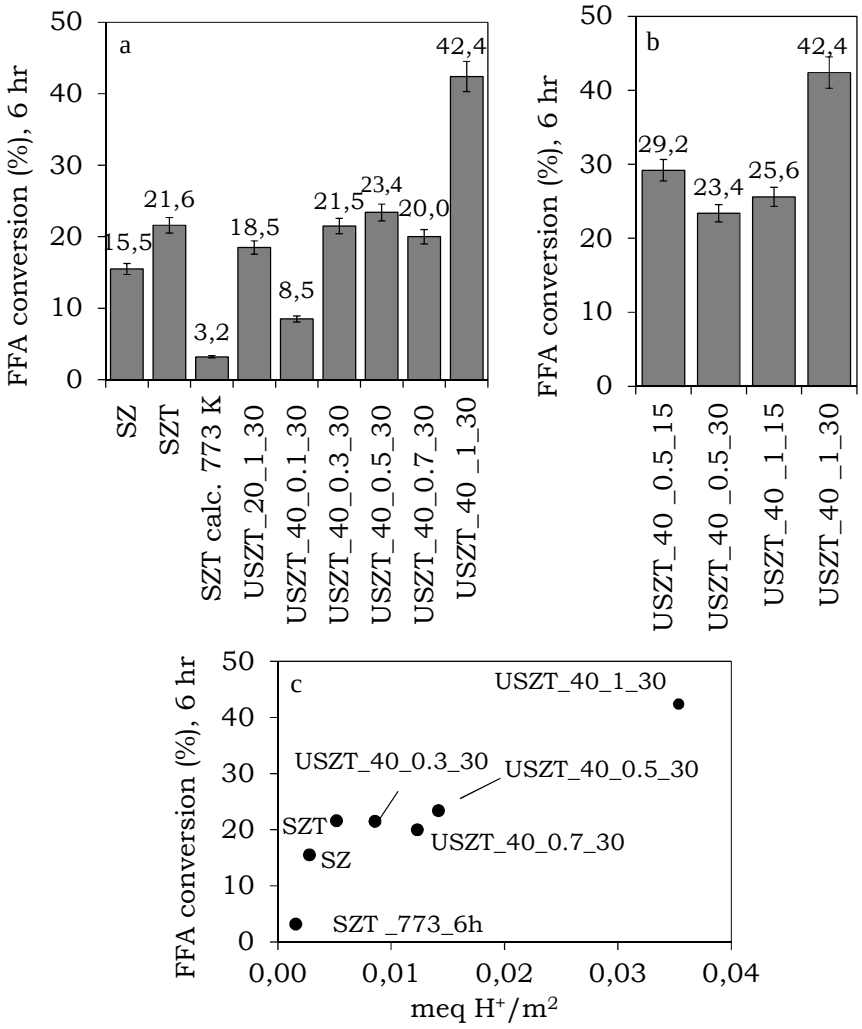

Fig. 3.5. FFA conversions of sulphated inorganic Zr-Ti systems synthesized with ultrasound-assisted sol-gel for a) the same amount of H_2O, b) different amount of H_2O used in the sol-gel synthesis, c) in function of the meq of H^+/g of catalyst

Both the addition of TiO_2 and the use of US during the synthesis are able to improve the properties of the catalysts and therefore the catalytic performance in the FFA esterification. The addition of TiO_2 is able to increase the Brønsted acidity and, as a consequence, the catalytic activity (compare entries 1 and 2 in Tab. 3.4).

The improvement in the properties of the catalysts due the use of US is probably caused by the effects generated by acoustic cavitation. Acoustic cavitation is the growth of bubble nuclei followed by the implosive collapse of bubbles in solution as a consequence of the applied sound field. This collapse generates transient hot-spots with local temperatures and pressures of several thousand K and hundreds of atmospheres, respectively (Sehgal et al., 1979). Very high speed jets (up to 100 m/s) are also formed.

As documented by Suslick and Doktycz (Suslick and Doktycz, 1990), in the presence of an extended surface, such as the surface of a catalyst, the formation of the bubbles occurs at the liquid-solid interface and, as a consequence of their implosion, the high speed jets are directed towards the surface. The use of sonication in the synthesis of catalysts can therefore improve the nucleation production rate (i.e. sol-gel reaction production rate) and the production of surface defects and deformations with the formation of brittle powders (Suslick and Doktycz, 1990).

For the samples obtained with the US pulses with on/off ratio from 0.3/0.7 on, the conversion does not increase much more compared to the one achieved with the sample obtained via traditional sol-gel synthesis. Their conversion is in fact comparable (see samples USZ_40_0.3_30, USZ_40_0.5_30, USZ_40_0.7_30 and SZT in Fig. 3.5a. The similarity in the catalytic performance of these catalysts may be ascribable to the fact that they are characterized by comparable values of SSA (entries 2, 5, 8, 10 in Tab. 3.4) and, in the case of the catalysts obtained with pulses, also by comparable acidities (entries 5, 8, 10 in

Tab. 3.4). A high SSA may in fact be disadvantageous for the catalysis of the reaction here studied for the reasons already highlighted in the previous sections. The best catalytic performance is reached by the sample USZT_40_1_30, i.e. the one obtained using continuous US at higher power. This catalyst results in fact in a doubled catalytic activity with respect to the samples prepared either with the traditional synthesis or with the use of pulsed US. In spite the acidity of this catalyst is lower than that of the samples obtained with the US pulses, it is characterized by a rather low surface area (entry 12 in Tab. 3.4) that can be associated with a localization of the active sites mainly on its outer surface. As evidenced by the FTIR measurements (not reported for the sake of brevity), it is also important to highlight, that only in the case of the USZT_40_1_30 sample, a not negligible number of medium-strong Lewis acid sites is present at the surface, together with a high number of strong Brønsted acid centres.

The XRD patterns of the samples were typical of amorphous systems, due to the low calcination temperatures. Samples calcined for a long time (SZT_773_6h) exhibit almost no catalytic activity (results not reported for the sake of brevity). This catalytic behaviour might be ascribable to the loss of part of the sulphates occurred during the calcinations step that result also in a very low acid capacity (see Tab. 3.4). For the sake of clarity, in Fig. 3.5c the FFA conversions as a function of the concentration of the acid sites normalized to the surface area are reported for the most significant samples.

For what concerns how the water/precursors ratio affects the catalysts acidity, some general observations can be made: increasing it up to a certain amount increases the H^+ concentration (compare entries from 6 to 9 and 11 to 12 in Tab. 3.4) because the rate of the hydrolysis and the number of H_2O molecules that can be chemically bounded increases. Nevertheless, increasing the water/precursor ratio over a certain amount (30 for pulsed and 15 for continuous US, entries 8 and

11 in Tab. 3.4, respectively), seems to have a negative effect on the acidity concentration. In fact, the risk of the extraction of acid groups by the excess of water increases as well and the US power density decreases.

3.3 Sonochemically-assisted esterification and transesterification

Esterification

In Tab. 3.5 a list of the sonochemically-assisted esterification experiments is displayed together with the final acidities achieved after 4 hours of reaction. The reactor used for these experiments, provided with both an US horn (20 kHz) and a MW emitter (2450 MHz) is described elsewhere in detail (Ragaini et al., 2012). Standard calorimetric measurements were carried out to measure the actual emitted power (Suslick and Lorimer, 1989).

Considering entries from 1 to 6 (rapeseed oil with high acidity), a final acidity lower than 0.5%$_{wt}$ is achieved within 4 hours operating at the conventional temperature of 336 K with all the methods, while this does not happen operating at lower temperatures. In particular, the lowest acidity is achieved at 336 K with MW. Considering entries from 7 to 12, inherent to the raw tobacco oilseed, final acidities lower than 0.5%$_{wt}$ are achieved only with the use of US. It is remarkable that at the temperature of 293 K the FFA esterification reaction rate results 6X faster than the conventional process at the same temperature. In the case of the rapeseed oil with low acidity (entries from 13 to 20), the use of MW increases the FFA conversion at 293 K and 313 K but not at 336 K. Moreover, the higher the applied power, the higher the FFA conversion.

	Oil	Initial acidity (%wt)	Cat.	Technique	Temp. (K)	Emitted power (W)	$T_{thermostat}$ (K)	Final acidity (%wt), 4 hr
1	Rapeseed oil (5)*	4.2-5.0	A46	conventional	313	-	315	1.18
2					336		338	0.50
3				ultrasound	313	38.5	293	0.55
4					336		313	0.48
5				microwaves	313	61.4	293	0.69
6					336		313	0.32
7	Tobacco	1.17	A46	conventional	293	-	293	0.97
8					313		315	0.55
9					336		338	0.45
10				ultrasound	293	38.5	277	0.48
11					313		293	0.46
12					336		313	0.30
13	Rapeseed oil (2)*	2.0-2.3	D5081	conventional	293	-	277	0.82
14					313		315	0.44
15					336		338	0.25
16				microwaves	293	31.7	277	0.73
17					313	31.7	293	0.34
18						61.4	293	0.37
19					336	31.7	313	0.29
20						61.4	313	0.25

Tab. 3.5. Sonochemically-assisted esterification experiments.

The positive effects of acoustic-cavitation in liquid-solid systems are ascribable to the asymmetric collapse of the bubbles in the vicinity of the solid surface. When a cavitation bubble collapses violently near a solid surface, liquid jets are produced and high-speed jets of liquid are driven into the surface of a particle. These jets and shock waves improve both the liquid–solid and liquid-liquid mass transfer (Mason and Lorimer, 1988). MW is considered as a non-conventional heating system: when MW pass through a material with a dipole moment, the molecules composing the material try to align with the electric field (Mingos et al., 1997). Polar molecules have stronger interactions with the electric field. Polar ends of the molecules tend in fact to align themselves and oscillate in step with

the oscillating electric field. Collisions and friction between the moving molecules results in heating (Toukoniitty et al., 2005).

The increase of the FFA conversion as the power increases may be attributed to the fact that more power is delivered to the system and, therefore, the enhanced temperature effects caused by electromagnetic irradiation are increased with respect to lower powers. Differently the reason why a too high power was detrimental at the temperature of 336 K could be accounted for by two factors: i) the acoustic cavitation is enhanced at lower temperatures due to the higher amount of gas dissolved; ii) possible generation of too high temperatures inside the reaction medium that could have caused the removal of methanol from the system through constant evaporation or pyrolysis.

Transesterification

Transesterification experiments were performed on rapeseed oil both in batch and continuous mode. For the batch experiments two kinds of reactors were used: a traditional reaction vessel and a Rosett cell reactor, both with two ultrasound horns with different tip diameters (13 and 20 mm), and operating powers. A Rosett cell is a reactor designed to promote hydrodynamic cavitation through its typical loops placed at the bottom of vessel.

Sonicators used in this work were provided by Synetude Company (Chambery, France).

In Fig. 3.6, results from the conventional and the US-assisted batch experiments are compared. The US methods allows to attain very high yields in much shorter times than the traditional method and using less reagents (see Tab. 2.3) in just one step. The beneficial effects given by the US are attributable to the generation of acoustic cavitation inside the reaction medium leading to the phenomena

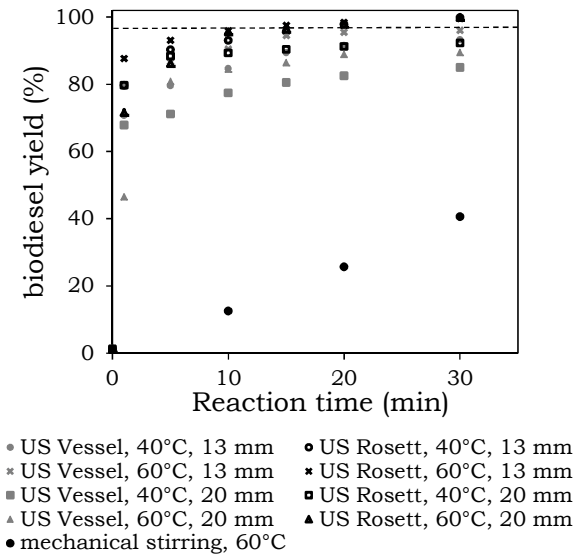

Fig. 3.6 Comparison between the US-assisted and conventional tranesterification

already described in the case of esterification reaction. In particular, with the use of the Rosett cell reactor, BD yields of 96.5% (dotted lined) are achieved after 10 minutes of reaction. This is likely due to the combined approach exploiting acoustic cavitation along with hydrodynamic cavitation, which is able to provide a very efficient mixing inside the system. The use of the Rosett cell reactor provided transesterification reaction rates up to 15X faster than the conventional process.

Continuous experiments were performed using two tubular reactors with different volumes (0.070 L at 35 KHz and 0.700 L at 20 kHz) and different US powers (19.3 and 68.3 W, respectively). The volume of the treated reagents was varied to obtain the same power density in both the reactors. Results are presented in Fig. 3.7. BD yields higher than 96.5% were obtained in the case of the small reactor within a reaction time of ~5 minutes. It is remarkable that BD yields higher than 90% were obtained using pulsed US (2 seconds on, 2 seconds off) after only 18 seconds, corresponding to just one passage in the reactor. In this case the transesterification reaction rate was 300X faster than the conventional process.

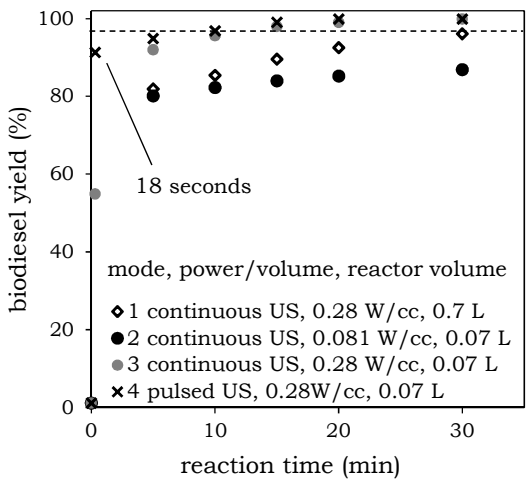

Fig. 3.7 Results of the US-continuous experiments.

The beneficial effects of pulses for the reactivity of the transesterification have been extensively reported (Chand et al., 2010; Kumar et al., 2010). In particular, as reported by Chand, when pulses are adopted, excessive heating of the reaction medium is not promoted, so preventing the loss of the gases dissolved in the system that are necessary for the acoustic cavitation to occur. Moreover, excessive heating during the transesterification reaction might lead to evaporation followed by pyrolysis of methanol and its subsequent removal from the reaction environment.

4. Conclusions

As a conclusion to this work, some final remarks can be claimed:

- Feedstocks with a high potential for biodiesel (BD) production are *Brassica juncea* oilseed, which can be used as feedstock for BD100, *Carthamus tinctorus*, tobacco, animal fat and waste cooking oil to be used in BD blends with other oils or in diesel blends. However, blending different oils among them or with diesel already during the free fatty acids (FFA) esterification reaction may increase the reaction rate due to the lowered viscosity.

- Free fatty acids esterification over acid ion exchange resins in slurry reactors remains the preferred method of oils deacidification due to the optimal contact between the reagents and the catalyst and the good durability over time.
- The final high BD yields obtained for the oils de-acidified with the pre-esterification method over sulphonic ion exchange resins demonstrate its effectiveness in lowering the acidity and the possibility of obtaining high quality biodiesel from the selected feedstocks.
- Surface acidity and specific surface area of sulphated inorganic systems can be increased by both adding TiO_2 and using ultrasound (US) in precise experimental conditions to assist the sol-gel synthesis of the catalysts. Changing the experimental conditions of US during the sol-gel synthesis makes also possible to tune the properties of the catalysts. In spite of not satisfying FFA conversions were obtained, US-assisted sol-gel synthesis turns out to be an extremely interesting method to obtain catalysts with high acidity and surface area.
- Both US and microwaves (MW) enhanced the FFA esterification reaction rate at temperatures lower than the one used conventionally (336 K). The positive effects of US are attributable to the phenomena generated inside the reaction medium by the acoustic cavitation, while MW are able to generate temperature effects localized in the proximity of the catalyst surface and to increase MeOH-oil solubility.
- US-assisted transesterification reaction is much faster than conventional transesterification: BD yields higher than 96.5% were achieved in most of the cases within 10 minutes of reaction, whereas the conventional method requires 150

minutes, besides higher reagents amount and higher temperatures. In particular, BD yields higher than 90% were obtained using a continuous reactor and pulsed US within 18 seconds, corresponding to just one passage in the reactor. In this case the transesterification reaction rate resulted to be 300X faster than the conventional process.

Suggestions for the continuations of the work concern the further study of the synthesis of sulphated inorganic systems such as SO_4^{2-}/ZrO_2 or SnO_2 or TiO_2 with US and MW.

Future work should also be devoted to the optimization of the experimental variables related to the use of MW and US to promote both FFA esterification and transesterification reactions.

References

Barrett E.P., Joyner L.G., Halenda P.P., "The determination of pore volume and area distributions in porous substances. I. Computations from nitrogen isotherms", *J. Am. Chem. Soc.* **1951**, 73, 373.

Bianchi C.L., Boffito D.C., Pirola C., Ragaini V., "Low temperature de-acidification process of animal fat as a pre-step to biodiesel production", *Catal. Lett.*, **2010**, 134, 179.

Bianchi C.L., Pirola C., Boffito D.C., Di Fronzo A., Carvoli G., Barnabè D., A. Rispoli, R. Bucchi, "Non edible oils: raw materials for sustainable biodiesel", in Stoytcheva M., Montero G. (Eds.): *Biodiesel Feedstocks and Processing Technologies*, Intech, **2011**, pp. 3-22.

Boffito D.C., Pirola C., Galli F., Di Michele A., Bianchi C.L., "Free Fatty Acids Esterification of Waste Cooking Oil and its mixtures with Rapeseed Oil and Diesel", *Fuel*, **2012a**, accepted on 19th October 2012, DOI: 10.1016/j.fuel.2012.10.069.

Boffito D.C., Crocellà V., Pirola C., Neppolian B., Cerrato G., Ashokkumar M., Bianchi C.L., "Ultrasonic enhancement of the acidity, surface area and free fatty acids esterification catalytic activity of sulphated ZrO_2-TiO_2 systems", *J. Catal.*, **2012b**, http://dx.doi.org/10.1016/j.jcat.2012.09.013

Boffito D.C., Pirola C., Bianchi C.L., "Heterogeneous catalysis for free fatty acids esterification rea.ction as a first step towards biodiesel production", *Chem, Today*, **2012c**, 30, 14.

Brunauer S., Hemmett P., Teller E., “Adsorption of Gases in Multimolecular Layers”, *J. Am. Chem. Soc.* **1938**, 60, 309.

López D. E., Suwannakarn K., Bruce D. A., Goodwin JG. “Esterification and transesterification on tungstated zirconia: Effect of calcination temperature”, *J Catal* **2007**, 247, 43.

Mason T.J., Lorimer J.P., “Sonochemistry, Theory, Applications and Uses of Ultrasound in Chemistry“, Efford, J. Wiley, New York, **1988**.

Mingos D.M.P.,Baghurst D.R., “Applications of Microwave Dielectric Heating Effects to Synthetic Problems in Chemistry“, Microwave-Enhanced Chemistry, American Chemical Society,Washington, DC, USA, **1997**.

Perego C., Ricci, M., “Diesel fuel from biomass”, *Catal. Sci. Technol.*, **2012**, 1, 1776.

Pirola C., Boffito D.C., Carvoli G., Di Fronzo A., Ragaini V., Bianchi C.L., “Soybean oil deacidification as a first step towards biodiesel production”, in D. Krezhova (Ed.): Recent Trends for Enhancing the Diversity and Quality of Soybean Products, Intech, **2011**, pp. 321-44.

Pirola C., Bianchi C.L., Boffito D.C., Carvoli G., Ragaini V., “Vegetable oil deacidification by Amberlyst : study of catalyst lifetime and a suitable reactor configuration”, *Ind. Eng. Chem. Res.*, **2010**, 49, 4601.

Ragaini V., Pirola C., Borrelli S., Ferrari C., Longo I., “Simultaneous ultrasound and microwave new reactor: Detailed description and energetic considerations”, *Ultrasonics Sonochemistry* **2012**, 19, 872

Sehgal C., Steer R.P., Sutherland R.G., Verrall R.E., “Sonoluminescence of argon saturated alkali metal salt solutions as a probe of acoustic cavitation”, *J. Chem. Phys.*, **1979**, 70, 2242.

Suslick K. S., Doktycz, S. J., "The Effects of Ultrasound on Solids" in Mason, T.J.: *Advances in Sonochemistry*, JAI Press: New York, **1990**, vol.1, pp. 197-230.

Toukoniitty B., Mikkola J.P., Murzin D.Yu., Salmi T., “Utilization of electromagnetic and acoustic irradiation in enhancing heterogeneous catalytic reactions”, *Appl. Catal. A* **2005**, 279, 1

Winayanuwattikun P., Kaewpiboon C., Piriyakananon K., Tantong S., Thakernkarnkit W., Chulalaksananukul W. et al. “Potential plant oil feedstock for lipase-catalyzed biodiesel production in Thailand”, *Biomass. and Bioen.* **2008**, 32, 1279.

CHAPTER 1:
GENERAL INTRODUCTION

1.1 The current energy situation

Today's economy, society and culture are largely based on the availability of cheap energy, mostly produced by burning fossil fuels: coal, oil, and natural gas. The era of fossil fuels is far from being over, but their dominance decreases. According to the World Energy Outlook (WEO) 2011 by the International Energy Agency (IEA), the consumption of all fossil fuels increases, but their share of the global demand for primary energy decreases slightly slipping from 81% in 2010 to 75%, expected in 2035. In this perspective, natural gas is the only fossil fuel that increases its share in the global energy mix. Worldwide, the use of energy from all sources increases in the projection. Nevertheless, we are facing increasing concern about the exploitation of the fossil fuels, basically due to a couple of major reasons. On the one side, the observed climate change, particularly global warming, is widely held as a consequence of the increase of atmospheric CO_2 concentration due to fossil fuel combustion. On the other side, people are increasingly aware that fossil fuels reserves are huge but not unlimited and given expectations that oil prices will remain relatively high, petroleum and other liquids are the world's slowest-growing energy sources. Moreover, expansion and social progress is however boosting a further increase of energy demand, particularly in the transportation sector. Energy consumption in non-OECD Asia, led by China and India, shows the most robust growth among the non-OECD regions, rising by 91% from 2010 to 2035. However, strong growth also occurs in much of the rest of the non-OECD regions (Annual Energy Outlook 2012, U.S. Energy Information Administration, EIA) (Fig. 1.1). High energy prices and concerns about the environmental consequences of

greenhouse gases (GHG) emissions lead a number of national governments to provide incentives in support of the development of alternative energy sources, making renewables the world's fastest-growing source of energy in the outlook (Fig. 1.2).

All these are the reasons why carbon-neutral biofuels are largely considered a possible way to satisfy the energy demand without dramatically increasing the CO_2 content of the atmosphere (Perego and Ricci, 2012).

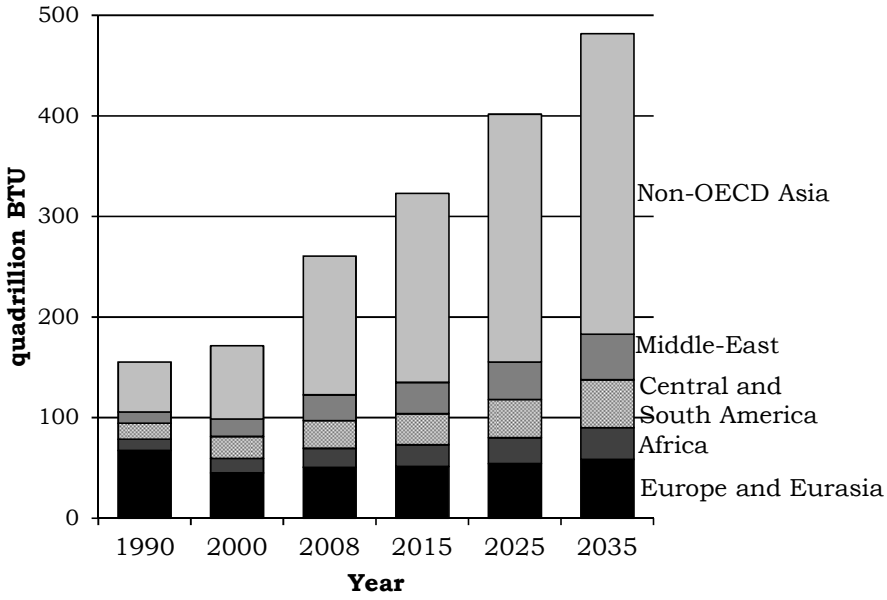

Fig. 1.1. World energy consumption by region. Source: Annual Energy Outlook 2012, EIA.

1.2 General biodiesel interest and challenge

Biodiesel is a liquid biofuel that is defined as fatty acid methyl ester fulfilling certain standards. Biodiesel is obtained by the transesterification or alcoholysis of natural triacilglycerols (TAG), also known as triglycerides, contained in vegetable oils, animal fats,

waste fats and greases, waste cooking oils (WCO) or side-stream products of refined edible oil production with short-chain alcohols, usually methanol or ethanol and using an alkaline homogeneous catalyst (Perego and Ricci, 2012; Okoronkwo et al., 2012; Veljković et al., 2012; Ganesan et al., 2009).

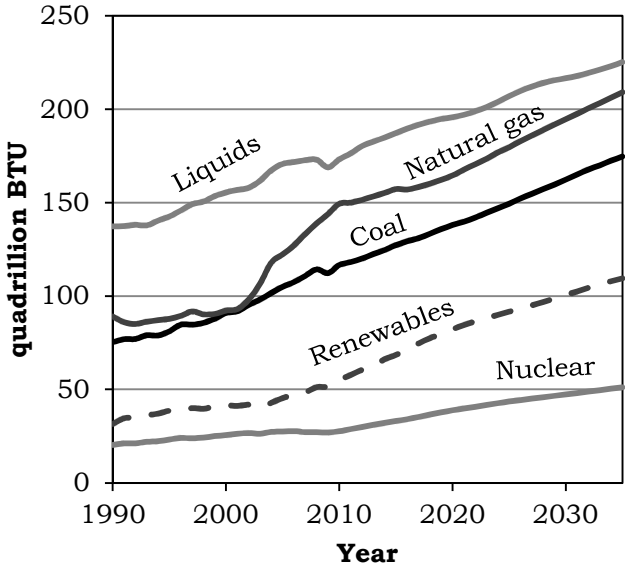

Fig. 1.2. World energy consumption by fuel type. Source: Annual Energy Outlook 2012, EIA.

Biodiesel present several advantages over petroleum-based diesel such as:

- Biodegradability;
- Lower unburned hydrocarbons and particulate emissions;
- Lower CO emissions;
- Lower SO_x emissions;
- Absence of aromatics;
- Closed CO_2 cycle.

It has been estimated that biodiesel is able to reduce carcinogenic air toxins (particulate matter, unburned hydrocarbons, carbon

monoxides and sulphates) by 75–90% compared to diesel (Antolin et al., 2002; Lang et al., 2001) (Fig. 1.3).

Moreover, biodiesel can be used in any compression diesel engine without major modifications.

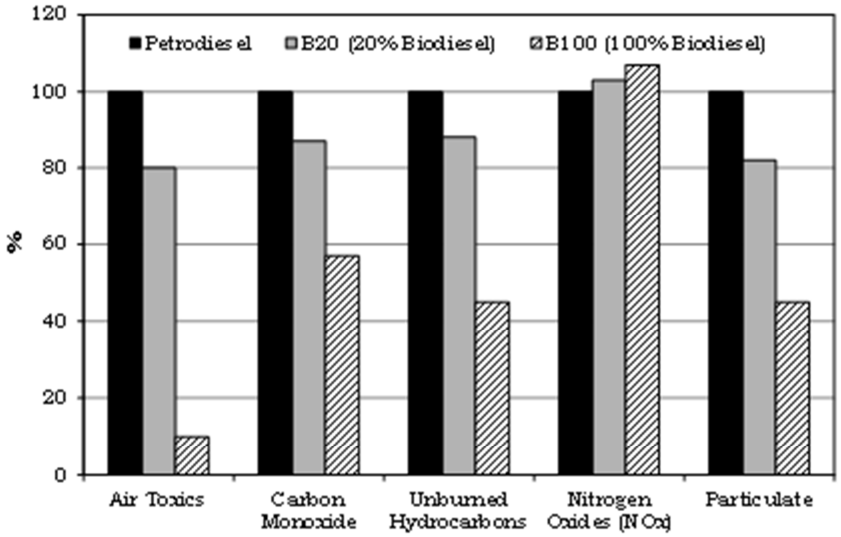

Fig. 1.3. B20 and B100 emissions compared to petrodiesel.

The recent EU directive 2009/28/EC sets the targets of achieving, by 2020, a 10% share of energy from renewable sources in each Member State's transport energy consumption. In this context special consideration is paid to the role played by the development of a sustainable and responsible biofuels production, with no impact on food chain. Nowadays most biodiesel (BD) is produced through triglycerides transesterification of edible oils with methanol in the presence of an alkaline catalyst (Santori et al., 2012; Arzamendi et al., 2008; Lotero et al., 2005; Ma and Hanna, 1999) (Fig.1.4).

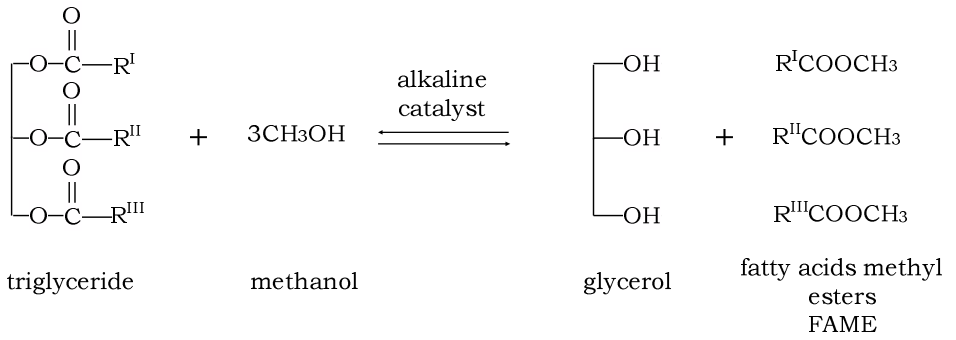

Fig. 1.4. Transesterification reaction.

Refined, low acidity oilseeds (e.g. those derived from sunflower, soy, rapeseed, etc.) may be easily converted into BD, but their exploitation significantly raises the production costs, resulting in a biofuel that is uncompetitive with the petroleum-based diesel (Santori et al., 2012; Lotero et al., 2005).

Moreover, the aforementioned oils derived from food crops, are characterized by substantial water requirements. In Europe vegetable oil production is mainly based on soybean, sunflower and rapeseed cultures: their competition with alimentary applications caused a slowing down of BD production in 2007 with plants exploiting only 50% of their production capacity (source: Wall Street Journal 27/12/2007).

This generated a hot debate about a possible food vs. fuel conflict, i.e. about the risk of diverting farmland or crops for biofuels production at the expense of food supply. It is so highly desirable to produce BD from crops specifically selected for their high productivity and low water requirements (Bianchi et al., 2011; Pirola et al., 2011), or from low-cost feedstocks such as used frying oils (Boffito et al., 2012a) and animal fats (Bianchi et al., 2010).

The value of these second generation biofuels, i.e. produced from crop and forest residues and from non-food energy crops, is

acknowledged, for instance, by the European Community which, in its RED directive, states:

"For the purposes of demonstrating compliance with national renewable energy obligations […], the contribution made by biofuels produced from wastes, residues, non-food cellulosic material, and ligno-cellulosic material shall be considered to be twice that made by other biofuels".

(European Union, RED Directive 2009/28/EC).

For commercial fuel use, the finished biodiesel must be analysed using sophisticated analytical equipment to ensure it meets international standards. A few specifications have been set but the ASTM D 6751 and EN 14214. Comparison is given in Tab. 1.1.

Property	Unit of measure	EN 14214	ASTM 6751
Density (15°C)	g/cm^3	0.86-0.90	-
Viscosity (40°C)	mm^2/s	3.5-5.0	1.9-6.0
Distillation	% (°C)		90%(360°C)
Flash point	°C	>101	>93
Sulphur	mg/kg	≤10	≤15
CCR 100%	%m/m		≤0.05
Carbon residues (10% dist. residue)	%m/m	≤0.3	
Sulphated ash	%m/m	≤0.02	≤0.02
Water	mg/kg	≤500	≤500
Total contamination	mg/kg	≤24	
Cu corrosion max.	3 h (50°C)	1	3
Oxidation stability	h (110°C)	≥6	≥3
Cetane number	min	>51	>47
Acid value	mg KOH/g	≤0.5	≤0.5
Methanol	%m/m	≤0.2	≤0.2
Ester content	%m/m	≥96.5	
Monoglyceride	%m/m	≤0.8	
Diglyceride	%m/m	≤0.2	
Triglyceride	%m/m	≤0.2	
Free glycerol	%m/m	≤0.02	≤0.02
Total glycerol	%m/m	≤0.25	≤0.24
Iodine value	$gI_2/100g$	≤120	
Linoleic acid methyl esters	%m/m	≤12	
C(x:4) and greater unsaturated esters	%m/m	≤1	
Phosphorous	mg/kg	≤4	
Group I metals	mg/kg	≤5	≤5
Group II metals	mg/kg	≤5	≤5

Tab. 1.1. Biodiesel European and American standards.

1.3 History of biodiesel

The roots of what eventually became known as “biodiesel” extend back to the discovery of the diesel engine by Rudolf Diesel (Fig. 1.5) (Songstad et al. 2009). The first vehicle biodiesel-powered was Rudolf Diesel's first engine model, a single 10 feet iron cylinder with a flywheel at its base, that ran with this fuel for the first time in Augsburg in 1893. Diesel’s engine was first demonstrated in the 1900 World Fair in Paris using peanut oil as a fuel (Nitske, Wilson 1965), receiving the "Grand Prix" at the World Fair in Paris, France in 1900. Diesel believed that the utilization of a biomass fuel was the future of his engine, as he stated in his 1912 speech saying "the use of vegetable oils for engine fuels may seem insignificant today, but such oils may become, in the course of time, as important as petroleum and the coal-tar products of the present time" (Biodiesel Magazine, 15th July 2009).

Fig. 1.5. Rudolf Diesel (185-1913).

In 1916, Gutierrez tested castor oil as alternative fuel for the first diesel engine imported into Argentina (Gutierrez, 1916).

1937 was a landmark year in the history of biodiesel. In this year a Patent was granted to G. Chavanne from the University of Brussels for the: "Procedure for the transformation of vegetable oils for their uses as fuels" that describes the use of ethyl esters of palm oil (although other oils and methyl esters are mentioned) as diesel fuel. The patent describes the process of alcoholysis (also called transesterification) of vegetable oils using ethanol in order to separate the fatty acids from the glycerol by replacing the glycerol with short linear alcohols (Chavanne, 1937).

Of particular interest is a related extensive report published in 1942 on the production and use of palm oil ethyl ester as fuel (van den Abeele, 1942). The work describes what is probably the first urban bus operating with biodiesel. A bus fuelled with palm oil ethyl ester served the commercial passenger line between Brussels and Louvain in the summer of 1938. Performance of the bus operating on that fuel was reported to be satisfactory. It was noted that the viscosity difference between the esters and conventional diesel fuel is considerably less than that between the parent oil and conventional diesel fuel. Also, the author(s) point out that the esters are miscible with other fuels.

Prompted by shortage of fuel, during the World War II year, export of cottonseed oil was prohibited in Brazil so it could be used as a substitute for diesel (Anonymous, 1943) and in China, tung oil and other vegetable oils were used to produce a version of gasoline and kerosene (Cheng, 1945). During this period research on conversion of a variety of vegetable oils to diesel was conducted in India (Chowhury et al., 1942) and in the USA research was performed to evaluate cottonseed oil as a diesel fuel (Okoronkwo, 2012).

The Arab petroleum embargo in 1974 reignited interest in alternative liquid fuels, and during the 1970s and 1980s much research was done on a wide variety of oils (Shay, 1993).

The first commercial biodiesel plant went into operation in 1991 in Austria. Then, for several years both plants' capacity and actual production and consumption experienced extremely high average annual growth close, e.g., to 50% in the 2002–2006 period. This explosive development, however, resulted in some overcapacity, and further growth is expected to slow down (Perego and Ricci, 2012).

1.4 The numbers of biodiesel in the World, Europe and Italy

In Fig. 1.6 daily biodiesel production by World region and year is presented.

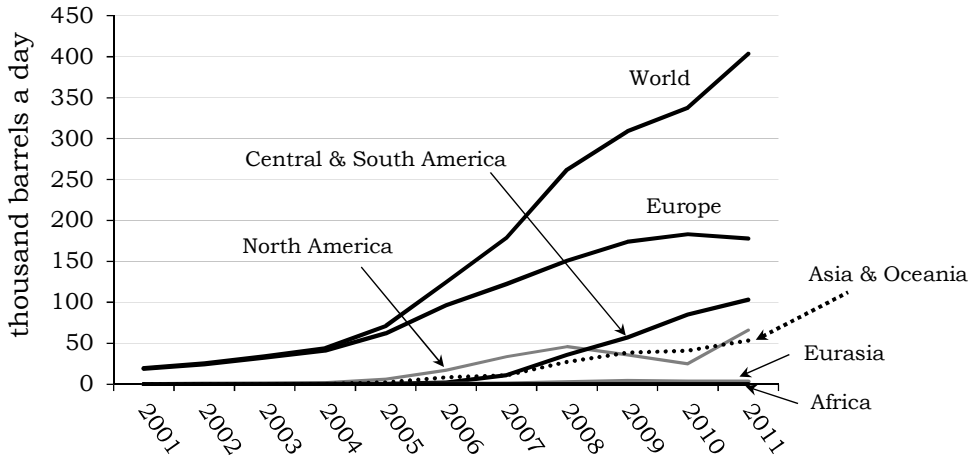

Fig. 1.6. World biodiesel production by region and year. Source: Energy Information Administration, International Energy Statistics, Biofuels Production. The above graph was derived from an interactive table and generated on November 25, 2012.

Europe has been the dominant region for biodiesel production with increased production each year since 2001, followed by North

America, whose biodiesel production is led by the United States, until 2007. In 2007 Central & South America surpassed North America's in biodiesel production. In 2009, U.S. biodiesel production fell by over 10 thousand barrels per day, while continued growth in Central & South America and Asia & Oceania surpassed North America in production of biodiesel for the first time. The declining biodiesel production in the United States beginning in 2008 is likely due to changes in Federal subsidies for biodiesel as well as changes in foreign trade policy and the downturn of the economy (U.S. Energy Department, 2010).

During the first two quarters of 2011 biodiesel production in Europe decreased. According to the European Biodiesel Board, biodiesel production in Europe grew by 5.5 % from 2009 to 2010, by 17 % from 2008 to 2009 and by 35 % from 2007 to 2008) (European Biodiesel Board - EBB, 2011).

In Tab. 1.2 biodiesel production capacities of European Countries are listed for years 2010 and 2011.

Germany and France continue to lead the EU in biodiesel production, followed by Spain and Italy. As of July 2011, total biodiesel production capacity in Europe reached 22 million tons (6.6 billion gallons) from 254 existing production facilities. However, according to EBB only 44% of the capacity is in operation. The EBB states that during the first two quarters of 2011, only 44 % of capacity was being utilized.

Few European countries have experienced a growth in production capacity over the past year. Belgium, Greece, the Netherlands, Poland, Slovenia, and Spain reported slight increases. Bulgaria, Germany, Italy, Romania, and the U.K. reported slight reductions in production capacity.

Country	2010 capacity (000 tons)	2011capacity (000 tons)
Austria	560	560
Belgium	670	710
Bulgaria	425	348
Cyprus	20	20
Czech Republic	427	427
Denmark	250	250
Estonia	135	135
Finland*	340	340
France	2 505	2 505
Germany	4 933	4 932
Greece	662	802
Hungary	158	158
Ireland*	76	76
Italy	2 375	2 265
Latvia	156	156
Lithuania	147	147
Luxemburg	0	0
Malta	5	5
Netherlands	1 328	1 452
Poland	710	864
Portugal	468	468
Romania	307	277
Slovakia	156	156
Slovenia	105	113
Spain	4 100	4 410
Sweden	277	277
UK	609	404
TOTAL	21.904,00	22.117,00

Tab. 1.2. 2010 and 2011 biodiesel production capacity of the European Countries (European Biodiesel Board, 2011).

According to EBB, the increased imports from third countries such as Argentina, Indonesia as well as circumvention measures from North America are mostly likely to have contributed to lessen European domestic production.

In 2011, EBB successfully addressed the challenge of circumvention of the anti-dumping and countervailing duties applicable to US biodiesel (B99). However, besides the circumvention of the EU duties in B99, the general trend in EU biodiesel imports is raising concerns. In 2010 the EU imported at least 1.9 million tons (570 million gallons) of biodiesel. Approximately 61% of these

imports were from Argentina, 26% from Indonesia, with lower quantities from Canada, Malaysia, India, Singapore and the rest of the World. During the first quarter of 2011, 71% of the imported biodiesel entering the EU came from Argentina, while 27% came from Indonesia. As a result, the EBB supports the recent proposal by the European Commission to remove Argentina and Malaysia from the list of countries benefiting from the Generalized System of Preferences.

The EBB also addresses indirect land use change in the statement it published regarding the release of its new statistics. "In the view of the EBB, it is essential that efforts to implement the Renewable Energy Directive and its 2020 objectives are not diverted by the current debate over biofuels (ILUC)," said the Board in a published release. "In view of this, it cannot be a reasonable way forward for the EU to let its 2020 objectives of climate change mitigation and energy security being knocked-off course on the basis of the elusive ILUC concept and questionable modelling exercises".

"The important contribution of biofuels to the EU's GHG reduction, energy security and economic growth objectives has never been so evident as today. The EU biodiesel industry stands ready. Yet, this contribution will only materialize in the future if a suitable policy framework and market environment is maintained at EU level. This requires a prompt and seamless implementation of the RED and a level-playing field with imported biofuels." (European Biodiesel Board, press release 18 October 2011).

In Tab. 1.3. the production capacities of Italian biodiesel manufacturers are listed for the year 2011.

Manufacturer	Locality	Productive capacity (tons/year)
ALCHEMIA ITALIA SRL	Rovigo (RO)	15.000
BIO-VE-OIL OLIMPO SRL	Corato (BA)	100.000
CEREAL DOCKS SPA	Vicenza (VI)	150.000
COMLUBE SRL	Castenedolo (BS)	120.000
DP LUBRIFICANTI SRL	Aprilia (LT)	155.520
ECOIL	Priolo (SR)	200.000
F.A.R. Fabbrica Adesivi Resine Spa Divisione Polioli	Cologno Monzese (MI)	100.000
ECO FOX SRL	Vasto (CH)	199.416
ITAL BI OIL SRL	Monopoli (BA)	190.304
ITAL GREEN OIL SRL	San Pietro di Morubio (VR)	365.000
GDR BIOCARBURANTI	Cernusco sul Naviglio (MI)	50.000
MYTHEN SPA	Vicenza (VI)	200.000
NOVAOL SRL	Castenedolo (BS)	250.000
NOVAOL SRL	Aprilia (LT)	200.000
OIL.B SRL	Vicenza (VI)	200.000
OXEM S.p.A.	Castenedolo (BS)	200.000
TOTAL		2.395.240

Tab. 1.3. Italian biodiesel manufacturers and 2011 biodiesel productive capacity (Assocostieri, Unione produttori biocarburanti, 2012).

The overall production capacity of biodiesel plants in Italy indicated in Tab. 1.3 for the year 2011 remained practically unchanged from the previous year. Moreover, according to Assocostieri, only 33.4% and 26% of the total capacity was exploited in 2010 and 2011, respectively. On the other hand, the amount of imported biodiesel is increasing dramatically, from 780 000 tons in 2010 to more than 1 000 000 tons in 2011, while biodiesel export market increased from 101 000 to 158 000 tons from 2010 to 2011. The amount of biodiesel consumed accounts for 1 460 000 tons and remained practically unchanged from the previous year.

The reasons of this unfortunate situation are to be found once again in the biodiesel imports from foreign countries, which can rely on a more favourable tax regime with respect to Italy. Moreover with

the financial act "legge finanziaria" promulgated in 2010, the incentive for biofuels producers was cut of 90%, contributing in worsening biodiesel situation in Italy.

The hope is that the anti-dumping duty posed by the European Community (EC/444/2011) against imports from the United States and Canada will improve the situation in the forthcoming years and be possibly extended countries importing biodiesel in Italy.

1.5 Present situation of biodiesel technology: state of art

There are basically four ways of making biodiesel from refined or waste greases, namely:

- direct use and dilution/blending (Kaya et al., 2009; Kansedo et al., 2009);
- microemulsions (Sahoo and Das, 2009);
- thermal cracking (pyrolysis) (Santos et al., 2009; Srivastava and Prasad, 2000);
- transesterification (Perego and Ricci, 2012; Okoronkwo et al., 2012; Veljković et al., 2012; Ganesan et al., 2009).

The most commonly used method is transesterification of vegetable oils and animal fats (Okoronkwo et al., 2012), which will be described in detail in this section.

There are currently four main technologies for biodiesel production by transesterification:

- Catalytic transesterification (homogeneous, heterogeneous and enzymatic);
- Non-catalytic supercritical-alcohol transesterification;
- Sonochemically-assisted transesterification.

It has to be stressed that although transesterification is the most important step in biodiesel production, additional steps are necessary to obtain a product that complies with international standards (Meher, 2006).

1.5.1 Catalytic transesterification

Catalytic transesterification may be performed using homogeneous, heterogeneous or enzymatic catalysts.

Among homogeneous and heterogeneous catalysts, both basic and acid materials may be adopted.

Homogeneous base-catalysed transesterification

Homogeneous base-catalysed transesterification is the most commonly used technique as it is the most economical process to obtain biodiesel (Singh et al. 2006). Basic catalysts are used since, compared to acidic ones, they are more active (up to 4000 times) (Formo, 1954) and pose fewer corrosion problems. Catalysts such as sodium methoxide or potassium or sodium hydroxide are most frequently used. The transesterification is usually carried out at 333 K and at high methanol/oil ratio, so as to obtain high conversions (Perego and Ricci, 2012). The transesterification reaction is known to be an equilibrium-limited reaction and it is therefore usually performed in two steps unless a very large excess of methanol is used in first step. A second step is necessary to convert the unreacted mono- and di-glycerides to glycerol and methyl esters. FAME yields around 90% are usually obtained after the first step (Çaylı and Küsefoğlu, 2012; Gole and Gogate, 2008). A scheme of the homogeneous base-catalysed transesterification industrial process is

displayed in Fig. 1.7. However, the process still has a few drawbacks. The presence of free fatty acids in the feedstock, occurring in particular in the case of not refined oils, causes the formation of soaps as a consequence of the reaction with the alkaline catalysts (RCOOH + NaOH → RCOONa + H_2O). Soaps distribute among the two phases, hindering the contact between reagents and, eventually, the products separation (Fig. 1.8). As a consequence, the process can only accept a restricted range of feedstock, typically with less than 0.5% of free fatty acids and 0.2% of moisture (Perego and Ricci, 2012; Boffito et al., 2012a, 2012b, Bianchi et al., 2010; Pirola et al., 2010) . Another drawback given by the use of alkaline homogeneous catalysts lies in the need of neutralization (and wastewater disposal) and the non-recovery of the catalyst.

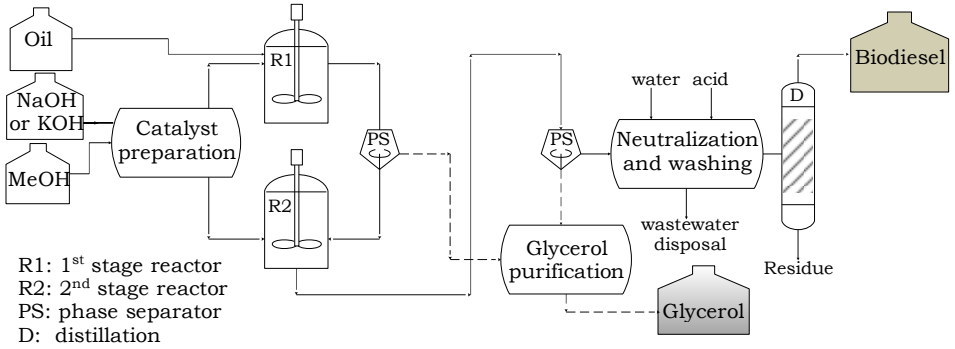

Fig. 1.7. Scheme of the industrial alkali-catalysed transesterification process.

Many methods have been proposed to eliminate FFA during or prior to transesterification, i.e. neutralization with alkali, deacidification with selective solvents, neutralizing distillation and FFA pre-esterification (Santori et al., 2012). Among these the FFA pre-esterification method is a very interesting approach to lower the acidity of biodiesel feedstocks with high initial FFA concentration

(Boffito et al., 2012a, 2012b; Bianchi et al., 2010, 2011; Pirola et al., 2010, 2011). The method allows to lower the acid value of the raw material as well as to obtain methyl esters already in this preliminary step. The FFA esterification reaction will be described in detail later.

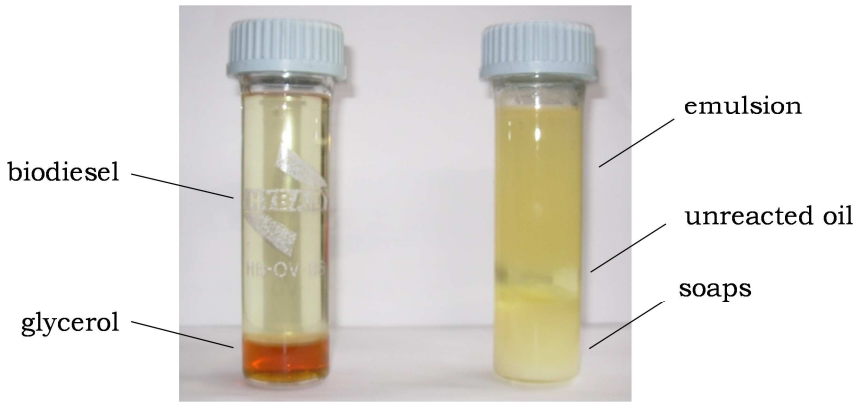

Fig. 1.8. Alkali-catalysed transesterification products obtained from a rapeseed oil with 0.1%$_{wt}$ FFA (on the left) and 5%$_{wt}$ FFA (on the right).

Homogeneous acid-catalysed transesterification

Sulphuric acid, sulfonic acid and hydrochloric acid are usually adopted as catalysts in the acid catalysed reactions and are advantageous for oils having high FFA content, as acids catalyse the FFA esterification to produce fatty acid methyl esters. The main drawback of acid-catalysed transesterification lies in the need of high catalyst concentrations (Balat, Balat 2008). Moreover long reaction times and considerable alcohol requirements are necessary in order to obtain good product yields in practical reaction times (Canakci and Van Gerpen, 1999). However, ester yields do not proportionally increase with molar ratio (Lotero et al., 2006).

Heterogeneous alkali and acid-catalysed transesterification

Heterogeneous acid and basic catalysts could be classified as Brønsted or Lewis catalysts, though in many cases both types of

sites could be present and it is not easy to evaluate the relative importance of the two types of sites in the reaction. In this case the transesterification reaction occurs between alcohol adsorbed on catalyst and triglycerides by the Eley–Rideal mechanism (Sharma et al., 2011). Solid acid catalysts have the strong potential to replace liquid acids as transesterification aids as they can eliminate separation, corrosion and environmental problems associated with liquid acid transesterification. Heterogeneous catalytic systems present lower methanolysis and ethanolysis activities when compared with the traditional acid and basic ones (Abreu et al. 2004). Another general drawback of heterogeneous catalysts lays their preparation and reaction conditions which are energy intensive (Sharma, Singh & Korstad 2011).

Despite all these difficulties, IFP (Institute Francais du Petrole) developed an industrial process (Esterfip-Ht) which is currently commercialized by Axens. The Esterfip-Ht is a two-step continuous process using zinc aluminate mixed oxide as a catalyst (Bournay, 2005).

Enzymatic transesterification

Lipases-catalysed transesterification reactions have been reported to have many advantages: they are highly specific and chemically clean, proceed regardless of the initial moisture content and FFA concentration in the raw material and yield glycerol with higher purity than other methods (Ma and Hanna, 1999). The main problem of the lipase-catalysed process is the high cost of the lipases (Royon et al. 2007). Processes using biocatalysts (pure lipases and organisms secreting lipase enzymes) are efficient in terms of by product glycerol removal; mild reaction conditions, initial moisture content and FFA present in raw material do not

interfere with the reaction. Deactivation of the lipase when exposed to high concentration of methanol, higher reaction time and cost of enzymes are the major disadvantages of enzymatic processes (Ganesan et al., 2009).

1.5.2 Non catalytic supercritical-alcohol transesterification

Supercritical-alcohol transesterification is carried out at temperatures ranging from 200 °C and 400°C, pressures up to 200 bars and methanol to oil ratios up to 42:1. The process presents some advantages such as improved phases miscibility and consequent overcoming of mass transfer limitations, high reactions rates and easy separation and purification of the products. The supercritical process may also be carried out in presence of moisture and high FFA concentrations, since also FFA are easily converted into methyl esters. It has also been reported that a possible advantage of the process might be thermal decomposition of glycerol to low molecular weight esters, ethers and hydrocarbons on reaction with methanol (Sharma, et al., 2011).

However, its application in large scale production is still limited by high cost involved because of high temperature and pressure, and high alcohol to oil molar ratio (Okoronkwo et al., Ganesan et al., 2009).

1.5.3 Sonochemically-assisted transesterification

Recent developments in sonochemistry allow the use of ultrasonic irradiation as a new, more efficient mixing tool in biodiesel production. Ultrasound biodiesel production from various feedstocks

is the focus of many research groups all over the World in the last decade. The use of low-frequency ultrasound (LFU) in biodiesel production has several advantages over the classical synthesis. The positive effect of LFU on biodiesel production from vegetable oils via transesterification may ascribable to different phenomena connected with the occurrence of the acoustic cavitation inside the reaction medium. Veljković and co-authors (Veljković et al., 2012) give an extensive explanation of the effects caused by the acoustic cavitation occurring during the transesterification reaction.

Ultrasound can have physical and chemical effects on heterogeneous reaction systems through cavitation bubbles (Verziu et al., 2009). The physical effects are connected with the formation of emulsions between liquid reactants that are usually not miscible, as well as triglycerides and methanol. The microturbulence generated by the collapse of the cavitation bubbles would be able to disrupt the phase boundary leading to the formation of the microemulsion. The increased interfacial area of exchange between the micro-phases of triglycerides and methanol enhances the reaction rates as well as a very vigorously mechanically agitated reactor. These emulsions are reported to have drops smaller in size and be more stable than those obtained using conventional techniques, which is very beneficial for liquid-liquid reaction systems (Georgogianni et al., 2008a).

The chemical effects are due to the radicals formation caused by the collapse of the transient cavitation bubbles. The transesterification reaction may be governed by the in situ generation of methoxy radicals, provided that the temperature generated by the collapse of the cavitation bubbles is high enough to allow their formation (Georgogianni et al., 2008b). Ultrasonically generated radicals increase reaction rate in bulk mixture. Few

researchers also reported that ultrasonic cavitation can also provide the activation energy required for initiating the transesterification reaction (Siatis et al., 2006). A more detailed explanation of this process will be given later.

Another possibility for accelerating the transesterification reaction is to use microwave irradiation. Microwave irradiation has been an alternative heating system in transesterification over the past few years (Azcan and Danisman, 2008). As a result, drastic reductions in the quantity of by-products and a short separation time have been obtained (Hernando et al., 2007).

1.6 Chemistry of the transesterification

As already discussed above, the transesterification reaction may be alkali- or acid-catalysed. Both mechanisms are shown in Fig. 1.9.

The reaction mechanism of the alkali-catalysed transesterification is formulated in four steps. First, methoxide anions are formed from the reaction between methanol and the alkaline catalyst (I). Then, the next step involves the nucleophilic attack of a methoxide anion to the carbonyl carbon, forming a tetrahedral intermediate (II). From the intermediate, a fatty alkyl methyl ester (III) and diglyceride are then yielded and the catalyst is obtained in its original form (IV).

The mechanism of acid-catalysed transesterification of vegetable oils starts with the protonation of the carbonyl of one ester group, thus promoting the formation of a carbocation (I), which after a nucleophilic attack of the alcohol produces a tetrahedral intermediate (II). The tetrahedral intermediate, after tautomerization, eliminates a methyl ester and re-generates the acid catalyst (III).

In Fig. 1.9., only the first step of the transesterification, i.e. the formation of the diglyceride is shown.

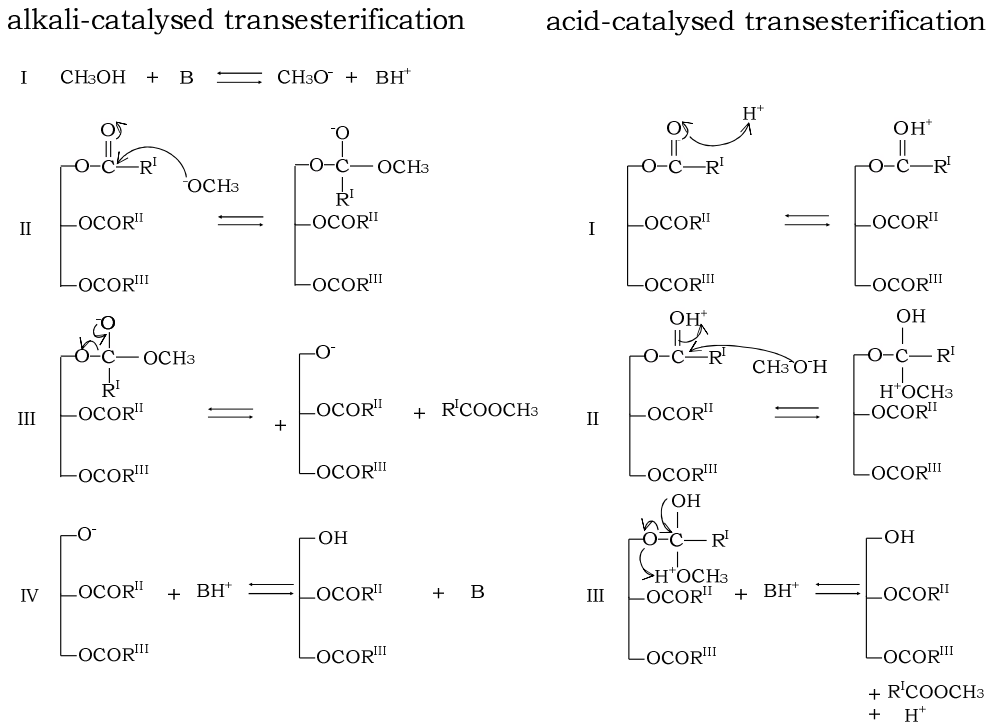

Fig. 1.9. Transesterification reaction mechanisms.

The reaction proceeds in three reversible steps: the conversion of triglycerides to diglycerides, followed by the conversion of diglycerides to monoglycerides, and of monoglycerides to glycerol, yielding one methyl ester molecule per mole of glyceride at each step, as reported hereinafter.

$$\text{triglyceride} + CH_3OH \rightleftharpoons \text{diglyceride} + \text{FAME}$$
$$\text{diglyceride} + CH_3OH \rightleftharpoons \text{monoglyceride} + \text{FAME}$$
$$\text{monoglyceride} + CH_3OH \rightleftharpoons \text{glycerol} + \text{FAME}$$

1.7 Free fatty acids esterification for biodiesel production

As already evidenced in the section concerning the alkali-catalysed transesterification, free fatty acids esterification may be a valid solution to lower the acidity of the feedstock prior to the transesterification. This method is considered particularly attractive because, besides lowering the FFA concentration of the oils, it also

$$RCOOH + CH_3OH \xrightleftharpoons{\text{acid catalyst}} RCOOCH_3 + H_2O$$

allows to increase the final yields in methyl esters, according to the scheme represented in Scheme 1.2.

Scheme 1.2. Free fatty acids esterification reaction.

The mechanism of the reaction is shown in Fig. 1.10. The first step is the protonation of the carbonyl group (I), followed by the nucleophilic attack of methanol to the carbonyl carbon, forming a tetrahedral intermediate (II). The tetrahedral intermediate rearranges through tautomerization and a water molecule is yielded (III). In the final step the methyl ester forms and the catalyst is re-obtained (IV).

The free fatty acids esterification reaction may be also an alternative process to transesterification reaction when low-quality oils and fats are used as feedstock. Esterification is normally carried out in a homogeneous phase in the presence of acid catalysts such as H_2SO_4, H_3PO_4, HCl and p-toluene sulfonic acid (Bourges and Diaz, 2012).

However, the use of these catalysts results in some obvious drawbacks, such as corrosion, impossibility of catalyst recovering and safety issues. Therefore, acid heterogeneous catalysts can be considered as a valid alternative to overcome all this problems and reduce biodiesel production costs. Heterogeneous catalysts can be in

fact easily separated and recovered from reaction mixture. For this reason many efforts regarding the use of solid acid catalysts for the FFA esterification were recently carried out (Boffito et al., 2012a, 2012b; Bianchi et al., 2010; Pirola et al., 2010; Marchetti and Errazu 2008).

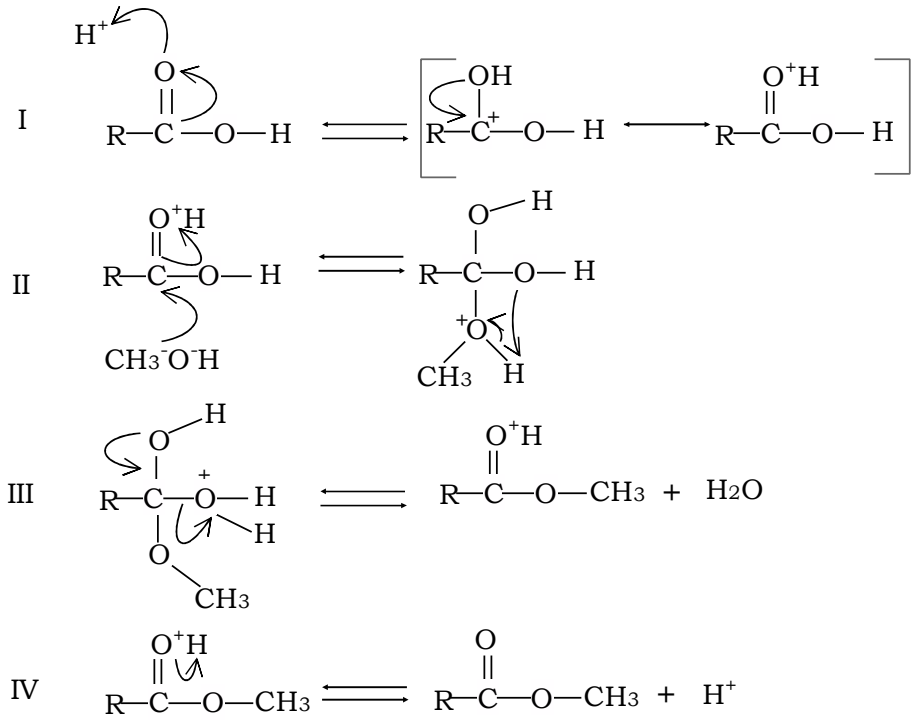

Fig. 1.10. Free fatty acids esterification reaction mechanism.

Several acid solids have been tested in the FFA esterification reaction, such as: zirconium oxide, titanium oxide, tin oxide, sulfonic ion-exchange resin, sulfonic modified mesostructure silica, sulphonated carbon-based catalyst, heteropolyacids (HPAs) (Bourges and Diaz, 2012). However in the last year the use of aluminosilicates (mordenite, halloysite, kaolinite) (Nascimento et al., 2011; Zatta et al., 2011; Carmo et al., 2009), zirconium oxides (Boffito et al, 2012a,

2011) and cation-exchange resins (Boffito 2012b, 2012c; Bianchi et al., 2010; Pirola et al., 2010) seem to be most worthy options.

Another possible advantage given by the use of an acid heterogeneous catalyst lies in the possibility of performing simultaneously the free fatty acids esterification and the transesterification reactions, though temperatures higher than 120°C are necessary (Bourges and Diaz, 2012).

Large part of this thesis will be devoted to the study of the heterogeneously catalysed free fatty acids esterification.

1.8 Aims of the work

The aims of this work are framed in the context of the entire biodiesel production chain, ranging from the choice of the raw material, through its standardization to the actual biodiesel production. The objectives can be therefore summarized as follows:

- Assessing the potential of different vegetable or waste oils for biodiesel production by their characterization, deacidification and final transformation into biodiesel;
- To test different ion exchange resins and sulphated inorganic systems as catalysts in the FFA esterification; this was accomplished through activity tests in FFA esterification reaction and catalysts characterization;
- To assess the use of ultrasound to assist the sol-gel synthesis of inorganic sulphated oxides to be used as catalysts in the FFA esterification by activity tests and their characterization;
- To assess the use of sonochemical techniques such as ultrasound (US) and microwaves (MW) to promote both the FFA esterification and transesterification by performing the

reactions in different experimental conditions (varying US and MW power, temperature, using batch or continuous reactors).

References

Abreu F.R., Lima D.G., Hamú E.H., Wolf C., Suarez P.A.Z., "Utilization of metal complexes as catalysts in the transesterification of Brazilian vegetable oils with different alcohols", *J. Mol. Catal. A: Chem.*, **2004**, 209(1-2), 29.

Antolin G., Tinaut F.V., Briceno Y., "Optimization of biodiesel production by sunfloweroil transesterification", *Bioresour. Technol.,* **2002**, 83, 111.

Arzamendi G., Arguinarena E., Campo I., Zabala S., Gandia L.M,. "Alkaline and alkaline-earth metals compounds as catalysts for the methanolysis of sunflower oil". Catal. Today, **2008**, 133, 305.

Assocostieri, Unione produttori biocarburanti, **2012**. Available at: http://www.assocostieribiodiesel.com/produttori.asp, accessed on 25 November 2012.

Azcan N., Danisman A., "Microwave assisted transesterification of rapeseed oil.", *Fuel*, **2008**, 87, 1781.

Balat M., Balat H. "A critical review of bio-diesel as a vehicular fuel", *Energ. Conv. Manage.*, **2008**, 49(10), 2727.

Bianchi C.L., Boffito D.C., Pirola C., Ragaini V., "Low temperature de-acidification process of animal fat as a pre-step to biodiesel production", *Catal. Lett.*, **2010**, 134, 179.

Bianchi C.L., Pirola C., Boffito D.C., Di Fronzo A., Carvoli G., Barnabè D., A. Rispoli, R. Bucchi, "Non edible oils: raw materials for sustainable biodiesel", in Stoytcheva M., Montero G. (Eds.): *Biodiesel Feedstocks and Processing Technologies*, Intech, **2011**, pp. 3-22.

Boffito D.C., Pirola C., Galli F., Di Michele A., Bianchi C.L., "Free Fatty Acids Esterification of Waste Cooking Oil and its mixtures with Rapeseed Oil and Diesel", *Fuel*, **2012a**, accepted on 19th October 2012, DOI: 10.1016/j.fuel.2012.10.069.

Boffito D.C., Crocellà V., Pirola C., Neppolian B., Cerrato G., Ashokkumar M., Bianchi C.L., "Ultrasonic enhancement of the acidity, surface area and free fatty acids esterification catalytic activity of sulphated ZrO_2-TiO_2 systems", *J. Catal.*, **2012b**, http://dx.doi.org/10.1016/j.jcat.2012.09.013

Boffito D.C., Pirola C., Bianchi C.L., "Heterogeneous catalysis for free fatty acids esterification rea.ction as a first step towards biodiesel production", *Chem. Today***, 2012c**, 30, 14.

Borges, M.E., Díaz, "Recent developments on heterogeneous catalysts for biodiesel production by oil esterification and tranesterification reactions: a review"., *Renew. Sustain. Energy Rev.*, **2012**, 16, 2839.

Bournay L., Casanave D., Delfort B., Hillion G., Chodorge J.A., "New heterogeneous process for biodiesel production: A way to improve the

quality and the value of the crude glycerine produced by biodiesel plants", *Catal. Today*, **2005**, 106, 190.

Canakci M., Van Gerpen J., "Biodiesel production via acid catalysis", *Trans ASAE*, **1999**, 42(3), 1203.

Carmo Jr A.C., de Souza L.K.C., da Costa C.E.F., Longo E., Zamian J.R., da Rocha Filho G.N. "Production of biodiesel by esterification of palmitic acid over mesoporous aluminosilicate Al-MCM-41", *Fuel*, **2009**, 88,461.

Çaylı G., Küsefoğlu S., "Increased yields in biodiesel production from used cooking oils by a two step process: Comparison with one step process by using TGA", *Fuel Proc. Technol.*, **2008**, 89, 118.

Chavanne C.G., Belgian Patent 422,877, Aug. 31, **1937**.

Cheng F., "China produces fuel from vegetable oils", *Chem. Metall. Eng*, **1945**, 52, 99.

Chowhury D.H., Mukerji S.N., Aggarwal J.S., Verman L.C., "Indian vegetable fuel oils for diesel engines", *Gas Oil Power*, **1942**, 37, 80.

European Biodiesel Board, **2011**. Available at http://www.ebb-eu.org/stats.php, accessed on 25 November 2012.

European Biodiesel Board, press release 18 October **2011**. Available at http://www.ebb-eu.org/EBBpress.php, accessed on 25 November 2012.

EIA, Annual Energy Outlook **2012**. Available at http://www.eia.gov/totalenergy/data/annual/index.cfm , accessed on 30 October 2012.

European Union, RED Directive 2009/28/EC on the promotion of the use of energy from renewable sources, 23 April **2009**, Article 21. Available at http://eur-lex.europa.eu/LexUriServ/LexUriServ.do?uri=OJ:L:2009:140:0016:0062:en:PDF., accessed on 30 October 2012.

Formo, M.W., "Ester reactions of fatty materials", *J. Am. Oil Chem. Soc.*, **1954**, 31, 548.

Ganesan D., Rajendaran A., Thangavelu V., "An overview on the recent advances in the transesterification of vegetable oils for biodiesel production using chemicals and biocatalysts" *Rev. Environ. Sci. Biotechnol.*, **2009**, 8, 367.

Georgogianni K.G., Kontominas M.G., Pomonis P.J., Avlonitis D., Gergis V., "Alkaline conventional and in situ transesterification of cottonseed oil for the production of biodiesel", *Energy Fuels*, **2008a**, 22, 2110.

Georgogianni K.G., Kontominas M.G., Pomonis P.J., Avlonitis D., Gergis V., " Conventional and in situ transesterification of sunflower seed oil for the production of biodiesel", *Fuel Process. Technol.*, **2008b**, 89, 503.

Gole V.L., Gogate P.R., "Intensification of synthesis of biodiesel from nonedible oils using sonohchemical reactors", *Ind. Eng. Chem. Res.*, **2012**, 51, 11866.

Gutierrez R.J., "Use of Vegetable oil in Internal Combustion Engine", *1st South American Engineering Congress, Buenos Aires*, **1916**.

Hernando J., Leton P., Matia M.P., Novella J.L., "Alvarez-Builla J, et al. "Biodiesel and fame synthesis assisted by microwaves. Homogeneous batch and flow process", *Fuel*, **2007**, 86,1641.

Kansedo J., Lee K.T., Bhatia S. "Cerbera odollam (sea mango) oil as a promising non-edible feedstock for biodiesel production", *Fuel*, **2009**, 88(6), 1148.

Kaya C., Hamamci C., Baysal A., Akba O., Erdogan S., Saydut A., "Methyl ester of peanut (Arachis hypogea L.) seed oil as a potential feedstock for biodiesel production", *Renew. Energ.*, **2009**, 34, 1257.

Lang X., Dalai A.K., Bakhshi N.N., "Preparation and characterization of bio-diesels from various bio-oils" *Bioresour. Technol.,* **2001**, 80, 53.

Lotero E., Liu Y., Lopez D.E., Suwannakaran K., Bruce D.A, Goodwin Jr. J.G., "Synthesis of biodiesel via acid catalysis", *Ind. Eng. Chem. Res.*, **2005**, 44, 5353.

Lotero, E., Goodwin, J.G., Bruce, D.A., Suwannakarn, K., Liu,
Y. & Lopez, D.E. 2006, "The catalysis of biodiesel synthesis",
Catalysis, vol. 19, pp. 41-83.

Marchetti J. M., Errazu A. F., "Comparison of different heterogeneous catalysts and different alcohols for the esterification reaction of oleic acid", *Fuel*, *2008*, 87, 3477.

Meher L.C., Vidya Sagar D., Naik S.N., "Technical aspects of Biodiesel production by transesterification: a review", *Renew. Sustain. Energy Rev.*, **2006**, 10(3), 248.

Ma F., Hanna M.A., "Biodiesel production: a review[1]", *Bioresour. Technol.*, **1999**, 10, 1.

Nascimento L.A.S., Angélica R.S., da Costa C.E.F., Zamian J.R., da Rocha Filho G.N., "Comparative study between catalysts for esterification prepared from kaolins", *Applied Clay Science* **2011**,51, 267.

Nitske R.W., Wilson C.M., "Rudolf Diesel: Pioneer of the age of power", University of Oklahoma Press, Norman, OK, **1965**.

Okoronkwo M.U., Galadima A., Leke L., "Advances in Biodiesel synthesis: from past to present", *Elixir Appl. Chem*. **2012**, 43 6924.

Perego C., Ricci, M., "Diesel fuel from biomass", *Catal. Sci. Technol.*, 2012, 1, 1776.

Perego, C., Bosetti A., "Biomass to fuels: The role of zeolite and mesoporous materials*", Microporous. Mesoporous. Mater.*, **2011**, 144, 28.

Pirola C., Boffito D.C., Carvoli G., Di Fronzo A., Ragaini V., Bianchi C.L., "Soybean oil deacidification as a first step towards biodiesel production", in D. Krezhova (Ed.): Recent Trends for Enhancing the Diversity and Quality of Soybean Products, Intech, **2011**, pp. 321-44.

Pirola C., Bianchi C.L., Boffito D.C., Carvoli G., Ragaini V., “Vegetable oil deacidification by Amberlyst : study of catalyst lifetime and a suitable reactor configuration”, *Ind. Eng. Chem. Res.*, **2010**, 49, 4601.

Royon D., Daz M., Ellenrieder G., Locatelli S. “Enzymatic production of biodiesel from cotton seed oil using t-butanol as a solvent”. *Bioresour. Technol.*, **2007**, 98(3), 648.

Santori G., Di Nicola G., Moglie M., Polonara F., “A review analyzing the industrial biodiesel production practice starting from vegetable oil refining”. *Appl. Energy*, **2012**, 109.

Santos F.F.P., Malveira J.Q., Cruz M.G.A., Fernande F.A.N., "Production of biodiesel by ultrasound assisted esterification of Oreochromis niloticus oil", *Fuel*, **2010**, 89(2), 275.

Sahoo, P.K., Das, L.M., "Process optimization for biodiesel production from Jatropha, Karanja and Polanga oils", **2009**, *Fuel*, 88(9), 1588.

Sharma Y.C., Singh B., Korstad J. "Latest developments on application of heterogenous basic catalysts for an efficient and ecofriendly synthesis of biodiesel: A review", **2011**, *Fuel*, 90(4), 1309.

Shay E.G., “Diesel fuel from vegetable oils: Status and opportunities”, *Biomass. Bioenerg.*, **1993**, 4, 227.

Songstad D.D., Lakshmanan P., Chen J., Gibbons W., Hughes S., Nelson R., "Historical perspective of biofuels: learning from the past to rediscover the future", *In Vitro Cell. Dev. Biol.-Plant,* **2009**, 45, 189.

Siatis N.G., Kimbaris A.C., Pappas C.S., Tarantilis P.A., Polissiou M.G., “Improvement of biodiesel production based on the application of ultrasound: monitoring of the procedure by FTIR spectroscopy”, *J Am Oil Chem. Soc.*, **2006**, 83, 53.

Srivastava A., Prasad R., "Triglycerides-based diesel fuels", *Ren. Sust. Energy Rev.*, **2000**, 4(2), 111.

US Department of Energy, Energy, Efficinecy & Renewable Energy, **2010**. Available at http://www1.eere.energy.gov/vehiclesandfuels/facts/2011_fotw662.html, accessed on 25 November 2012.

van den Abeele, “L'Huile de palme, matiere premiere pour la preparation d'un carburant lourd utilisable dans les moteurs à combustion interne (Palm oil as raw material for the production of a heavy motor fuel)”, *Bull. Agr. Congo Belge*, **1942**, 33, 3.

Veljković V.B., Avramović J.M., Olivera, Stamenković O.S., “Biodiesel production by ultrasound-assisted transesterification: State of the art and the perspectives”, *Ren. Sust. Energy Rev.*, **2012**, 16, 1193

Verziu M., Florea M., Simon S., Simon V., Filip P., Parvulescu V., Hardacre C., “Transesterification of vegetable oils on basic large mesoporous alumina supported alkaline fluorides—evidences of the nature of the active site and catalytic performances”, J. Catal., **2009**, 263, 56.

Zatta L., da Costa Gardolinski J.E.F., Wypych F., “Raw halloysite as reusable heterogeneous catalyst for esterification of lauric acid. *Applied Clay Science*, **2011**, 51,165.

CHAPTER 2:
GENERAL EXPERIMENTAL PART

This chapter is aimed to provide both the description and the experimental procedures of routine methods and analyses that were most commonly used in the present work.

2.1 Catalysts

In this work two main types of catalyst were used to promote the free fatty acids (FFA) esterification.

- Sulphonic ion exchange resins;
- Sulphated inorganic catalytic systems.

2.1.1 Ion exchange resins

In this work three different acid ion exchange resins were used as catalysts in the FFA esterification:

- Amberlyst®15 (Dow Chemical) – A15
- Amberlyst®46 (Dow Chemical) – A46
- Purolite®D5081 (Purolite) – D5081

Ion exchange resins involve mostly the use of functionalized styrene and divinylbenzene copolymers with different surface properties and porosities. The functional group is generally of the sulphuric acid type. These resins are supplied as macroreticular spherical beads. Amberlysts® polymeric resins have been used for 40 years in a wide variety of reactions and purification processes (www.amberlyst.com).

These resins are obtained through so-polymerization of styrene and divinylbenzene in suspension and successive sulphonation as displayed in the scheme in Fig. 2.1.

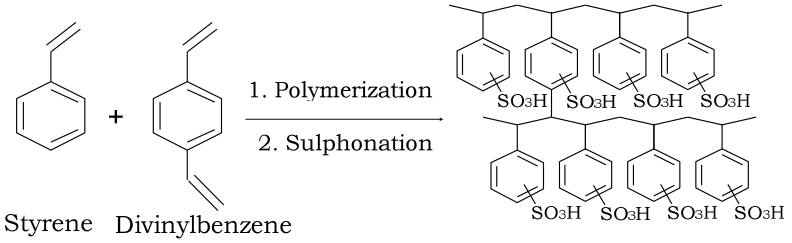

Fig. 2.1. Synthesis of sulphonic ion exchange resins.

The amount of crosslinking component determines the main physical characteristics (surface area and pore size distribution) of these catalysts (Öezbay et al., 2008). The higher the DVB amount added during the copolimeration, the higher the reticulation degree and, as a consequence, the smaller the pores. Indeed, the amount of DVB plays the major role in controlling the physical features of these catalysts. The strong $-SO_3H$ acid groups formed on the resin during the sulphonation step are the active sites responsible for the catalysis in the FFA esterification.

A scheme of the structure of the used resins is given in Fig. 2.2.

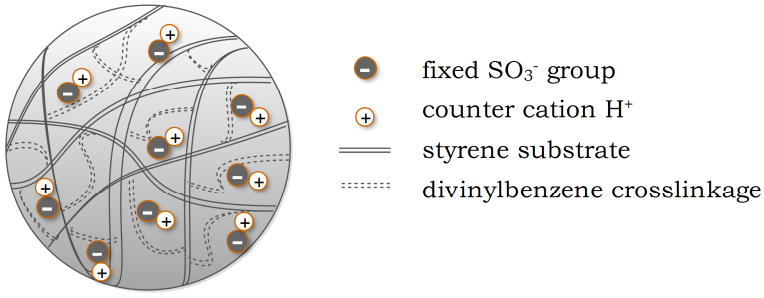

Fig. 2.2. Scheme of a sulphonic ion exchange's bead.

In Tab. 2.1 the main features of the three catalysts as available from the producers are shown.

Catalyst	A15	A46	D5081
Physical form	opaque beads		
Type	Macroreticular		
Matrix	Styrene-DVB		
Cross-linking degree	medium	medium	high
form	dry	wet	wet
Surface area ($m^2\ g^{-1}$)	53	75	514[a]
Ave. D_p (Å)	300	235	37[a]
Total V_p (ccg^{-1})	0.40	0.15	0.47
Declared Acidity (meq H^+g^{-1})	4.7	0.43	0.90-1.1
Moisture content ($\%_{wt}$)	1.6	26-36	55-59
Shipping weight ($g\ l^{-1}$)	610	600	1310[a]
Max. operating temp (°C)	120	120	130

[a] (Abidin et al., 2012)

Tab. 2.1. Features of the ion exchange resins used as catalysts.

The higher the amount of DVB used in the copolymerization, the greater the degree of crosslinking and therefore the smaller the size of the pores. This may results in a penalized diffusion inside the internal pores, however, in favour of a greater surface area.

A typical phenomenon related to the resins is their swelling capacity and shrinking (narrowing). The first occurs when the active sites of the resin interact with solvents of polar type, thereby retaining the solvent molecules within the pores by means of non-bonding interactions. It follows that the resin increases in size, properly "swells". In this way pores "widen" and become more accessible to the reagent species, thus exposing also some active sites that in absence of swelling would not be accessible. Following an ion exchange, the resin will undergo a further bulge, or will contract depending on the ionic form in which it is located. Normally

a resin undergoes shrinking when treated with a non-polar solvent. It is well known that low degrees of crosslinking originate a greater swelling capacity of the resin (Hokela et al., 2005; Klepakova et al., 2005), since in this case the structure is less rigid and more prone to swell.

The three resins adopted as catalysts are described in detail hereinafter.

2.1.1.1 Amberlyst®15

It is a strongly acidic ion exchange resin, developed specifically to be used in the heterogeneous catalysis of a wide variety of organic reactions. It is also used for the removal of cationic impurities in non-aqueous systems. Its macroreticular structure allows the easy access of the liquid or gaseous reagents to the active acid sites localized within the granule of catalyst, thus ensuring good performance even in organic non-swelling media.

The resin A15 is mainly used in applications such as alkylations, esterifications, etherifications and condensation reactions (www.amberlysts.com).

2.1.1.2 Amberlyst®46

Distinguishing feature of this resin is that it is sulphonated only superficially and therefore has few "swellable" domains. It is characterized by a rather high percentage of DVB, which results in permanent opening of the macropores, even in the absence of swelling.

Being sulphonated only superficially, this type of catalyst greatly reduces the possible formation of dialkyl ethers given by the auto-condensation of the molecules of alcohol inside the pores.

The presence of catalytically active sites on the catalyst surface, it is advantageous with regard to the studied reaction system. Free fatty acids molecules are in fact highly sterically hindered molecules that hardly penetrate inside the catalysts pores (Redaelli, 2006).

2.1.1.3 Purolite®D5081

Not much information is available on this resin, since it is not commercialized yet. The available information was provided by the manufacturer.

D5081 is sulphonated only on its outer surface and characterized by an high percentage of DVB, as well as A46. The higher crosslinking degree brings to a dense net of mesopores of narrow size and high specific surface area (see Tab. 2.1).

The main difference from A46 lays in the acid capacity, that is more than two-fold the one of the Amberlyst.

2.1.1 Sulphated inorganic systems

2.1.1.1 Properties

Sulphated inorganic oxides are solids that have recently received much attention due to their acid properties. These materials are active because of the presence of both Brønsted acid centres and Lewis acid sites (i.e. coordinatively unsaturated (cus) M^{n+} cations) at the surface, as evidenced by Morterra et al. (Morterra et al., 2001).

Sulphated zirconia is an acid solid that have recently received much attention in the field of catalysis. In sulphated zirconia the sulphate groups are supported on zirconium oxide (ZrO_2), commonly known as zirconia. ZrO_2 is a compound with very strong bonds given

by their partially ionic character. The difference of electronegativity between Zr and O is responsible for its special. Properties. Sulphonic groups linked to the surface of ZrO_2 are variously hydrated and form therefore Brønsted acid sites, which are responsible of the catalytic action together with the Lewis acid centres.

Like most of the oxides of the transition metals, zirconia is affected by the phenomenon of polymorphism: in fact exist in four different crystalline forms: cubic, tetragonal, monoclinic and orthorhombic (Levin and McMurdie, 1975). The sulphate groups are better supported by tetragonal zirconia. Sulphate groups stabilize tetragonal zirconia at room temperature, condition at which zirconia exists just in monoclinic form (known in nature as baddeleyite).

The sulphate groups are bound to the zirconia support generally by means of two hydroxyl groups, which may come from one or two atoms of Zr. The first case is referred to as a chelating bidentate sulphate, while the second case to as a sulphate bridge (Ward and Ko, 1995) (Figure 2.3).

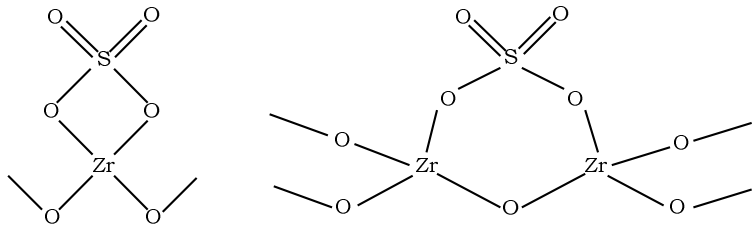

bidentate sulphate sulphate bridge

Fig. 2.3. Attachment modes of the sulphates to the zirconia support.

The proximity of the zirconium atom to the sulphate group, strongly electron-attractor, generates an acid site. The acid sites thus generated may be Brønsted or Lewis sites (Fig. 2.4). The Brønsted acidity is generated by strongly chemisorbed water

molecules (Ardizzone et al., 2009). The Lewis acidity is instead generated by the desorption of H_2O, which leaves an empty orbital on Zr (Mastikhin et al., 1995).

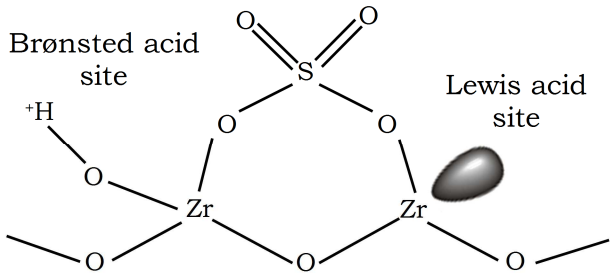

Fig. 2.4. Acid sites on the sulphated inorganic systems.

Sulphated zirconia has frequently been defined as one of the strongest solid superacids (Corma, 1995; Corma et al., 1994; Kurosaka et al., 1998; Furuta et al., 2004; Sejidov et al., 2005), with a value of the acid strength lower than -16 in the Hammett scale (Furuta et al., 2004). Its catalytic activity has often been attributed to this extreme intrinsic acidity, but there is much disagreement in the scientific community about how sulphated zirconia really fulfils its catalytic activity. Some claim that the superacidity is the only factor responsible for the catalytic properties (Corma, 1995; Corma et al., 1994; Kurosaka et al., 1998; Furuta et al., 2004). Some others are inclined to a combined action of Brønsted and Lewis sites, claiming also that the term "superacid" referred to sulphated zirconia is improper, since both types of sites are not particularly strong if considered singularly within their own category (Morterra et al., 1997; 2001; 2003; Ardizzone et al., 2009; Kustov et al., 2004).

Sulphated tin oxide (SO_4^{2-}/SnO_2) is another potential catalyst for esterification reaction due to its strong surface acidity that is

reported to be stronger than SO_4^{2-}/ZrO_2 (Matsuhashi et al., 1990; Lam et al., 2009). Nevertheless, study concerning the usage of SO_4^{2-}/SnO_2 catalyst in biodiesel production is still limited (Kiss et al., 2006; Lam et al., 2009).

Some recent studies have reported that the acidity of the sulphated systems may be increased by adding another metal oxide such as TiO_2 to ZrO_2 (Boffito et al., 2012b; Neppolian et al., 2007) or SnO_2 so to create charge imbalances responsible for the creation of additional acidity on the solid.

2.1.1.2 Synthesis methods

Sol-gel

There are several techniques to produce hydrous oxides, but in the field of catalysts those carried out in the liquid phase and in a particular way the sol-gel technique prevail (Richardson, 1989). Sol-gel technique allows to obtain powders characterized by better chemical homogeneity and higher purity compared to other techniques, with the possibility of working at room temperature and atmospheric pressure and to control the particle size and the morphological characteristics of the material (for example with the template synthesis). The obtained materials are characterized by high surface area and porosity. Disadvantages are the high preparation costs and long times (Llewellyn et al., 1997).

The word sol-gel indicates that a colloidal solution is initially prepared from the salts of the metal, and then, through a precipitation process, which is achieved by adjusting the pH, the same salt increases the viscosity of the medium, forming a gel that is referred as the precursor of the catalyst. Depending on whether the

solvent is water or an alcohol, the precursor takes the name of hydrogel or alcoholgel, respectively.

In Fig. 2.5 the steps of the sol-gel process are shown.

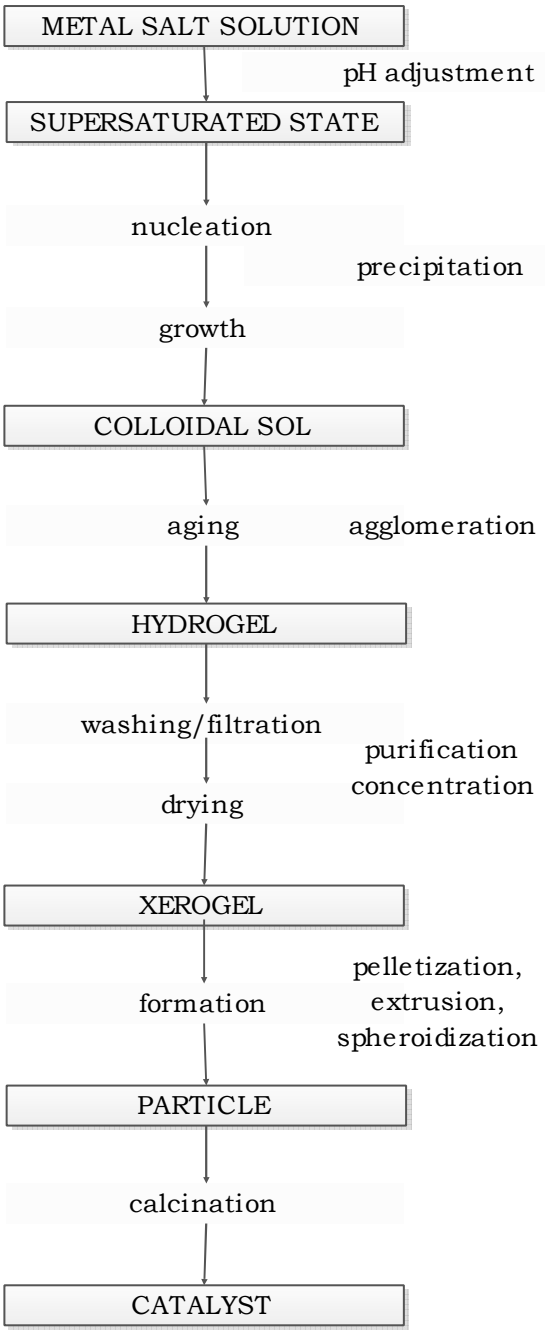

Fig. 2.5. Preparation steps for hydrous oxides.

After its formation, the gel is subjected to a drying treatment, whereby most of the solvent is lost, and becomes what is called "xerogel". The passage from hydrogel (or alcoholgel) to xerogel involves remarkable changes in the structure of the material. Evaporation of the solvent from the pores of the gel causes their collapse, especially of those of smaller dimensions (according to the Kelvin law).

After the drying step the material still possesses 25-30% of solvent. Depending on the final use one can proceed or not with the calcination step. Calcination step involves the heating of the sample at high temperatures (473-1073 K) in static atmosphere or under the flow of different

gases depending on the desired active phase. During this step several processes occur: loss of water and CO_2 chemically bound, changes in the distribution of pores sizes, generation of the active phase, surface conditioning, and stabilization of the mechanical properties.

The sol-gel synthesis is mostly used also for the synthesis of mixed oxides. In this case the co-precipitation of the metals salts occurs and high dispersion and interactions are attained (Richardson, 1989).

In this work zirconium tetra-n-propoxide was chosen as a metal salt to synthesize sulphated zirconia because of its high reactivity.
The hydrolysis of the salt was promoted in acid conditions by HNO_3, while ammonium sulphate was used as sulphating agent in most of the cases. These choices were dictated by the results previously attained in similar works, whereby samples obtained with HNO_3 and $(NH_4)_2SO_4$ exhibited higher activity in the esterification of benzoic acid than the samples obtained using NaOH or H_2SO_4 (Ardizzone et al., 2004; 2009). In Fig. 2.6 the mechanism of the hydrolysis of zirconium tetra-n-propoxide in acid conditions is displayed.
Initially the protonation of one of the four oxygen atoms occurs with consequent increase of its electronegativity. At this point also a base as weak as water is able to attack the atom of Zr, which is activated by the inductive effect of electronic acquisition (-I) of the adjacent oxygen atom. The successive stage involves the simultaneous water attack and the breaking of the Zr – O bond, with the expulsion of a molecule of n-propanol. The expulsion mechanism of the other protoxide groups is the same but it is facilitated by the mesomeric effect of electronic transfer (+M) introduced by the hydroxyl group (I).

During the synthesis, however, also two condensation reactions, which are responsible for the formation of a pseudo reticular structure and which transform the sol in gel, occur.

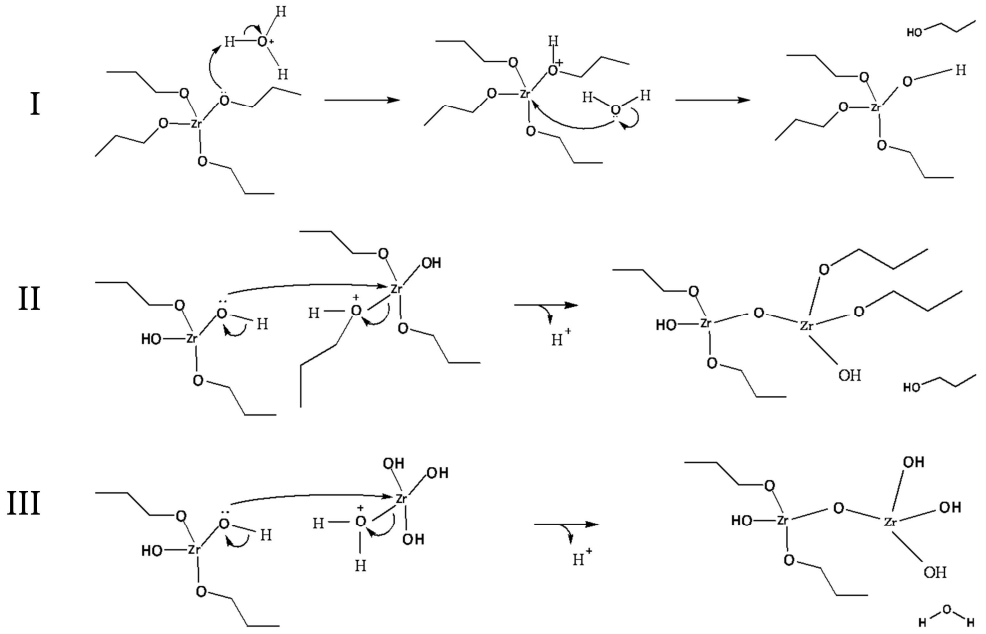

Fig. 2.6. Mechanism of the hydrolysis of zirconium tetra-n-propoxide under acid conditions.

In the first condensation reaction (II) the attack of the hydroxyl group bound to a Zr to the Zr of another molecule tales place along with the expulsion of a molecule of n-propanol.

In the second condensation reaction (III) the attack of the hydroxyl group bound to a Zr to the Zr of another molecule takes place along with the expulsion of a molecule of water.

At the beginning of the synthesis, the favoured reaction is the simple hydrolysis (I), but when most of the propoxide groups moves into solution, the condensation reactions (I and II) prevail.

Impregnation

Impregnation is also known as “incipient wetness” and is the simplest and most direct method of deposition. The objective is to fill the pores with a solution of metal salt of sufficient concentration to give the desired loading. The support, usually in particle form, is heated or evacuated to remove pores moisture. Then, the solution of the metal salt is added in an amount just sufficient to fill the pores and wet the particles outside. The solution amount has to be determined from pores volume measurement.

Drying is necessary to crystallize the salt in the pores and the surface. If not performed properly, this step can result in irregular and uneven concentration distributions. Only experiments can establish the best procedure, but some nonuniformity must always be expected.

The following step of calcination, if required, is very important in these circumstances since converts the salt to an oxide or metal and essentially “freezes” the distribution. Other calcination effects, such as solid state reactions also take place (Richardson, 1989).

2.2 Characterization of the catalysts

2.2.1 Acidity of the catalysts

The acidity of solid catalysts has proved to be a key factor in determining the catalytic activity in many organic reactions such as acylations (Yadav and Kamble, 2012), alkylations (Sohn and Seo, 2003, Dijs et al., 2003), isomerizations (Moreno and Poncelet, 2001; Ivanov et al., 1998), alcohols dehydrations (Dijs et al., 2003; Chaabene et al., 2004) and esterifications (Juan et al. 2007a;

20007b; 2008; Morterra et al., 1994; Boffito et al., 2012a; 2012b; 2012c).

The qualitative and quantitative determination of acid sites is therefore a key issue in relating the properties of a catalyst with its catalytic performance and to design an optimized catalytic system.

2.2.1.1 Determination of acid sites concentration

The quantification of the Brønsted acidity of the catalysts was carried out through ion exchange. About 0.2 g of catalyst are weighted and left in contact with 10 ml of a NaCl saturated solution for 30 hours. The H^+ concentration can be then evaluated by either pH-metry or acid-base titration with a 0.1 M NaOH aqueous solution. The number of H^+ milliequivalents per gram of catalyst was then calculated as follows as in similar works (López et al., 2007; Boffito et al., 2012a, 2012b):

$$meqH^+/g_{cat} = \frac{V \times C}{W} \qquad 2.1$$

where V is the volume in ml of the NaOH solution required for the titration, C is the molarity of the NaOH solution expressed in mmol ml^{-1} and W is the weight in grams of the catalyst's sample.

2.2.1.2 FTIR measurements

Theoretical notes

Infra-red (IR) spectroscopy of the adsorption / desorption of basic molecules such as ammonia, pyridine and its derivatives, is a method often used to characterize the surface acidity of solids as it

is considered able to determine the concentration and strength of superficial acid sites (Morterra et al., 1994).

The first studies (Mapes and Eischens, 1954) aimed at identifying the nature of the acid sites of some commercial samples of silica-alumina utilized ammonia as a probe molecule. Brønsted acid sites interact with the adsorbed NH_3 to form NH^{4+}, thus giving rise to two bands near 1450 and 3130 cm^{-1}, while the adsorbed NH_3 as such on the Lewis acid sites gives rise to two bands near 1630 and 3330 cm^{-1}. This study was followed by many others using NH_3 as a probe molecule to determine the nature of the acid sites of silica-alumina, alumina, and other oxides (Anderson, 1984). However, in many cases NH_3 is not the most appropriate base for the determination of acid sites, because it is a relatively strong base, and thus able to interact both with the weaker and stronger acid sites. An alternative was given by Parry in 1963 (Parry, 1963), who used pyridine as a probe molecule. Pyridine, being a weaker base than ammonia, was proved to be able to interact only with the stronger acid sites. The adsorption band near 1540 cm^{-1} is characteristic of pyridinium ion, while the spectral differences between the regions 1640-1580 cm^{-1} and 1500-1440 cm^{-1} make possible to distinguish the physically adsorbed pyridine from the one coordinated to the acid sites of Lewis. The adsorption of pyridine and its derivates is currently widely used to characterize the surface acidity of various oxides, both in the case of catalysts or supports, of zeolites and other solids with high surface area.

Depending on the type of sample to be analysed, other basic probes that can be used are: hydrocarbons (especially olefins and aromatics), CO, CO_2 and NO.

Initially the IR spectrometers were dispersive, i.e. they were equipped with a dispersive element, usually a monochromator,

which separated the radiation in the various wavelengths striking the sample at different times. With the advent of computers, Fourier transform (FTIR-Fourier Transform Infrared) were developed. Compared to the normal dispersive spectrometers, FTIR show a series of further advantages such as time saving (few seconds vs. several minutes), better signal / noise ratio, high precision of wavenumbers and constant resolution along the entire spectral range.

Experimental procedure

The FTIR analyses were carried out at the laboratories of Prof. G. Cerrato at Università di Torino (Dipartimento di Chimica IFM).

The spectrometer used was a Brucker IFS113v, connected to a vacuum glass line allowing a residual pressure $<10^{-5}$ Torr. The spectrometer is divided into two compartments: one containing the optical system and the detector, and the other containing the sample cell. The sample to be analysed is deposited over a silicon plate, which is then introduced into the cell. The cell is entirely of quartz, except for the window through which the IR beam passes. The window is in fact in KBr, which is transparent to IR and glued to the cell with an epoxy resin.

The vacuum was achieved through the combination of a rotative pump (which allows obtaining a pressure equal to 10^{-2} Torr) and a turbomolecular pump (which allows reaching the vacuum required for the analysis).

The probe molecule mostly used for the qualitative determination of acid sites of the catalysts described in this work is 2,6-dimethylpyridine (2,6-DMP), known as lutidine.

The adsorption of 2,6-DMP allows to obtain information about the total acidity (Lewis and Brønsted) of the systems with which it comes

into contact (Ardizzone et al., 2009). 2,6-DMP behaves like a Lewis base, being able to donate one pair of electrons present on N atom of the aromatic ring. It gives therefore interactions with species capable of accepting electrons (it can donate a pair of electrons to the metal species coordinatively unsaturated, or it can interact by means of these solitary electrons to give hydrogen bonds with surface hydroxyl species). Depending on the species with which it interacts absorption occurs at different frequencies: the higher the absorption frequency, the greater the strength of the interaction.

2,6-DMP can also behave as a Brønsted base; in fact, interacting with the sample, can give rise to lutidinium species (by binding an H^+ ion to the nitrogen atom), which presents the characteristic bands in the IR spectrum between 1630 and 1680 cm^{-1}. The formation of this species requires that the compound with which the 2,6-DMP is in contact is characterized by Brønsted acidity. In general, the interaction of Brønsted type is quite strong.

The absorption of this molecule is generally conducted at room temperature, interposing a vial containing 2,6-DMP between the sample cell and the vacuum line by means of special connections and joints. Furthermore, a liquid nitrogen trap was interposed between the compartment containing the sample cell and the vial of 2,6-DMP in order to prevent any impurities present in the 2,6-DMP to reach the sample. The following steps were then followed (Morterra et al., 2001):

- A large excess of the 2,6-DMP (~ 5 Torr) was made come in contact with the surface of the sample for a short period (2-5 minutes) at the temperature of the IR beam;
- Degassing at increasing times (1, 2, 5 and 15 minutes) was performed to eliminate the excess of 2,6-DMP;
- Spectra were recorded for the different degassing times.

2.2.3 Determination of the specific surface area

Adsorption methods may be used to provide information about the total surface area of a catalyst, the surface area of the phase carrying the active sites, or possibly even the type and number of active sites. The interaction between the adsorbate and the adsorbent may be chemical (chemisorption) or physical (physisorption). Physical adsorption is used in the BET method to determine the total surface area of a solid. "BET" derives from the names of the inventors of the so-called BET equation (Brunauer, Emmett and Teller, 1938) that allows to determine the parameter V_m (monostrate volume), i.e. the total volume of the first layer of the molecules adsorbed on the solid. V_m is then used to calculate the specific surface area of the solid sample, usually expressed in $m^2\,g^{-1}$.

BET technique uses the adsorption of an inert gas (usually nitrogen) varying the relative pressure (ratio between the partial pressure of nitrogen and its vapour pressure in the liquid state).

The concept of the BET theory is an extension of the Langmuir theory, which concerns the adsorption of a monolayer, to multilayer adsorption. BET theory bases on the following hypotheses: (a) gas molecules physically adsorb on a solid forming an infinite number of layers; (b) there is no interaction between each adsorption layer and (c) the Langmuir theory can be applied to each layer. The resulting BET equation is therefore the following:

$$\frac{V}{V_m} = \frac{c\frac{p}{p^0}}{\left[\left(1-\frac{p}{p^0}\right)\right]\left[1+(c-1)\frac{p}{p^0}\right]} \qquad 2.1$$

where V is the volume of adsorbed gas at pressure p, $p°$ is the gas saturation pressure, at temperature T, $p/p°$ is relative pressure and c the BET constant, expressed as in the following equation:

$$c = (q_1 - q_L)/RT \qquad 2.2$$

where q_1 is the heat of adsorption of the first layer and q_L the heat of adsorption from the second to infinite layers.

For the calculation of V_m, equation 2.1 needs to be linearized. The linear relationship of this equation is maintained only in the range of $0.05 < p / p^0 < 0.35$:

$$\frac{\frac{p}{p^0}}{V\left[1-\left(\frac{p}{p^0}\right)\right]} = \frac{\pi r^2}{CV_m} + \frac{(c-1)\frac{p}{p^0}}{cV_m} \qquad 2.3$$

Equation 2.3 is an adsorption isotherm and can be plotted as a straight line with $1 / V[(p° /p) - 1]$ on the y-axis and p / p^0 on the x-axis. according to experimental results. The surface area is then determined as follows:

$$SA = \frac{V_m N_{AV} A_{mol}}{V_{mol}} \qquad 2.4$$

where N_{AV} is the number of Avogadro, A_{mol} is the area of the cross section of the adsorbed molecule (for N_2 = 16.2 Å^2) and V_{mol} is the molar volume of gas (22414 ml/mol).

The specific surface area (SSA) is then obtained dividing the SA for the weight of the sample.

2.2.4 Determination of pores dimensions

The method usually adopted to calculate the dimensions of the pores is the BJH method (Barrett, Joyner and Halenda, 1951), so called from the initials of the scientists who proposed it. The method is based on the assumption that the pores of the solid material under analysis are all cylindrical and there is no communication among them.

The dimensions of the pores are calculated using the Kelvin equation:

$$ln\frac{p}{p^0} = -\frac{2\gamma V_{mol}}{r_K RT} \qquad 2.5$$

where p is the actual vapour pressure, p^0 the saturated vapour pressure, γ is the surface tension, V_{mol} the molar volume, R and T are the universal gas constant and temperature, respectively. r_k is the "Kelvin radius" and corresponds to the radius of the meniscus of the condensed adsorbate inside the pore. The pore radius r_p can be then calculated by summing the Kelvin radius and the film thickness t of the layer of adsorbate inside the pore:

$$r_p = r_k + t \qquad 2.6$$

The method also allows calculating the total pores volume and the distributions of pores volume and area.

2.2.5 Determination of the swelling capacity of a resin

The swelling capacity of the resins can be evaluated in different swelling media. In this work the swelling media of interest were: water, methanol and oils containing FFA. For this purpose, about 2 g of dry catalyst were placed into a graduated tube to measure the dry volume and then transferred into a flask and left in contact under agitation with 20 ml of the swelling medium for 6 hours, i.e. the usual duration of the FFA esterification tests performed in this work. The catalyst was then filtered, weighted and transferred into the measured tube to calculate the gain by weight and volume, respectively.

Percentage gains by weight and volume were calculated according to the following equations, as in other works (Öezbay et al., 2008):

$$swelling\ (\%_{wt}) = \frac{swollen\ weight\ (g)}{dry\ weight\ (g)} \quad 2.7$$

$$swelling\ (\%_{vol}) = \frac{swollen\ volume\ (vol)}{dry\ volume\ (vol)} \quad 2.8$$

2.3 Characterization of the oils

2.3.1 Determination of the acidity of the oils

The acidity of all the oils was determined through titration analysis with KOH 0.05 M or 0.1 M in ethanol.

The neutralization reaction of the FFA is a saponification reaction, schematized as follows:

$$CH_3(CH_2)_7CH{=}CH(CH_2)_7COOH + KOH \rightarrow CH_3(CH_2)_7CH{=}CH(CH_2)_7COOK + H_2O$$

Since oil and ethanol are not miscible, a mixture of diethylether: ethanol 9:1 by volume was used as co-solvent for the titration. Phenolphthalein 2% in ethanol was used as indicator. The percentage of FFA content per weight was calculated as follows, as usual in similar works (Boffito et al., 2012a; 2012b; Bianchi et al., 2010; Pirola et al., 2010; Russbueldt et al., 2009; Pasias et al., 2006):

$$FFA = \frac{V \times \overline{MW} \times C}{W} \times 100 \qquad 2.9$$

where V is the volume of KOH solution employed for the titration (mL), $\overline{MW}$ is the average molecular weight of the free fatty acids contained in the oil, obtained from the analysis of the acidic composition by GC. If the acidic composition is missing, the MW of the acid that is present in higher concentration may be used. C is the concentration of KOH (mmol mL^{-1}) and W is the weight of the analysed sample (mg).

All the reagents were Fluka products and were used without further purification.

2.3.2 Determination of the moisture content

The Karl Fischer titration method is one of the most used methods in the industrial field for the determination of water in various types of solids and organic liquids, as it is capable of detecting traces of water in a sample down to a few parts per million.

The method was developed by the chemist Karl Fischer and consists of a titration whose end point is usually automatically detected amperometrically.

The method is based on an oxidation / reduction that is relatively specific for the water (Skoog et al., 1998).

The used titrant is the Karl Fischer reagent, which contains I_2, SO_2, pyridine and anhydrous methanol or another suitable solvent.

The classical reaction occurs in two stages. In the first stage, I_2 and SO_2 react in the presence of pyridine and water to form the pyridine sulphite and iodide.

(I) $C_5H_5N{\cdot}I_2 + C_5H_5N{\cdot}SO_2 + C_5H_5 + H_2O \rightarrow 2\ C_5H_5N{\cdot}HI + C_5H_5N{\cdot}SO_3$

(II) $C_5H_5N^{+}{\cdot}SO_3^{-} + CH_3OH \rightarrow C_5H_5N(H)SO_4CH_3$

where I_2, SO_2 and SO_3 are complexed by pyridine. Sulphite in pyridine is also capable of consuming water:

(III) $C_5H_5N^{+}{\cdot}SO_3^{-} + H_2O \rightarrow C_5H_5NH + SO_4H^{-}$

This latter reaction can be avoided using a large excess of methanol. Reactions I and II indicate that the stoichiometry of the Karl Fischer titration, which involves the consumption of one mole of iodine, one mole of sulphur dioxide and three moles of pyridine for each mole of water. When all the water has been consumed by these two reactions, an excess of free iodine occurs. This has the effect of depolarizing the electrodes, i.e. to allow the passage of current, which is the index of the end of titration and activate therefore the automatism blocking the burette which adds the reagent.

The used titrator was a dead-stop automatic titrator (Amel, model 231).

The solvent (methanol) has to be "cleared" before the analysis.

To obtain the amount of water contained in an organic sample, it is necessary to calibrate the reagent, i.e. to know how many millilitres are required to titrate a given quantity of water expressed in grams.

The calibration may be performed by the addition of small amounts of water to 25-30 ml of methanol previously neutralized. It is however preferable not to use pure water, but solutions or substances of known composition containing water. In this work sodium tartrate dihydrate ($C_4H_4Na_2O_6 \cdot 2H_2O$) has been used to determine the title of the Karl Fischer reagent. Knowing that for each mole of tartrate two moles of water are released into solution, it is possible to construct the calibration curve for the used Karl Fischer reagent.

In Fig. 2.7 the calibration curve of the Karl Fischer is reported.

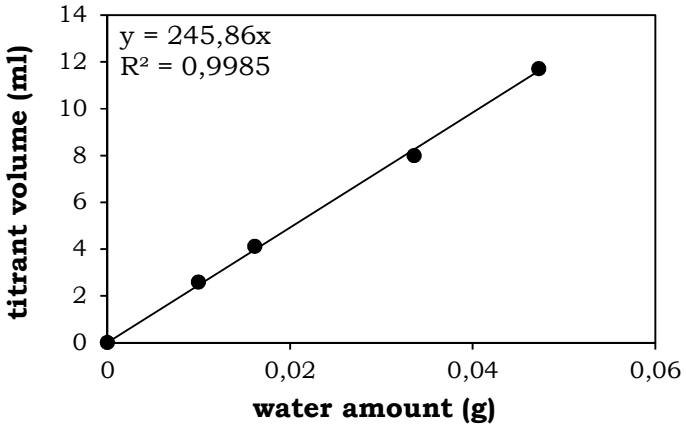

Fig. 2.7. Calibration curve of the Karl Fischer reagent.

To determine the % of water contained in the samples, the following equation (2.10) was used.

$$\%\, H_2O = \frac{V \times t}{W} \times 100 \qquad 2.10$$

where V is the volume in ml of Karl Fischer titrant given at the end point, *t* indicates the grams of water titrated by 1 ml of reagent, obtained from the calibration curve and W is the weight in grams of the sample.

2.3.3 Determination of fatty acids composition

Fatty acids composition was determined following the normative UNI EN 14103 for the determination of esters and linoleic acid methyl ester content. The analysis was performed on the oils either after the esterification reaction or after the transesterification reaction to determine the overall biodiesel (FAME) content.

About 250 mg of the sample were dissolved in 2.50 mL of a standard solution 0.1 M of methylheptadecanoate or methylnonadecanoate. Methylheptadecanoate (>99% and methylnonadecanoate (>99%), were used as internal standard and heptane as a solvent. The capillary GC column OmegaWax (Sigma Aldrich) was used in a splitless GC Fision Carlo Erba (currently Thermo) model 8000 series for the analyses carried out at the University of Milan, while a PerkinElmer Instruments AutoSystem XLGas Chromatograph (with split) was used for the experiments concerning BD synthesis and carried out at the University of Savoie. Both the GC were equipped with flame ionization detector (FID) fed with hydrogen (50 kPa) and air (100 kPa) and the temperature of both the injector and detector was kept at 250°C. In both the cases an isotherm at 210°C was used and He was used as a carrier at 70 kPa. The biodiesel yield, i.e. the FAME content, expressed as mass %, was calculated using the following equation (2.11):

$$C_{FAME}=\frac{(\sum A)-A_{std}}{A_{std}}\times\frac{C_{std}\times V_{std}}{W}\times 100 \qquad 2.11$$

where ΣA is the total peak area of the methyl esters, A_{std} is the peak area corresponding to methylheptadecanoate or methylnonadecanoate; C_{std} and V_{std} are the concentration (mg ml^{-3}) and the volume (ml), respectively, of methylheptadecanoate or methylnonadecanoate solution being used; W is the mass of the sample in mg.

The content of each methyl ester, expressed as mass %, was determined using the following equation (2.12):

$$C_i=\frac{A_i}{A_{std}}\times\frac{W_{std}}{W_i}\times 100 \qquad 2.12$$

where A_i and A_{std} are the peaks areas corresponding to each ester and the used standard, respectively, and W_i and W_{std} are the mass (mg) of the sample and the used standard, respectively.

Average molecular weights ($\overline{MW}$) were calculated from the acidic composition using the following equation (2.13):

$$\overline{MW}=\sum MW_i\times A_i \qquad 2.13$$

where MW_i is the molecular weight of the methyl ester and A_i is its weight percentage of each methyl ester as resulted from the GC analysis.

All the reagents were Fluka products and were used without further purification.

In Fig. 2.7. a typical gaschromatogram of a transesterified oil showing the peaks corresponding to the FAME is displayed for the case of Brassica juncea.

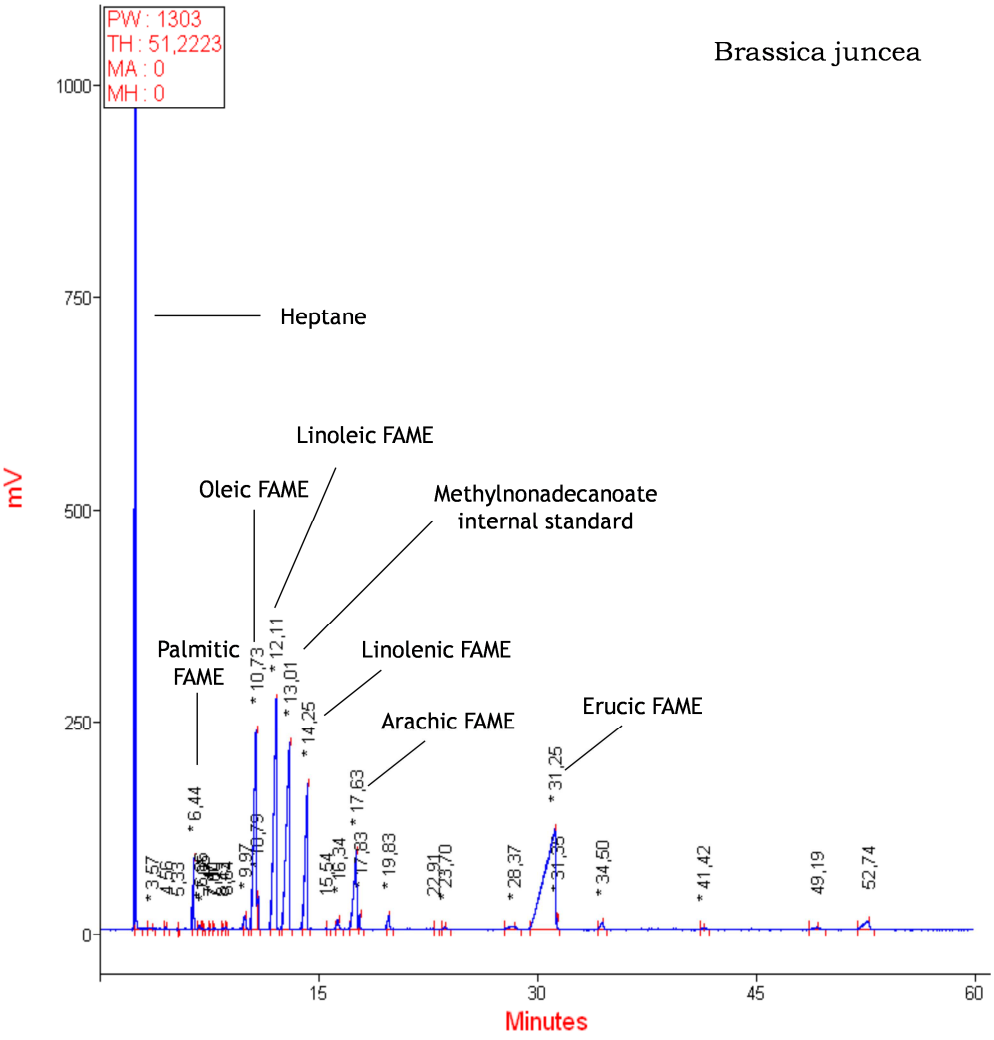

Fig. 2.8. Gaschromatogram of a transesterified Brassica juncea oilseed.

2.3.4 Determination of iodine value

The iodine value (IV), corresponding to the mass of I_2 contained in 100 g of sample and indicating the number of unsaturations in the oil, was obtained by the Hannus method (EN 14111:2003).

In this reaction, iodine monochloride reacts with the unsaturated bonds to produce a di-halogenated single bond, of which one carbon has bound an atom of iodine:

$CH_3(CH_2)_7CH=CH(CH_2)_7COOH + ICl \rightarrow CH_3(CH_2)_7IH\text{-}CClH(CH_2)_7COOK$

After the reaction is complete, the amount of iodine that has reacted is determined by adding a solution of potassium iodide to the reaction product. This causes the remaining unreacted ICl to form molecular iodine:

$ICl + KI \rightarrow KCl + I_2$

The I_2 is then titrated with a standard solution of sodium thiosulfate:

$I_2 + 2Na_2S_2O_3 \rightarrow 2\ NaI + Na_2S_2O_4$

Concurrently, a blank test, i.e., a test containing the solvent and the reagents in identical amounts with the exception of the sample was carried out.

In this work the Wijs reagent (ICl in acetic acid) was used as a source of ICl and a mixture of glacial acetic acid (>99%) and cyclohexane (>99%) in 1:1 volume ratio was used as a solvent. A KI aqueous solution 0.1 M was used to create the iodine excess. $Na_2S_2O_3$ 0.1 M and starch solution 1% in H_2O were used as a titrating agent and indicator, respectively. Amylose forms a blue to black solution with iodine and is colourless when iodine is titrated.

All the reagents were Fluka products and where used without further purification.

Two 250 ml- flasks were used for the analyses, one for the sample and one for the blank, respectively. About 0.3 g of the oil were weighted for each analysis, dissolving it in 20 ml of solvent. 25 ml of Wijs reagent were added and made react for 2 hours in the dark. Afterwards, 20 ml of the KI solution and 150 ml of deionized water were added. The mixture was then titrated with a 0.1 M $Na_2S_2O_3$ standard solution. The IV was then calculated with the following equation (2.14):

$$IV\ (gI_2/g\ oil)=\frac{12.69 \times C \times (V_1-V_2)}{W} \qquad 2.14$$

where 12.69 is the equivalent weight of iodine (PM/2), C is the concentration of the solution, V_1 and V_2 are the volume of the solution required by the titration of the blank and the sample, respectively and W is the weight of the oil sample.

A precaution that should be observed is to add the starch indicator solution only near the end point (the end point is near when fading of the yellowish iodine colour occurs) because at high iodine concentration starch is decomposed to products whose indicator properties are not entirely reversible.

The IV can be also calculated theoretically from the acidic composition of the oil, using the following equation (2.15) (Azam et al., 2005):

$$IV\ (gI_2/g\ oil) = \sum (254 \times D \times A_i)\ MW_i \qquad 2.15$$

where D is the number of double bonds, A_i the weight % and MW_i the molecular weight of each fatty acid contained in the oil.

2.3.5 Determination of saponification number

Saponification value (or "saponification number", also referred to as "sap" in short) represents the number of milligrams of potassium hydroxide or sodium hydroxide required to saponify 1g of fat under the conditions specified. It is a measure of the average molecular weight (or chain length) of all the fatty acids present.

The long chain fatty acids found in fats have low saponification value because they have a relatively fewer number of carboxylic functional groups per unit mass of the fat as compared to short chain fatty acids.

The calculated molar mass is not applicable to fats and oils containing high amounts of unsaponifiable material, free fatty acids (>0.1%), or mono- and diacylglycerols (>0.1%).

Saponification number measurement is based on a back-titration: the sample is treated with a known amount of solution of potassium hydroxide in ethanol in excess and heated to reflux for at least 1 hour. At the end of the hour, after cooling, the excess of potassium hydroxide, which has not reacted, is quantified by titration with a solution of hydrochloric acid in the presence of phenolphthalein as indicator.

In this work 25 ml of KOH solution 0.5 M were added to 2 g of the sample. Concurrently, a blank test, i.e., a test containing only the KOH solution was carried out. Both the mixtures were kept in reflux for 1 hour and titrated with HCl aqueous solution 0.5 M. The saponification value was then determined as follows (2.16):

$$SV\ (mg\ KOH\ /\ 100g\ oil) = \frac{56.1 \times C \times (V_1 - V_2)}{W} \qquad 2.16$$

where *56.1* is the molecular weight of KOH (mg $mmol^{-1}$), *C* is the concentration of the KOH solution in ethanol used for the titration, V_1 and V_2 are volume of the KOH solution required for the titration of the blank and the oil sample, respectively, and *W* is the weight of the oil sample.

The SN can be also calculated theoretically from the acidic composition of the oil, using the following equation (2.17) (Azam et al., 2005):

$$SN=\sum(560 \times A_i)/MW_i \qquad 2.17$$

where A_i and MW_i are the weight % and the molecular weight of each fatty acid contained in the oil, respectively.

2.3.6 Determination of peroxide number

The peroxide number provides a measure of the extent to which oil has undergone primary oxidation (Chakrabarty, 2003) and is therefore an index of the conservation conditions of oil.

The peroxide number (PN) was determined following the AOC standard method that is an iodimetric method (Lea, 1946).

The peroxide value is determined by measuring the amount of iodine which is formed by the reaction of peroxides (formed in fat or oil) with iodide ion:

$$2\ I^- + H_2O + ROOH \rightarrow ROH + 2OH^- + I_2$$

Note that the base produced in this reaction is taken up by the excess of acetic acid present. The iodine liberated is titrated with sodium thiosulphate.

$2Na_2S_2O_3 + I_2 \rightarrow Na_2S_4O_6 + 2NaI$

The acidic conditions (excess acetic acid) prevents formation of hypoiodite (analogous to hypochlorite), which would interfere with the reaction.

The indicator used in this reaction is a starch solution where amylose forms a blue to black solution with iodine and is colourless where iodine is titrated.

A precaution that should be observed is to add the starch indicator solution only near the end point (the end point is near when fading of the yellowish iodine colour occurs) because at high iodine concentration starch is decomposed to products whose indicator properties are not entirely reversible.

In this work about 1 g of oil sample was weighted and 10 ml of chloroform were added. After the dissolution of the sample, 15 ml of acetic acid and 1 ml of KI saturated solutions were added and the solution was left stand in the dark for 5-10 minutes. Afterwards 75 ml of deionized water were added and the mixture titrated with $Na_2S_2O_3$ 0.01 M standard solution. The PN was then calculated as follows (2.16):

$$PV\ (meq O_2/kg\ oil) = \frac{V \times C}{W} \qquad 2.18$$

where V is the volume of the solution required for the titration and C is its concentration, W is the weight of the oil sample.

2.3.7 Determination of cetane number

Cetane number (CN) is a significant expression of diesel fuel quality among a number of other measurements that determine overall diesel fuel quality. CN is a measure of a fuel's ignition delay, the time period between the start of injection and start of combustion of the fuel. Fuels with higher CN, which have shorter ignition delays, provide more time for the fuel combustion process to be completed. Hence, higher speed diesels operate more effectively with higher CN fuels. This is one of the important parameters which are considered during the selection of oil to be used as feedstock for biodiesel. The different countries or organizations have specified different minimal values. Biodiesel standards set by ASTM 6751-and European Standards Organization (EN14214:2003) are 47 and 51, respectively (Winayanuwattikun et al., 2008).

CN is usually determined using Cooperative Fuel Research (CFR) engines, with which it is possible to measure the time delay between the start of fuel injection and the start of significant combustion through auto-ignition of a pre-measured amount of diesel in a constant volume chamber.

However it is possible to calculate CN theoretically using the following equation (2.17) (Krisnangkura, 1986) as also carried out in other works (Winayanuwattikun et al., 2008):

$$CN=46.3+\frac{5458}{SN}-0.225\times IV \qquad 2.19$$

where *SN* and *IV* are the saponification number and iodine value of the oil, respectively.

2.4 Free fatty acids esterification

2.4.1 Reactors

2.4.1.1 Batch reactors

In the present work, only batch reactors were used for the study of the FFA esterification reaction.

A batch reactor is a "closed reactor" that, once charged, receives no further inputs of mass or energy and permits no outputs of waste materials. Batch reactors usually work according to charge-reaction and discharge cycles. Batch reactors may be stirred or not stirred but in any case, conditions in the reactor are constantly changing. For this reason batch reactors are also defined as discontinuous reactors.

Batch reactors with different configurations were used in this work. In Tab. 2.2 the conditions adopted for each reactor are listed and a description of the used reactors follows.

Rector	oil (+ FFA) (g)	MeOH (g)	catalyst amount	Temp. (K)
Vial	21	3.4	$5\%_{wt}/g_{FFA}$ sulphated inorganic catalysts	336
Slurry	100	16	- 10 g ion exchange resins - $5\%_{wt}/g_{F\ FA}$ sulphated inorganic catalysts	336
Slurry with MeOH recycle	350	56	$5\%_{wt}/g_{FFA}$ sulphated inorganic catalysts	336 363
Carberry	300	48	10 g (5 g in each basket)	

Tab 2.2. Reaction conditions for the adopted reactors.

Slurry reactors

Slurry reactors are rectors in which the catalyst is suspended in the reaction medium through agitation. Slurry reactors are characterized by efficient mass transfer of the reagents towards the catalyst and inside its pores. However, the major drawback of slurry reactors lies in catalyst mechanical stress that can lead to its fragmentation during the reaction and its consequent loss during the discharge operations. This may pose problems to the re-usability of heterogeneous catalysts (Pirola et al., 2011).

Different kinds of slurry reactors were used in this work for the FFA esterification:

- vials;
- classical slurry reactor;
- slurry reactor with methanol recycle.

25 ml vials were adopted for preliminary tests on all the homemade catalysts, to assess the extent of their catalytic activity.

In most of the cases, a classical slurry reactor, as the one schematized in Fig. 2.9, was adopted.

The used slurry-type reactor consists of a 250 mL three-neck glass flask, equipped with a thermometer and a coil condenser. The third neck was reserved for sampling. The temperature of 336±1 K was reached by means of a thermostat. Stirring rate was kept constant at 100 rpm with a mechanical stirrer.

A variation in the use of the classical slurry reactor was made by using a slurry reactor with methanol recycle, as schematized in Fig. 2.10.

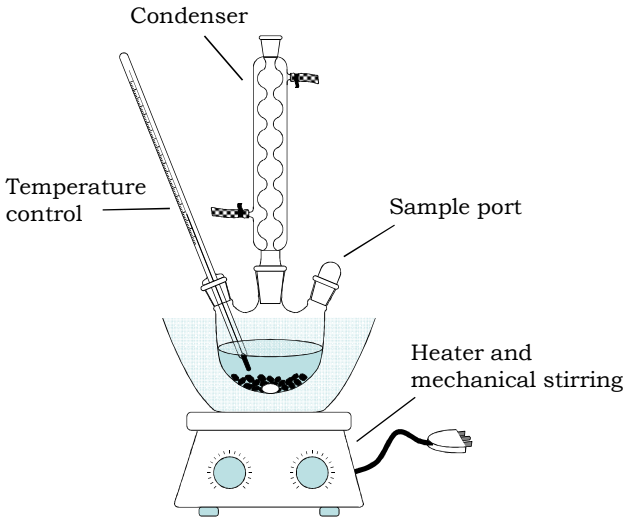

Fig 2.9. Classical slurry reactor.

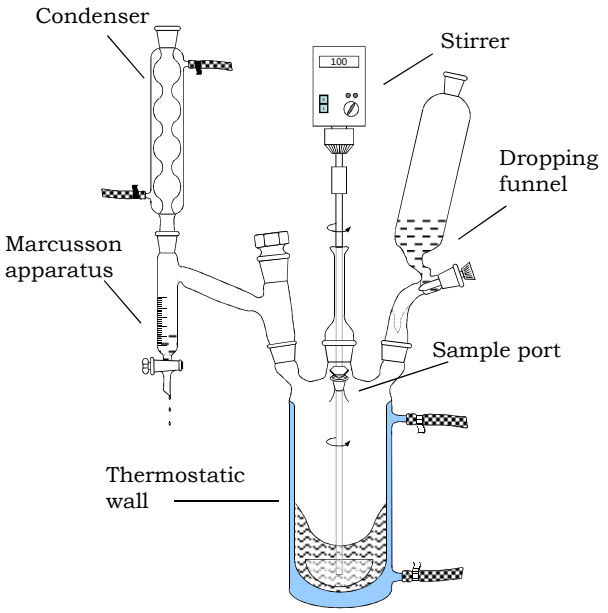

Fig 2.10. Slurry reactor with methanol recycle.

The slurry reactor with methanol recycle was used to test the catalytic activity of zirconium sulphate. It consists of a jacketed

reaction vessel of 1 litre of capacity and equipped with 5 necks to host the mechanical stirrer, the Marcusson apparatus, the dropping funnel and the sample port

This kind of reactor is useful to subtract water from the FFA esterification reaction equilibrium, so accelerating the achievement of the maximum conversion (Boffito et al., 2012a). This reactor can in fact be operated at temperatures higher than the incipient boiling temperature of methanol (337.8 K), which is evaporated from the reaction mixture together with water and condensed in the Marcusson apparatus. Fresh methanol has therefore to be added during the reaction through the dropping funnel.

Carberry reactor (catalyst confined)

Carberry-type reactor or "spinning baskets reactor" is a kind of batch reactor who was designed by Carberry in 1964 with the aim of preventing catalyst fragmentation by confining it in two perforated baskets. A scheme of the Carberry reactor is represented in Fig. 2.11.

As already described in a previous work (Ragaini et al., 2006), the Carberry type reactor consists of a glass container provided with a mechanical stirrer (kept at 100 rpm), a thermometer and a coil condenser. The reactor is provided with two stainless steel perforated baskets (h = 0.067 m, diameter = 0.032 m) where to lodge the catalyst and attached to the stirrer arm. Catalyst is introduced inside these baskets and confined into one portion of the reactor. Temperature was reached and maintained at 336±1 K by pre-heated diathermic oil flowing through the outer jacket surrounding the reactor.

The amount of the catalyst to introduce inside the baskets of the Carberry reactor had to be limited to 10 g to ensure a good

fluidization of the catalysts by the reagents. Higher amounts of catalyst would prevent the reagents to enter in an effective way inside the baskets (Redaelli, 2006). Oil had to be 300 g as minimum, so to ensure the complete immersion of the baskets inside the reaction medium. 300 g of oil were therefore used for all the tests conducted in the Carberry reactor.

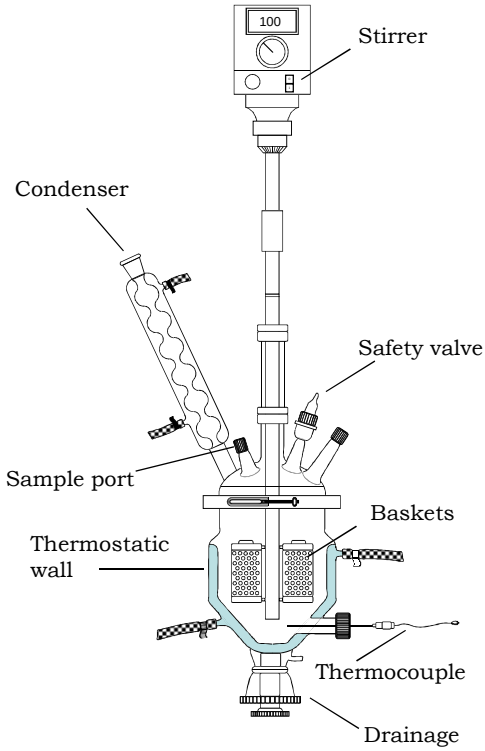

Fig 2.11. Carberry-type reactor.

Despite the use of Carberry reactor is reported to limit catalyst's fragmentation, its use may be associated with bad catalyst fluidization and scarce contact with the reagents (Boffito et al., 2012c).

2.4.1.2 Continuous reactors

In the present work continuous reactors were not used for the study of the FFA esterification reaction. However, the batch esterification process is reported to be labour intensive and not well adapted to automation. By comparison a continuous-flow process has advantages including the adjustability of the production costs and time for producing small amounts of biodiesel, the ability to produce a larger quantity per unit of labour and the capacity for making equipment-design improvements for the optimization of biodiesel quality (Behzadi et al., 2009). Accordingly, the use of a continuous-flow esterification process can save time and money, thereby increasing productivity and profit and contributing to the likelihood that biodiesel eventually becomes a viable energy source (Chen et al., 2010).

The use of a continuous packed bed reactor would prevent the previously mentioned problems connected with the mechanical stress of the catalyst.

In a recent work by Pirola (Pirola et al., 2010) and carried out in this research group a semi-continuous/continuous reactor configuration was studied for the FFA esterification reaction.

As highlighted in the work by Pirola, it is essential to feed the reactor with an oil/methanol emulsion that is stable for the whole length of the reactor, i.e. for a time at least equal to its residence time τ in the reactor. A possible solution may be represented by the use of an emulsificator between the feeding chamber and the packed bed reactor, as represented in 2.12.

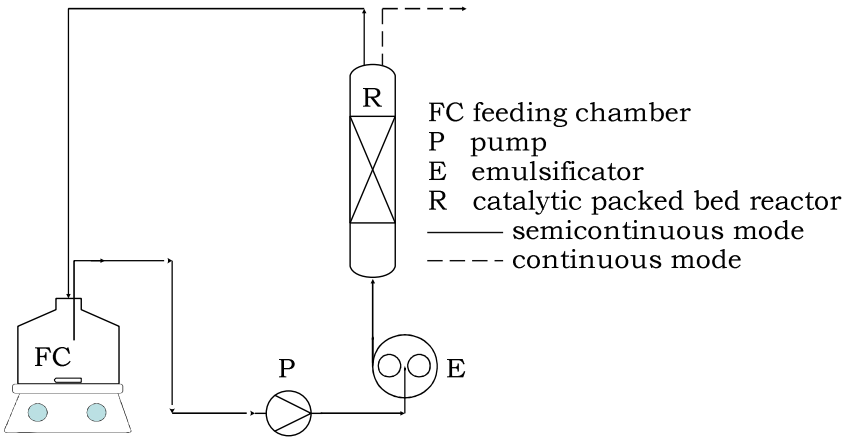

Fig 2.12. Continuous or semi-continuous experimental setup.

2.4.2 Reaction conditions

Choice of methanol and methanol amount

Different alcohols could be used for the FFA esterification (Rinaldi, 2007). Nevertheless, the most commonly preferred one is methanol because of its low price and physical and chemical advantages (polarity and the shortest chain). Methanol was found to be the most efficient alcohol to be used. Moreover, alcohols different from methanol requires higher temperatures to reach the same conversion given by methanol at the same reaction time (Rinaldi, 2007). When performing a bibliographic, it is seen that the number of investigations that were conducted with an alcohol apart from methanol are limited.

The reaction conditions adopted in the FFA esterification reaction for the different reactors utilized in this work are listed in Tab. 2.2.

A methanol: oil weight ratio of 16:100, corresponding to a molar ratio of ~ 4.5 was adopted for all the FFA esterification tests.

The stoichiometric alcohol/acid ratio for the esterification reaction is 1:1, but it is advisable to use a higher amount of alcohol to shift the reaction towards the desired products. Moreover, it is necessary to take into account the high viscosity of the feedstock treated, which can limit mass transfer of the reagents towards the catalyst. For these reasons the amount of methanol was calculated based on the actual oil mass inside the reactor rather than on reaction stoichiometry. The 4.5:1 MeOH: oil molar ratio has been already adopted in in several works (Bianchi et al., 2010; 2011; Pirola et al., 2010; 2011; Boffito et al., 2012a; 2012b; 2012c; Marchetti and Errazu, 2008a; 2008b; Marchetti et al., 2007).

Catalyst amount

Ion exchange resins were used in most of the cases in the weight ratio of 10:100 to the oil, unless otherwise specified. This ratio was proved to correspond to the optimal amount of catalyst Amberlyst®46 in order to reach a FFA concentration lower than $0.5\%_{wt}$ within the standard reaction time fixed at 6 hours (Bianchi et al., 2010).

Choice of the temperature

The temperature was maintained in most of the cases at 336 K, i.e. at a temperature slightly lower than the boiling temperature of methanol (337.8 K), unless otherwise specified. A temperature higher than 336 K was found to be necessary to achieve a FFA concentration lower than $0.5\%_{wt}$ within the standard reaction time fixed at 6 hours (Bianchi et al., 2010). The esterification reaction is an endothermic reaction, therefore, increasing the temperature, the time required for the achievement of the reaction equilibrium decreases along (Bianchi et al., 2011, Pirola et al., 2011).

Nevertheless, the choice of a temperature below the boiling temperature of methanol allows avoiding the use of costly equipment such as pressure reactors.

2.4.3 Activity tests

Activity tests were conducted withdrawing oil samples from the reactors at pre-established times. Usually: 60, 120, 240, 360 minutes. The samples were then analysed through acid-base titrations as described in the experimental part, to calculate the residual acidity (equation 2.18).

The FFA conversion into methyl esters was then calculated as follows as already reported (Boffito et al., 2012a; 2012b;2012c; Pirola 2011).

$$FFA\ conversion\ (\%)=\frac{FFA_{t=0}-FFA_t}{FFA_{t=0}}\times 100 \qquad 2.20$$

Where $FFA_{t=0}$ is the FFA concentration by weight of the starting oil and FFA_t is the FFA concentration of the oil sample at time *t*.

To verify the extent of the reaction, also Karl Fischer titrations were performed on some oil samples. Experimental procedure for Karl Fischer analyses has been already reported at paragraph 2.3.2.

2.5 Transesterification

In this work transesterification reaction was conducted in most of the cases to verify the effectiveness of the pre-esterification method performed with different oils and in different conditions.

Transesterification reaction was performed using methanol as alcohol and KOH or sodium methoxide (CH_3ONa) as basic catalysts.

Among all the alcohols used in biodiesel production, the most commonly preferred one is methanol because of the same reasons already highlighted in the case of the FFA esterification. When the related literature is searched, the number of investigations that were conducted with an alcohol apart from methanol and a catalyst apart from an alkaline one is fairly limited. This may be due to the fact that other alcohols are more expensive than methanol and, in the case of different alcohols usage, transesterification gets harder because of their low reactivity and consequently the reaction time required for completeness of the reaction becomes longer (Sanli and Canakci, 2008).

The reaction was performed in two-steps, utilizing the conditions reported in Tab. 2.3.

	g MeOH/10'0 g oil	g cat/100 g oil	Temp (K)	Time (min)
1st step	20	1	333	90
		Products separation		
2nd step	5	0.5	333	60
		Products separation		

Tab. 2.3. Experimental conditions of the transesterification reaction.

The catalyst, either KOH or CH_3ONa, was dissolved in the reagent methanol before the reaction.

A slurry reactor as the one described in the section 2.4.1.1. was used for all the traditional transesterification experiments. Some transesterification experiments with the aid of ultrasound were also carried out. The experimental details will be described in a chapter aside (chapter 8).

References

Abidin S.Z., Haigh K.F., Saha B., "Esterification of Free Fatty Acids in Used Cooking Oil Using Ion-Exchange Resins as Catalysts: An Efficient Pretreatment Method for Biodiesel Feedstock", *Ind. Eng. Chem. Res.* **2012,** 51, 14653.

Ardizzone S., Bianchi C.L., Cappelletti G., Annunziata R., Cerrato G., Morterra C., Scardi P., "Fe- and Mn-promoted sulphated ZrO_2 as liquid phase catalysts", *Appl. Catal. A* **2009,** 360, 137.

Ardizzone S., Bianchi C.L., Cappelletti G., Porta F., "Liquid-phase catalytic activity of sulfated zirconia from sol–gel precursors: the role of the surface features", *J. Catal.* **2004,** 227, 470.

Azam M.M., Waris A., Nahar N.M., "Prospects and potential of fatty acid methyl esters of some non-traditional seed oils for use as biodiesel in India", *Biomass Bioenergy* **2005,** 29, 293.

Barrett E.P., Joyner L.G., Halenda P.P., "The determination of pore volume and area distributions in poroussubstances. I. Computations from nitrogen isotherms", *J. Am. Chem. Soc.* **1951,** 73, 373.

Behzadi S., Farid M.M., "Production of Biodiesel Using a Continuous Gas-Liquid Reactor", *Bioresour. Technol.* **2009,** 100, 683.

Ben Chaabene S., Bergaoui L., Ghorbel A., Lambert J.F., "In situ preparation of zirconium sulfate pillared clay: study of acidic properties", *Appl. Catal. A* **2004,** 268(1-2), 25.

Bianchi C.L., Boffito D.C., Pirola C., Ragaini V., "Low temperature de-acidification process of animal fat as a pre-step to biodiesel production", *Catal. Lett.* **2010,** 134, 179.

Bianchi C.L., Pirola C., Boffito D.C., Di Fronzo A., Carvoli G., Barnabè D., Bucchi R., Rispoli A., Non edible oils: raw materials for sustainable biodiesel, in: Feedstocks and Processing Technologies, M. Stoytcheva (Ed.), ISBN: 978-953-307-713-0, InTech 2011, pp. 3-22.

Boffito D.C., Crocellà V., Pirola C., Neppolian B., Cerrato G., Ashokkumar M., et al., Ultrasonic enhancement of the acidity, surface area and free fatty acids esterification catalytic activity of sulphated ZrO_2-TiO_2 systems, J Catal 2012, accepted on September 2012., DOI: 10.1016/j.jcat.2012.09.013.

Boffito D.C., Pirola C., Bianchi C.L., "Heterogeneous catalysis for free fatty acids esterification reaction as a first step towards biodiesel production", *Chim. Oggi - Chem Today* **2012,** 30(1), 42.

Boffito D.C., Pirola C., Galli F., Di Michele A., Bianchi C.L., Free Fatty Acids Esterification of Waste Cooking Oil and its mixtures with Rapeseed

Oil and Diesel, Fuel, 2012a, accepted on 19th October 2012, DOI: 10.1016/j.fuel.2012.10.069.

Brunauer S., Hemmett P., Teller E., "Adsorption of Gases in Multimolecular Layers", *J. Am. Chem. Soc.* **1938,** 60, 309.

Chakrabarty M.M., "Chemistry and Technology of Oils and Fats", Allied Publishers Pvt. Ltd, **2003**, ISBN : 81-7764-495-5.

Chen Y.H., Wang L.C., Tsai C.H., Shang N.C., "Continuous-flow Esterification of Free. Fatty Acids in a Rotating Packed Bed", *Ind. Eng. Chem. Res.* **2010,** 49, 4117.

Corma A., Martinez A., Martinez C., "Influence of Process Variables on the Continuous Alkylation of Isobutane with 2-Butene on Superacid Sulfated Zirconia Catalysts", *J. Catal.* **1994,** 149, 52.

Corma A., "Inorganic Solid Acids and Their Use in Acid-Catalyzed Hydrocarbon Reactions", *Chem. Rev.* **1995,** 95, 559.

Dijs I.J., Geus J.W., Jenneskens L.W., "Effect of Size and Extent of Sulfation of Bulk and Silica-Supported ZrO_2 on Catalytic Activity in Gas- and Liquid-Phase Reactions", *J. Phys. Chem. B* **2003,** 107, 13403.

EN 14111, Fat and oil derivatives. Fatty acid methyl esters (FAME). Determination of iodine value, CEN Brussels, Belgium., 2003.

Furuta S., Matsuhashi H., Arata K., "Catalytic action of sulfated tin oxide for etherification and esterification-comparison with sulfated zirconia", *Appl. Catal. A* **2004,** 269, 187.

Ivanov A.V., Vasina T.V., Masloboishchikova O.V., Khelkovskaya-Sergeeva E.G., Kustov L.M., Zeuthen P., "Study of alkane isomerization on superacidic catalysts on the basis of SO_4/ZrO_2", *Kinet. Catal.* **1998,** 39(3), 367.

Juan J.C., Jiang Y., Meng X., Cao W., Yarmo M.A., Zhang J., "Supported zirconium sulfate on carbon nanotubes as water-tolerant solid acid catalyst", *Mater. Res. Bull.* **2007,** 42(7), 1278.

Juan J.C., Zhang J., Yarmo M.A, "Study of catalysts comprising zirconium sulfate supported on a mesoporous molecular sieve HMS for esterification of fatty acids under solvent-free condition", *Appl. Catal. A* **2008,** 347(2), 133.

Juan J.C., Zhang J., Yarmo M.A., "Structure and reactivity of silica-supported zirconium sulfate for esterification of fatty acid under solvent-free condition", *Appl. Catal. A* **2007,** 332(2), 209.

Kiss A.A., Omota F., Dimian A.C., Rothenberg G., "The heterogeneous advantage: biodiesel by catalytic reactive distillation", *Top. Catal.* **2006,** 40, 141.

Komiyama M., "Design and Preparation of Impregnated Catalysts", *Catal. Rev. - Sci. Eng.* **1985,** 27, 341.

Krisnangkura K., "A simple method for estimation of cetane index of vegetable oil methyl ester", *J. Am. Oil Chem. Soc.* **1986,** 63, 552.

Kurosaka T., Matsuhashi H., Arata K., "Dehydrogenative Coupling of Methane Catalyzed by Platinum-Added Sulfated Zirconia and Characterization of the Catalyst Surface", *J. Catal.* **1998,** 179, 28.

Kustov L.M., Kazansky V.B., Figueras F., Tichit D., "Investigation of the Acidic Properties of ZrO_2 Modified by SO2−4 Anions", *J. Catal.* **2004,** 150, 143.

Lam M.K., Lee K.T., Mohamed A.R., "Sulfated tin oxide as solid superacid catalyst for transesterification of waste cooking oil: An optimization study", *Appl. Catal. B* **2009,** 93, 134.

Lea C.H., "The determination of the peroxide values of edible fats and oils: The iodimetric method", *J. Soc. Chem. Ind.* **1946,** 65(10), 286.

Levin E.M., McMurdie H.F., Phase Diagrams for Ceramists, The American Ceramic Society (**1975**)

Llewellyn P., Montanaro L., Rouquerol F., "Investigation of the dehydration of Y-TZP gels by controlled transformation Rate Thermal Analysis", *Solid State Ionics* **1997,** 95, 23.

López D.E., Suwannakarn K., Bruce D.A., Goodwin J.G., "Esterification and transesterification on tungstated zirconia: Effect of calcination temperature", *J. Catal.* **2007,** 247, 43.

Mapes J.E., Eischens R.P., "The infrared spectra of ammonia chemisorbed on cracking catalysts ", *J. Phys. Chem.* **1954,** 58, 1059.

Marchetti J.M., Errazu A.F., "Esterification of free fatty acid using sulfuric acid as catalyst in the presence of triglycerides", *Biomass Bioenergy* **2008,** 32, 892.

Marchetti J.M., Errazu A.F., "Comparison of different heterogeneous catalysts and different alcohols for the esterification reaction of oleic acid", *Fuel* **2008,** 87, 3477.

Marchetti J.M., Miguel V.U., Errazu A.F., "Heterogeneous esterification of oil with high amount of free fatty acid", *Fuel* **2007,** 86, 906.

Mastikhin V.M., Nosov A.V., Filimonova S.V., Terskikh V.V., Kotsarenko N.S., Shmackova V.P., Kim V.I., "High-resolution solid-state NMR studies of sulfate-promoted zirconia in relation to n-pentane isomerization", *J. Mol. Catal. A: Chem.* **1995,** 101(1), 81.

Moreno J.A., Poncelet G., "Isomerization of n-Butane over Sulfated Al- and Ga-Promoted Zirconium Oxide Catalysts. Influence of Promoter and Preparation Method", *J. Catal.* **2001,** 203(2), 453.

Morterra C., Cerrato G., Meligrana G., "2,6-dimethylpyridine as an analytical tool to test the surface acidic properties of oxidic systems", *Langmuir* **2001,** 17, 7053.

Morterra C., Cerrato G., Pinna F., Signoretto M., "BrØnsted Acidity of a Superacid Sulfate-Doped ZrO_2 System", *J. Phys. Chem.* **1994,** 98, 12373.

Öezbay N., Oktar N., Tapan N.A., "Esterification of Free Fatty Acids in Waste Cooking Oils (WCO): Role of Ion-exchange Resins", *Fuel* **2008,** 87, 1789.

Parry E.P., "An infrared study of pyridine adsorbed on acidic solids. Characterization of surface acidity", *J. Catal.* **1963,** 2(5), 371.

Pasias S., Barakos N., Alexopoulos C., "Heterogeneously Catalyzed Esterification of FFAs in Vegetable Oils", *Chem. Eng. Technol.* **2006,** 29, 1365.

Peri J.B., Infrared spectroscopy in catalytic research, in Anderson, J. R. and Boudart, M.(Eds), Catalysis Science and Technology, **1984**,Vol. 5, Springer-Verlag, Berlin, pp. 171–221.

Pirola C., Bianchi C.L., Boffito D.C., Carvoli G., Ragaini V., "Vegetable oil deacidification by Amberlyst : study of catalyst lifetime and a suitable reactor configuration", *Ind. Eng. Chem. Res.* **2010,** 49(10), 4601.

Pirola C., Boffito D.C., Carvoli G., Di Fronzo A., Ragaini V., Bianchi C.L., Soybean oil deacidification as a first step towards biodiesel production, In: D. Krezhova., editor., Recent Trends for Enhancing the Diversity and Quality of Soybean Products: Intech, **2011**, p. 321-44.

Ragaini V., Bianchi C.L., Pirola C., Carvoli G., "Increasing the value of dilute acetic acid streams through esterification: Part I. Experimental analysis of the reaction zone", *Appl. Catal. B* **2006,** 64, 66.

Redaelli B., Metodo innovativo, via esterificazione, per l'abbattimento dell'acidità di oli vegetali da destinarsi alla produzione di biodiesel, Master degree thesis, 2006, this research group.

Richardson J.T., Principles of Catalyst Development, 1989 Plenum Press New York

Rinaldi R., Deacidificazione su catalizzatori commerciali di oli vegetali per la produzione di biodiesel in impianti batch attraverso reazioni di esterificazione con alcoli di diversa natura , Master Degree thesis, 2007, this research group.

Russbueldt B.M.E., Hoelderich W.F., "New sulfonic acid ion-exchange resins for the preesterification of different oils and fats with high content of free fatty acids", *Appl. Catal. A* **2009,** 362, 47.

Sanli H., Canakci M., "Effects of Different Alcohol and Catalyst Usage on Biodiesel Production from Different Vegetable Oils", *Energy Fuels* **2008,** 22, 2713.

Sejidov F.T., Mansoori Y, Goodarzi N., "Esterification Reaction Using Solid Heterogeneous Acid Catalysts under Solvent-Less Condition", *J. Mol. Catal. A: Chem.* **2005,** 240, 189.

Skoog D.A., West D.M., Holler F.J., Crouch S.R., Fondamenti di Chimica Analitica, EdiSES (**1998**) 580

Sohn J.R., Seo D.H., "Preparation of new solid superacid catalyst, zirconium sulfate supported on γ-alumina and activity for acid catalysis ", *Catal. Today* **2003,** 87, 219.

Winayanuwattikun P., Kaewpiboon C., Piriyakananon K., Tantong S., Thakernkarnkit W., Chulalaksananukul W. et al. "Potential plant oil feedstock for lipase-catalyzed biodiesel production in Thailand", *Biomass and Bioen* **2008**, 32, 1279.

CHAPTER 3:
CHARACTERIZATION AND PROCESSING OF THE OILS

Abstract

Different oils, both refined and raw ones, were considered as potential feedstock for biodiesel production. They were characterized for what concerns acidity, free fatty acids composition, saponification number, peroxide value and cetane number and then submitted to free fatty acids esterification to lower the acidity. Some of them were finally transformed into biodiesel. Most of the oils were successfully deacidified over sulphonic ion exchange resins Amberlyst®15, 46 and Purolite®D5081. A46 and D5081 also demonstrated to be able to maintain a good catalytic activity over several recycles of use, differently from A15. A46 and D5081 are in fact characterized by the only superficial location of the active sites that confers to them stability and reproducibility of the performance. The results achieved with A46 and D5081 were compared with the ones simulated using the pseudohomogeneous kinetic model achieving a good correlation.

Brassica juncea oilseed and blends of waste cooking oil with rapeseed oil and tobacco oilseed turned out to have the highest potential to be transformed into biodiesel, being characterized by optimal intrinsic properties (composition of free fatty acids resulting in optimal values of iodine and cetane number).

The high transesterification yields resulted from the final transformation of the deacidified oils into biodiesel confirmed the effectiveness of the deacidification method.

3.1 Introduction

3.1.1 Feedstock for biodiesel production

Potentially, any kind of vegetable oil or animal fat might be used as an input for biodiesel production. In Tab. 3.1 the characteristics of the most studied oils for biodiesel production are displayed.

The production of biodiesel demands new land or lands previously dedicated to food crops or forests. This may result in deforestation and shortage of food. Only when marginal lands or agricultural residues are used the environmental advantages of biodiesel are maximal.

This section includes a description of both the most common sources of triglycerides currently used for biodiesel production and the ones with high potential. This description also includes the crops used as biodiesel feedstock in the present work.

Rapeseed and Canola

Canola oilseed is a low erucic acid rapeseed oil (*Brassica napus*) and the second largest oil crop after soybean (Lopes and Neto, 2011) in the World.

Canola oil makes up the greatest percentage of the biodiesel raw material used in the global market (84%), followed by sunflower (13%), soybean (2%), palm (1%), and other oilseeds.

The reason why canola covers the highest portion of biodiesel market, besides is wide availability, is given by its ratio of unsaturated/saturated fatty acids, yielding methyl esters whose properties are comparable with those of conventional diesel fuels. It has also been reported that the lubricity of diesel fuel can be

enhanced by 60% with the addition of 1 vol% of canola derived methyl ester (Lopes and Neto, 2011). Its unsaturated/saturated fatty acids ratio also allows high oxidation stability, which enables high quality biodiesel manufacturing (Lee et al., 2010) and, at the same time, prevents engine blockage due to the low solidification point (276-277 K) (Xie et al., 2007).

Sunflower

The sunflower (*Helianthus annuus*) is an annual plant and is one of the four most important oilseed crops in the World.

Sunflower is grown in many semi-arid regions of the world from Argentina to Canada but it can grow in a wide range of soil types from sands to clays (Zabanioutou et al. 2008). Moreover it is tolerant to low temperatures. The nutritional quality of its edible oil ranks among the best vegetable oils (Skoric et al., 2008).

Due to the fact that sunflower oil does not have a fixed quality, but different qualities depending on weather conditions and agricultural practises, many researchers are restive about using sunflower oilseed as biodiesel feedstock (Lopes and Neto, 2008).

Moreover, some assessments regarding the biodiesel production from sunflower oil highlighted the negative result in terms of energy output (Pimentel and Patzek, 2005; Pimentel, 2001). Sunflower seeds, in fact, have higher oil content than soybeans but seeds yields per hectare is nearly half that of soybean. (Pimentel and Patzek, 2005).

Oil	Oil yield (kg /ha)	η_{FAME} ($cSt_{40°C}$)	IV (gI_2/ 100 g)	SN (mg KOH /g)	CN	Fatty acids composition ($\%_{wt}$)
Canola	1000[a]	3.53[b]	112	199	48.5	12:0 (0.06) 14:0 (0.07) 16:0 (4.65) 16:1 (0.13) 18:0 (1.64) 18:1 (65.93) 18:2 (21.16) 18:3 (5.16) 20:0 (0.93) 22:0(0.27)[b]
Sunflower	1040[b]	3.28[b]	142	200	41.6	14:0 (0.05) 16:0 (6.59) 16:1 (0.09) 18:0 (3.14) 18:1(22.43) 18:2 (66.20) 18:3 (0.92) 20:0(0.15) 22:0(0.43)[b]
Soybean	210[b]	3.28[b]	139	201	42.2	14:0 (0.03) 16:0 (10.70) 18:0 (3.02) 18:1(24.02) 18:2 (56.58) 18:3 (5.35) 20:0 (0.11) 22:0 (0.19)[b]
Palm	4000[c]	4.00[l]	63.0	207	58.5	16:0 (40.3) 18:0(3.1) 18:1 (43.4) 18:2 (13.2)[h]
Tobacco	1800[d]	3.81[b]	148	201	40.2	16:0 (10.52) 18:0 (2.67) 18:1 (11.01) 18:2 (74.99) 18:3 (0.81)[b]
Brassica juncea	880[e]	n.a.	118	186	49.1	16:0 (3.6) 18:0(1.10) 18:1 (13.90) 18:2 (21.50) 18:3 (13.70) 20:0 (8.70) 22:1 (37.50)[g]
Brassica carinata	n.a.	n.a.	124	189	47.3	16:0 (3.90) 18:0 (0.80) 18:1 (12.9) 18:2 (20.40) 18:3 (17.00) 20:0 (6.30) 22:1 (38.70)[g]
Safflower	1090[b]	3.21[b]	152	201	39.3	14:0 (0.11) 16:0 (6.44) 16:1 (0.05) 18:0 (2.20) 18:1(14.13) 18:2 (76.57) 18:3 (0.15) 20:0 (0.20) 22:0 (0.15)[b]
Jatropha curcas	610[f]	n.a.	104	202	49.9	14:0 (0.1) 16:0 (14.7) 16:1 (0.7) 18:0 (6.85) 18:1 (40.0) 18:2 (37.0) 18:3 (0.25) 20:0 (0.25) 22:0 (0.15)[h]
Castor oil	880[b]	3.49[b]	88.0	188	55.5	16:0 (0.7) 18:0 stearic (0.9) 18:0 dihydroxystearic (0.5) 18:1 oleic (2.8) 18:1 ricinoleic (90.2) 18:2 (4.4) 18:3 (0.2) 20:0 (0.20) 22:0 (0.15)[i]
Animal fat	-	n.d.	60.3	204	59.5	12:0 (0.1) 14:0 (1.5) 16:0 (24.8) 16:1 (2.8) 18:0 (15) 18:1 (42.3) 18:2 (10.0) 18:3 (0.5) 20:0 (1.7) 22:0 (1.3)[m]

[a](Fukuda et al., 2001); [b](Winayanuwattikun et al., 2008); [c](AOCS lipid library, 2012); [d](Fogher, 2008); [e](Ali and Shah, 1982); [f](Dar, 2007); [g](Velasco et al., 1998) [h](Berchmans and Hirata, 2008); [i](Sarin et al., 2007); [l](Mejia et al., 2013); [m](Feddern et al., 2012)

Tab. 3.1. Indicative values of some properties of oils used for biodiesel production.

Soybean

Soybean (*Glycine max*) is a major crop throughout much of North America, South America and Asia. The United States is the World's

greatest soybean producer, with approximately 32% of the World's soybeans followed by Brazil with 28%.

Soybean acreage is much greater than other oilseed crops leading to substantial soybean oil production and its availability as a biofuels feedstock. Use of soybean oil for biodiesel was greatly influenced by the promotion from U.S. soybean farmers through the United Soybean Board (USB) and subsequent creation of the National Biodiesel Board (NBB).

Besides biodiesel production has been widely studied by researchers who have proven its potential for this purpose (Pirola, 2011; Lopes and Neto, 2011), the high iodine value of soybean oil (~ 140 gI_2/100 g oil) (Winayanuwattikun et al., 2008) makes it unsuitable to be used as pure biodiesel (compare with Tab. 1.1, Chapter 1). Use of soybean oil-derived methyl esters as biofuel results anyway possible and beneficial in blends with diesel (Tat and Van Gerpen, 1999).

Palm

Palm is now one of the major economic crops in a large number of countries, which triggered the expansion of plantation area around the World. Also, the renewable/fossil energy relation for oil palm biodiesel is higher in comparison with the one attained for other crops. The main reason for this is the high productivity of palm oil and the oxidation stability due to the presence of high concentration of saturated fatty acids chains. One of the major problems associated with the use of biodiesel, especially prepared from palm oil is its poor low temperature flow property, measured in terms of cloud point, pour point and cold filter plugging point (CFPP). This makes of palm oil biodiesel (POB) a good candidate to use in blends

with diesel or other oil characterized by lower viscosities (Sarin et al., 2007).

In 2005, Malaysia and Indonesia produced nearly 80% of 35 million tonnes of the total World production of palm oil. This created much attention towards the specific palm oil biodiesel (POB) and biodiesel in general (Beckman et al., 2007).

Though current production of POB (1%) is insignificant compared to biodiesel production from rapeseed oil, POB remains one of the most attractive candidates for energy generation.

Tobacco

Tobacco (*Nicotiana tabacum*) is an annual herbaceous plant widespread in North and South America, commonly grown for the collection of leaves. The seeds are very small (up to 10,000/g) and contain 36 to 39% of oil having a high percentage of linoleic acid (Giannelos et al., 2002). Currently, the common varieties directed to leaf production reach the modest order of 1 to 1.2 t seeds/ha (Patel, 1998, as cited in Usta, 2005) as a result of selection to reduce the amount of seeds produced. Recently researchers were able to over-express, through genetic engineering, genes responsible for the oil production in the leaves (Andrianov et al., 2010). However, the seeds potential for oil production is much higher. In this sense, another recent outcome on tobacco improvement is a variety that can at least triple seeds (up to 5 t/ha) and oil production. The energy tobacco varieties exist both in the non GMO and the GMO version for resistance factors against herbicides and insects (Fogher, 2008). Its high oil yield makes it very competitive in front of mainstream oil crops as rapeseed, sunflower and soybean. In addition, the presence of consolidate agricultural practices and know-how make clear the

advantage of using a well-known species as tobacco as alternative feedstock for biodiesel.

The research on Energy Tobacco has also found new economies for the transplant management as well as direct sowing techniques are currently under test (Bianchi et al., 2011).

Brassica juncea

B. juncea (also known as wild mustard or Indian mustard) varieties are grown for edible leaves or for condiment mustard only in some countries, while its use as an oilseed crop is increasingly growing. Canadian plant breeders have developed B. juncea cultivars with canola characteristics (Potts et al., 1999). As a result, canola varieties of B. napus and canola-type B. juncea have similar compositional characteristics. The key differences between B. napus and canola-type B. juncea lie in their agronomic characteristics. B. juncea tolerates high temperatures and drought better than B. napus, and thus it is better suited for the warmer, drier climates as the Upper Plains of the U.S. or the Mediterranean area. Green manure of B. juncea is a current practice in some countries (e.g. Italy and U.S.) making use of the GSL-Myrosinase system as a natural biofumigant. At the same time, this practice supplies organic matter to soil. To make the most of its biocidal activity against soilborne pests and diseases, the mulching and incorporation to soil must be done at flowering time (Curto and Lazzeri, 2006).

Brassica carinata

The recent interest in B. carinata (also known as Ethiopian or Abyssinian mustard) is mainly a result of its high resistance to biotic and abiotic stresses such as drought tolerance. B. carinata, is an annual crop noted to be highly resistant to many rapeseed pests

(Pan, 2009). According to Razon (2009), B. carinata, together with E. sativa ssp. oleifera, is the most promising oilseed for biodiesel purpose in temperate zones, not just for the yield but also for its adaptability to hard pedo-climatic conditions.

It may be used in a crop rotation system with cereals and on low nutrient soils. Best results are achieved sowing on autumn (IENICA, 2004). The vegetable oil obtained from B.carinata is characterized by the presence of erucic acid, making it unsuitable for human consumption. On the other hand, its physico-chemical properties meet the European specifications defined for biodiesel destination by the normative EN 14214:2002. Beyond its oil production capabilities, it was pointed out that the B. carinata's lignocellulosic biomass can also be used to generate power and especially heat (Gasol et al., 2007), revealing an even greater potential.

Safflower

Recent studies (Ilkılıç et al., 2011; Rashid and Anwar, 2008) demonstrated that the biodiesel produced through methanolysis of safflower (*Carthamus tinctorius*) oil under a given set of experimental conditions has fuel properties quite comparable to those of mineral diesel.

Safflower has been cultivated for long mainly for its seeds that are source of edible oil, and as a source of yellow and red dyes (Gyulai, 1996). It is reported to require few inputs in terms of irrigation and fertilizer, and to grow on semi-arid or abandoned land (Liu and Benson, 2011).

India, U.S.A., and Mexico are the principle producers of safflower; however, the crop has also been cultivated in many other countries, such as Kazakhstan, Ethiopia, Argentina, China, Uzbekistan, Australia, Russian Federation, Pakistan, and Spain (Gyulai, 1996).

Safflower seeds are a potential source of linoleic acid (C18:2 n-6) rich oil with an approximate yield of 36-41%. Another type, i.e., high oleic safflower oil, has also been introduced in the marketplace.

Although safflower has been grown for decades in different countries as a source of dye, folk medicine, and human food, it did not attract any significant attention as an oilseed crop and its cultivation has been limited until recently. Nevertheless, some domestic renewable energy resources can play an important role in fulfilling the energy demands of some countries, thus contributing and reducing their dependence on fossil-derived fuels. An example is given by Pakistan (Rashid and Anwar, 2008).

In view of rapidly growing energy demands, exploration of some aboriginal, renewable energy resources has to play a crucial role.

Jatropha curcas

J. curcas is native to American tropics (Pramanik, 2003) but naturally grows in tropical and subtropical countries, like sub-Sahara Africa, India, South East Asia, and China (Tamalampudi et al., 2008).

Jatropha plantations have been established in tropical and subtropical regions worldwide (Li et al. 2010) and during the last 10 years, it has gained considerable attention as a potential feedstock of biodiesel due to its multiple attributes, uses and considerable potential (Openshaw 2000). The seeds usually mature 3–4 months after flowering and once this plant becomes an adult, it will continue producing seeds for 50 years. The oil is covering approximately 40% of the seed content (Jain and Sharma, 2010a). Due to leaf-shedding activity, jatropha plant becomes highly adaptable in harsh environments because decomposition of the shed leaves would provide nutrients for the plant and reduces water loss during dry

season. Thus, it is well adaptable to various types of soil, including soils that are poor in nutrition such as sandy, saline and stony soils. Jatropha plant also has the ability to tolerate a wide range of climate and rainfall (Kumar and Sharma, 2008; Makkar and Becker, 2009) but cannot grow in waterlogged land. As a drought-resistant plant, jatropha is a good candidate for eco-restoration in wastelands (Kumar et al., 2008; Kumari et al., 2009). Jatropha cultivation in wastelands would help the soil to regain its nutrients and will be able to assist in carbon restoration and sequestration (Makkar and Becker, 2009).

Castor oil

Castor oil (*Ricinus communis*) is an oilseed crop that belongs to the Euphorbiaceae family, which includes other energy crops as cassava (*Manihot esculenta*), rubber tree (*Hevea brasiliensis*) and physic nut (*Jatropha curcas*). Among non-edible oils, the one extracted from castor bean is the most used for a wide variety of industrial purposes. Its oil is primarily of economic interest having cosmetic, medical and chemical applications. The presence of a high proportion of ricinoleic acid makes it suitable for the production of high-quality lubricants (Sanzone & Sortino, 2010). The use of castor oil is particularly supported in Brazil, with attempts to extract the ethyl esters using ethanol from sugarcane fermentation (although less reactive than methanol), making it a complete natural and renewable product (Pinto et al., 2005). Though the actual productivity is not very high, between 600 and 1,000 kg seeds/ha year, this value could triplicate with genetic improvements (Holanda, 2004). With the recent report on the draft genome sequence of castor bean revealing some key genes involved in oil synthesis (Chan et al., 2010), this possibility becomes even more palpable. In addition to

this, the ease with which it can be cultivated in unfavourable environments contributes to its appeal as a raw material for sustainable biodiesel. In agreement to this, a two years field experiment conducted in south Italy using local ecotypes yielded around 2.3 t/ha of seeds, with up to 38% oil content, a quite high number for the dry conditions of the region (Sanzone & Sortino, 2010). The main limitation is the hand harvest, the current practice in the biggest producer countries as India, Brazil and China. However mechanization of harvesting is recently available for the collection of dwarf hybrid plants (Clixoo, 2010).

Waste vegetable oils

In most parts of the World edible oils are used in frying pans or fryers and after a variable time of use are discarded. The used cooking oils have different properties from those of refined and crude vegetable oils. The presence of heat and water during the frying accelerates the hydrolysis of triglycerides and increases the content of free fatty acids (FFA) in the oil (Marmesat et al., 2007). The FFA and water content have significant negative effects on the transesterification reaction negatively as already highlighted in the general introduction. Especially, the viscosity of the oil increases considerably, because of the formation of dimeric and polymeric acids and glycerides in used cooking oils. Molecular mass and iodine values decrease while saponification value and density increase (Marmesat et al., 2007; Kulkarmi and Dalai, 2006).

At present there is no systematic method of processing used oils from households and most of the used oil is poured into the sewer system of the cities and is finally discharged to surface waters, leading to water pollution. Moreover, more than 80% of the oil is consumed at home; the control of this disposal behaviour becomes a

huge problem because of the large volumes involved (Alcantara et al., 2000).

Despite the gains made in biodiesel production techniques, the cost of biodiesel is still higher than petroleum-based diesel and this has been a major barrier to its commercialization. The main barriers are given by the cost of the raw materials that may constitute up to 80% of the overall biodiesel production cost. The use of waste cooking oil instead of virgin (neat) oil to produce biodiesel has been found to be an effective way to reduce the raw material cost. Hence reusing of the waste cooking oil has both the benefit of producing an environmentally benign fuel and solving the problem of waste oil disposal.

The high WCO potential is recognized also by the EU directive 2009/28/EC, where waste vegetable or animal oil BD is reported to save about the 88% of greenhouse emissions, a quite high value if compared to biodiesel from common vegetable oils, whose greenhouse emission savings range from 36 to 62% (2009/28/EC).

Animal fats

In the last years, meat production has increased significantly. World meat production reached 237.7 million tons in 2010, from which 42.7%, 33.4%, 23.9% corresponds respectively to pork, poultry and beef (USDA, 2010). Consequently, a larger amount of residues from animal processing-plants has been generated in countries with intensive livestock production. Within agro-industrial residues, lipid sources may be used as feedstock to biodiesel supply, helping to solve inappropriate environmental disposal, besides contributing to energy demand.

Animal fats are readily available because slaughter industries are generally well managed for product control and handling

procedures. However, there is a biosafety issue related to animal fats that could come from the contaminated animals. The future research to ensure biodiesel quality from animal waste (cradle to grave) has been highlighted (Janaun and Ellis, 2010). Biodiesel made from animal fat is less resistant to cold weather than biodiesel made from virgin soybean oil or most other virgin oils. As additives are developed specifically for the biodiesel industry, even this distinction could soon disappear (Tickell, 2006).

Animal greases are generally described as follows:

- Tallow: extracted from residues of bovine slaughter and it can be filtered or not since it has guaranteed that the product contains minimum 90% total fatty acids, unsaponifiable impurities maximum 1.5% and no FFA or fat degradation products;
- Lard: extracted from swine slaughter residues, being its specification and quality guarantees the same as for tallow;
- Chicken fat: extracted from broiler slaughter residues and it can be filtered or not since it has guaranteed that the product contains minimum 90% total fatty acids, maximum 3% unsaponifiable impurities, without FFA or fat degradation products;
- Animal fat mix: extracted from slaughter residues of mammals or birds. It can be filtered or not since it has guaranteed that the product contains total fatty acids minimum 90%, maximum 2% unsaponifiable impurities, without FFA or products of fat degradation unless the ones generated even with good production practices implemented (Feddern et al., 2011).

Algae

Algae are among the most potentially significant sources of sustainable biofuels in the future of renewable energy. A feedstock with virtually unlimited applicability, algae can produce products with a wide variety of compositions and uses. These products include lipids, which can be processed into biodiesel; carbohydrates, which can be processed into ethanol; proteins, which can be used for human and animal consumption.

Algae-based biofuel production has a number of potential advantages:

- Biofuels and by products can be synthesized from a large variety of algae;
- Rapid growth rate;
- Possibility of being grown in brackish coastal water and seawater;
- Some land areas that are unsuitable for agricultural can be used to cultivate algae;
- Algae nutrients may be high nitrogen, silicon, phosphate, and sulphate nutrients from human or animal waste (e.g. municipal wastewater, carbon dioxide from industrial flue gas) (Menetrez, 2012).

In addition to the algae-derived liquid biofuels, various petroleum-like products and end products can be generated from microalgae. An additional biofuel, for example, comes from the microalga *Chlamydomonas reinhardtii*, which has been demonstrated to grow in the laboratory to produce hydrogen (Beer et al., 2009; Mullner and Happe, 2007).

Developing this technology into a commercial success, however, will be a challenge. Many issues must be addressed for the algae industry to advance from its current state to commercial success. Of

these issues, environmental impact end effects on human health are paramount. A typical process might in fact involve microorganisms such as bacteria, mold, and yeast, including GMO that could also have potential human health risks such as those from infection and exposure to allergens, toxins, carcinogens (Dermibas, 2011; Graham et al., 2008;).

Moreover, the process of generating biofuel from algae involves several steps: growth, concentration, separation, and conversion of microalgae biomass. After separating the desired biofuel product or products from the microalgae biomass, a significant portion of by-product remains (Menetrez, 2012). It is important that the remaining by-products have a useful and safe purpose for the economic feasibility and environmental sustainability of the process.

3.1.2. Deacidification over sulphonic exchange resins

The presence of free fatty acids (FFA) in the feedstock is very common in the case of not refined oils. As a consequence soaps form during the transesterification reaction as a result of the saponification reaction ($RCOOH + NaOH \rightarrow RCOONa + H_2O$). Soaps hinder the contact between reagents and, eventually, the products separation (Perego and Ricci, 2012; Boffito et al., 2012a, 2012b, Bianchi et al., 2010; Pirola et al., 2010).

Many methods have been proposed to eliminate FFA during or prior to transesterification, i.e. neutralization with alkali, deacidification with selective solvents, neutralizing distillation and FFA pre-esterification (Santori et al., 2012). Among these, FFA pre-esterification method is a very interesting approach to lower the acidity of biodiesel feedstocks with high initial FFA concentration

(Boffito et al., 2012a, 2012b; Bianchi et al., 2010, 2011; Pirola et al., 2010, 2011).

Many efforts regarding the use of solid acid catalysts for the FFA esterification were recently carried out (Boffito et al., 2012a, 2012b; Bianchi et al., 2010; Pirola et al., 2010; Marchetti and Errazu, 2008). Solid acid catalysts present typical advantages over homogeneous catalyst, such as easier separation and recovery and absence of problems related to corrosion.

Acid sulphonic ion exchange resins have been extensively studied by the author of this thesis. Ion exchange resins demonstrated to be highly active in the FFA esterification and able to main excellent catalytic performances over time (Pirola et al., 2010; 2011; Bianchi et al., 2011; Boffito et al., 2012a). In particular, in a recent work (Pirola et al., 2010) a study on the lifetime of the ion exchange resin Amberlyst®46 was carried out. In this work the same batch of catalyst was recycled for 90 consecutive kinetic experiments for a total time of 540 operating hours. The results of this study show how the resin does not deactivate unless loss of catalytic material from the system occurs.

In this chapter the results of the FFA esterification reaction performed with Amberlyst®15, Amberlyst®46 (Dow Chemical) and Purolite®D5081 (Purolite) on both refined and crude oils with very different characteristics are presented and analysed in detail.

In particular, much attention was devoted on catalysts' recycle of use.

3.2. Materials and Methods

3.2.1 Catalysts characterization

Characterization of the resins was performed following the experimental procedures already described in the general experimental part at section 2.2.

Swelling capacities (§ 2.2.5) were measured in different media: water, methanol and acid oil (rapeseed acid oil with ~2.2%$_{wt}$ FFA) ((Öezbay et al., 2008; Boffito et al., 2012c). Acidity was determined as meq of H^+ per gram of catalyst by ion exchange (§ 2.2.1) with a saturated solution of NaCl and successive titration (López et al., 2007; Boffito et al., 2012a, 2012b).

In addition, some magnifications (40X or 100X) of the resins in dry and swollen form were performed using a Wild (Herbrugg), Photomakroskop, model M400, 1,25x.

3.2.2 Oils characterization

Procedures description for oils characterization is given in the general experimental part at section 2.3.

Oils were characterized for what concern acidity (§ 2.3.1), moisture content (§ 2.3.2), composition (§ 2.3.3), iodine number (IV) (§ 2.3.4), saponification number (SN) (§ 2.3.5), peroxide number (PN) (§ 2.3.6) and cetane number (CN) (§ 2.3.7). IV and SN were determined both experimentally and theoretically from the acidic compositions. CN was only determined theoretically from both the experimental and calculated IV and SN (Krisnangkura, 1986; Winayanuwattikun et al., 2008).

3.2.3 Activity tests

Activity tests in the FFA esterification reaction were carried as described in the general experimental part at section 2.4. A classical slurry reactor (§ 2.4.1) was used for the work described in this chapter. All the tests were carried out at 336 K and atmospheric pressure, using a weight ratio MeOH:oil and catalysts: oil of 16:100 and 10:100, respectively, unless specified differently. The choice of the reaction conditions is explained in § 2.4.2. FFA conversions were calculated carrying out acid/base titrations (§ 2.3.1) on samples of oil withdrawn from the reactor at pre-established times and calculated taking into account the initial acidity of the oil, as described in § 2.4.3.

3.2.4 Transesterification reaction

Transesterification reaction was performed on deacidified oils following the procedure already described in § 2.5. The final transformation into biodiesel had the scope of proving the effectiveness of the pre-esterification method. Both KOH and sodium methoxide (CH_3ONa) were used as homogeneous catalysts adopting the conditions reported in Tab. 2.3. Biodiesel yield (corresponding to the content of FAME) was determined by GC analysis.

3.3 Results and Discussion

3.3.1 Catalysts characterization

The main features of the adopted catalysts are reported in Tab. 3.2. Information about Amberlysts® were available from products data sheets by Dow Chemical, whereas information about Purolite®D5081 was available directly from the sheets provided by the manufacturer since this product is still at the development stage.

Catalyst	A15	A46	D5081
Physical form	opaque beads		
Type	Macroreticular		
Matrix	Styrene-DVB		
Cross-linking degree	medium	medium	high
form	dry	wet	wet
Surface area ($m^2\ g^{-1}$)	53	75	514[a]
Ave. D_p (Å)	300	235	37[a]
Total V_p (ccg^{-1})	0.40	0.15	0.47
Declared Acidity (meq H^+g^{-1})	4.7	0.43	0.90-1.1
Moisture content ($\%_{wt}$)	1.6	26-36	55-59
Shipping weight ($g\ l^{-1}$)	610	600	1310[a]
Max. operating temp (°C)	120	120	130

[a] (Abidin et al., 2012)

Tab.3.2. Features of the catalysts.

All the used resins have the appearance of opaque quasi-perfect spherical beads, with dimensions ranging from 0.3 to 1 mm, with higher distribution near the upper limit. The matrix structure of both Amberlysts® and Purolite®D5081 consists of a copolymer of styrene and divinylbenzene (DVB) forming a macroporous polymer functionalized with strong -SO_3H acid sites (Brønsted acidity).

Polymer structure of resins is characterized by a certain content of the crosslinking component (DVB), which determines surface area and pore size distribution besides the ”rigidity” of the resin. Images of the resins obtained with the optical microscopy are given in Fig. 3.1. The images of the resins are displayed as they are provided by the manufacturer (dry for A15 and wet for A46 and D5081), after drying (A46 and D5081) and after swelling in methanol. When the resin is provided as “wet” it means that it is in its swollen state in water. In this case it is in fact required to dry the resins for 16 hour at 383 K in an oven to make the acid sites available for the catalysis before using them.

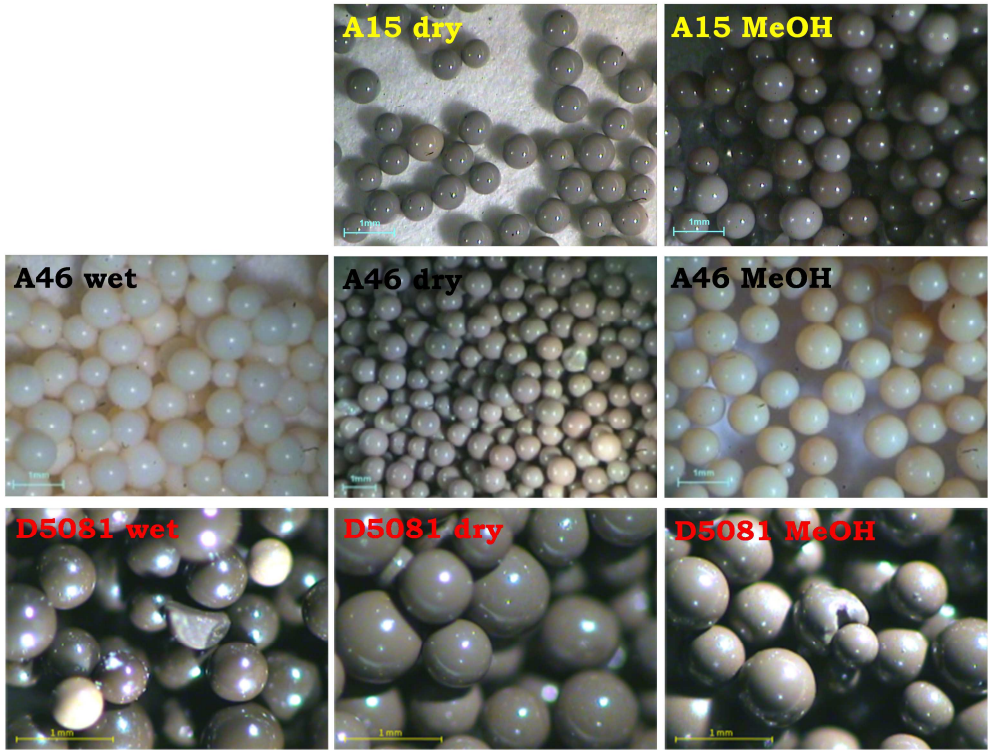

Fig. 3.1. 40X magnification of the resins A15 and A46 and 100X magnification of the resin D5081. Images of the resins as they were provided (dry for A15 and wet for A46 and D5081), after drying pretreatment and swelling in MeOH.

The reason of the choice of A15 and A46 among the other Amberlysts® is due to their different features concerning both physical and chemical properties such as surface area, porosity and acidity, as given in Tab. 3.2. Distinguishing feature of A46 and D5081 is the only surface functionalization. Consequently, A46 and D5081 are characterized by a lower number of acid sites than A15 and other Amberlysts® (Bianchi et al., 2010), which are sulphonated also internally.

The higher content of DVB for D5081 results in a higher surface area than the other two catalysts since a denser net of mesopores is created. As a consequence, the average pores diameter is lower for D5081 than for A15 and A46.

The H^+ ions exchange capacities determined experimentally are reported in Tab. 3.2. The acidity value obtained for A46 is higher, whereas the one obtained for A15 is slightly lower than the one reported by the manufacturer. This is probably due to the high accessibility by the exchange solution to the acid sites of A46, which are located exclusively externally. Differently, the value obtained for D5081 is perfectly in range with the one declared by the manufacturer. Resin A15 is therefore the most acid among the tested resins. Nevertheless, the use of resins characterized by the only surface functionalization brings some advantages in spite of the lower acidity. These comprise minimization of side products formation and absence of mass transfer limitations. An easy understanding of the catalyst's behaviour is therefore possible, as already experimented by Pirola and co-authors in a recent work (Pirola et al., 2010).

The results of the swelling tests are summarized in Tab. 3.3. The swelling capacities by both weight and volume in water and methanol increase in this order: A46 < D5081 < A15 and A46 < A15

< D5081, respectively. This result can be explained considering that water molecules are able to penetrate inside the pores of A15 under the driving force caused by the attractive interaction of polar nature between the sulphonic acid sites and the polar molecules. For A46 and D5081 the same interaction can occur only on their external surface as no sulphonic groups are located inside the catalyst beads. The higher swelling capacity in water of D5081 compared to A46 can be easily explained by its higher acidity. The higher the number of H^+ sites interacting with the polar swelling medium, the greater the mass and volume gains.

Swelling medium	Water		MeOH		Acid Oil (2%$_{wt}$ oleic acid)	
gain (%)	wt	vol	wt	vol	wt	vol
A15	122	90	87	25	39	0
A46	37	20	50	5	48	0
D5081	95	35	99	25	56	10

Tab. 3.3 Results of the swelling tests performed on the resins.

Results obtained using acid oil (~2%$_{wt}$ of FFA) as a swelling medium gave a very interesting outcome. The amount of adsorbed FFA molecules can be in fact directly correlated with the interaction between FFA (the reagent) and the catalytic active sites. This measurement is therefore indicative of the activity of the catalyst. The swelling capacities in the acid oil follow in fact inverse order with respect to the capacities in the polar media: A15 < A46 < D5081, indicating a possible order of increasing catalytic activity. This result can be explained considering that internal sites of A15 are too narrow (around 300 Å) to be accessible by the FFA, which are sterically hindered molecules. As a consequence, FFA can be adsorbed only on the external surface of the catalyst, differently

from water and methanol, which can penetrate inside the pores of A15. The number of external acid sites of A46 and D5081 is supposed to be higher than the one of A15 and they are consequently able to bind a higher number of FFA molecules on the external surface. Consequently, the weight gain of D5081 and A46 is higher than A15. The higher weight and volume gain of D5081 compared to A46 may be always ascribable to its higher acid capacity, resulting in an interaction with a higher number of FFA molecules.

3.3.2 Characterization of the oils

The results of the characterization of the oils utilised in this work is given in Tab. 3.4. The number in parentheses indicates the theoretical value of a property, calculated as explained in the previous chapter.

It can be noticed that the oils are characterized by very different values of the properties.

Considering the crude oils, the values of the acidities range from 0.50 to 2.20 $\%_{wt}$, with the exception of the tobacco oil obtained with the second pressing (tobacco2). Winterized sunflower, crude rapeseed, safflower and brassica oilseeds were all pressed in extra-virgin conditions by the same oil manufacturer (TopAgri, Roverchiara, Italy), while information about the pressing of the two stocks of tobacco oil, as well as palm oil, were not available.

Oil	Acidity ($\%_{wt}$)	IV[1] (gI_2/ 100 g)	PN[2] ($meqO_2$ /kg)	SN[3] (mg KOH/g)	CN[4]	Fatty acids composition (%wt)
animal fat (lard)*	5.87	51	2.3	199	62.3	n.d.
soybean*	5.24	138	3.8	201	42.4	n.d.
tobacco1	1.68	143 (149)	21.9	199 (202)	41.6 (39.8)	C14:0 (2.0) C16:0 (8.3) C18:0 (1.5) C18:1 (12.0) C18:2 (75.3) C18:3 (0.6) C20:0 (0.1) C22:0 (0.2)
sunflower*	3.79	126	3.7	199	45.4	n.d.
WSO[5]	0.50	118 (129)	71.3	187 (200)	48.9 (44.6)	C16:0 (6.9) C18:0 (0.9) C18:1 (40.1) C18:2 (50.9) C18:3 (0,3) C20:0 (0.1) C20:1 (0.4) C22:0 (0.4)
palm	2.71	54.0 (53.0)	12.3	201 (208)	61.3 (60.6)	16:0 (43.9) 18:0 (5.6) 18:1 (40.5) 18:2 (8.6)
WCO[6]	2.10	53.9 (50.7)	11.0	212 (196)	59.9 (62.7)	C16:0 (38.8) C18:0 (4.1) C18:1 (47.9) C18:2 (4.2)
WCO: CRO=3:1	2.12	69.0 (75.5)	30.1	200 (212)	58.1 (55.1)	C16:0 (30.1) C18:0 (3.1) C18:1 (51.9) C18:2 (12.0) C18:3 (2.6%) C20:0 (0.2) C22:0 (0.1)
WCO: CRO=1:1	2.19	76.8 (90.7)	51.3	188 (203)	58.1 (52.8)	C16:0 (21.5) C18:0 (2.1) C18:1 (55.8) C18:2 (14.7) C18:3 (5.1) C20:0 (0.8) C22:0 (0.1)
WCO: CRO=1:3	2.24	84.5 (104)	62.4	177 (202)	58.1 (49.9)	14:0 (0.1) 16:0 (14.7) 16:1 (0.7) 18:0 (6.85) 18:1 (40.0) 18:2 (37.0) 18:3 (0.25) 20:0 (0.25) 22:0 (0.15)
rapeseed (CRO[7])	2.20	118 (123)	71.6	165 (200)	52.8 (45.9)	C16:0 (4.1) C18:0 (0.1) C18:1 (63.7) C18:2 (20.2) C18:3 (10.2) C20:0 (1.5) C22:0 (0.2)
rapeseed*	4.17-5.12	108 (107)	3.5	203 (200)	48.9 (49.5)	C16:0 (7.6) C18:0 (1,3) C18:1 (64.5) C18:2 (23.7) C18:3 (2.4) C20:0 (0.5)
Brassica juncea	0.74	109 (110)		178 (185)	52.4 (51.1)	C16:0 (2.4) C18:0 (1.1) C18:1 (19.9) C18:2 (19.2) C18:3 (10.9) C20:0 (7.2) C20:1 (1.7) C22:0 (0.9) C22:1 (34.8) 24:0 (1.9)
safflower	1.75	139	48.9	170	47.1	n.d.
WCO: tobacco2 =1:1	4.34	119 (112)	56.0	191 (203)	48.1 (48.0)	C16:0 (22.5) C18:0 (3.2) C18:1 (32.0) C18:2 (42.1) C18:3 (0.2)
tobacco2	6.17	141 (151)	33.4	183 (201)	44.4 (39.5)	C16:0 (8.7) C18:0 (1.6) C18:1 (12.8) C18:2 (76.0) C18:3 (0.7) C20:0 (0.1) C22:0 (0.1)

[1]Iodine value; [2]Peroxide number; [3]Saponification number; [4]Cetane number; [5]Winterized sunflower oil, [6]Waste cooking oil; [7]Crude rapeseed oil; * refined, commercial oils acidified with pure oleic acid up to the indicated value.

Tab. 3.4. Results of the characterization of the oils.

The acidity of all the oils exceeds the $0.5\%_{wt}$. This value corresponds to an acidity value of ~0.5 mgKOH/g, i.e. the one

recommended by both the European normative on biodiesel (EN 14214) and American standard ASTM 6751. FFA could in fact cause the corrosion of the engine. Moreover, a FFA concentration lower than 0.5%$_{wt}$ is also required to perform the homogeneously alkali-catalysed transesterification. FFA higher than 0.5%$_{wt}$ could in fact form an amount of soaps such that contact among the reagents and products separation is prevented (Perego and Ricci, 2012; Boffito et al., 2012a, 2012b, Bianchi et al., 2010; Pirola et al., 2010).

The iodine values (IV) is regulated by the EN 14214, which poses a limit of 120 gI_2/100 g not to be exceeded. In fact, the number of saturated fatty chains in the fuel determines its behaviour at low temperatures, influencing parameters such as the cloud point, the CFPP (cold filter plugging point) and the freezing point (Saloua et al., 2010; Encinar et al., 2005; Winayanuwattikun et al., 2008).

The oils with IV higher than 120, i.e. soybean, tobacco, sunflower and sunflower) are therefore not recommended as feedstock for B100 (100% biodiesel), but they have to be used in blends with diesel or with BD deriving from oils with a lower concentration of unsaturated fatty alkyl chains. Differently, some oils such as palm, animal fat, and waste cooking oil (WCO) are characterized by low IV that might influence their behaviour at cold temperatures. The use of blends of different oils may be therefore beneficial to the biodiesel properties (Bianchi et al., 2010, Boffito et al., 2012c). Examples are given by the mixtures of WCO with crude rapeseed oil (CRO) and tobacco oil.

Other oils, such as rapeseed and brassica juncea oilseeds show IV that are at the same time below 120 gI_2/100 g and not so low as to affect the diesel behaviour in cold climates.

The measured iodine values (IV) are in most of the cases similar to the ones calculated theoretically from the acidic compositions and

indicated in parentheses. When the experimental IV differs from the theoretical one, it is in most of the cases underestimated. This can be explained considering the peroxide numbers (PN) listed in Tab. 3.4 for all the oils. Oils with high IV usually have a high concentration of peroxides, whereas fats with low iodine numbers have a relatively low concentration of peroxide at the start of rancidity (King et al., 1933). Oxidative rancidity of oils is in fact associated with the degradation of oils by oxygen in the air. Via a free radical process, the double bonds of an unsaturated fatty acid can undergo cleavage and release volatile aldehydes and ketones.
Observing Tab. 3.4, it may be noticed that oils with high IV, also exhibit high PN. The cleavage of the double bonds of these oils as a consequence of oxidation leads to a decrease in the number of unsaturations and as a consequence, to a decrease in the iodine values.

The peroxide number provides a measure of the extent to which oil has undergone primary oxidation (Chakrabarty, 2003) and is therefore an index of the conservation conditions of an oil. The nature of the fat, the temperature at which it is stored, the amount of oxygen available, the surface exposed, the presence or absence of light and perhaps other factors influence the on the peroxide value.

The high PN obtained for the oils utilised in this work might be due to the fact that they were delivered from weeks to months later after the pressing.

Although PN is not specified in the current biodiesel fuel standards, it may affect cetane number (CN), a parameter that is regulated by the standards concerning biodiesel fuel. Increasing PN increases CN, altering the real ignition delay time (Dunn, 2005). However, a CN higher than 51 is required by the EN 14214. A high

CN results in a more regular engine functioning and reduces particulate emissions.

Saponification number (SN) is an index of the number of the fatty alkyl chains that can be saponified. The long chain fatty acids have a low SN because they have a relatively fewer number of carboxylic functional groups per mass unit of fat compared to short chain fatty acids.

In Tab. 3.4 the SN measured for all the oils are reported. It can be noticed that in most of the cases the experimental SN are lower than the ones calculated theoretically. This can be explained always considering the PN of the oils, indicating a high concentration of oxygen bound to the fatty alkyl chains. The presence of oxygen in the oil brings to an underestimation of the saponification value because, on an equal weight, an oxygenated sample contains less triglyceride molecules than the same oil sample not oxygenated. Differently, the SN of the refined rapeseed oil is very close to the calculated one and the SN of all the other refined oils (sunflower, soybean, animal fat) are anyway in range with the ones reported in literature (compare with Tab. 3.1).

3.3.3 Deacidification of different oils over sulphonic exchange resins

A typical trend of the FFA esterification performed with acid ion exchange resins is given in Fig. 3.2. for the rapeseed oil. The conversion increases with the time until the achievement of the plateau of conversion according to the reaction equilibrium (Bianchi et al., 2010, Boffito et al., 2012a).

The results of the FFA esterification performed on the different oils adopting the experimental conditions mentioned in the section on materials and methods is given in Fig. 3.3.

The dotted line represent a FFA concentration equal to 0.5%$_{wt}$, i.e. the limit required by both the European and American directives on biodiesel fuel and to perform the transesterification reaction avoiding excessive soaps formation.

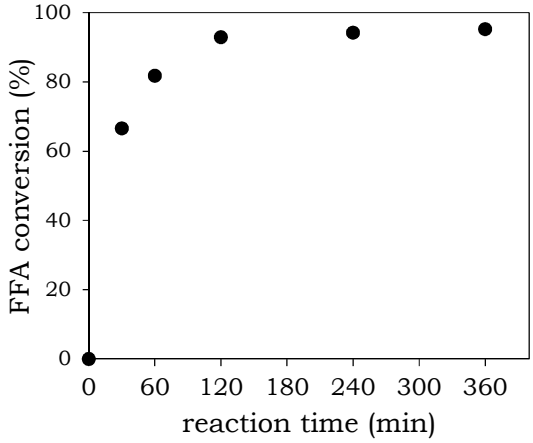

Fig. 3.2. Typical trend of the FFA esterification kinetic. Acid rapeseed oil (~5%$_{wt}$ FFA), slurry reactor, 336 K, MeOH:oil=16:100.

The FFA esterification method is able to lower the acidity of most of the oils using the ion exchange resins Amberlyst®46 and Purolite®D5081 as catalysts in the adopted reaction conditions. The use of one catalyst, rather than the other, depended on their availability during the experimentation. The differences in the acidic composition seem not to affect the final yield of the reaction. What appears to influence the FFA conversion is the refinement degree of the oil. WCO is in fact harder to be processed in comparison to refined oils (Bianchi et al., 2010; Boffito et al., 2012c), probably due

to its higher viscosity which results in limitations to the mass transfer of the reagents towards catalysts. Indeed, the required acidity limit is not achieved within 6 hours of reaction. A FFA concentration lower than 0.5%$_{wt}$ is not achieved also in the case of WCO mixture 3:1 with CRO and 1:1 with tobacco oil and in the case of the second stock of tobacco oil (tobacco2). This is attributable to the very low quality of these oils due to the waste nature of the oil itself, in the case of WCO, or to the bad conservation conditions as already highlighted in the previous paragraph concerning the characterization of the oils. In the particular case of tobacco oilseed, the low FFA conversion was also ascribed to the presence of phospholipids, able to deactivate the resin.

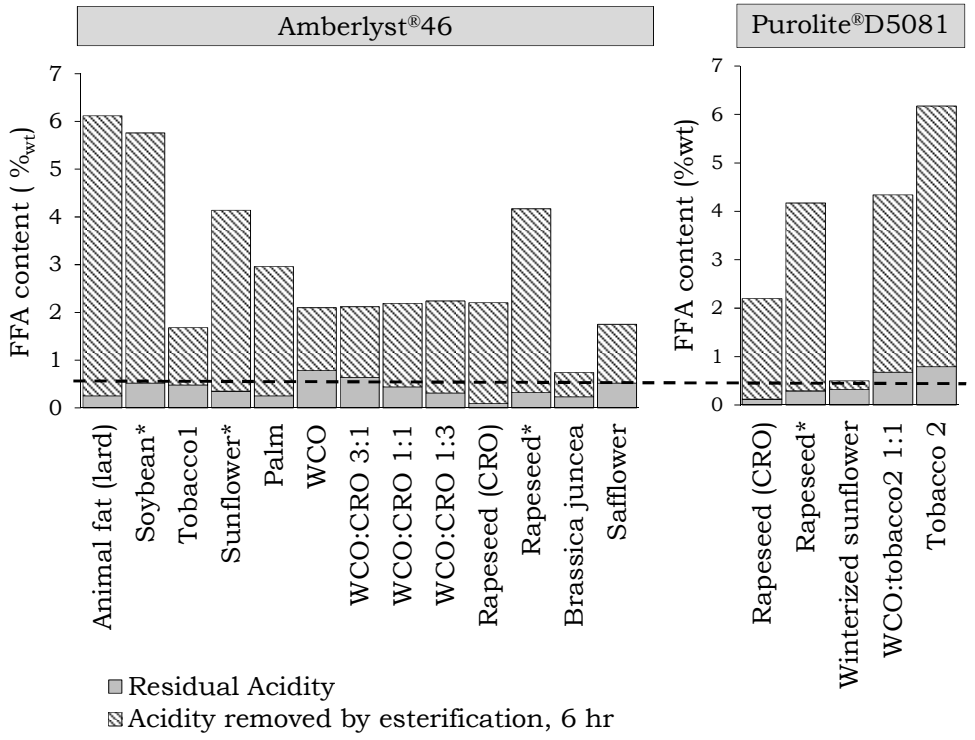

Fig. 3.3. Results of the deacidification of different oils by FFA esterification reaction. Slurry reactor, 336 K, catalyst:oil=10:100, MeOH:oil=16:100.

3.3.4 Comparison between Amberlyst®46 and Purolite®D5081

In the graphs in Fig. 3.4a and 3.4b a comparison between Amberlyst®46 (A46) and Purolite®D5081 (D5081) at different catalyst loadings and different temperatures is shown, respectively.

In Fig. 3.4a it can be seen that D5081 brings to the achievement of the plateau of conversion within 6 hours at all the catalyst loadings, while A46 gives the same result just when used in the ratio 10:100 with respect to the oil weight, that is the usual loading adopted for this catalyst (Bianchi et al., 2010; Pirola et al., 2011; Boffito et al., 2012a; 2012c). Lower amounts of A46 do not allow the achievement of the maximum conversion within the pre-established reaction time.

The better performance of D5081 over A46 is likely due to the higher number of active acid sites located on its surface. In fact, as already remarked in the discussion of the results of the characterization of the catalysts, a higher number of superficial active sites are able to adsorb more efficiently both methanol and FFA (as described in § 3.3.1). It is noteworthy that, by loading the 10% of D5081 it is possible to achieve the maximum conversion within a reaction time of two hours, as displayed in Fig. 3.4a.

It is interesting to notice how loading 6% of D5081 and 10% of A46 practically results in two almost perfectly overlapping kinetic curves. For the sake of clarity, these curves are represented in Fig. 3.4a by continuous lines. This result can be explained considering the acid sites concentration on each of the two catalysts (0.60 and 1.0 meq H^+/g for A46 and D5081, respectively). Multiplying the acid site concentration for the catalyst loading, the number of active acid sites present in the reaction medium is obtained:

0.6 meqH^+/g_{cat} x 10 g_{cat}= 6 meq H^+ (A46)

1.0 meqH^+/g_{cat} x 6 g_{cat}= 6 meq H^+ (D5081)

Therefore, the acid sites concentration in the reaction medium in the case of 6 and 10% of catalyst loading of A46 and D5081, respectively, is the same. As a consequence the same conversion is obtained at constant time.

In Fig. 3.4b, the comparison between A46 and D5081 at different temperatures and in absence of drying pretreatment (wet catalyst) is displayed. As expected, D5081 performs better than A46 in all the adopted conditions. Nevertheless, the maximum conversion within a reaction time of 6 hours is not achieved by none of the catalysts both operating at 318 K and in absence of drying pretreatment. This suggests that the pretreatment of the ion exchange resins before the FFA esterification reaction is important in order to remove all the moisture content from the catalyst. The presence of water at the reaction time t=0 can in fact decelerate the esterification reaction rate and limit the reaction equilibrium.

In conclusion to this paragraph, it can be stated that D5081 is more active than A46 in all the studied reaction conditions.

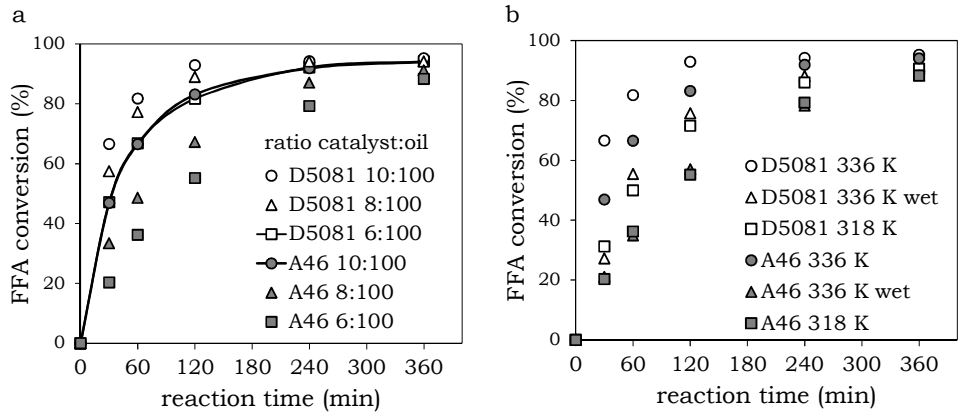

Fig. 3.4. Comparison between catalysts Amberlyst®46 and Purolite®D5081 at a) different catalyst loadings and b) different temperatures and in absence of drying pre-treatment (wet catalyst). Acid rapeseed oil (~5%$_{wt}$ FFA), slurry reactor, 336 K, MeOH:oil=16:100.

3.3.5 Recycles of use of the ion exchange resins

Although the catalysts deactivation and decay with time are crucial issues for industrial applications, only little data dealing with catalyst duration or catalyst recycle are reported in the literature. When available, these data refer to relatively short periods of use with a limited number of cycles. For example, Pasias et al. (Pasias et al., 2006) studied the deactivation of A15 across 8 runs of 12 h each; likewise, Ni and Meunier (Ni and Meunier, 2007) tested the catalysts for 4 cycles, each lasting 3 h. Needless to say, these results do not allow any estimation of the performance trend of the catalysts in long-term operations, as requested by industrial applications. Moreover, the catalyst stability depends on the operating mode of the reactor employed (batch, semibatch, continuous) and on the operating parameters (stirring velocity, temperature and pressure, amount of catalyst, etc.). A deep study concerning A46's lifetime in order to conceive an optimized system for the FFA esterification is already reported in a previous study (Pirola et al., 2010). In this work, 90 consecutive runs, each lasting 6 hours for a total operating time of 540 hr was performed using A46 as a catalyst for the FFA esterification. The results of this work show that A46 does not incur in chemical deactivation even after very long operating times, but it is necessary to avoid loss of the catalyst from the system to maintain a stable catalytic performance. Loss of the catalyst from the system may occur during the reactor discharge operations from one run to the other, as a consequence of catalyst fragmentation. Mechanical stress caused by the stirring may in fact provoke the fragmentation of the catalyst into smaller debris that remain in the oil and are lost during slurry reactor discharge operations. These drawbacks can be

avoided by the use of a continuous reactor to be fed with a stable MeOH/oil emulsion (Pirola et al., 2010).

The results presented hereinafter were carried out taking care that mechanical shovel used to stir the reaction medium did not come directly in contact with the catalyst at the bottom of the slurry reactor.

In Fig. 3.5. the results of the recycles of use of catalysts A15, A46 and D5081 are shown. It can be seen that A46 and D5081 maintain very good versions, higher than 90%, in all the recycles of use, differently from A15.

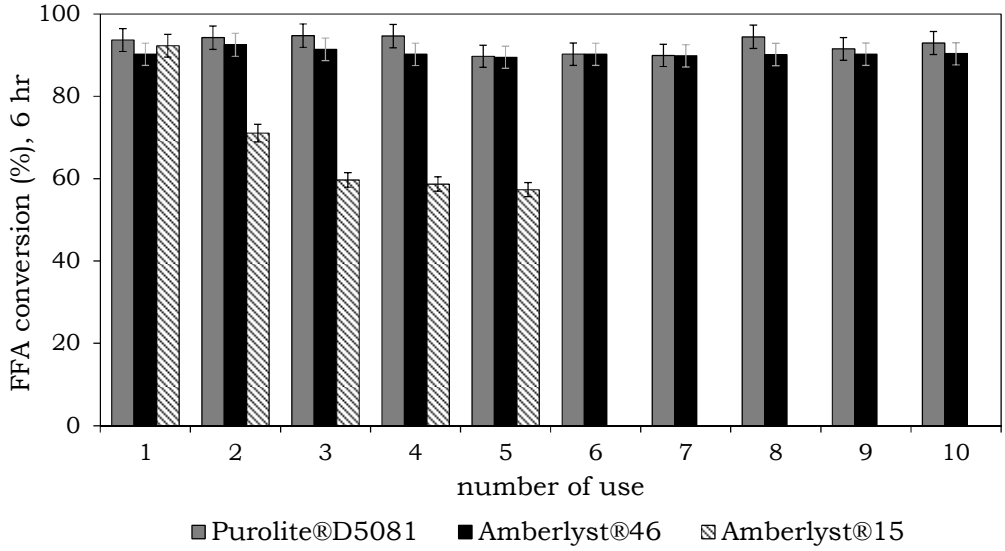

Fig. 3.5. Results of the deacidification by FFA esterification reaction with different ion exchange resins as a catalyst. Acid rapeseed oil (~5%$_{wt}$ FFA), slurry reactor, 336 K, catalyst:oil=10:100, MeOH:oil=16:100.

A good conversion is obtained with A15 at the first use of the catalyst, but then its catalytic activity drastically drops after each recycle. The total loss of activity was estimated to be around 30% within the 5 recycles. A possible explanation concerning this loss of activity may be related to the adsorption of the water yielded by the esterification on the active sites, which can make them unavailable

for the catalysis. In the first run the catalytic action takes places on both inner and outer surface of the grains of A15. More in detail, methanol is firstly adsorbed on the active sulphonic acid sites, thus forming a sort of wreath around the particles and increasing the pores diameter due to the swelling action. FFA diffuse towards the catalyst, and dissolve in the methanol. Then, they penetrate inside the pores of the catalyst and undergo to the catalysis both on the inner and the outer surface. When water molecules are formed inside the pores, they are not able to give internal retro-diffusion due to their strong interaction with H^+ sites and form an aqueous phase inside the pores. The formation of this phase prevents FFA from reaching internal active sites due to repulsive effects. In this way the number of active sites available for the catalysis drastically drops within few recycles of use. Catalyst A46 shows a lower activity than A15 at the first use, but it is able to maintain a better performance over time. Differently from A15, in fact, A46 and D5081 has only superficial active sites, as well as D5081. This confers absence of mass transfer limitation, minimization of side products formation and stable catalytic activity (Pirola et al., 2010; Bianchi et al., 2011; Boffito et al., 2012a; 2012b).

No loss of activity is observed for A46 and D5081 in the slurry reactor. A fluctuation in the FFA conversions is rather recognizable. This is worthy for A46 as well as for D5081. To better explain this result, in Fig. 3.6 the results of 15 consecutive recycles performed on D5081 are shown.

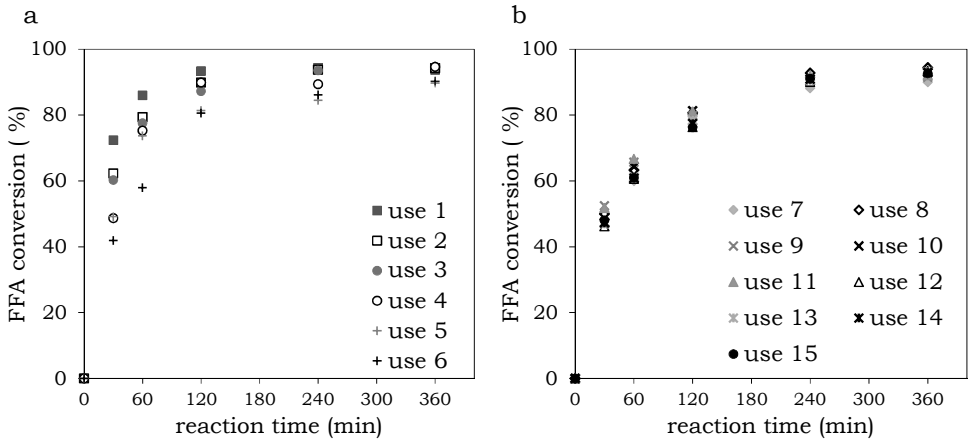

Fig. 3.6. Results of the deacidification by FFA esterification reaction with D5081 as a catalyst. Acid rapeseed oil (~5%$_{wt}$ FFA), slurry reactor, 336 K, catalyst:oil=10:100, MeOH:oil=16:100.

As it can be observed, the kinetic curves of the first six recycles of use are not reproducible and the FFA conversion at the same time fluctuates for the various uses. Differently, from 7th recycle of use on, the kinetic curves overlap almost perfectly. This behaviour was already observed for the two catalysts in a recent work (Boffito et al., 2012a) and is ascribable to the catalyst that has to settle in the system. A stable performance of the catalyst, is usually observed from the 8th to the 10th use, depending on the kind of substrate (Bianchi et al., 2011; Boffito et al., 2012a).

Due to the high reproducibility of this data, they were deemed suitable for kinetic modelling. The results will be shown in the next paragraph.

Recycles of catalyst use were also performed on brassica juncea and on the second stock of tobacco (tobacco2) oilseeds. The results are displayed in Fig. 3.7.

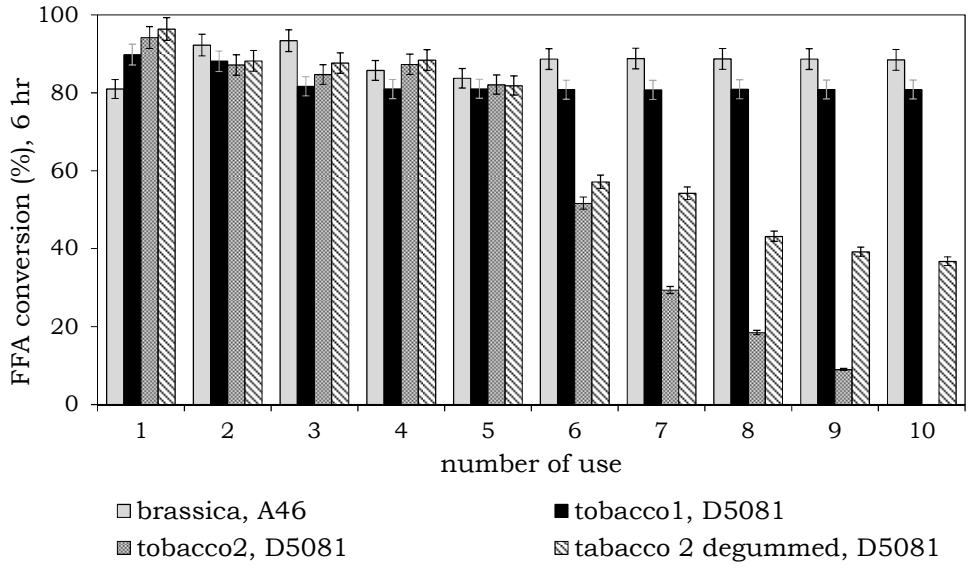

Fig. 3.7. Results of the deacidification by FFA esterification reaction of different oils, slurry reactor, 336 K, catalyst:oil=10:100, MeOH:oil=16:100.

As it can be seen the resins adopted as catalysts are able to maintain excellent catalytic performances also in raw oils such as brassica juncea and tobacco oilseeds. Nevertheless, a dramatic decrease of the FFA conversion was observed in the case of the deacidification of the 2nd stock of tobacco oil (tobacco2). A46's catalytic activity drops of the 100% within the first ten recycles of use. It was thought that this phenomenon might have been related to the presence of phospholipids (gums) in the oil.

The common oilseeds as soybean, cottonseed, sunflower and rapeseed are rich sources of phospholipids (Indira et al., 2000; Willem et al., 2008). Phospholipids pose many problems for the storage and processing of the crude oil and are usually removed from oil during refining by a process known as degumming (Brekke, 1975). In the case of the present work, none of the raw oils underwent to the degumming process.

There are two types of phospholipids: hydratable (HPL) and nonhydratable (NHPL). Most of the phospholipids in crude sunflower and rapeseed oils are hydratable and can be removed by water degumming (Carelli et al. 1997). NHPL are not hydratable with water, cannot swell and form gels or precipitate from oil (Szydlowska-Czerniak 2007). Removing of NHPL requires more complex processes at increased temperature with the use of phosphoric acid, citric acid or other degumming substances (Zufarov et al., 2008).

A hypothesis concerning the deactivation of D5081 is related to the absorption of HPL on the resin, and, in particular, on the active acid sites responsible for the catalysis. As a consequence, it was decided to perform a standard degumming process with sulphuric acid, followed by a new set of deacidification runs. The results are displayed in Fig. 3.7. D5081's deactivation is much slower in the case of degummed than for the non-degummed tobacco oil. However, the overall catalyst activity drops of the 60% within the 10 recycles in any case. This might be due to the presence of other impurities in the tobacco oil or to an insufficient degumming.

3.3.6 Process simulation

In order to develop a process simulation of the FFA esterification, able to predict the reaction progress, thermodynamic and kinetic analyses were performed.

3.3.6.1 Thermodynamic aspects

The considered reaction system turns out to be a highly non-ideal system, being formed by a mixture of oil, methylester, methanol,

FFA and water. The interactions among these molecules are absolutely not ideal, in fact they are only partially soluble and a two phase system is formed if the quantity of methanol is greater than 6%$_{wt}$. Indeed, the activity coefficients are used not only for the phase and chemical equilibria calculations, but also for the kinetic expressions. Modified UNIFAC model was used adopting the parameters available in literature and published by Gmehling et al. (Gmehling et al., 2002). The modified UNIFAC model adopted is known as "Dortmund modified UNIFAC" and was already available in the simulation software used (PROII, Simsci-Esscor) referred as "UFT2".

3.3.6.2 Reaction kinetic

The considered reaction is the following:

$$\text{FFA} + \text{MeOH} \underset{k_{-1}}{\overset{k_1}{\rightleftharpoons}} \text{methylester} + \text{water}$$

where the forward reaction is the FFA esterification and the backward reaction is the hydrolysis.

The oil is considered as non-reacting solvent, being present in large quantity.

A pseudo-homogeneous model was used for describing the kinetic behaviour of the reaction (Pöpken et al., 2000). The adopted model is displayed in the following equation (3.1.):

$$r=\frac{1}{m_{cat}}\frac{1}{\upsilon_i}\frac{dn_i}{dt}k_1 a_{FFA}a_{methanol}-k_{-1}a_{methylester}a_{water} \qquad 3.1$$

where

r= reaction rate

m_{cat}= dry mass of catalyst, in grams;
υ_i= stoichiometric coefficients of component i;
n_i= moles of component i;
t = reaction time;
k_1= kinetic constant of direct reaction;
k_{-1}= kinetic constant of indirect reaction;
a_i= activity of component i

Being the system non ideal, activities are calculated using the activity coefficients according to equation 3.2:

$$a_i=\gamma_i c_i \qquad 3.2$$

where a_i, γ_i and c_i are the activity, the activity coefficient and the concentration of the component *I*, respectively.

The temperature dependence of the rate constant is expressed by the Arrhenius law, shown in equation 3.3.

$$k_i=k_{i,0}exp\left(\frac{-E_{a,i}}{RT}\right) \qquad 3.3$$

where $k_{i,0}$ and $E_{a,i}$ are the pre-exponential factor and the activation energy of the reaction i (i=1 for the direct reaction, i=-1 for the indirect reaction), respectively, T is the absolute temperature and R the Universal Gas Constant.

The adopted parameters set is the same reported by Steinigeweg and Gmehling (Steinigeweg and Gmehling, 2003). The absolute values of pre-exponential factors were however corrected as reported in Tab. 3.5 for both A46 and D5081, so to take into account the presence of both a second liquid phase and a different type of

catalyst. The ratio of pre-exponential factors was kept constant at: $Keq(T) = k^0_1/k^0_{-1} = 60.78$.

Reaction	k^0_i D5081 (mol kg^{-1} s^{-1})	k^0_i A46 (mol kg^{-1} s^{-1})	$E_{A,i}$ ($kJmol^{-1}$)
esterification (1)	3039.0	1306.8	68.71
hydrolysis (-1)	50.00	21.50	64.66

Tab. 3.5. Pre-exponential factors (k^0_i) and activation energies ($E_{A,i}$) adopted in the pseudo-homogeneous model for the different catalysts.

All the simulations were carried using Batch Reactor of the simulation software PRO II (Simsci – Esscor).

3.3.6.3 Comparison theoretical vs. experimental.

In Fig. from 3.8 to 3.10 the comparison between the FFA conversions measured experimentally and the ones calculated with the theoretical model as described above are shown.

data are reported, while above the outgoing arrow the calculated and experimental FFA conversions are shown for each case.

In Fig. 3.8. the results of the FFA conversions calculated with the conventional UNIFAC model are displayed. The adopted modified UNIFAC thermodynamic model, the “Dortmund” model, reproduces the experimental data much better than the conventional UNIFAC model.

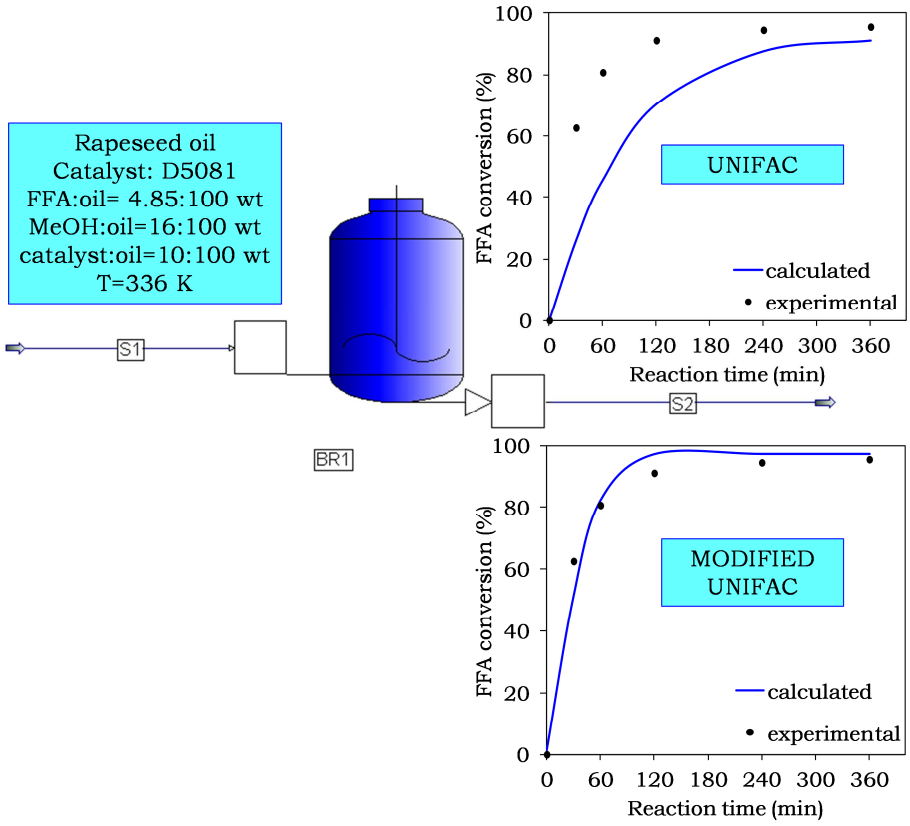

Fig. 3.8. Input data and comparison experimental and calculated FFA conversions for the FFA esterification of an acid rapeseed oil at 336 K, 10th recycle of catalyst use. Catalyst: D5081.

The correlation between the calculated and the experimental FFA conversions is quite good. In particular, the chosen kinetic model, together with the thermodynamic one, allows predicting the time for achievement of the plateau of conversion in a rather good way. The modified UNIFAC (Dortmund) parameters allow a reliable prediction of phase equilibria involved in the studied reaction. Moreover, being a predictive model, it does not require experimental data regression, that could result very laborious in some cases.

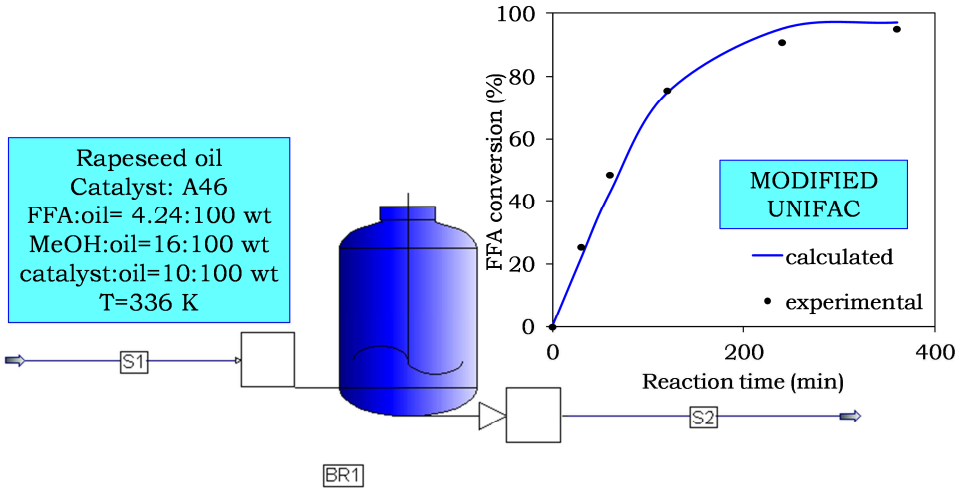

Fig. 3.9. Input data and comparison experimental and calculated FFA conversions for the FFA esterification of an acid rapeseed oil at 336 K, 10th recycle of catalyst used. Catalyst: A46.

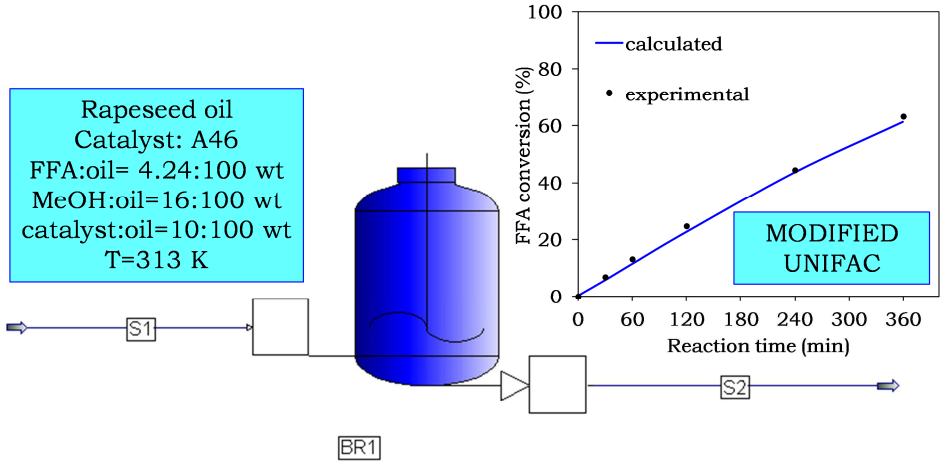

Fig. 3.10. Input data and comparison experimental and calculated FFA conversions for the FFA esterification of an acid rapeseed oil at 313 K, 10th recycle of catalyst use. Catalyst: A46.

3.4 Transesterification reaction

In the Tab. 3.6. the results of the transesterification reaction are reported. The acidic compositions of the oil have been already reported in Tab. 3.4.

Oil	Initial acidity (%wt FFA)	Acidity after esterification acidity (%wt FFA)	Cat.	Trans. yield (%wt FAME)	BD content (%wt FAME)
tobacco2 (deacidified 2 times)	6.17	0.10	CH_3ONa	93.8	99.9
			KOH	88.9	95.0
crude rapeseed oil	2.20	0.09	CH_3ONa	96.8	98.9
			KOH	89.4	91.5
Rapeseed oil	4.17	0.32	CH_3ONa	92.7	96.5
			KOH	92.5	96.3
Winterized sunflower	0.50	0.32	CH_3ONa	92.4	96.6
			KOH	95.2	95.4
Brassica juncea	0.74	0.23	CH_3ONa	97.5	98.0
			KOH	96.7	97.2

Tab. 3.6. Transesterification yields and biodiesel (BD) content of the deacidified oils transformed into BD.

The transesterification reaction is known to be an equilibrium-limited reaction and it is therefore usually performed in two steps, as described in the experimental part. A second step is necessary to convert the unreacted mono- and di-glycerides to glycerol and methyl esters. Biodiesel yields around 90% were obtained in this work at the end of the first step (90 minutes). This result is in agreement with what also Gole (Gole et al., 2012) and Çayli (Çayli et al., 2008) found in the same experimental conditions adopted in this work. After the first step, the separation of glycerol and the addition of fresh catalyst and methanol were required to shift the reaction equilibrium towards the products. The second step was then carried

out for an additional hour to obtain biodiesel yields higher than 96.5%, which is the minimum FAME concentration required by the European normative on biodiesel (EN 14214).

The transesterification yields reported in Tab 3.4 represent the % of triglycerides transformed into FAME, while the BD content represents the total concentration of FAME (in $\%_{wt}$) yielded by both the esterification and the transesterification.

The limit set by the EN 14214 is achieved in all the case using CH_3ONa and in the case of Brassica juncea also using KOH.

The higher transesterification yields obtained with CH_3ONa might be due to the establishment of the following equilibrium in presence of methanol:

$$CH_3ONa + CH_3OH \rightleftharpoons CH_3O^- + Na^+ + CH_3OH$$

where the formation of the nucleophile CH_3O^- is accompanied by the formation of methanol instead of water, which occurs when KOH or NaOH are used as catalysts:

$$KOH + CH_3OH \rightleftharpoons CH_3O^- + K^+ + H_2O$$

However, quite high yields were obtained for both the refined rapeseed oil and the raw oilseeds, in spite of their bad conservation state.

Considering the rather high transesterification yields obtained, it can be concluded that the pre-esterification method was effective in substantially reducing the free acidity of the raw oils, so making possible to perform easily their transformation into BD.

3.5 Conclusions

Considering the results of the characterization of the oils, feedstock with high potential to be used as raw materials for pure biodiesel (B100) are *Brassica juncea* oilseed and blends of waste cooking oil (WCO) with rapeseed and tobacco oilseeds. Also other oils present very good intrinsic properties to be transformed into BD, but they are foodstuff. In this work the benefits of blending have been demonstrated: mixing WCO with rapeseed oil or tobacco oil not only improves the properties of the feedstock but also fasten the FFA esterification reaction rate. All the oils, both refined and raw ones, were in fact successfully deacidified, bringing the FFA content below the 0.5%$_{wt}$, i.e. the limit imposed by European Normative on biodiesel (EN 14214) and also required by the transesterification. This limit was not achieved in the case of the tobacco oilseed referred as tobacco2 and in the case of the WCO.

All the sulphonic acid ion exchange resins adopted (Amberlyst®15, 46 and Purolite®D5081) exhibit a very good activity in the FFA esterification reaction. However, just A46 and D5081 demonstrated to be able to maintain the good performance over time, being recycled several times. This is attributable to their particular egg-shell configuration, whereby the acid active sites are located just on their external surface and not inside the pores. This ensures avoidance of mass transfer limitations, stability of the performance over time and minimization of side products formation.

Given the stability of the performance of A46 and D5081, a kinetic modelling was performed and the results were compared with the experimental ones. A good correlation between the experimental and the calculated data was achieved using the pseudohomogeneous kinetic model and activities instead of

concentrations. The adoption of the modified-UNIFAC Dortmund model resulted to give the best experimental-theoretical correlation.

Transesterification experiments performed on deacidified oils resulted in rather high yields, demonstrating that the pre-esterification method was effective in lowering the free acidity so allowing performing a trouble-free transformation into BD.

References

Alcantara R., Amores J., Canoira L., Fidalgo E., Franco M.J., Navarro A., "Catalytic production of biodiesel from soy-bean oil, used frying oil and tallow", *Biomass Bioenergy* **2000,** 18, 515.

Ali N., Shah S.A.H., "Seed yield and oil contents in poorbi raya (Brassica Juncea) as affected by number and time of irrigations", *Pak. J. Agric. Res.* **1982,** 3(2), 138.

Andrianov V., Borisjuk N., Pogrebnyak N., Brinker A., Dixon J., Spitsin S., Flynn J., et al., "Tobacco as a Production Platform for Biofuel: Overexpression of Arabidopsis DGAT and LEC2 genes Increases Accumulation and Shifts the Composition of Lipids in Green Biomass", *Plant Biotechnol. J.* **2010,** 8, 277ISSN 1467-7644.

AOCS Lipid library, http://lipidlibrary.aocs.org/market/palmoil.htm .

Beckman, C., "Vegetable Oils: Situation and Outlook", Bi-weekly Bulletin, 2007, Vol. 20, No.7. Market Analysis Division. Research and Analysis Directorate Strategic Policy Branch and Agriculture and Agri-Food Canada, Manitoba, Canada.

Beer L.L., Boyd E.S., Peters J.W., Posewitz M.C., "Engineering algae for biohydrogen and biofuel production", *Curr. Opin. Biotechnol.* **2009,** 20, 264.

Berchmans H.J., Hirata S., "Biodiesel production from crude Jatropha curcas L. seed oil with a high content of free fatty acids", *Bioresour. Technol.* **2008,** 99, 1716.

Bianchi C.L., Boffito D.C., Pirola C., Ragaini V., "Low temperature de-acidification process of animal fat as a pre-step to biodiesel production", *Catal. Lett.* **2010,** 134, 179.

Bianchi C.L., Pirola C., Boffito D.C., Di Fronzo A., Carvoli G., Barnabè D., Bucchi R., Rispoli A., "Non edible oils: raw materials for sustainable biodiesel", in: Feedstocks and Processing Technologies, M. Stoytcheva (Ed.), ISBN: 978-953-307-713-0, InTech **2011**, pp. 3-22.

Boffito D.C., Pirola C., Bianchi C.L., "Heterogeneous catalysis for free fatty acids esterification rea.ction as a first step towards biodiesel production", *Chem, Today***, 2012a**, 30, 14.

Boffito D.C., Crocellà V., Pirola C., Neppolian B., Cerrato G., Ashokkumar M., et al., "Ultrasonic enhancement of the acidity, surface area and free fatty acids esterification catalytic activity of sulphated ZrO2-TiO2 systems", *J. Catal.* **2012b**, accepted on September 2012., DOI: 10.1016/j.jcat.2012.09.013.

Boffito D.C., Pirola C., Galli F., Di Michele A., Bianchi C.L., "Free Fatty Acids Esterification of Waste Cooking Oil and its mixtures with Rapeseed

Oil and Diesel", *Fuel* **2012c**, accepted on 19th October 2012, DOI: 10.1016/j.fuel.2012.10.069.

Brekke O.L., In Handbook of Soy Oil Processing, Ed. Oil Degumming and Soybean Lecithin and Utilization. Vol 1, pp 71-78, American Soybean Association, St. Louis, and American Oil Chemists' Society, Champaign, Illinois, **1975**.

Carelli A.A., Brevedan M.I.V., Crapiste G.H., "Quantitative Determination of Phospholipids in Sunflower Oil", *J. Am. Oil Chem. Soc.* **1997,** 74, 511.

Çayli G., Küsefoğlu S., "Increased yields in biodiesel production from used cooking oils by a two step process: Comparison with one step process by using TGA", *Fuel Proc. Technol.* **2008**, 89, 118.

Chakrabarty M.M., "Chemistry and Technology of Oils and Fats", Allied Publishers Pvt. Ltd, 2003, ISBN : 81-7764-495-5.

Chan A.P., Crabtree J., Zhao Q., Lorenzi H., Orvis J., Puiu D., Melake-Berhan A., et al., "Draft genome sequence of the oilseed species Ricinus communis", *Nat. Biotechnol.* **2010,** 28, 951; ISSN 1087-0156.

Clixoo, "Preview of Comprehensive Castor Oil Report", In: Castor Oil Industry Reference & Resources, 30.05.2011, Available from http://www.castoroil.in.

Curto G., Lazzeri L., "Brassicacee, un Baluardo Sotterraneo Contro i Nematodi", *Agricoltura* **2006,** 34(5), 110.

Dar W.D., "Research needed to cut risks to biofuel farmers", Science and Development Network, 6 December 2007, http://www.scidev.net/en/opinions/research-needed-to-cut-risks-to-biofuel-farmers.html.

Demirbas M.F., "Biofuels from algae for sustainable development", *Appl. Energy* **2011,** 88, 3473.

Dunn R.O., "Effect of antioxidants on oxidative stability of methyl soyate", *Fuel Process. Technol.* **2005,** 86, 1071.

Encinar J.M., Gonzalez J.F., Rodriguez-Reinares A., "Biodiesel from used frying oil. Variables affecting the yields and characteristics of the biodiesel", *Ind. Eng. Chem. Res.* **2005,** 44, 5491.

Feddern V., Cunha Jr. A., Prá M.C., Abreu P.G.De, Santos Filho J.I.Dos, Higarashi M.M., Sulenta M., Coldebella A., "Animal fat wastes for biodiesel production." In: Stoytcheva M., Montero G. (Ed.), Biodiesel: feedstocks and processing technologies. Rijeka: Intech Open, 2011. p. 45-70.

Fogher C., "Sviluppo di un Ideotipo di Tabacco per la Produzione di Seme da Usare a Fini Energetici", Presented at the workshop "La Filiera del Tabacco in Campania: Ristrutturazione e/o Riconversione. La ricerca come motore per l'innovazione tecnologica, la sostenibilità e la competitività della filiera", Portici, Italy, February, **2008**.

Fukuda H., Kondo A., Noda H., "Biodiesel fuel production by transesterification of oils", *J. Biosci. Bioeng.* **2001,** 92, 405.

Gasol C.M., Gabarrella X., Antonc A., Rigolad M., Carrascoe J., Ciriae P., Solanoe M.L., Rieradeva J., "Life Cycle Assessment of a Brassica carinata Bioenergy Cropping System in Southern Europe", *Biomass Bioenergy* **2007,** 31(8), 543; ISSN 0961-9534.

Gmehling J., Wittig R., Lohmann J., Joh R., "A Modified UNIFAC (Dortmund) Model. 4. Revision and Extension", *Ind. Eng. Chem. Res.* **2002,** 41, 1678.

Gole V.L., Gogate P.R., "Intensification of synthesis of biodiesel from nonedible oils using sonohchemical reactors", *Ind. Eng. Chem. Res.* **2012**, 51(37), 11866.

Graham L.E., Graham J.E., Wilcox L.W., "Algae", 2nd ed., Benjamin-Cummings Publishing: Menlo Park, CA, 2008; ISBN: 0321559657.

Gyulai J., "Market outlook for safflower", Proceedings of North American Safflower Conference, Great Falls, MT, 1996, p 15.

Holanda A., "Biodiesel e Inclusão Social", Câmara dos Deputados, Coordenação de Publicações, Brasília, Brazil, 2004, Retrieved from http://www2.camara.gov.br/acamara/altosestudos/pdf/biodiesel-e-inclusao-social/biodiesel-e-inclusao-social.

IENICA, "Agronomy Guide, Generic guidelines on the agronomy of selected industrial crops", Interactive European Network for Industrial Crops and their Applications, August **2004**, Retrieved from http://www.ienica.net/agronomyguide/agronomyguide05.pdf.

Ilkiliç C., Aydin S., Behcet R., Aydin H., "Biodiesel from safflower oil and its application in a diesel engine", *Fuel Process. Technol.* **2011,** 92(3), 356.

Indira T.N., Hemavathy J., Khatoon S., Gopala Krishna A.G., Bhattacharya S., "Water degumming of rice bran oil: a response surface approach", *J. Food Eng.* **2000,** 43(2), 83.

Janaun J., Ellis N., "Perspectives on biodiesel as a sustainable fuel", *Renewable Sustainable Energy Rev.* **2010,** 14(4), 1312; ISSN 1364-0321.

King A.E., Roschen H.L., Irwin W.H., "An accelerated stability test using the peroxide value as an index", *J. Am. Oil Chem. Soc.* **1933,** 10(6), 105.

Krisnangkura K., "A simple method for estimation of cetane index of vegetable oil methyl ester", *J. Am. Oil Chem. Soc.* **1986,** 63, 552.

Kulkarni M.G., Dalai A.K., "Waste cooking oil-an economical source for biodiesel: a review", *Ind. Eng. Chem. Res.* **2006,** 45, 2901.

Kumar A., Sharma S., "An evaluation of multipurpose oil seed crop for industrial uses (Jatropha curcas L.): a review", *Ind. Crops Prod.* **2008,** 28, 1.

Kumar G.P., Yadav S.K., Thawale P.R., Singh S.K., Juwarkar A.A., "Growth of Jatropha curcas on heavy metal contaminated soil amended with

industrial waste and Azotobacter - a greenhouse study", *Bioresour. Technol.* **2008,** 99, 2078.

Kumari A., Mahapatra P., Garlapati V.K., Banerjee R., "Enzymatic transesterification of Jatropha oil", *Biotechnol. Biofuels*, **2009**, doi:10.1186/1754-6834-2-1.

Lee S.B., Han K.H., Lee J.D., Hong I.K., "Optimum process and energy density analysis of canola oil biodiesel synthesis", *J. Ind. Eng. Chem.* **2010,** 16, 1006.

Li Z., Lin B.L., Zhao X., Sagisaka M., Shibazaki R., "System approach for evaluating the potential yield and plantation of Jatropha curcas L. on a global scale", *Environ. Sci. Technol.* **2010,** 44, 2204.

Liu B., Benson A.G., "Winter Safflower Biodiesel: A Green Biofuel for the Southern High Plains.", Presentation at the Southern Agricultural Economics Association meetings, Corpus Christi, TX, 2011.

López D. E., Suwannakarn K., Bruce D. A., Goodwin JG. "Esterification and transesterification on tungstated zirconia: Effect of calcination temperature", *J. Catal.* **2007**, 247, 43.

Makkar H.P.S., Becker K., "Jatropha curcas, a promising crop for generation of biodiesel and value-added coproducts", *Eur. J. Lipid Sci. Technol.* **2009,** 111, 773.

Marmesat S., Rodriguez-Macado E., Velasco J., Dorbangarnes M.C., "Used frying fats and oils: comparison of rapid tests based on chemical and physical oil properties", *Int. J. Food Sci. Technol.* **2007,** 42, 601.

Mejia J.D., Salgado N., Orrego C.E., "Effect of blends of Diesel and Palm-Castor biodiesels on viscosity, cloud point and flash point", *Ind. Crops Prod.* **2013,** 43, 791.

Menetrez M.Y., "An Overview of Algae Biofuel Production and Potential Environmental Impact", *Environ. Sci. Technol.* **2012,** 46, 7073.

Mullner K., Happe T., "Biofuel from algae-photobiological hydrogen production and CO2-fixation", *Int. J. Energy Technol. Policy* **2007,** 5, 290.

Ni J., Meunier F.C., "Esterification of Free Fatty Acids in Sunflower Oil over Solid Acid Catalysts Using Batch and Fixed-Bed Reactors", *Appl. Catal. A* **2007,** 333, 122.

Öezbay N., Oktar N., Tapan N.A., "Esterification of Free Fatty Acids in Waste Cooking Oils (WCO): Role of Ion-exchange Resins", *Fuel* **2008,** 87, 1789.

Openshaw K., "A review of Jatropha curcas: an oil plant of unfulfilled promise", *Biomass Bioenergy* **2000,** 19, 1.

Pan X., "A Two Year Agronomic Evaluation of Camelina sativa and Brassica carinata in NS, PEI and SK", Master degree thesis, 2009, Dalhousie University, Halifax, Canada, Retrieved from Digital Repository Unimib

database of Dalhousie University at http://dalspace.library.dal.ca/handle/10222/12370.

Pasias S., Barakos N., Alexopoulos C., "Heterogeneously catalyzed esterification of FFAs in vegetable oils", *Chem. Eng. Technol.* **2006,** 29, 1365.

Perego C., Bosetti A., "Biomass to fuels: The role of zeolite and mesoporous materials", *Microporous Mesoporous Mater.* **2011,** 144, 28.

Perego C., Ricci M., "Diesel fuel from biomass", *Catal. Sci. Technol.* **2012,** 1, 1776.

Pimentel D., Patzek T.W., "Ethanol Production Using Corn, Switchgrass, and Wood; Biodiesel Production Using Soybean and Sunflower", *Nat. Resour. Res.* **2005,** 14(1), 65; DOI: 10.1007/s11053-005-4679-8.

Pimentel D., Patzek T.W., "Ethanol Production Using Corn, Switchgrass, and Wood; Biodiesel Production Using Soybean and Sunflower", in Food, Energy and Society, Third Edition, Edited by Marcia H . CRC Press **2007**, Pages 311-331.

Pimentel D., "The limitations of biomass energy", in Meyers, R., ed., Encyclopedia of Physical Science and Technology (3rd edn.), **2001**, Vol. 2: Academic, San Diego, CA, p. 159-171.

Pinto A.C., Guarierio L.L.N., Rezende M.J.C., Ribeiro N.M., Torres E.A., Lopes W.A., Pereira P.A.de P., "Biodiesel: an Overview", *J. Braz. Chem. Soc.* **2005,** 16(6b), 1313; ISSN 0103-5053.

Pirola C., Bianchi C.L., Boffito D.C., Carvoli G., Ragaini V., "Vegetable oil deacidification by Amberlyst : study of catalyst lifetime and a suitable reactor configuration", *Ind. Eng. Chem. Res.* **2010,** 49(10), 4601.

Pirola C., Boffito D.C., Carvoli G., Di Fronzo A., Ragaini V., Bianchi C.L., "Soybean oil deacidification as a first step towards biodiesel production", In: D. Krezhova., editor., Recent Trends for Enhancing the Diversity and Quality of Soybean Products: Intech, **2011**, p. 321-44.

Pöpken T., Götze L., Gmehling J., "Reaction Kinetics and Chemical Equilibrium of Homogeneously and Heterogeneously Catalyzed Acetic Acid Esterification with Methanol and Methyl Acetate Hydrolysis", *Ind. Eng. Chem. Res.* **2000,** 39, 601.

Potts D.A., Rakow G.W., Males D.R., "Canola-Quality Brassica juncea, a New Oilseed Crop for the Canadian Prairies", Proceedings of the 10th International Rapeseed Congress, Canberra, Australia, September 1999.

Pramanik K., "Properties and use of Jatropha curcas oil and diesel fuel blends in compression ignition engine", *Renewable Energy* **2003,** 28, 239.

Razon L.F., "Alternative Crops for Biodiesel Feedstock", *CAB Reviews: Perspectives in Agriculture, Veterinary Science, Nutrition and Natural Resources* **2009,** 4(56), 1ISSN 1749-8848.

Saloua F., Saber C., Heidi Z., "Biodiesel production and characterization", *Bioresour. Technol.* **2010,** 101, 3091.

Santori G., Di Nicola G., Moglie M., Polonara F., "A review analyzing the industrial biodiesel production practice starting from vegetable oil refining", *Appl. Energ.* **2012,** 92, 109.

Sanzone E., Sortino O., "Ricino, Buone Prospettive Negli Ambienti Caldo-Aridi", *Terra e Vita - ed. Edagricole Il Sole 24 Ore* **2010,** 7, 28; ISSN 0040-3776.

Sarin R., Sharma M., Sinharay S., Malhotra R.K., "Jatropha-Palm biodiesel blends: An optimum mix for Asia", *Fuel* **2007,** 86, 1365.

Skoric D., Jocic S., Sakac Z., Lecic N., "Genetic possibilities for altering sunflower oil quality to obtain novel oils.", *Can. J. Physiol. Pharmacol.* **2008,** 86(4), 215.

Steinigeweg S., Gmehling J., "Esterification of a Fatty Acid by Reactive Distillation", *Ind. Eng. Chem. Res.* **2003,** 42, 3612.

Szydłowska-Czerniak A., "MIR Spectroscopy and Partial Least-Squares Regression for Determination of Phospholipids in Rapeseed Oils at Various Stages of Technological Process", *Food Chem.* **2007,** 10(3)5, 1179.

Tamalampudi S., Talukder M.R., Hama S., Numata T., Kondo A., Fukuda H., "Enzymatic production of biodiesel from Jatropha oil: a comparative study of immobilized-whole cell and commercial lipases as a biocatalyst", *Biochem. Eng. J.* **2008,** 39, 185.

Tickell J., "Biodiesel America: How to achieve energy security, Free America from middle-east oil dependence and make money growing fuel", Yorkshire Press, 2006, USA, ISBN 9780970722744.

USDA, Foreign Agricultural Service, March 18 2010, Available from: http://www.fas.usda.gov/psdonline/ .

Velasco L., Goffman F.D., Becker H.C., "Variability for the fatty acid composition of the seed oil in a germplasm collection of the genus Brassica", *Genet. Resour. Crop Evol.* **998,** 45(4), 371.

Willem V.N., Mabel C.T., "Update on vegetable lecithin and phospholipid technologies", *Eur. J. Lipid Sci. Technol.* **2008,** 110, 472.

Winayanuwattikun P., Kaewpiboon C., Piriyakananon K., Tantong S., Thakernkarnkit W., Chulalaksananukul W., et al., "Potential plant oil feedstock for lipase-catalyzed biodiesel production in Thailand", *Biomass Bioenergy* **2008,** 32, 1279.

Xie W., Huang X., Li H., "Soybean oil methyl esters preparation using NaX zeolites loaded with KOH as a heterogeneous catalyst", *Bioresour. Technol.* **2007,** 98(4), 936.

Zabanioutou A.A., Kantarelis E.K., Theodoropoulos D.C., "Sunflower shells utilization for energetic purposes in an integrated approach of energy

crops: laboratory study pyrolysis and kinetics", *Bioresour. Technol.* **2008,** 99(8), 3174.

Zufarov O., Schmidt Š., Sekretár S., "Degumming of rapeseed and sunflower oils", *Acta Chimica Slovaca* **2008,** 1(1), 321.

CHAPTER 4:
WASTE COOKING OIL FOR BIODIESEL PRODUCTION

Abstract

The choice of waste cooking oil (WCO) as a raw material for biodiesel production is recognized to be an attractive and Economic alternative to the use of vegetable oils. However, the presence of free fatty acids, impurities and high viscosity of WCO may require several pretreatments before the transesterification. In this study WCO deacidification by esterification is investigated: the results show how both Amberlyst®46 and Purolite®D5081 catalysts maintain their performance in a Carberry reactor (where catalyst is confined to minimize mechanical stress) and a slurry reactor after several recycles. A46 was tested in the free fatty acids esterification of blends of WCO with different ratios of crude rapeseed oil and diesel as a solvent. The results show how both the use of the blends with another oil with lower viscosity and diesel are both beneficial to the reaction rate and to the properties of the finished biodiesel.

4.1 Introduction

Nowadays, there is an enormous amount of waste lipids generated from restaurants, food processing and industries, which regrettably is mostly poured into the sewer system of the cities. This practice contributes to the pollution of rivers, lakes, seas and underground water, which is very harmful to the environment and human health. This opens a wide opportunity for the use of waste cooking oil (WCO) as a feedstock for liquid biofuels.

The high WCO potential is recognized also by the EU directive 2009/28/EC, where waste vegetable or animal oil BD is reported to save about the 88% of greenhouse emissions, a quite high value if compared to biodiesel from common vegetable oils, whose

greenhouse emission savings range from 36 to 62%. The main issue posed by such a raw material is the need of its standardization, especially with regard to the decrease of acidity. Several methods have been proposed to solve this problem. Among them (Xingzhong et al., 2009, Rao et al., 2009; Ono et al., 1979) the free fatty acids (FFA) pre-esterification method (Lotero et al., 2005; Pirola et al., 2011; 2010; Bianchi et al., 2011; 2010; Boffito et al., 2012a; 2012b), has recently received much attention since it improves the final yield in methyl esters, i.e. BD, as reported in Scheme 1.2.

Recent work has focused on the use of inorganic catalysts (Boffito et al., 2012a; 2012b) and ion exchange acid resins (Pirola et al., 2011; 2010; Bianchi et al., 2011; 2010) as catalysts for the FFA esterification performed in several different raw oils. Very high FFA conversions were obtained using crude animal fat as a feedstock, with different kinds of Amberlysts as catalysts (Bianchi et al., 2010).

In this chapter a study of the effects of blending WCO with another oil on the FFA esterification reaction and the properties of the finished biodiesel is reported. The effect of using diesel as a solvent for the FFA esterification of WCO is also investigated for the first time.

Solid acid resins as heterogeneous catalysts: Amberlyst®15, Amberlyst®46 and Purolite®D5081 were used as heterogeneous catalysts. The reaction was carried out at very mild conditions, i.e. at a temperature of 336 K and atmospheric pressure. A slurry batch reactor and a Carberry reactor were used. In the slurry reactor the catalyst is suspended in the reaction medium, while in the Carberry reactor the catalyst is confined inside two baskets.

Although catalyst deactivation and decay with time are crucial issues for industrial applications, little data on these subjects have been published in literature (Russbuduelt et al., 2009).

In a recent work (Pirola et al., 2010), Pirola and co-authors investigate the mechanical and chemical stability of Amberlyst®46 (Dow Chemical) over long operating times (540 hours) in presence of different vegetable oils. The outcomes of this study show how Amberlyst®46 maintains a stable performance over the whole period. This makes of Amberlyst®46 a potential candidate for industrial application of FFA esterification of vegetable oil. To mention an open issue, the use of WCO might lead to the rapid chemical deactivation of the catalyst due to the presence of metals, in particular of sodium, deriving from the NaCl directly added to the food during the frying process and of a certain amount of iron(II), deriving from the iron cookware (Kröger-Ohlsen et al., 2002). Metals can easily replace the H^+ active sites of sulphonic groups, causing chemical deactivation. In this work the ion exchange capacity of Amberlyst®46 and metals content were quantified at the end of each of 6 consecutive deacidification runs of WCO and compared with the one of the fresh catalyst.

Besides to the high content of metals, another drawback of the use of the cooking oil in biodiesel production lies in its high viscosity, which makes WCO hardly processable. This aspect is particularly marked when the WCO is mainly composed by triglycerides with saturated fatty chains. It becomes therefore important to enrich the oil of unsaturated fatty chain and/or to add a solvent to lower its viscosity during the processing. In this work the FFA esterification of blends of WCO and crude rapeseed oil (CRO) in different ratios and the effect of diesel as a solvent is investigated.

4.2 Materials and Methods

4.2.1 Materials

WCO was kindly provided by a restaurant in Milan. WCO was first submitted to a rough filtration followed by drying under vacuum and vacuum filtration in order to remove water and solid deposits, respectively. The acidity content of each sample was measured before and after the filtrations.

Crude rapeseed oil (CRO) with an initial acidity of 2.2%$_{wt}$ was used.

The adopted catalysts were two Amberlysts®, namely A15d (A15) and A46w (A46) commercially available, provided by Dow Chemical, and one resin from Purolite®, D5081, which is still at the laboratory development stage.

All the resins used in this work are macroreticular strongly acidic cationic exchanger available in the dry or in the wet form. A46 and D5081 were provided in wet form, whereas A15 in dry form. Dry resins do not require any pre-treatment as the active sites are already free and available on the surface of the catalyst, whereas wet resins are swollen in a liquid medium, usually water, and the active sites are covered by a liquid phase. For this reason wet resins were preliminary submitted to a drying treatment at 383 K for 16 hours to completely remove water, so making the active sites available.

4.2.2. Characterization of the catalysts

The swelling capacity of A15, A46 and D5081 was evaluated in different swelling media: water, methanol and the acid crude

rapeseed oil. For this purpose, about 2 g of dry catalyst was placed into a graduated tube to measure its dry volume and then transferred into a flask and left in contact under agitation with 20 ml of the swelling medium for 6 hours, i.e. the duration of a FFA esterification test as performed in this study. The catalyst was then filtered, weighted and transferred into the measured tube to calculate the weight and volume gains respectively.

Percentage gains by weight and volume were calculated according to the equations 2.7 and 2.8, respectively (§ 2.2.5), as in other works Öezbay et al., 2008).

Acid capacity of the resins was quantified through an ion exchange with a saturated solution of NaCl and successive titration with NaOH 0.1 M, as done by López et al. (López et al., 2007). The presence of metals (Na, K, Ca, Mg and Fe) on fresh and used catalyst was verified by SEM-EDX analysis (FEG-LEO 1525 and Bruker Quantax EDS).

4.2.3 Characterization of the oils

All the reagents used are Fluka products and were used without further purification.

Viscosities and densities of the WCO and its blends with CRO were determined with the Anton Paar SVM 3000 Stabinger Viscosimeter. This instrument allows the measurements of dynamic viscosity and density (g/cm^3 at 15°C) at the same time, according to ASTM D7042 standard method. Kinematic viscosity (cSt at 40°C) is then automatically calculated by the instrument which delivers a measurement equivalent to ASTM D445 standard method. The Iodine value (IV), corresponding to the mass of I_2 contained in 100 g of sample and indicating the number of unsaturations in the oil, was

obtained by the Hannus method (EN 14111:2003). A mixture of glacial acetic acid (>99.85%) and cyclohexane (>99%) in 1:1 volume ratio was used as a solvent and KI aqueous solution 0.1 M to create the iodine excess. $Na_2S_2O_3$ 0.1 M and starch solution 1% in H2O were used as titrating agent and indicator, respectively.

Oil acidity was determined through titration analysis with KOH 0,05 M in ethanol (made by dilution of KOH 0.1 M). A mixture of diethylether: ethanol 9:1 by volume and phenolphthalein 2% in ethanol were used as titrating agent and indicator, respectively. The percentage of FFA content per weight was calculated as follows, as usual in similar works (Pirola et al. 2011; 2010; Bianchi et al., 2011, 2010):

$$FFA = \frac{V \times \overline{MW} \times C}{W} \times 100 \qquad 4.1$$

where V is the volume of KOH solution necessary for the titration (mL), $\overline{MW}$ is the average molecular weight of the acid contained in major quantity (mg mmol^{-1}), C is the concentration of KOH (mmol mL^{-1}) and W is the weight of the analysed sample (mg).

The acidic composition of the oils was determined by gas chromatography of the methyl esters yielded by the esterification. The capillary GC column OmegaWax (Sigma Aldrich) was used. The analysis was performed in isotherm at 210°C. He was used as a carrier at 70 kPa. Methylnonadecanoate (>99%, Fluka product) was used as internal standard and heptane as a solvent.

Average molecular weights of the FFA were calculated from the acidic composition using the following formula:

$$\overline{MW} = \sum MW_i \times A_i \qquad 4.2$$

where MW_i is the molecular weight and A_i the percentage of each fatty acid.

4.2.4 Esterification Tests

All the FFA esterification tests performed in this study, along with the adopted conditions, are listed in Tab. 4.1. WCO stands for Waste Cooking Oil while CRO for Crude Rapeseed Oil. The number next to WCO, CRO or diesel indicates the weight per cent of that specific component in the blend or the mixture.

The stoichiometric alcohol/acid ratio for the esterification reaction is 1:1, but it is advisable to use a higher amount of alcohol to shift the reaction towards the desired products. Moreover, it was necessary to take into account the high viscosity of the WCO, which can limit mass transfer of the reagents towards the catalyst. For these reasons the amount of methanol was calculated based on the actual oil mass inside the reactor rather than on reaction stoichiometry. Consequently 16 g of methanol were added per 100 g of oil in all the cases, corresponding to 4.5:1 MeOH:oil molar ratio, as already reported by the authors (Bianchi et al., 2011; 2010; Pirola et al., 2011; 2010; Boffito et al., 2012a; 2012b).

The used slurry-type reactor consists in a 250 mL three-neck glass flask, equipped with a thermometer and a coil condenser. The third neck was reserved for sampling. The temperature of 336±1 K was reached by mean of a thermostat. Stirring rate was kept constant at 100 rpm thanks to a mechanical stirrer.

In slurry-type reactors the catalyst is suspended in the reaction medium. 10 g of catalyst were used each 100 g of oil as in previous works (Bianchi et al., 2011; 2010; Pirola et al., 2011; 2010).

Carberry-type reactor, already described in a work by some of the authors (Ragaini et al., 2006), consists of a glass container provided with a mechanical stirrer (kept at 100 rpm), a thermometer and a coil condenser.

Entry	Feedstock	$\%_{wt}FFA_{t=0}$	Reactor	Cat.	g_{cat}/100 g oil	g_{cat}/100 g feedstock	Number of catalyst re-uses
1	WCO	2.10	Carberry	A15	3.3	3.3	6
2	WCO	2.10	slurry	A15	10	10	6
3	WCO	2.10	Carberry	A46	3.3	3.3	6
4	WCO	2.10	slurry	A46	10	10	6
5	WCO	2.10		D5081	10	10	6
6	CRO	2.20		A46	10	10	10
7	CRO	2.20		D5081		10	10
8	WCO	2.10		A46		10	0
9	WCO 75 CRO 25	2.12				7.5	
10	WCO 50 CRO 50	2.19				5.0	
11	WCO 25 CRO 75	2.24				2.5	
12	CRO	2.20				10	
13	WCO 75 DIESEL 25	1.74				7.5	
14	WCO 50 DIESEL 50	1.17				5.0	
15	WCO 25 DIESEL 75	0.65				2.5	
16	WCO 25 DIESEL 75 (higher FFA input)	2.44				2.5	

Tab. 4.1. Esterification tests on WCO.

The reactor is provided with two stainless steel perforated baskets (h = 0.067 m, diameter = 0.032 m) where to lodge the catalyst and attached to the stirrer arm. Catalyst is introduced inside these baskets and confined into one portion of the reactor. Temperature was reached and maintained at 336 K by pre-heated diathermic oil flowing through the outer jacket surrounding the reactor. A scheme

of the used Carberry reactor is represented in Fig. 4.1. The amount of the catalyst to introduce inside the baskets of the Carberry reactor was limited to 10 g to ensure a good fluidization of the catalysts by the reagents. Higher amounts of catalyst would prevent the reagents to enter in an effective way inside the baskets. Oil had to be 300 g as minimum, so to ensure the complete immersion of the baskets inside the reaction medium. 300 g of oil were therefore used for all the tests conducted in the Carberry reactor.

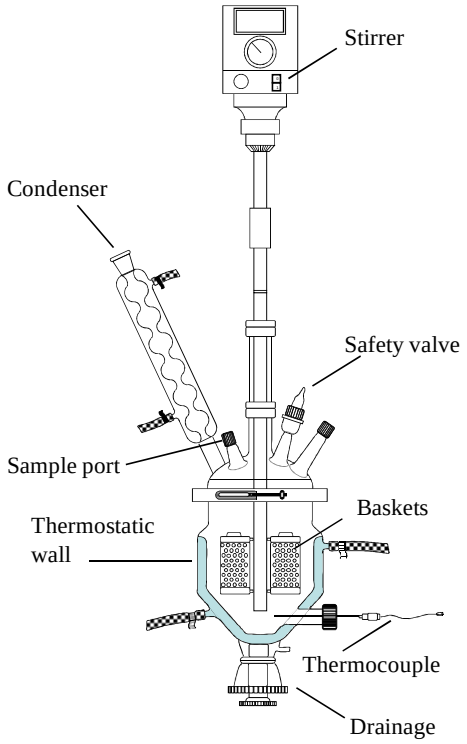

Fig.4.1: Carberry-type reactor.

In each test, when the system achieved the desired temperature, oil was sampled from the system and considered as initial acidity value, i.e. as the point at time zero. Each reaction was carried out for six hours, sampling at 60, 120, 240 and 360 minutes. Acidity

was determined as already explained in the section concerning the characterization of the oils.

FFA conversion, i.e. the percentage of acid converted in methylester was determined as follows as in similar works (Bianchi et al., 2011; 2010; Pirola et al., 2011; 2010; Boffito et al., 2012a; 2012b; Russbueldt et al., 2009; Pasias et al., 2006):

$$FFA\ conversion\ (\%)=\frac{FFA_{t=0}-FFA_t}{FFA_{t=0}}\times 100 \qquad 4.3$$

where $FFA_{=0}$ is the acidity of oil at zero time and FFA_t is the acidity of the oil at reaction time t.

Some recycles of use of the catalyst were performed with the aim of assessing catalyst deactivation in the presence of WCO. For this purpose the catalyst was left inside the reactor or inside the baskets after each recycle for the slurry and the Carberry reactor, respectively, without any treatment or purification.

4.6.3 Results and Discussion

4.3.1 Characterization of the catalysts

The main features of the adopted catalysts are reported in Tab. 4.2. Information about Amberlysts® were available from products data sheets by Dow Chemical, whereas information about Purolite®D5081 was available directly from the sheets provided by the manufacturer, since this product is still at the development stage.

Catalyst	A15	A46	D5081
Type		Macroreticular	
Matrix		Styrene-DVB	
Surface area ($m^2\ g^{-1}$)	53	75	N.a.
Ave. D_p (Å)	300	235	N.a.
Total V_p (ccg^{-1})	0.40	0.15	N.a.
Acidity (meq H^+g^{-1})	4.7	0.43	0.90-1.1
Measured acidity (meq H^+g^{-1})	4.2	0.60	1.0
Moisture content ($\%_{wt}$)	1.6	26-36	55-59
Shipping weight ($g\ l^{-1}$)	610	600	N.a.
Max. operating temp (°C)	120	120	130

Tab.4.2. Features of the catalysts.

All the used resins have the appearance of opaque quasi-perfect spherical beads, with dimensions ranging from 0.3 to 1 mm, with higher distribution near the upper limit. The matrix structure of both Amberlysts® and Purolite®D5081 consists of a copolymer of styrene and divinylbenzene (DVB) forming a macroporous polymer functionalized with strong $-SO_3H$ acid sites (Brønsted acidity). Polymer structure of resins is characterized by a certain content of the crosslinking component (DVB), which determines surface area and pore size distribution. The reason of the choice of A15 and A46 among the other Amberlysts® is due to their different features concerning both physical and chemical properties such as surface area, porosity and acidity, as given in Tab. 4.2. Distinguishing feature of A46 and D5081 is the only surface functionalization. Consequently, A46 and D5081 are characterized by a lower number of acid sites than A15 and other Amberlysts® (Bianchi et al., 2010), which are sulphonated also internally.

The H^+ ions exchange capacities determined experimentally are reported in Tab. 4.2. The acidity value obtained for A46 is higher, whereas the one obtained for A15 is slightly lower than the one

reported by the manufacturer. This is probably due to the high accessibility by the exchange solution to the acid sites of A46, which are located exclusively externally. Differently, the value obtained for D5081 is perfectly in range with the one declared by the manufacturer. Resin A15 is therefore the most acid among the tested resins. Nevertheless, the use of resins characterized by the only surface functionalization brings some advantages in spite of the lower acidity. These comprise minimization of side products formation and absence of mass transfer limitations. An easy understanding of the catalyst's behaviour is therefore possible, as already experimented by the authors (Pirola et al., 2010).

The results of the swelling tests are summarized in Tab. 4.3. The swelling capacities by both weight and volume in water and methanol increase in this order: A46 < D5081 < A15 and A46 < A15 < D5081, respectively. This result can be explained considering that water molecules are able to penetrate inside the pores of A15 under the driving force caused by the attractive interaction of polar nature between the sulphonic acid sites and the polar molecules. For A46 and D5081 the same interaction can occur only on their external surface as no sulphonic groups are located inside the catalyst beads. The higher swelling capacity in water of D5081 compared to A46 can be easily explained by its higher acidity. The higher the number of H^+ sites interacting with the polar swelling medium, the greater the mass and volume gains.

Results obtained using acid oil (~2%$_{wt}$ of FFA) as a swelling medium gave a very interesting outcome. The amount of adsorbed FFA molecules can be in fact directly correlated with the interaction between FFA (the reagent) and the catalytic active sites. This measurement is therefore indicative of the activity of the catalyst. The swelling capacities in the acid oil follow in fact inverse order

with respect to the capacities in the polar media: A15 < A46 < D5081, indicating a possible order of increasing catalytic activity. This result can be explained considering that internal sites of A15 are too narrow (around 300 Å) to be accessible by the FFA, which are sterically hindered molecules. As a consequence, FFA can be adsorbed only on the external surface of the catalyst, differently from water and methanol, which can penetrate inside the pores of A15. The number of external acid sites of A46 and D5081 is supposed to be higher than the one of A15 and they are consequently able to bind a higher number of FFA molecules on the external surface. Consequently, the weight gain of D5081 and A46 is higher than A15. The higher weight and volume gain of D5081 compared to A46 may be always ascribable to its higher acid capacity, resulting in an interaction with a higher number of FFA molecules. Further information about the used exchange resins are provided in § 2.1.1 and § 3.3.1.

Swelling medium	Water		MeOH		Acid Oil ($2\%_{wt}$ oleic acid)	
gain (%)	wt	vol	wt	vol	wt	vol
A15	122	90	87	25	39	0
A46	37	20	50	5	48	0
D5081	95	35	99	25	56	10

Tab. 4.3 Results of the swelling tests performed on the resins.

4.3.2 Characterization of the oils

The WCO used in this work had the appearance of a very dense, highly viscous mixture and, if let stand, it formed solid deposits. The solid part of the oil, mainly consisting of food residues, salt, etc.,

was removed first by rough filtration and then by vacuum filtering on a Buchner funnel.

The acidity of the oil after rough filtration was equal to the one measured just before the esterification tests, indicating that most of the acidity was due to the presence of the solid visible part. A simple filtration was effective in substantially decreasing the acidity of the oil. This operation was also necessary in order to avoid the clogging of the catalysts pores, so to prevent a possible cause of deactivation.

In Table 4.4, densities, viscosities and iodine values (IV) of WCO, crude rapeseed oil (CRO) and their blends are reported together with the acidic compositions determined by GC analysis and the calculated average molecular weights. As it can be seen, 100% WCO is characterized by a low IV (53.9 gI_2/100g WCO). Although this value respects the maximum limit of 120 imposed by the European normative on biodiesel (EN14214), it might be unsuitable for the application of WCO for BD100 (pure biodiesel), in particular in cold climates (EN14111:2003). Viscosity is another parameter that is influenced by the composition of the oil. Viscosity decreases quite linearly with the increase of IV (Saloua et al., 2010; Encinar et al., 2005; Winayanuwattikun et al., 2008). Consequently, low IV are accompanied by high viscosities. To the best of author's knowledge and according to the literature (Demirbas, 2008) viscosity is reduced to one tenth after the transesterification process. Considering that the range of viscosity required by the EN1421 is between 3.5 and 5.0 cSt (at 40°C), WCO 100 ($\mu_{40°C}$= 82.2 cSt) and WCO 75 ($\mu_{40°C}$= 63.1 cSt) are expected to results in a biodiesel whose viscosity is too high to be directly used as biodiesel. The blends WCO 50 and WCO 25 and the CRO 100 are instead characterized by higher IV as long as lower viscosities, possibly resulting in a biodiesel with properties

matching the EN14214. Densities do not practically change from WCO 100 to its blends and the CRO 100.

The IV reflects the acidic composition obtained by the GC analyses for all the feedstocks. WCO 100 is in fact characterized by a high percentage of palmitic acid (C16:0) and low content of linoleic acid (C18:2), resulting in a low IV. Contrariwise, CRO is rich in oleic (C18:1) and linoleic acid, resulting in an IV of 118, which is anyway below the limit of 120 gI_2/100 g oil.

Feedstock	ρ ($g/cm^3_{15°C}$)	η ($cSt_{40°C}$)	IV (gI_2/100g oil)	Acidic composition (%wt)	Ave. MW (g/mol)
WCO	0.918	82.2	53.9	C16:0 (38.8) C18:0 (4.1) C18:1 (47.9) C18:2 (0.2)	272.27
WCO 75 CRO 25	0.914	63.1	69.0	C16:0 (30.1) C18:0 (3.1) C18:1 (51.9) C18:2 (12.0), C18:3 (2.6) C20:0 (0.4), C22:0 (0.1)	274.49
WCO 50 CRO 50	0.914	52.8	84.5	C16:0 (21.5) C18:0 (2.1) C18:1 (55.8) C18:2 (14.7) C18:3 (5.1) C20:0 (0.8) C22:0 (0.1)	276.71
WCO 25 CRO 75	0.926	40.5	76.8	C16:0 (12.8), C18:0 (1.1) C18:1 (59.8) C18:2 (17.5) C18:3 (7.7), C20:0 (1.1) C22:0 (0.2)	278.93
CRO	0.922	37.0	118	C16:0 (4.1) C18:0 (0.1) C18:1 (63.7), C18:2 (20.2), C18:3 (10.2) C20:0 (1.5) C22:0 (0.2)	281.15

Tab. 4.4. Density (ρ), viscosity (η), iodine value (IV), acidic composition and average molecular weight (MW) of the FFA in WCO and its blends with crude rapeseed oil (CRO).

4.3.3. Esterification tests

4.3.3.1. Effect of different reactors and study of deactivation

The results of the FFA esterification tests performed in the two different reactors, related to entries from 1 to 5 in Tab. 4.1, are given in Fig. 4.2.

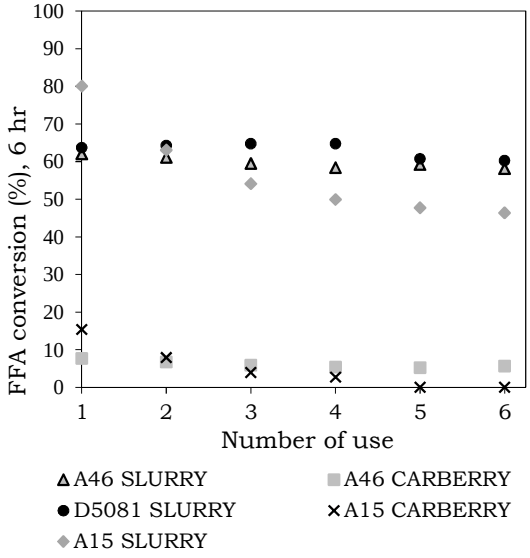

Fig. 4.2. FFA conversion of the recycles of use for different catalysts and reactors: 336 K. Reaction conditions reported in Tab. 4.1.

A blank test was first carried out in both the reactors confirming that in absence of the catalyst no FFA conversion takes place. As it can be seen, D5081 results in the best catalytic performance among the three catalysts. This is very likely due to the higher number of active acid sites located on its surface. In fact, as already remarked in the discussion of the results of the characterization of the catalysts, a higher number of superficial active sites are able to adsorb more efficiently both methanol and FFA.

A good conversion is obtained with A15 in the slurry reactor at the first use of the catalyst, but then its catalytic activity drastically

drops after each recycle. The total loss of activity was estimated to be around 43% within the 6 recycles. A possible explanation concerning this loss of activity may be related to the adsorption of the water yielded by the esterification on the active sites, which can make them unavailable for the catalysis. In the first run the catalytic action takes places on both inner and outer surface of the grains of A15. More in detail, methanol is firstly adsorbed on the active sulphonic acid sites, thus forming a sort of wreath around the particles and increasing the pores' diameter due to the swelling action. FFA diffuse towards the catalyst, and dissolve in the methanol. Then, they penetrate inside the pores of the catalyst and undergo to the catalysis both on the inner and the outer surface. When water molecules are formed inside the pores, they are not able to give internal retro-diffusion due to their strong interaction with H^+ sites and form an aqueous phase inside the pores. The formation of this phase prevents FFA from reaching internal active sites due to repulsive effects. In this way the number of active sites available for the catalysis drastically drops within few recycles of use.

Catalyst A46 shows a lower activity at the first use, but it is able to maintain a better performance over time than A15. Differently from A15, in fact, A46 has only superficial active sites, as well as D5081. This confers absence of mass transfer limitation, minimization of side products formation and stable catalytic activity (Pirola et al., 2010).

No substantial loss of activity is observed for A46 in the slurry reactor. A fluctuation in the FFA conversions is rather recognizable. This is worthy for A46 as well as for D5081. This behaviour was already observed for the two catalysts in a recent work of the authors (Boffito et al., 2012a) and is ascribable to the catalyst that has to settle in the system within the first recycles of use. A stable

performance of the catalyst is usually observed from the 8th to the 10th use, depending on the kind of substrate (Bianchi et al., 2011; Boffito et al., 2012a). Nevertheless, a possible cause of deactivation of the catalyst in WCO might be due to the substitution of the active H^+ sites of catalyst with metal cations such as Na^+ and Fe^{2+}, which may be present in the oil. In order to verify that these fluctuations were actually due the catalyst's settling in the system and not by the presence of metal cations in the feedstock, recycles of the use of both A46 and D5081 were performed on a CRO characterized by the same initial acidity of the WCO (entries 5 and 6 in Tab. 4.1). The results of this study are displayed in Fig. 4.3.

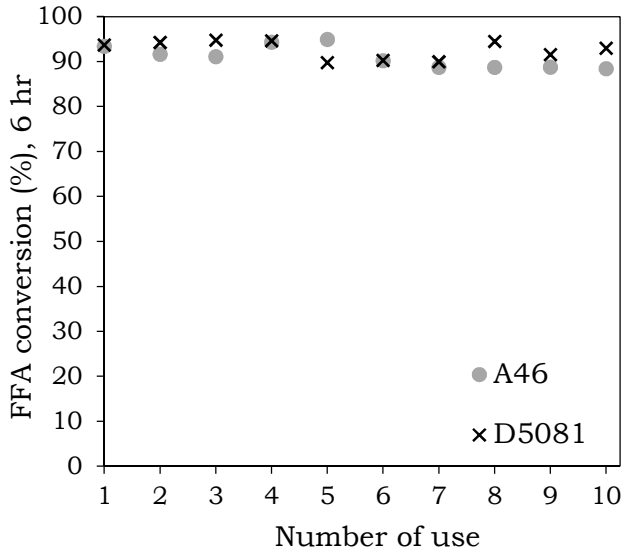

Fig. 6.3. FFA conversions of the recycles of use of A46 and D5081 in CRO and slurry reactor at 336 K. Reaction conditions reported in Tab. 4.1.

As it can be seen, A46 and D5081 do not give a stable performance of deacidification in CRO as well as in WCO. Fluctuations in the values of FFA conversions were calculated to be 6.3% and 6.4% for A46 and 6.1% and 5.2% for D5081, in the

recycles of use in WCO e CRO, respectively. As a consequence, A46 and D5081 showed no deactivation in WCO. To confirm this result, the ion exchange capacity of A46 was measured after each recycle and the presence of metals on fresh and used catalyst (6th recycle) was checked by EDX analysis. Results of ion exchange did not show any change in the concentration of H^+ sites on the catalyst. EDX analyses (results not shown here for the sake of brevity) could not detect a significative presence of metals both on the fresh and used catalyst. This confirms that in the present case, active sites were not replaced by the cations present in the feedstock.

Another cause of deactivation may be ascribable to the mechanical stress of the catalysts (Pirola et al., 2010; Mohibbe et al. 2005). Collisions of catalyst particles, one against the other and against the inner walls of the reactor may in fact cause fragmentation. The debris generated can collapse over the active sites, hindering their action. In addition, a small part of catalyst powder originated by fragmentation could have been lost during the discharge operations between two successive recycles (Pirola et al., 2010).

In the Carberry-type reactor, the effects due to the mechanical stress may be disregarded. The catalysts are in fact confined inside the rotating baskets. A15 and A46 were tested in the Carberry reactor and the results obtained are displayed in Fig. 4.2 along with the ones of the slurry reactor. Very low conversions were reached in both the cases. A46 maintains its activity, although low, while A15 loses the 100% of its activity within 6 recycles of use. This may be mainly ascribable to the poor contact between the reagents and the catalyst due to the configuration of the reactor. To come in contact with the catalysts, reagents need in fact to penetrate inside the baskets, winning the centrifugal force caused by the mechanical

rotation that push them towards the reactor's inner walls. Moreover, confining the catalysts inside the baskets, might have prevented an effective swelling in methanol. The swelling in methanol is very important for the reaction to occur. In fact, FFA molecules need first to dissolve in the methanol wreath formed around the catalysts to come in contact with its active sites.

In the view of the results obtained, Carberry-type reactor is not a potential good candidate for the industrial application of the FFA esterification catalysed by ion exchange resins.

In conclusion to this paragraph, the good maintenance of the catalytic activity for A46 and D5081 in slurry reactors is due to its particular frame. In fact, being sulphonated only on their external surface, their active sites are immediately available for the catalysis and diffusive aspects may be neglected, giving a very stable performance over time, as evidenced by Fig. 4.3. In addition, thanks to the only surface sulphonation achieved through a particularly high crosslinking degree (Lin et al., 2006), the matrix is more compact and resistant. Therefore, A46 and D5081 can better withstand mechanical stress.

4.3.3.2. Deacidification of blends of Waste Cooking Oil and Crude Rapeseed Oil

FFA esterification performed in the blends of WCO and CRO shows an increase of the reaction rate proportional to the content of the CRO. The kinetic curves of these experiments, related to experiments from entry 8 to 12 in Tab.4.1, are displayed in Fig. 4.4.

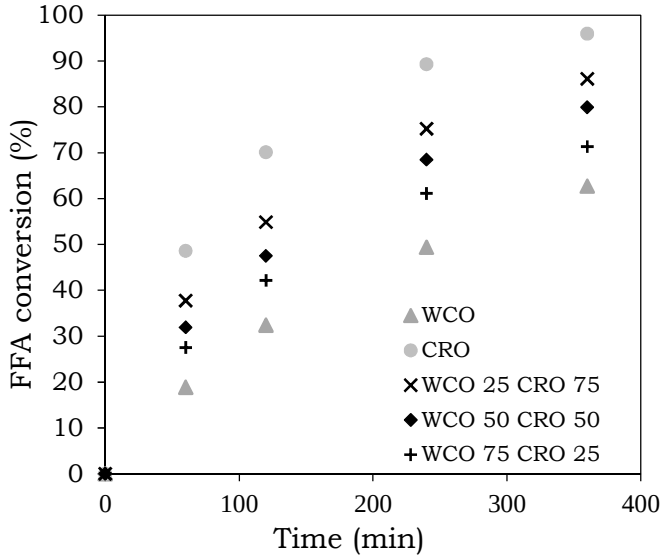

Fig. 4.4. FFA conversions of the FFA esterification of WCO and its blends with CRO, slurry reactor, 336 K. Reaction conditions reported in Tab. 4.1.

As it can be seen, the plateau of conversion is reached first by those blends with a higher content of CRO. Being all the blends characterized by the same initial FFA concentration (as given in Tab. 4.1), this results may be ascribable to the lower viscosity of the blends containing CRO. A low viscosity of the reacting medium can in fact enhance the mass transfer and facilitate the contact between the reagents and the catalyst. Viscosities of the various feedstocks are reported in Tab. 4.4 and show a decrease in their values as the content of WCO is increased. The IV value increases along with decrease of viscosity for the reasons already highlighted in the section concerning the results of the characterization of the oils. This demonstrates how the blends of WCO with other oils, characterized by lower viscosity and higher IV, can contribute to enhance the exploitation of WCO making it more easily processable. In this way, in fact, not only the properties of the feedstock result enhanced, so falling within the limits imposed by the regulations,

but also the reaction of deacidification is fastened and time saving can be achieved.

For a better understanding, in Fig. 4.5 the FFA esterification conversions at 6 hours and the viscosity of all the blends of WCO with CRO are reported. The image shows how the FFA conversion at the end of the reaction increases with the content of CRO, in spite of all the blends are characterized by the same initial acidity.

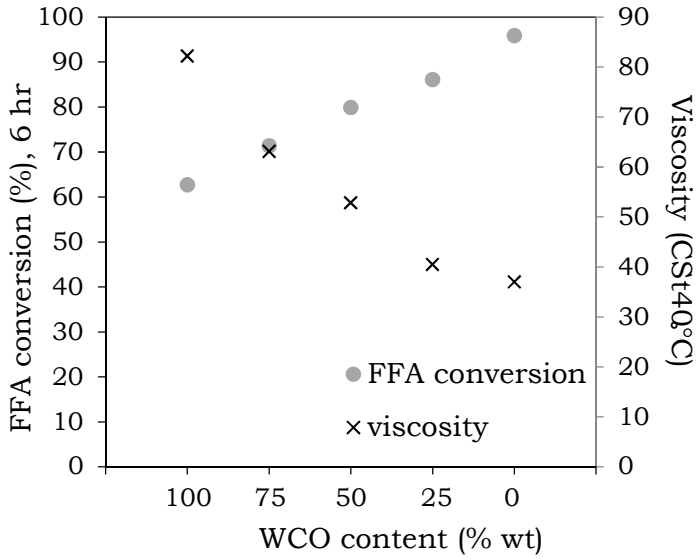

Fig. 4.5. FFA conversions of the FFA esterification and viscosities of WCO and its blends with CRO, slurry reactor, 336 K. Reaction conditions reported in Tab. 4.1.

When only CRO is used, the conversion increases up to 53% more and the viscosity decreases down to 55% less with respect to WCO. In particular, when WCO is blended with 75% of CRO (WCO 25 CRO 75), the viscosity halves and the FFA conversion increases of the 40% with respect to WCO, reaching a final FFA content of 0.38%$_{wt}$. This concentration is below the limit required by both the transesterification and the European Normative on biodiesel EN 14214.

4.3.3.3. Effect of diesel as a solvent

The kinetic curves obtained from the FFA esterification performed using different amounts of diesel as a solvent are given in Fig 4.6.

FFA conversions achieved with the mixture WCO 75 DIESEL 25 are sensibly higher than the ones achieved in the case of WCO, in spite its initial FFA concentration is lower. In the same way, the mixture WCO 50 DIESEL 50 results in the same conversion of WCO in spite the initial FFA concentration is even lower. This result indicates that the addition of diesel as a solvent brings beneficial effects to the esterification reaction rate.

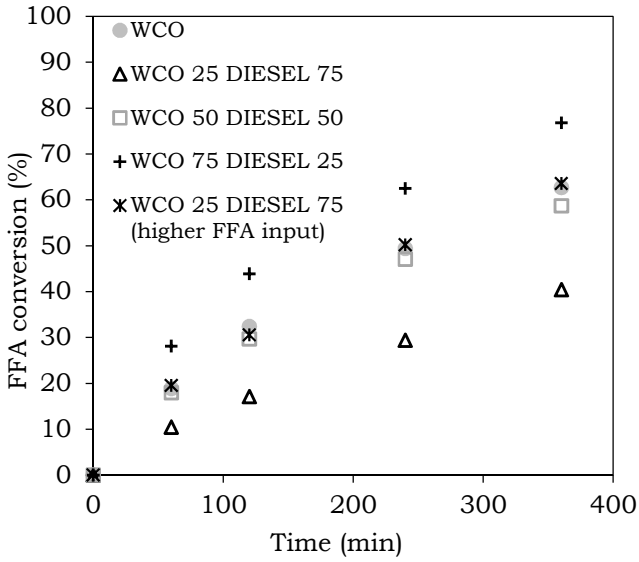

Fig. 4.6. FFA conversions for the FFA esterification of WCO and using diesel as a solvent, slurry reactor, 363 K. Reaction conditions reported in Tab. 4.1.

Differently, the sample WCO 25 DIESEL 75, that is characterized by the lowest initial FFA concentration, exhibits the lowest FFA conversion in spite the higher diesel content. A test was carried using a mixture of WCO 25 and DIESEL 75 with a higher FFA input (oleic acid). The kinetic curve is reported in Figure 6. It can be

observed that FFA conversion increases with respect to the solution WCO 25 DIESEL 75. This happens because the FFA esterification reaction rate directly depends on the FFA concentration, as already reported (Pirola et al., 2011; Bianchi et al., 2011; Boffito et al., 2012a).

The addition of diesel as a solvent decreases the initial FFA concentration, so slowing the reaction kinetic, but on the other hand it enhances the diffusive phenomena, improving the mass transfer and therefore the contact between the reagents and the catalyst. The conversions reported in Fig. 4.6 for the different mixtures of WCO and diesel are to be interpreted taking into consideration both these aspects.

In these experiments it was intentionally decided to keep the ratio catalyst/oil constant for all the feedstock. The actual amount of WCO treated in the mixtures with diesel is lower than pure WCO and, as a consequence, the ratio catalyst/feedstock changed according to the ratio WCO/diesel adopted (as given in Table 1). Therefore, conversions obtained for the mixtures of WCO with diesel could increase more using the same catalyst amount adopted for WCO.

The use of diesel as a solvent for the FFA esterification should be encouraged since no solvent separation stages are needed downstream. Moreover, as the results of this work prove, higher FFA esterification conversions are achieved in shorter times, so allowing time-saving and, as a consequence, cost-saving. The deacidified oil contained in different proportions in the diesel solvent could in fact be directly processed through the transesterification reaction to produce methyl esters. The so obtained biodiesel already dissolved in petro-diesel might be then directly fed into diesel engines.

4.4 Conclusions

Waste cooking oil (WCO) is a very attractive raw material for biodiesel production.

FFA esterification of WCO heterogeneously catalyzed by ion exchange resins in slurry reactor is a convenient and easy-to handle process to lower acidity. Resins Amberlyst®46 (Dow Chemical) and Purolite® D5081 demonstrated not to deactivate in WCO even after several recycles of uses in slurry modality. Carberry type reactor, besides preventing deactivation by mechanical stress of the resins is not suitable for the FFA esterification since a good contact between the reagents and the catalyst cannot be achieved.

Properties of WCO that make it hard to be processed to biodiesel or that are not in range with limits imposed by the law, can be improved blending the WCO with other crude oils. In this work the progressive improvement of the properties of the WCO was achieved by blending it with increasing amounts of crude rapeseed oil (CRO). These blends were moreover successfully deacidified by FFA esterification reaction, showing an increase of the FFA conversion with the content of CRO.

The effect of diesel as a solvent was also investigated, showing very interesting results. Higher FFA conversions were achieved in shorter times using diesel as a solvent other conditions being equal. This opens the opportunity for the use of diesel as a solvent for oils along the entire weaving factory for biodiesel production, since solvent separation steps are not required downstream.

References

Bianchi C. L., Boffito D. C., Pirola C., Ragaini V. "Low temperature de-acidification process of animal fat as a pre-step to biodiesel production", *Catal. Lett.* **2010**, 134, 179.

Bianchi C. L., Pirola C., Boffito D.C., Di Fronzo A., Carvoli G., Barnabè D., A. Rispoli, R. Bucchi, "Non edible oils: raw materials for sustainable biodiesel", in: Stoytcheva M., Montero G. (Eds.), *Biodiesel Feedstocks and Processing Technologies*, Intech, **2011**, pp. 3-22.

Boffito D. C., Pirola C., Bianchi C. L. "Heterogeneous catalysis for free fatty acids esterification reaction as a first step towards biodiesel production", *Chem Today* **2012a**, 30, 14.

Boffito D. C., Crocellà V., Pirola C., Neppolian B., Cerrato G., Ashokkumar M. at al. "Ultrasonic enhancement of the acidity, surface area and free fatty acids esterification catalytic activity of sulphated ZrO2-TiO2 systems", *J Catal* **2012b**, accepted on September 2012., DOI: 10.1016/j.jcat.2012.09.013.

Cheng Y. J., Brittin H. C. "Iron in Food: Effect of Continued Use of Iron Cookware", *J of Food Science* **1991**, 56, 584.

Demirbas A. "Relationships derived from physical properties of vegetable oil and biodiesel", *Fuel* **2008**, 87, 1743.

EN 14111:2003 "Fat and oil derivatives. Fatty acid methyl esters (FAME). Determination of iodine value", CEN Brussels., Belgium., **2003**.

Encinar J. M., Gonzalez J. F., Rodriguez-Reinares A. "Biodiesel from used frying oil. Variables affecting the yields and characteristics of the biodiesel", *Ind Eng Chem Res* **2005**, 44, 5491.

Graboski M. S., McCormick R. L. "Combustion of fat and vegetable oil derived fuels in diesel engines", *Prog. Energy Combust. Sci.* **1998**, 24, 125.

Kröger-Ohlsen M. V., Trùgvason T., Skibstes L. H., Michaelsen K. F. "Release of Iron into Foods Cooked in an Iron Pot: Effect of pH., Salt., and Organic Acids", *J of Food Science* **2002**, 67(9), 3301.

Lin Z. H., Guan C. J., Feng X. L., Zhao C. X. "Synthesis of macroreticular p-(omega-sulfonic-perfluoroalkylated)polystyrene ion-exchange resin and its application as solid acid catalyst", *J Molec Catal A Chem* **2006**, 247, 19.

López D. E., Suwannakarn K., Bruce D. A., Goodwin JG. "Esterification and transesterification on tungstated zirconia: Effect of calcination temperature", *J Catal* **2007**, 247, 43.

Lotero E., Liu Y., Lopez D. E., Suwannakara K., Bruce D. A., Goodwin J. G. "Synthesis of Biodiesel Via Acid Catalysis", *Ind Eng Chem Res* **2005**, 44(14), 5353.

Mohibbe Azam M., Amtul Waris A., Nahar N. M. “Prospects and potential of fatty acid methyl esters of some non-traditional seed oils for use as biodiesel in India”, *Biomass and Bioen* **2005**, 29, 293.

Öezbay N., Oktar N., Tapan N. A. “Esterification of Free Fatty Acids in Waste Cooking Oils (WCO): Role of Ion-exchange Resins”, *Fuel* **2008**, 87, 1789.

Ono T., Yoshiharu K., US Patent 4.,164., 506, 1979.

Pasias S., Barakos N., Alexopoulos C. “Heterogeneously Catalyzed Esterification of FFAs in Vegetable Oils”, *Chem Eng Technol* **2006**, 29, 1365.

Pirola C., Bianchi C. L., Boffito D. C., Carvoli G., Ragaini V. “Vegetable oil deacidification by Amberlyst : study of catalyst lifetime and a suitable reactor configuration”, *Ind Eng Chem Res* **2010**, 49, 4601.

Pirola C., Boffito D. C., Carvoli G., Di Fronzo A., Ragaini V., Bianchi C. L. “Soybean oil deacidification as a first step towards biodiesel production”. In: D. Krezhova., editor., Recent Trends for Enhancing the Diversity and Quality of Soybean Products: Intech, **2011**, p. 321-44.

Ragaini V., Bianchi C. L., Pirola C., Carvoli G. “Increasing the value of dilute acetic acid streams through esterification: Part I. Experimental analysis of the reaction zone”, *Appl Catal B: Environmental* **2006**, 64, 66.

Rao K.V., Krishnasamy S., Penumarthy V., WO 2009047793., 2009.

Russbueldt B. M. E., Hoelderich W. F. “New sulfonic acid ion-exchange resins for the preesterification of different oils and fats with high content of free fatty acids”, *Appl Catal A* **2009**, 362, 47.

Saloua F., Saber C., Heidi Z. “Biodiesel production and characterization”, *Biores Technol* **2010**, 101, 3091.

Winayanuwattikun P., Kaewpiboon C., Piriyakananon K., Tantong S., Thakernkarnkit W., Chulalaksananukul W. et al. “Potential plant oil feedstock for lipase-catalyzed biodiesel production in Thailand”, *Biomass and Bioen* **2008**, 32, 1279.

Xingzhong Y., Jia L., Guanming Z., Jingang S., Jingyi T., Guohe H. “Optimization of conversion of waste rapeseed oil with high FFA to biodiesel using response surface methodology”, *Renew En* **2009**, 33, 1678.

CHAPTER 5:
FREE FATTY ACIDS ESTERIFICATION IN SONOCHEMICAL REACTORS

Abstract

In this study the separate use of ultrasound and microwaves for the production of Fatty Alkyl Methyl Esters by free fatty acids esterification is i.e. biodiesel is investigated in the heterogeneously catalysed esterification of Free Fatty Acids. Experiments on both refined rapeseed oils and a raw tobacco oilseeds were conducted and compared with the conventional method. Ultrasound and microwave remarkably fasten the esterification reaction at temperatures lower than 336 K, which is the temperature normally used in the free fatty acids esterification. Conversions close to 70% were obtained in the tobacco oil with the conventional method at 336 K as well as with the ultrasound-assisted method at 293 K. The lower the temperature, the higher the enhancement brought by the sonochemical methods and the higher the microwave powers delivered to the systems the higher the conversions.

5.1 Introduction

The most recent challenge concerning biodiesel (BD) production deals with the processing of non-food, raw oils to make them suitable to be used as biofuels. Very often these oils require several standardization processes, which raise the overall cost for biodiesel manufacturing. The search for high efficiency transformation methods it is therefore a key issue in this context.

In this study, the effect of sonochemical techniques such as ultrasound (US) and microwave (MW) in the free fatty acids (FFA) esterification reaction is studied in presence of both refined and raw feedstock. Sulphonic ion exchange Amberlyst®46 and Purolite®D5081 were used as catalysts.

Acoustic cavitation-based technologies (such as US) have been regarded as a mean to eliminate or minimize mass-transfer (Vyas et al., 2005), while as a non-conventional way of heating (Gole et al., 2012)

Cavitation is a phenomenon of nucleation, growth, and subsequent collapse (quasi-adiabatic) of micro bubbles in a liquid medium. The collapse of bubbles forms hot spot characterized by very high temperatures (in the range of 1000−15000 K) and pressures (in the range of 500−5000 bar) locally but at millions of locations in the reactor. In addition to the generation of hotspots, cavitation also results in the generation of highly reactive free radicals, and strong turbulence. When a cavitation bubble collapses near a solid surface, liquid jets are produced and high-speed jets of liquid are driven into the surface of a particle (due to asymmetric collapse of bubbles), resulting in enhanced transport of the species towards the solid surface (Mason and Lorimer, 1988). For this reason US has been already adopted extensively to promote various reactions, among which also heterogeneous ones (Toukoniitt et al., 2005).

In presence of two immiscible liquids, US forms very fine emulsions, so increasing the surface area available for the reaction between the two phases. The cavitation may also lead to a localized increase in temperature at the phase boundary. As a consequence, also the reaction rate increases (Thompson and Doraiswamy, 1999). Emulsions produced by sonication are also reported to be more stable than those formed conventionally (Kardos et al., 2001).

US has been recently applied in fatty acids methyl esters production by FFA esterification (Santos et al., 2010; Gole and Gogate, 2012) and transesterification (Gole and Gogate, 2012;

Santos et al., 2009) due to enhancement of the miscibility between methanol and oil through the formation of micro-emulsions.

MW are a younger technique than US. Some studies have reported that MW can accelerate the FFA esterification reaction (Chemat et al., 1997; Kim et al., 2011; Vacek et al., 2000) and the transesterification (Jin et al., 2011; Yuan et al., 2009) reaction to produce fatty acids methyl esters.

In particular, use of MW associated with the use of heterogeneous catalysts has been reported to be beneficial for methyl esters production (Chen et al., 1997; Yuan et al., 2009; Chemat et al., 1997). If the catalyst is a strong MW absorption material, the radiation would directly act on the catalyst and the "microwave hot spots" would be formed under MW radiation (Chen et al., 1997; Zhang and Hayward, 2006). The "microwave hot spots" are extremely favourable to the endothermic reaction (Yuan et al., 2009), as in the case of FFA esterification reaction. At the same time, sulphonic groups, which are polar groups, also have a strong MW radiation absorbing function.

Also methanol shows strong MW absorption capacity, being a polar molecule. This makes of methanol a better alcohol than others to be used when MW are applied (Yuan et al., 2009).

The selection of a technology for biodiesel production would mainly depend on the advantages and disadvantages such as conversion efficiency, complexity, total cost, environmental friendliness and safety. According to previous researches, the esterification reactions, which are usually heated using conventional reactors (such as heaters and oil baths), are time-consuming (Ferrão-Gonzales et al., 2011). In order to reduce the reaction duration, MW-assisted reactors, may be a valid an effective alternative to conventional heating.

In this chapter the FFA esterification of refined rapeseed oils acidified with oleic acid and of a raw tobacco oilseed is investigated at different temperatures in presence of US or MW. In the case of the MW the effect of different powers was also studied.

5.2 Materials and Methods

5.2.1 Description of the sonochemical reactor

A batch reactor equipped with both a MW emitter and a US titanium horn was used for the experiments. A photo of the reactor, which was extensively described by Ragaini (Ragaini et al., 2012) is reported in Fig. 5.1.

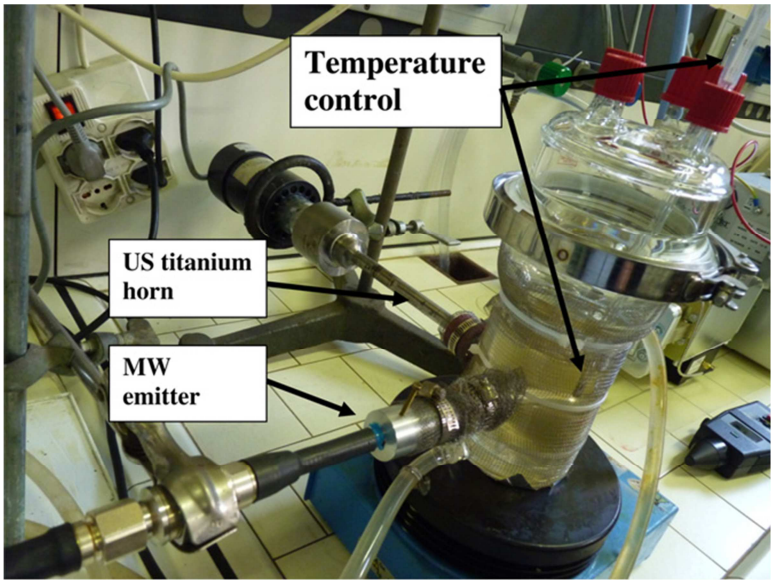

Fig. 5.1. Photo of the batch reactor with MWand US (titanium horn) immersed in the reacting liquid.

The apparatus is a 500 mL cylindrical pyrex vessel, closed on the top by a pyrex cover. The solution in the reactor may be continuously stirred by means of a magnetic stirrer or a rotating helix during the reaction or process under study.

An outer jacket, in which water passes, can be used to heat or to cool the liquid in the reactor by mean of a thermostat.

The temperature inside the reaction medium can be controlled and monitored by means of a thermocouple. The US horn and the MW emitter are located in the lower part of the reactor at the same height from the bottom (5.5 cm). The axes of the US horn and the MW emitter are nearly perpendicular each other. Such arrangement guarantees the best performance of the two sources when used together. The distance between the US horn and the MW emitter was fixed at 5 mm. The MW applicator consists of a short section of a semi-rigid 50 X, coaxial cable SC, as depicted in Fig. 5.2. It is a high power, high temperature corrugated cable (Andrew Corp., Rolando Park, IL, USA, model HST2-50), having an external diameter over copper outer conductor of 9.5 mm, with a power handling capability of about 900 W (average, continuous wave) at the operating frequency of 2450 MHz, and with a power attenuation coefficient of 22 dB/100 m at ambient temperature and sea level. At one end of the cable a short section of the external conductor EC was stripped off to obtain a k/4 dipole antenna. The active end having a maximum of MW power emission at point F, or feed point, was introduced inside the US + MW reactor through a horizontal glass well in order to protect the MW antenna, as shown in Fig. 5.1. This antenna was provided with a sliding coaxial k/4 (~30 mm) choke section CS placed near the input port of the glass reactor, to block microwaves reflections guided by the external surface of the cable.

Stray radiations emitted by the reactor, if any, were blocked using a shield made out of a thin metal netting, as depicted in Fig. 5.1.

The other end of the antenna was connected to the coaxial output port of the microwave generator, using a low attenuating flexible coaxial cable (not shown) and a type 7/16 female connector, FC.

MW were produced by an MW generator (Alter, Mod. TM A09-51), maximum nominal power gets from the electrical net: 900 W), and sent to the MW applicator above discussed, using a waveguide to coaxial adapter. Details of the microwave applicator and of the associated experimental techniques utilized for the in situ activation of chemical reactions can be found in previous works (Biffi, 2009 et al.; Ferrari, 2009 et al.).

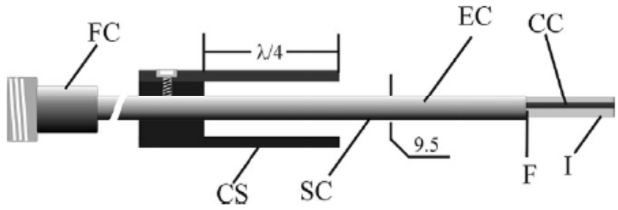

Fig. 5.2. Axial section of the MW applicator, FC: type 7/16 DIN female connector, SC: semi-rigid coaxial cable, 9.5 mm diameter over outer conductor, CS: choke section; CC: central conductor, EC: external conductor, I: insulator, F: point of maximum MW emission, or feed point.

The US treatment was performed using a Sonicator (Bandelin, Mod. Sonoplus GM 2200, maximum nominal power from the electrical net: 295 ± 2 W, as measured experimentally) with a frequency of 20 kHz and a tip diameter of 13 mm.

Both US and MW power emissions were determined following exactly the standard calorimetric method (Mason and Lorimer, 1988; Löning et al., 2000), i.e. measuring the temperature increase (ΔT), in the same vessel, of a weighted volume (300 ml) of water (300 g, 16.7 mol).

5.2.2 Esterification tests

In Tab. 5.1 the list of all the esterification experiments performed in this study is reported.

Entry	Oil	Initial acidity (%wt)	Cat.	Technique	Temp. (K)	Emitted power (W)	$T_{thermostat}$ (K)
1	Rapeseed oil (5)*	4.2-5.0	A46	conventional	313	-	315
2					336		338
3				ultrasound	313	38.5	293
4					336		313
5				microwaves	313	61.4	293
6					336		313
7	Tobacco	1.17	A46	conventional	293	-	293
8					313		315
9					336		338
10				ultrasound	293	38.5	277
11					313		293
12					336		313
13	Rapeseed oil (2)*	2.0-2.3	D5081	conventional	293	-	277
14					313		315
15					336		338
16				microwaves	293	31.7	277
17					313	31.7	293
18						61.4	293
19					336	31.7	313
20						61.4	313

* acidified with pure oleic acid up to the desired acidity.

Tab. 5.1. Conventional and sonochemically-assisted esterification experiments.

Catalysts' description and characterization is provided in the paragraphs 2.1.1 and 3.3.1, respectively.

In this study both refined rapeseed oil (acidified with pure oleic acid up to the desired initial acidity) and a raw tobacco oil were used.

The used rapeseed oils were characterized by different initial acidities: from 4.2 to 5%$_{wt}$ of FFA, referred as rapeseed oil (5) and ~2%$_{wt}$ of FFA, referred as rapeseed oil (2).

US were powered at 37%, while MW at 2O and 30% of the nominal power. Calorimetric measurements resulted in the emitted powers reported in Tab. 5.1., i.e. 38.5 W for US (37%), 31.7 and 61.4, for MW a 20% and 30%, respectively.

Temperatures inside the reactor were maintained by the use of the thermostat mentioned in the previous section. In order to maintain the desired temperature, it was necessary to set the temperatures reported in Tab. 5.1.

FFA conversions were determined withdrawing from the reactor samples of the reaction mixture at pre-established times. All the samples were centrifuged for 5 minutes at 13500 rpm and then analysed through acid-base titration as explained in 2.3.1. Acidity was then calculated according to equation 2.9 and FFA conversions calculated equation 2.18.

5.3 Results and Discussion

5.3.1. Comparison of the sonochemically-assisted method with the conventional method

In Fig. 5.3 and 5.4 the results of the FFA esterification tests performed on the rapeseed (5) and the tobacco oilseeds are shown.

The tests are referred to the entries 1 to 6 for the rapeseed oil (5) and to entries from 7 to 12, respectively.

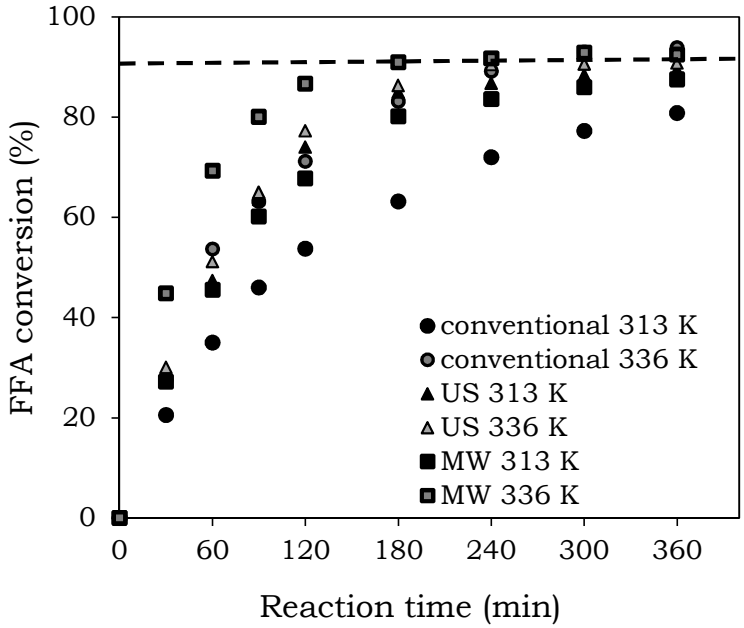

Fig. 5.3. FFA conversion vs. reaction time for the conventional and sonochemically-assisted FFA esterification of rapeseed oil (5) (FFA 5%$_{wt}$). Catalyst: A46.

The dotted line in both Fig. 5.3 and Fig 5.4. represents the conversion needed to achieve in the oil a final FFA concentration of 0.5%$_{wt}$, i.e. the maximum limit required by both the transesterification and the European normative on biodiesel (EN 14214).

In Fig. 5.3 the comparison among the conventional FFA esterification method and the MW- and US- assisted ones is displayed at two different temperatures. The limit of 0.5%$_{wt}$ of FFA is achieved within 6 hours, i.e. the standard reaction time for the FFA esterification kinetic (Bianchi et al., 2010; 2011; Pirola et al., 2010; 2011; Boffito et al., 2012a; 2012b; 2012c) by all the methods at 336 K, while at 313 K it is almost attained by the MW- and US-assisted methods.

At the shorter reaction time of 240 minutes, the desired FFA limit concentration is achieved only by the sonochemically-assisted

methods and almost by the conventional method at 336 K. However, with the exception of conventional method at 313 K and the MW-assisted esterification, there is not much difference among the FFA conversions attained in the other cases.

It is remarkable that at the lower temperature of 313 K, the sonochemically-assisted methods performs much better than the conventional one at the same temperature, US in particular.

In Fig. 5.4 the comparison among the conventional FFA esterification method and the US-assisted method is shown for the raw tobacco oilseed. Being an oil with a low starting acidity, the limit of 0.5%$_{wt}$ of FFA is attained with both the methods at all the different temperatures within 4 hours, with the exception of the conventional esterification carried out at 293 K. At a reaction time of 2 hours, the US-assisted method at 336 K is the only one allowing achieving the desired acidity limit. It is remarkable that at this temperature the FFA esterification reaction rate is 6X the one of the conventional process. However, in all the cases, temperature being equal, the US-assisted experiments lead to better results than the conventional method at all the experimented temperatures in the case of tobacco oilseed.

The difference in the FFA conversions obtained at 313 K and 336 K is not as remarkable as the one shown at 293 K. It is noteworthy that the US-assisted esterification at 293 K gives almost the same conversions attained with the same method at 313 K and with the conventional method at 336 K. The fact that US-assisted esterification gives the same results at two different temperatures in the presence of an endothermic reaction cannot be easily explained. However, the existence of an optimum temperature at which acoustic cavitation phenomena result enhanced have already been

documented for oil-methanol systems in the case of transesterification (Colucci et al., 2005; Gole et al., 2012).

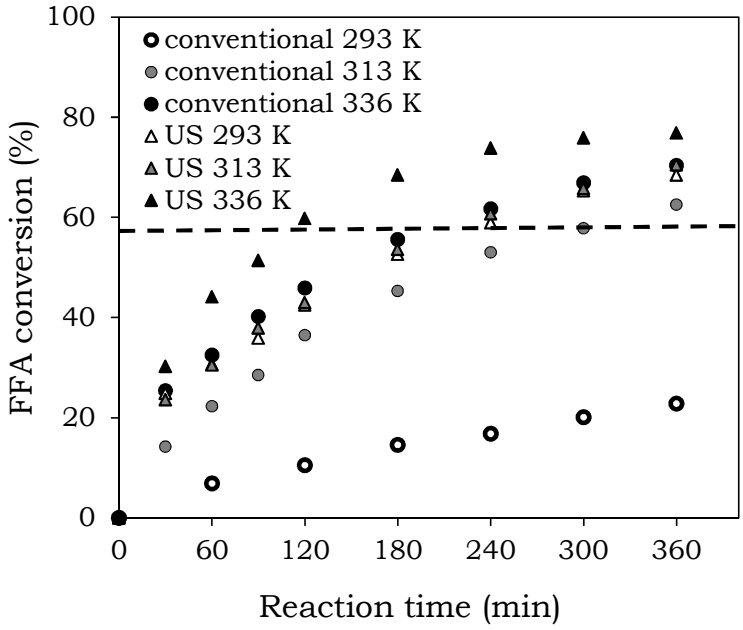

Fig. 5.4. FFA conversion vs. reaction time for the conventional and sonochemically-assisted FFA esterification of tobacco oil (FFA 1.17%$_{wt}$). Catalyst: A46.

The positive effects of MW and US on the FFA esterification reaction kinetic may be due to different reasons.

The benefits given by US are connected with the effects generated by the acoustic cavitation, as explained in the introduction.

The one of the FFA esterification is a “doubly-heterogeneous system” since it contains two kinds of heterogeneous systems: the oil-methanol liquid-liquid system and the oil-methanol-catalyst liquid-solid system. US has proved to be beneficial to both kinds of heterogeneous systems (Toukoniitty et al., 2005). First, US forms very fine emulsions in systems of two immiscible liquids that are more stable than the ones generated by conventional stirring

(Kardos et al., 2001). It means that the surface area available for the reaction between two phases is significantly increased and, therefore, also the reaction rate increases (Thompson and Doraiswamy, 1999).

For what concerns liquid–solid systems, the positive effects of acoustic-cavitation are ascribable to the asymmetric collapse of the bubbles in the vicinity of the solid surface. When a cavitation bubble collapses violently near a solid surface, liquid jets are produced and high-speed jets of liquid are driven into the surface of a particle. These jets and shock waves improve the liquid–solid mass transfer (Mason and Lorimer, 1988).

As already mentioned in the introduction, MW hot spots are beneficial to endothermic reactions (Yuan et al., 2009). However, MW cannot be regarded as just a mere alternative way of heating the reaction medium, since the conventional method carried out at equal temperature conditions results in lower FFA conversions, as also observed by Kim (Kim et al., 2011). The main difference from the conventional and the dielectric heating conditions concerns the localization of the enhanced temperature effects. MW hot spots are in fact localized on the surface of the solid catalysts adopted, as already observed in several works (Kabza et al., 2000; Chemat et al., 1997; Toukoniitty et al., 2005). Moreover, the interaction between the electromagnetic field and the materials is stronger if the material involved in the reaction possess a dipole moment.

When MW passes through a material with a dipole moment, the molecules composing the material try to align themselves with the electric field (Mingos et al., 1997). Polar molecules have stronger interactions with the electric field. Polar ends of the molecules tend in fact to align themselves and oscillate in step with the oscillating electric field of MW. Collisions and friction between the moving

molecules results in heating. Generally, the more polar a molecule is, the more effectively it will couple with microwaves. (Toukoniitty et al., 2005).

Sulphonic active groups supported on the resins used as catalysts possess a dipolar moment; moreover, resins like Amberlysts® have already been reported be strong MW absorbing media (Kabza et al., 2000). The use of MW radiation to promote esterification reactions was observed to be beneficial just in the case of the heterogeneously-catalysed reaction and not in the case of the same reaction promoted in homogeneous phase (Chemat et al., 1997).

The positive effect of MW irradiation on oil-methanol systems are known (Patile et al., 2011). Methanol's dipole quickly re-orientates under the MW irradiation, which destroys the two-tier structure of the interface of methanol and oil. Therefore, the solubility of methanol and oil is improved under MW irradiation (Patil et al., 2011), to the advantage of the esterification reaction.

However, one of the limitations of microwave heating is the depth of penetration of MW in absorbing materials. The use of continuous flow systems, however, reduces these problems (Pipus et al., 2000).

5.3.2 Effect of power and temperature in the microwave-assisted experiments

In Fig. 5.5 the results related to entries from 13 to 20 in Tab. 5.1 are shown. Also in this case the dotted line represents the conversion needed to achieve in the oil a final FFA concentration of 0.5%$_{wt}$, i.e. the maximum limit required by both the transesterification and the European normative on biodiesel (EN 14214).

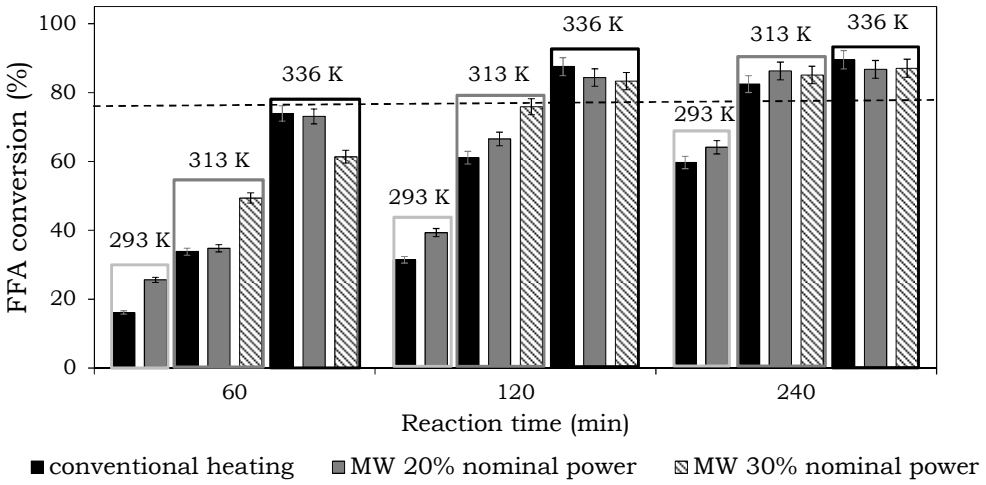

Fig. 5.5. Results of conventional and microwaves-assisted FFA esterification in different conditions of temperatures and powers. Catalyst; D5081.

Experiments were conducted at three different temperatures using the conventionally heated method and the MW-assisted one at two different powers as indicated in Tab. 5.1. At 293 K it was not possible to set a power higher than 20% of the nominal one because it would have required temperatures below 273 K in the thermostat.

The choice of the temperature of 293 K does not allow achieving the desired conversion within 6 hours at any of the adopted conditions. Differently, the desired FFA conversion is achieved within 4 hours operating at 313 K and 336 K at all the adopted conditions and within 2 hours at 336 K and at 313 K operating at the 30% of the nominal power. FFA conversions achieved at 336 K are higher than the ones attained at lower temperatures at all the adopted conditions. This can be simply due to the endothermic nature of the FFA esterification reaction that requires anyway high temperatures to occur.

With the exception of the conventional temperature for the FFA esterification (336 K), at all the experimented temperatures the use

of MW increases the FFA conversion at 293 K and 313 K. Moreover the higher the applied power, the higher the FFA conversion, always with the exception of the experiments carried out at the higher temperature (336 K), whereby the effect of the higher power seems to be detrimental for the reaction kinetic. Conversions attained with the conventional-heated method and at lower powers are in fact higher.

The increase of the FFA conversion at lower temperatures when MW are applied may be ascribed to the same reasons already highlighted in the previous paragraph.

The increase of the FFA conversion as the power increases may be attributed to the fact that more power is delivered to the system and, therefore, the enhanced temperature effects caused by electromagnetic irradiation are increased with respect to lower powers. Differently the reason why a too high power was detrimental at the temperature of 336 K could be explained by the possible generation of too high temperatures inside the reaction medium that could have caused the removal of methanol from the system through constant evaporation or pyrolysis.

5.4 Conclusions

The use of ultrasound (US) and microwaves (MW) increases the free fatty acids (FFA) conversions with respect to the conventional method at temperatures lower than 336 K, i.e. the temperature that is normally adopted for the FFA esterification method. The lower the temperature, the higher the difference between the sonochemically-assisted and the conventional method. Conversions attained operating at 293 K with US were as high as the ones achieved with the conventional method at 336 K and FFA esterification rate was

6X the one of the conventionally stirred process. However, highest reaction rates are still obtained in most of the cases with the conventional method at 336 K, whereby complete conversion can be attained within 2 hours of reaction using Purolite® D5081 as a catalyst.

The positive effects of US are connected with the phenomena enabled by acoustic cavitation in the reaction medium. The benefits brought by the use of MW are ascribable to the effects generated by the interaction of the electromagnetic radiation with the MW-absorbing media, such as the resins used as catalysts and methanol. Increasing the power of MW radiation increases the FFA conversions as well, due to the enhanced temperature effects and the improved methanol/oil solubility.

References

Bianchi C.L., Boffito D.C., Pirola C., Ragaini V., "Low temperature de-acidification process of animal fat as a pre-step to biodiesel production", *Catal. Lett.* **2010**, 134, 179.

Bianchi C.L., Pirola C., Boffito D.C., Di Fronzo A., Carvoli G., Barnabè D., A. Rispoli, R. Bucchi, "Non edible oils: raw materials for sustainable biodiesel", in Stoytcheva M., Montero G. (Eds.): Biodiesel Feedstocks and Processing Technologies, *Intech,* **2011**, pp. 3-22.

Biffi Gentili G., Linari M., Longo I., Ricci A.S., "A coaxial microwave applicator for direct heating of liquids filling chemical reactors", *IEEE Trans. Microwave Theory Tech.* **2009**, 57, 2268.

Boffito D.C., Pirola C., Bianchi C.L., "Heterogeneous catalysis for free fatty acids esterification reaction as a first step towards biodiesel production", *Chimica Oggi-Chemistry Today* **2012a**, 30(1), 42.

ical reactors", *IEEE Trans. Microwave Theory Tech.* **2009**, 57, 2268

Boffito D.C., Crocellà V., Pirola C., Neppolian B., Cerrato G., Ashokkumar M., Bianchi C.L., "Ultrasonic enhancement of the acidity, surface area and free fatty acids esterification catalytic activity of sulphated ZrO_2-TiO_2 systems", *J. Catal.*, **2012b**, http://dx.doi.org/10.1016/j.jcat.2012.09.013

Boffito D.C., Pirola C., Galli F., Di Michele A., Bianchi C.L., "Free Fatty Acids Esterification of Waste Cooking Oil and its mixtures with Rapeseed Oil and Diesel", Fuel, **2012c**, accepted on 19th October 2012, DOI: 10.1016/j.fuel.2012.10.069.

Chemat F., Poux M., Galema S.A., "Esterification of stearic acid by isomeric forms of butanol in a microwave oven under homogeneous and heterogeneous reaction conditions", *J. Chem. Soc., Perkin Trans.* **1997**, 2, 2371.

Chen C.L., Hong P.J., Dai S.S., Zhang C.C., Yang X.Y., "Microwave effects on the oxidative coupling of methane over Bi2O3-WO3 oxygen ion conductive oxides", *Reaction Kinetics and Catalysis Letters* **1997**, 61(1), 175.

Colucci J.A., Jose A., Borrero E.E., Alape F., "Biodiesel from an alkaline transesterification reaction of soybean oil using ultrasonic mixing", *J. Am. Oil Chem. Soc.* **2005**, 82(7), 525.

Ferrão-Gonzales A.D., Véras I.C., Silva F.A.L., Alvarez H.M., Moreau V.H., "Thermodynamic analysis of the kinetics reactions of the production of FAME and FAEE using Novozyme 435 as catalyst", *Fuel Process. Technol.* **2011**, 92, 1007.

Ferrari C., Longo I., Tombari E., Gasperini L., "A new integrated photoreactor for microwave assisted decolorization of acid orange 7 (AO7) in aqueous solutions", *Int. J. Chem. Reactor Eng.* **2009**, 8, A72

Gole V.L., Gogate P.R., "Intensification of Synthesis of Biodiesel from Nonedible Oils Using Sonochemical Reactors", *Ind. Eng. Chem. Res.* **2012**, 51(37), 11866.

Jin L., Zhang Y., Dombrowski J.P., Chen C.H., Pravatas A., Xu L., Perkins C., Suib S.L., "ZnO/La2O2CO3 layered composite: A new heterogeneous catalyst for the efficient ultra-fast microwave biofuel production", *Applied Catalysis B: Environmental* **2011**, 103, 200.

Kabza K.G., Chapados B.R., Gestwicki J.E., J.L. McGrath , "Microwave-Induced Esterification Using Heterogeneous Acid Catalyst in a Low Dielectric Constant Medium", *J. Org. Chem.* **2000**, 65, 1210.

Kardos N., Luche J.L., "Sonochemistry of cabohydrate compounds", *Carbohydr. Res.* **2001**, 332(2), 115.

Kim D., Choi J., Kim G.J., Seol S.K., Jung S., "Accelerated esterification of free fatty acid using pulsed microwaves", *Bioresource Technology* **2011**, 102, 7229.

Li J., Fu Y.J., Qu X.J., "Biodiesel production from yellow horn (Xanthoceras sorbifolia Bunge.) seed oil using ion exchange resin as heterogeneous catalyst", *Bioresource Technology* **2012**, 108, 112.

Löning J.M., Horst C., Hoffmann U., "Investigation on the energy conversion in sonochemical processes", *Ultrason. Sonochem.* **2002**, 9, 169.

Mason T.J., Lorimer J.P., "Sonochemistry, Theory, Applications and Uses of Ultrasound in Chemistry", Efford, J. Wiley, New York, **1988**.

Mingos D.M.P., Baghurst D.R., "Applications of Microwave Dielectric Heating Effects to Synthetic Problems in Chemistry", Microwave-Enhanced Chemistry, American Chemical Society,Washington, DC, USA, **1997**.

Patil P.D., Gude V.G., Mannarswamy A., Cooke P., Munson-McGee S., Nirmalakhandan N., Lammers P., Deng S.G., "Optimization of microwave-assisted transesterification of dry algal biomass using response surface methodology", *Bioresource Technology* **2011**, 102, 1399

Pipus G., Plazl I., Koloini T., "Esterification of benzoic acid in microwave tubular flow reactor", *Chemical Engineering Journal* **2000**, 76, 239.

Pirola C., Bianchi C.L., Boffito D.C., Carvoli G., Ragaini V., "Vegetable oil deacidification by Amberlyst : study of catalyst lifetime and a suitable reactor configuration", *Ind. Eng. Chem. Res.* **2010**, 49(10), 4601.

Pirola C., Boffito D.C., Carvoli G., Di Fronzo A., Ragaini V., Bianchi C.L., "Soybean oil deacidification as a first step towards biodiesel production", in D. Krezhova (Ed.): Recent Trends for Enhancing the Diversity and Quality of Soybean Products, Intech, **2011**, pp. 321-44.

Ragaini V., Pirola C., Borrelli S., Ferrari C., Longo I., "Simultaneous ultrasound and microwave new reactor: Detailed description and energetic considerations", *Ultrason. Sonochem.* **2012**, 19, 872.

Santos F.F.P., Malveira J.Q.,Cruz M.G.A., Fernandes F.A.N., "Production of biodiesel by ultrasound assisted esterification of Oreochromis niloticus oil", Fuel 2010, 89, 275.

Santos F.F.P., Matos L.J.B.L., Rodrigues S., F.A.N. Fernandes , "Optimization of the Production of Methyl Esters from Soybean Waste Oil Applying Ultrasound Technology", *Energy & Fuels* **2009**, 23, 4116

Thompson L.H., Doraiswamy L.K., "Sonochemistry: Science and engineering", *Ind. Eng. Chem. Res.* **1999**, 38(4), 1215.

Toukoniitty B., Mikkola J.P., Murzin D.Yu., Salmi T., "Utilization of electromagnetic and acoustic irradiation in enhancing heterogeneous catalytic reactions", *Appl. Catal. A* **2005**, 279, 1.

Vacek M., Zarevúcka M., Wimmer Z., Stránský K., Demnerová K., Legoy M.D., "Selective enzymic esterification of free fatty acids with n-butanol under microwave irradiation and under classical heating", *Biotechnology Letters* **2000**, 22, 1565.

Vyas A.P., Verma J.L., Subrahmanyam N., "A review on FAME production processes", Fuel 2010, 89, 1.

Yuan H., Yang B.L., Zhu G.L., "Synthesis of Biodiesel Using Microwave Absorption Catalysts, ", *Energy & Fuels* **2009**, 23, 548

Zhang X.L., Hayward D.O., "Applications of microwave dielectric heating in environment-related heterogeneous gas-phase catalytic systems", *Inorg. Chim. Acta* **2006**, 359, 3421.

CHAPTER 6:
FREE FATTY ACIDS ESTERIFICATION OVER INORGANIC SULPHATED SYSTEMS

Abstract

Sulphated Zr-based systems and Ti-Sn mixed oxides were synthesized with different methods (sol-gel, impregnation and physical mixing). They were characterized with particular regard to acidity and specific surface area and tested in the free fatty acids (FFA) esterification reaction. Zr-based catalysts show poor FFA conversions (below 45%) compared to the commercial zirconium sulphate ($Zr(SO_4)_2.4H_2O$) which exhibits conversions higher than 90%. Zr sulphate is characterized by a high concentration of active sites and low specific surface area that exposes most of the active sites on its surface making them immediately available for the catalysis. Differently the other sulphated Zr-based systems have relatively low acidities if compared to the rather high surface areas. However Zr sulphate deactivated within few recycles of use probably due to active groups leached into the reaction mixture and its partial solubility in water (yielded by the FFA esterification reaction). The water removal from the system resulted in delaying the deactivation of the catalysts from 1 to 3 uses.

Sulphated mixed Sn-Ti oxides were obtained with TiO_2 content ranging from 0 to 20% by weight. These catalysts exhibit increasing acidity as the content of Ti increases while specific surface area remains practically unchanged. FFA conversions increase as the acidity increase up to 76% for the catalyst with 20% of TiO_2. Recycles of use of catalyst and Sheldon test revealed however that the catalysis for the home-made sulphated Sn-Ti oxides is mainly due to the active species leached into solution.

6.1 Introduction

The presence of free fatty acids (FFA) in the feedstock, that is very common in the case of not refined oils, causes the formation of soaps as a consequence of the reaction with the alkaline catalysts ($RCOOH + NaOH \rightarrow RCOONa + H_2O$). Soaps distribute among the two phases, hindering the contact between reagents and, eventually, the products separation (Perego and Ricci, 2012; Boffito et al., 2012a, 2012b, Bianchi et al., 2010; Pirola et al., 2010). As a consequence, the process can only accept a restricted range of feedstock, typically with less than 0.5% of free fatty acids and 0.2% of moisture (Perego and Ricci, 2012; Boffito et al., 2012a, 2012b, Bianchi et al., 2010; Pirola et al., 2010) . Another drawback given by the use of alkaline homogeneous catalysts lies in the need of neutralization (and wastewater disposal) and the non-recovery of the catalyst. A solution could be represented by the use of acid catalysts. Acid catalysts, besides being tolerant to the FFA, also catalyse their esterification.

Sulphuric acid, hydrochloric acid and p-toluene sulphonic acids (Bourges and Diaz, 2012) are usually adopted as catalysts in the FFA esterification. However, the use of these catalysts results in some obvious drawbacks, such as corrosion, impossibility of catalyst recovering and safety issues. A clear challenge is the development of heterogeneous catalysts with high efficiency and sustainable costs of manufacturing. Solid acid catalysts have the strong potential to replace liquid acids in the transesterification reaction as they can eliminate separation, corrosion and environmental problems associated with liquid acid transesterification, besides also promoting the FFA esterification.

Moreover, the FFA esterification reaction may be also an alternative process to transesterification reaction when low-quality oils and fats are used as feedstock.

For this reason many efforts regarding the use of solid acid catalysts for the FFA esterification were recently carried out (Boffito et al., 2012a, 2012b; Bianchi et al., 2010; Pirola et al., 2010; Marchetti and Errazu, 2008).

Among various solid acid catalysts available, many studies have highlighted the application of sulphated metal oxides (Lotero et al., 2005; Jacobson et al., 2008; Jiputti et al., 2006; Boffito et al., 2012a; 2012b).

Zirconium sulphate has been widely studied for the FFA esterification reaction (Boffito et al., 2012a, Juan et al., 2007) due to its high activity. Sulphated zirconia is widely studied for other different kinds of reactions, such as isomerizations, alkylations and esterification of other carboxylic acids (Ardizzone et al., 2004) but its use for FFA esterification directly performed in the oil is reported in few studies (Dijs et al., 2003). Nevertheless, SO_4^{2-}/ZrO_2 is reported to exhibit high activity in the biodiesel production through transesterification (Lotero et al., 2005; Jacobson et al., 2008, Jiputti et al., 2006).

Sulphated tin oxide (SO_4^{2-}/SnO_2) is another potential catalyst for transesterification reaction due to its strong surface acidity that is reported to be stronger than SO_4^{2-}/ZrO_2 (Matsuhashi et al., 1990; Lam et al., 2009). Nevertheless, study concerning the usage of SO_4^{2-}/SnO_2 catalyst in biodiesel production is still very limited.

These materials are active because of the presence of both Brønsted acidic centres and Lewis acid sites (i.e. coordinatively unsaturated (cus) Zr^{4+} cations) at the surface, as evidenced by Morterra et al. (Morterra et al., 2001).

In this chapter, the preparation of different sulphated catalysts such as SO_4^{2-}/ZrO_2, SO_4^{2-}/SnO_2 and SO_4^{2-}/SnO_2-TiO_2 is described. All the catalysts were characterized with special regard to the surface acidity. The results of their characterization were then related to the activity in the FFA esterification reaction.

Moreover, since catalysts durability is a crucial issue from an industrial standpoint, much attention was devoted to catalysts re-use.

6.2 Materials and Methods

6.2.1 Synthesis of sulphated Zr-based systems

In Tab. 6.1 the sulphated Zr-based catalysts prepared using traditional techniques, i.e. sol-gel or impregnation methods are listed along with the method used for their preparation (entries 1 to 5). These catalysts are referred as SZ. Commercial zirconium sulphate, referred as ZS in Tab. 6.1 (entry 6), was characterized and tested in the free fatty acids (FFA) esterification for the sake of comparison with the other catalysts.

Catalysts from entry 1 to 3 in Tab. 6.1, i.e., SZ1, SZ2a and SZ2b (SO_4^{2-}/ZrO_2), were synthesized using sol-gel technique under acid hydrolysis conditions (HNO_3). Zirconium tetra-n-propoxide (ZTNP) and i-PrOH were used for all the sol-gel synthesis as precursor and solvent, respectively, adopting a molar ratio i-PrOH: ZTNP= 15 (Ardizzone et al., 2004). Molar ratio between water and the ZTNP was kept constant at 30 and the amount of sulphates, either from sulphuric acid or from $(NH_4)_2SO_4$, was the same for all preparations (molar ratio SO_4/Zr = 0.15) (Ardizzone et al., 2009). In a typical

synthesis, an aqueous solution containing HNO_3, and $(NH_4)_2SO_4$ in the case of one-pot sol-gel synthesis, was added to the precursor solution under stirring at a rate of 1-2 drops per minute. The solution was then kept under stirring for 90 minutes. The obtained product was dried at 353 K in static air obtaining a xerogel.

	Sample	Comp.	Prep. method	precursors	T calc.	SSA (m^2g^{-1})	V_p (cm^3g^{-1})	meq H^+g^{-1}
1	SZ1	SO_4^{2-}/ZrO_2	one-pot sol-gel	ZTNP[1] $(NH_4)_2SO_4$	893 K O_2, 6 hr	107	0.09	0.90
2a	SZ2a	SO_4^{2-}/ZrO_2	two-pots sol-gel	ZTNP H_2SO_4	893 K static, 3h	102	0.10	0.11
2b	SZ2b	SO_4^{2-}/ZrO_2	two-pots sol-gel	ZTNP H_2SO_4	653 K static, 3h	110	0.10	0.12
3	SZ3	SO_4^{2-}/ZrO_2	Solvent free	$ZrOCl_2.8H_2O$ $(NH_4)_2SO_4$	873 K static	81	0.11	1.3
4	SZ4	$Zr(SO_4)_2/SiO_2$	Impregnation	$Zr(SO_4)_2.4H_2O$ SiO_2	873 K static, 3h	331	0.08	1.4
5	SZ5	$Zr(SO_4)_2/Al_2O_3$	Impregnation	$Zr(SO_4)_2.4H_2O$ Al_2O_3	873 K static, 3h	151	0.09	0.67
6	ZS	$Zr(SO_4)_2.4H_2O$ (commercial)	-	-	-	13	0.12	9.6

[1] Zr-tetra-n-propoxide, $Zr(OC_3H_7)_4$

Table 6.1: Sulphated Zr-based systems.

The xerogel was ground in a mortar and sulphates were added by impregnation through incipient wetness of the zirconia hydrous precursor in the case of samples SZ2a and SZ2b. The xerogels were then calcined in the conditions reported in Tab. 6.1. All the samples listed in Tab. 6.1 from entry 1 to 5 were calcined with a heating rate of 2.5 K/min). The choice of the low calcination temperature of the sample SZ2b, along with the slow heating rate and duration of the treatment, was dictated by the need to preserve the largest number

of sulphate groups after the calcination, as suggested by Dijs (Dijs et al., 2003). SZ3 was prepared by a solvent free synthesis (Sun et al., 2005). In this synthesis zirconyl chloride and $(NH_4)_2SO_4$ were grounded in a mortar at room temperature for 20 minutes and then left ageing at room temperature for 18 hours. Calcination was performed in static air at 873 K (heating rate: 2.5 K/min). Also in this case, the molar ratio SO_4/Zr was kept constant at 0.15.

Samples SZ4 and SZ5, i.e., $Zr(SO_4)_2/SiO_2$ and $Zr(SO_4)_2/Al_2O_3$, respectively, were prepared by the impregnation of 3 g of support with 25 mL of a MeOH solution 0.4M of $Zr(SO_4)_2$. The solvent was then evaporated at 323 K under vacuum and the samples calcined at 873 K in static air (heating rate: 2.5 K/min), as reported in Tab. 6.1.

$Zr(SO_4)_2.4H_2O$ (98 % purity + metal basis) was an Alfa Aesar product. All the other reagents are Fluka products and were used without further purification.

6.2.2 Synthesis of sulphated SnO_2-TiO_2 systems

In Tab. 6.2 the sulphated SnO_2-TiO_2 systems are listed. Different TiO_2 weight amounts were added to the SnO_2. As an example, STTO_5 in Table 2 indicates a sample containing 95% of SnO_2 and 5% of TiO_2 by weight. Sulphated SnO_2-TiO_2 samples were all prepared grounding SnO_2 (Sigma Aldrich, ~325 mesh) with TiO_2 P25 (Degussa, SSA= 52 m^2g^{-1}) in a mortar for 20 minutes at room temperature, followed by impregnation by incipient wetness of a water solution. In a typical synthesis, 3 g of compound were impregnated with 25 ml of water solution containing sulphuric acid in an amount such as to have a ratio SO_4^{2-}/(Sn+Ti)=0.15 (Ardizzone at al., 2004). Water was then evaporated at 338 K under vacuum

and the samples calcined in static air at 773 K for 3 hours (heating rate: 2.5 K/min), as indicated in Tab. 6.2.

	sample	composition	Prep.	T calc.	SSA (m^2g^{-1})	V_p (cm^3g^{-1})	meq H^+g^{-1}
1	STTO_0	SO_4^{2-}/SnO_2	Physical mixing + impregnation	773 K static	16.8	0.10	3.15
2	STTO_5	SO_4^{2-}/95%SnO_2-5%TiO_2			15.9	0.11	3.43
3	STTO_10	SO_4^{2-}/ 90%SnO_2-10%TiO_2			16.5	0.09	5.07
4	STTO_15	SO_4^{2-}/ 85%SnO_2-15%TiO_2			14.9	0.11	7.13
5	STTO_20	SO_4^{2-}/ 80%SnO_2-20%TiO_2			16.9	0.09	7.33

Tab. 6.2. Sulphated SnO_2-TiO_2 systems.

All the chemicals used for the syntheses are Fluka products and were used without further purification.

6.2.3 Catalysts characterization

Specific surface area and pores volume were measured for all the samples by N_2 adsorption.

N_2 adsorption – desorption isotherms were measured at 77 K using Sorptometer 1042 instrument system (Costech, Milano). This system does not perform pores sizes distribution analysis. All samples were degassed at 393 K for 12 hours on a vacuum line and then pretreated for 3 hours in a nitrogen flow. The standard multi-points Brunauer–Emmett–Teller (BET) method was utilized to calculate the specific surface area (SSA).

FTIR spectra were run at 4 cm^{-1} resolution with a Bruker IFS 113v spectrophotometer equipped with MCT detector. The powder samples were investigated in the form of thin layer depositions (~ 10 mg cm^{-2}) on a pure Si wafer, starting from aqueous suspensions of the powders. After drying, all samples were activated in controlled

atmosphere at 623 K in a homemade IR quartz cell, equipped with KBr windows, connected to a conventional vacuum glass line capable of a residual pressure < 1×10^{-5} Torr, which allowed to perform strictly in situ adsorption/desorption experiments of molecular probes.

CO adsorption was performed to determine whether differences existed in Lewis acidity of the surface of the samples of interest. Approximately 100 Torr of carbon monoxide was exposed to the samples at ambient temperature. Desorption was performed in stages allowing 50, 25, 10, 5, 2, 1, and 0 Torr of carbon monoxide to remain in contact with the sample.

The quantification of the Brønsted acidity was carried out through ion exchange with NaCl saturated solution, leaving it in contact with the catalysts for 30 hours (López et al., 2007). The evaluation of H^+ concentration was carried out using a pH-meter. The number of H^+ milliequivalents released per gram of catalyst was then calculated as in equation 2.1.

6.2.4 Activity tests

A list of the experimental conditions adopted in the activity tests are listed in Tab. 6.3 for all the catalysts.

All the reactors used in this study have already been fully described in the general experimental part at paragraph 2.4.1.

The selected feedstock for all the activity tests was a commercial rapeseed oil (initial acidity 0.1%$_{wt}$), acidified with oleic acid up to 5%$_{wt}$, in order to obtain a high initial acidity.

FFA conversions were determined withdrawing oil samples at pre-established times (60, 120, 240, 360 minutes) and analysing the acidity through acid/base titrations as described in the general

experimental part in § 2.3.1. FFA conversion was then determined by equation 2.20 in § 2.4.3.

Catalyst	Reactor	Temp. (K)	Initial acidity (%wt)	Recycle of use
From SZ1 to SZ5 (Table 4.1)	vial	336	5.0	
ZS (Table 4.1)	vial	336	5.0	
	slurry	336		✓
	slurry with methanol recycle	363		✓
From STTO_0 to STTO_20 (Table 4.2)	vial	336	5.0	
STTO_20 (Table 4.2)	slurry	336	5.0	✓

Tab. 6.3. FFA Esterification experiments.

6.3 Results and Discussion

6.3.1 Catalysts characterization

The results of the characterization of sulphated Zr systems, i.e., BET surface area (SSA_{BET}), pores volume (V_p) and acidities (meq H^+/g) are given in Tab. 6.1. ZS is characterized by the highest acidity and lowest surface area. The coexistence of these two characteristics has already proven to be beneficial to the FFA esterification reaction activity (Boffito et al., 2012 a; 2012 b). In this case, in fact, the active sites on the catalyst's surface can be easily reached by sterically hindered molecules such as FFA.

Differently, the other sulphated Zr-based catalysts have significantly lower acidities and higher SSA than ZS. This might result in a low activity in the FFA esterification.

The samples SZ2a and SZb, i.e. the ones obtained by $Zr(OH)_4$ impregnation with sulphates, exhibit the lowest acidity. A hypothesis might be related to the poor absorption of sulphate groups on the ZrO_2 structure due to the choice of depositing the active groups in a second step. Since both these samples are characterized by very low and similar acidities, in spite being calcined at different temperature, a role of the calcination temperature in determining acidic properties cannot be stated in this case.

The quite high acidity and low surface area of sample SZ3 might potentially render this sample a better candidate for the FFA esterification than the other catalysts.

It has been reported (Lam et al., 2009) that the addition of sulphate groups causes part of the catalyst surface area to collapse. Nevertheless, the impregnated sulphate groups increase the pores width and volume of the catalyst. This phenomenon is important in biodiesel synthesis using solid acid catalysts, as catalysts with larger pores will minimize diffusion limitations especially for molecules having long alkyl chain. Primarily, catalysts with mesopores (10–50 nm) are preferred. On the other hand, the addition a support like SiO_2 or Al_2O_3 is reported to increase the BET surface area but retaining its mesopores properties. This is the case of samples SZ4 and SZ5.

Tab. 6.2 shows the BET surface area (SSA_{BET}), pore volume (V_p) and acidities (meq H^+/g) for the different sulphated SnO_2-TiO_2 systems. As it can be observed, the acidity of the samples, that was found to be a key issue in the FFA esterification activity, increases along the TiO_2 content. There are no data in literature on the acidic properties of sulphated SnO_2-TiO_2 systems but the increase of acidity with the TiO_2 content might be ascribable to the charge imbalance resulting from the heteroatoms linkage for the generation

of acid centres, as already described by Kataota and Dumesic in the case of the sulphated mixed Zr-Ti oxides (Kataota and Dumesic, 1988). The content of TiO_2 seems not to affect the specific surface area. Consequently, the number of acid active sites per unit of area increases with the content of TiO_2, as indicated in Tab. 6.2. This might results in a higher catalytic activity for sample with the highest TiO_2 content, i.e. STTO_20.

In case of CO adsorption, approximately 100 Torr of carbon monoxide was exposed to the samples at ambient temperature in order to determine whether differences existed in Lewis acidity of the surface of the samples of interest. Desorption was performed in stages allowing 50, 25, 10, 5, 2, 1, and 0 Torr of carbon monoxide to remain in contact with the sample.

No spectra will be reported for the sake of brevity, as all SnO_2-TiO_2 samples exhibit almost the same trend, both in the background profile and in the differential spectral features obtained for CO adsorption. In summary, it can be reported that:

i) Surface sulphate groups exhibit the spectral features typical of covalent species, as reported in the literature so far (Sarzanini et al., 1995), and, as a function of the increasing TiO2 content, the presence of polynuclear sulphate groups is evident;

ii) Lewis acidity, as tested by CO adsorption at room temperature, is present in very little amount, and can be ascribed, on the basis of both experimental evidences and literature data, to the presence of coordinatively unsaturated (cus) Ti^{4+} species present at the surface of the examined samples (Cerrato et al., 2009). No specific trend is evident as a function of the TiO_2 content.

6.3.2 Activity tests

In Fig. 6.1 a typical trend of the FFA esterification reaction is represented as an example for the sample of zirconium sulphate (entry 6 in Tab. 6.1). The FFA conversion increases with the time until the achievement of the plateau of conversion, according the reaction equilibrium (Boffito et al., 2012a; Bianchi et al., 2011; Pirola et al., 2011).

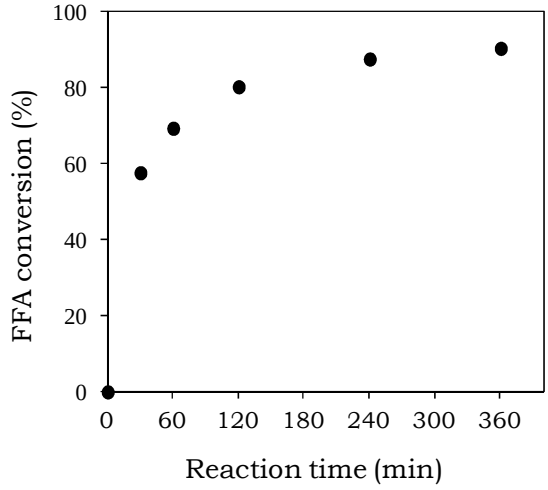

Fig. 6.1. FFA conversion vs. reaction time for zirconium sulphates, reaction vessel, 363 K.

As it can be observed, ZS allows to achieve a very high FFA conversions within 6 hours of reaction. This is ascribable to its high H^+ exchange capacity together with low SSA, for the reasons already highlighted in the section concerning catalysts characterization. A role in catalytic activity of ZS may be also played by Zr^{4+} Lewis acid sites, as evidenced in literature (Morterra et al., 1994; 1996; 1998; 2011; 2002). For this reason ZS is widely studied as a catalyst for various reactions, among which the FFA esterification. Due to the

high activity of ZS, it was decided to recycle it few times in the conditions usually adopted for the FFA esterification, i.e., 363 K and atmospheric pressure. Nevertheless, the major drawback of ZS lies in its fast deactivation due its partial solubility in water. Consequently recycles of catalyst use at 373 K with continuous evaporation of methanol and water yielded by FFA esterification were also performed. In this case, fresh methanol was continuously added into the reactor. The results of these experiments are displayed in Fig. 6.2. As it can be noticed, the catalyst deactivation is just slightly delayed operating at a temperature of 363 K instead of 336 K. Karl Fischer analyses performed on both evaporated methanol and the deacidfied oil after 6 hours of reaction, detected the presence of water just in the evaporated methanol but not in the oil, indicating that water removal from the system was actually achieved in the experiments at 336 K. Nevertheless, leaching of active sulphate groups from ZS might occur in presence of a liquid phase regardless of its polar nature. The presence of methanol might also have played a role in the loss of the sulphate groups from the catalyst.

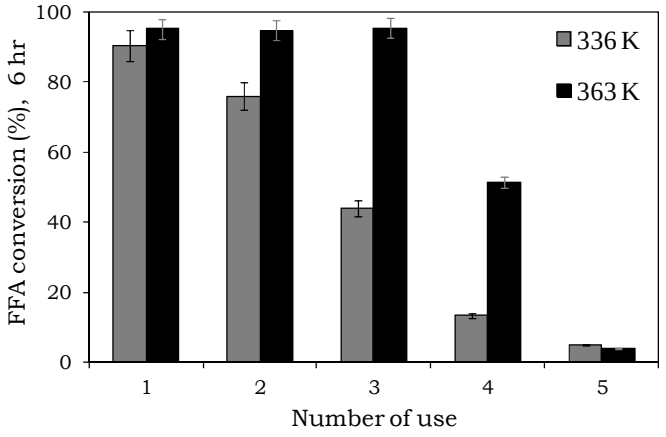

6.2. Results of the recycles of use of catalyst ZS.

Possible alternative to zirconium sulphate are represented by the sulphated zirconias (Chen et al., 2007; Lotero et al., 2005) or suphated supported catalysts (Jiménez-Morales, 2011; Juan et al., 2008).

The FFA esterification results of the sulphated ZrO_2 systems studied in this work are presented in Fig. 6.3.

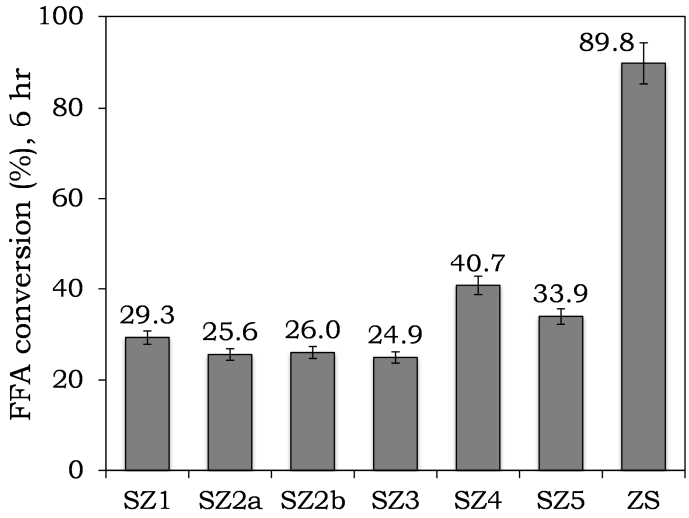

Fig. 6.3. FFA esterification results of the Zr-based sulphated systems.

The results displayed in Fig. 6.3 show that Zr-based sulphated systems do not provide a satisfactory performance in the FFA esterification, probably due to their low acid sites concentration related to their high SSA. Even if catalysts such as SZ3 and SZ4 exhibit higher surface area if compared to other catalysts, it is essential that this acidity is located mainly on the catalyst surface to be effectively reached by the FFA molecules. The author of this thesis have recently studied sulphonic ion exchange resins that are characterized by lower acidities than catalysts described in this chapter, but that perform better in the FFA esterification due to the

surface localization of the acid sites (Boffito 2012a; 2012c; Bianchi et al., 2011; 2010; Pirola et al. 2010; 2011).

In Fig. 6.4 the results of the FFA esterification tests on the sulphated Ti and Sn mixed oxides are shown. Other conditions being equal, these catalysts perform better than the sulphated Zr-based systems just described. This is more likely due to the higher acidity along with a low surface area. With increasing the TiO_2 content, the acidity increases as well. This might be ascribable to the charge imbalance resulting from the heteroatoms linkage for the generation of acid centres, as already explained in the case of the mixed Zr-Ti oxides in the previous paragraph (Kataota and Dumesic, 1988).

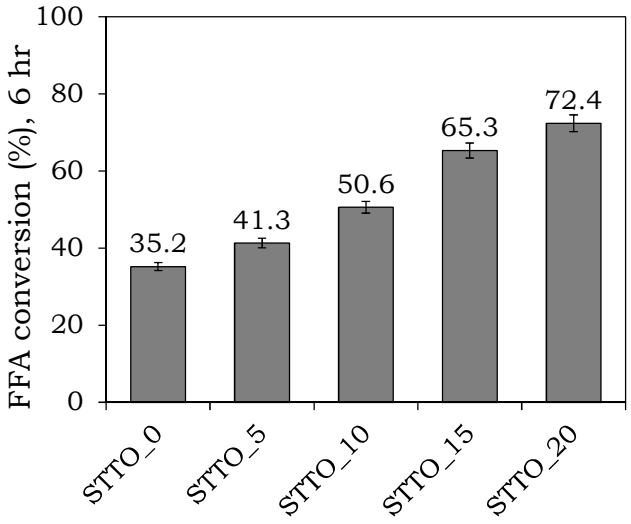

Fig. 6.4. FFA esterification results of the sulphated SnO_2-TiO_2 systems for different catalysts.

As a consequence, the activity in the FFA esterification increases with the TiO_2 content along with the acidity of the samples. For the sake of clarity, in Fig. 6.5 the FFA esterification conversions are represented as a function of the number of active sites per unit of

surface area of the samples: the FFA conversion increases with the number of meq H^+/m^2.

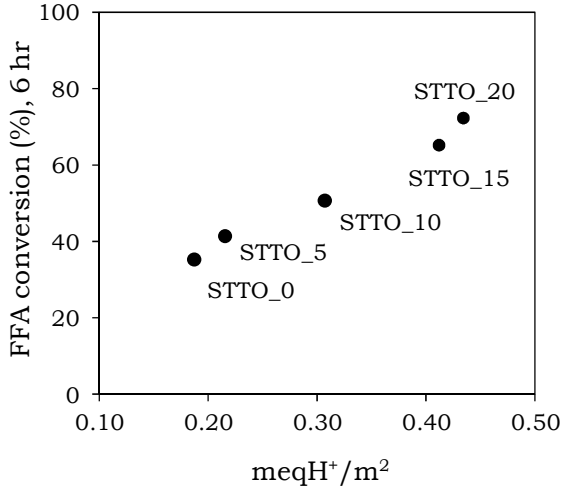

Fig. 6.5. FFA esterification results of the sulphated SnO_2-TiO_2 systems for different catalysts in function of the concentration of acid sites.

The best performing catalyst, i.e., the one with the highest TiO_2 content, was recycled few times to verify its stability in the FFA esterification. Results are shown in Fig. 6.6, whereby it can be noticed that the activity of the STTO_20 drastically drops already after the first recycle. This might be due to the leaching of sulphates groups during the first use and their consequent loss during discharge operations. To confirm this hypothesis also Sheldon test (Sheldon et al., 1998) was carried out on sample STTO_20. Sheldon test is a very simple way of checking if a catalyst is a real heterogeneous catalyst or if its activity is due to the active groups released into the reaction medium as a consequence of leaching. With this purpose, STTO_20 was removed from the reactor after 60 minutes of reaction. Results are represented in Fig. 6.7. As it can be seen, further FFA conversion was observed even after catalyst,

meaning that the catalysis of FFA esterification is due in large part to the active species leached into the solution.

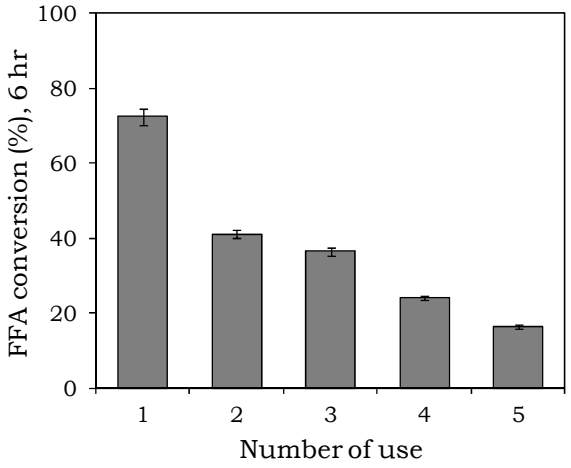

Fig. 6.6. FFA esterification results of the recycles of use of catalyst STTO_20.

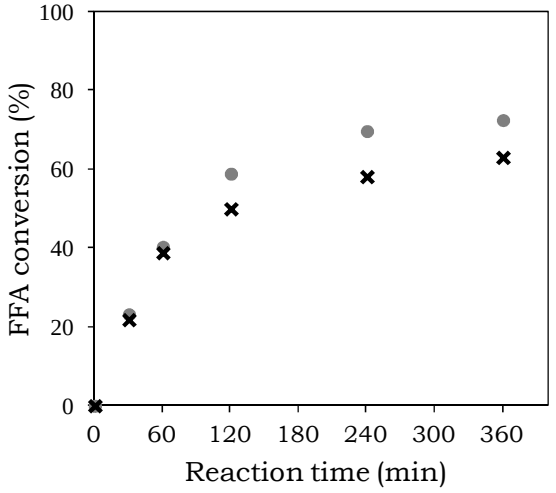

Fig. 6.7. FFA esterification results of Sheldon test of catalyst STTO_20.

6.4 Conclusions

Among all the tested sulphated Zr-based catalysts, commercial zirconium sulphate shows the highest activity in the free fatty acids (FFA) esterification, due to its high acidity. The main drawbacks of the use of $Zr(SO_4)_2$ still remain its partial solubility in water yielded by the reaction and the leaching of the active groups in methanol. Water removal from the system in the course of the reaction resulted to delay catalyst deactivation for insufficient times. Possible alternatives to $Zr(SO_4)_2$ are given by sulphated zirconia or supported sulphated materials. Nevertheless, these catalysts resulted in unsatisfactory catalytic performances due to the partial localization of the active sites inside the pores of the catalysts. This region cannot in fact be easily reached by sterically hindered molecules such as FFA.

Sulphated TiO_2-SnO_2 systems with TiO_2 content from 0 to 20%$_{wt}$ were obtained. These catalysts exhibit higher acidity than the sulphated ZrO_2 systems and their acidity increases with the TiO_2 content. Consequently, also their activity in the FFA esterification is higher. However, also TiO_2-SnO_2 systems deactivate in the adopted reaction conditions due to the leaching of the active species, as demonstrated by the results of recycles of use and the Sheldon test.

References

Ardizzone S., Bianchi C.L., Cappelletti G., Annunziata R., Cerrato G.,Morterra C., Scardi P. “Liquid phase reactions catalyzed by Fe- and Mn-sulphated ZrO2”, *Applied Catalysis A: General* **2009**, 360, 137.

Ardizzone S., Bianchi C.L., Cappelletti G., Porta F. “Liquid-phase catalytic activity of sulfated zirconia from sol–gel precursors: the role of the surface features”, *Journal of Catalysis* **2004**, 227, 470.

Arzamendi G., Arguinarena E., Campo I., Zabala S., Gandia L.M. “Alkaline and alkaline-earth metals compounds as catalysts for the methanolysis of sunflower oil”, *Catal. Today* **2008**, 133, 305.

Bianchi C.L., Boffito D.C., Pirola C., Ragaini V. “Low temperature de-acidification process of animal fat as a pre-step to biodiesel production”, *Catal. Lett.* **2010**, 134, 179.

Bianchi C.L., Pirola C., Boffito D.C., Di Fronzo A., Carvoli G., Barnabè D., A. Rispoli, R. Bucchi, “Non edible oils: raw materials for sustainable biodiesel”, in Stoytcheva M., Montero G. (Eds.): Biodiesel Feedstocks and Processing Technologies, Intech, **2011**, pp. 3-22.

Boffito D.C., Pirola C., Bianchi C.L. “Heterogeneous catalysis for free fatty acids esterification reaction as a first step towards biodiesel production”, *Chem. Today***, 2012a**, 30, 14.

Boffito D.C., Crocellà V., Pirola C., Neppolian B., Cerrato G., Ashokkumar M., Bianchi C.L., “Ultrasonic enhancement of the acidity, surface area and free fatty acids esterification catalytic activity of sulphated ZrO_2-TiO_2 systems”, J. Catal., **2012b**
http://dx.doi.org/10.1016/j.jcat.2012.09.013

Boffito D.C., Pirola C., Galli F., Di Michele A., Bianchi C.L., “Free Fatty Acids Esterification of Waste Cooking Oil and its mixtures with Rapeseed Oil and Diesel”, Fuel, **2012c**, accepted on 19th October 2012, DOI: 10.1016/j.fuel.2012.10.069.

Bourges M.E., Díaz L. “Recent developments on heterogeneous catalysts for biodiesel production by oil esterification and tranesterification reactions: a review”, *Renew. Sustain. Energy Rev.* **2012**, 16, 2839.

Cerrato G., Magnacca G., Morterra C., Montero J., Anderson J.A., “Modification to the Surface Properties of Titania by Addition of India”, *J. Phys. Chem. C* **2009**, 113(47), 20401.

Chen X.R., Ju Y.H, Mou C.Y. “Direct Synthesis of Mesoporous Sulfated Silica-Zirconia Catalysts with High Catalytic Activity for Biodiesel via Esterification”, *J. Phys. Chem.* **2007**, 111, 18731.

Dijs I.J., Geus J.W., Jenneskens L.W. “Effect of Size and Extent of Sulfation of Bulk and Silica-Supported ZrO2 on Catalytic Activity in Gas- and Liquid-Phase Reactions”, *J. Phys. Chem. B* **2003**, 107, 13403.

Jacobson K., Gopinath R., Meher L., Charan D., Ajay K. “Solid acid catalyzed biodiesel production from waste cooking oil”, *Applied Catalysis, B: Environmental* **2008**, 85(1.

Jiménez-Morales I., Santamaría-González J., Maireles-Torres P., Jiménez-López A. “Calcined zirconium sulfate supported on MCM-41 silica as acid catalyst for ethanolysis of sunflower oil”, *Appl. Catal. B: Environment* **2011**, 103, 91.

Jitputti J., Kitiyanan B., Rangsunvigit P., Bunyakiat K., Attanatho L., and Jenvanitpanjakul P. “Transesterification of crude palm kernel oil and crude coconut oil by different solid catalysts”, *Chem. Eng. J.* **2006**, 116(1), 61.

Juan J.C., Jiang Y., Meng X., Cao W., Yarmo M.A., Zhang J. “Supported zirconium sulfate on carbon nanotubes as water-tolerant solid acid catalyst”, *Mat. Res. Bullettin* **2007**, 42, 1278.

Juan J.C., Zhang J., Yarmo M.A . “Study of catalysts comprising zirconium sulfate supported on a mesoporous molecular sieve HMS for esterification of fatty acids under solvent-free condition”, *Applied Catalysis A: General* **2008**, 347(2), 133.

Kataoka T., Dumesic J.A. “Acidity of unsupported and silica-supported vanadia, molybdena, and titania as studied by pyridine adsorption”, *J. Catal.* **1988**, 112, 66.

Lam M.K., Lee K.T., Mohamed A.R. “Sulfated tin oxide as solid superacid catalyst for transesterification of waste cooking oil: An optimization study”, *Applied Catalysis B: Environmental* **2009**, 93, 134.

López D.E., Goodwin Jr. J.G., Bruce D.A. “Transesterification of triacetin with methanol on Nafion acid resins”, *J. Catal.* **2007**, 245, 381.

Lotero E., Liu Y., Lopez D.E., Suwannakaran K., Bruce D.A, Goodwin Jr. J.G. “Synthesis of biodiesel via acid catalysis”, *Ind. Eng. Chem. Res.* 2005, 44, 5353.

Lotero, E., Goodwin, J.G., Bruce, D.A., Suwannakarn, K., Liu, Y. & Lopez, D.E. “The catalysis of biodiesel synthesis”, *Catalysis* **2006**, 19, 41.

Ma F., Hanna M.A. “Biodiesel production: a review”, *Bioresour. Technol.* **1999**, 70, 1.

Marchetti J.M., Errazu A.F. “Comparison of different heterogeneous catalysts and different alcohols for the esterification reaction of oleic acid”, Fuel **2008**, 87, 3477.

Matsuhashi H., Hino M., Arata K. “Solid catalyst treated with anion: XIX. Synthesis of the solid superacid catalyst of tin oxide treated with sulfate ion”, *Applied Catalysis* **1990**, 59(2), 205.

Morterra C., Cerrato G., Ardizzone S., Bianchi C.L., Signoretto M., Pinna F. "Surface features and catalytic activity of sulfated zirconia catalysts from hydrothermal precursors", *Phys. Chem. Chem. Phys.* **2002**, 4, 3136.

Morterra C., Cerrato G., Di Ciero S. "IR study of the low temperature adsorption of CO on tetragonal zirconia and sulfated tetragonal zirconia", *Appl. Surf. Sci* **1998**, 126, 107.

Morterra C., Cerrato G., Meligrana G. "2,6-dimethylpyridine as an analytical tool to test the surface acidic properties of oxidic systems", *Langmuir* **2001**, 17, 7053.

Morterra C., Cerrato G., Pinna F., Signoretto M. "BrØnsted Acidity of a Superacid Sulfate-Doped ZrO_2 System", *J. Phys. Chem.* **1994**, 98, 12373.

Morterra C., Cerrato G., Signoretto M. "On the role of the calcination step in the preparation of superacid sulfated zirconia catalysts", *Catal. Lett.* **1996**, 41, 101.

Perego C., Ricci, M. "Diesel fuel from biomass", Catal. Sci. Technol. 2012, 1, 1776.

Pirola C., Bianchi C.L., Boffito D.C., Carvoli G., Ragaini V. "Vegetable oil deacidification by Amberlyst : study of catalyst lifetime and a suitable reactor configuration", *Ind. Eng. Chem. Res.* **2010**, 49, 4601.

Pirola C., Boffito D.C., Carvoli G., Di Fronzo A., Ragaini V., Bianchi C.L., "Soybean oil deacidification as a first step towards biodiesel production", in D. Krezhova (Ed.): Recent Trends for Enhancing the Diversity and Quality of Soybean Products, Intech, **2011**, pp. 321-44.

Sarzanini C., Sacchero G., Pinna F., Cerrato G. Morterra C., "Amount and nature of sulfates at the surface of sulfate-doped zirconia catalysts", *J. Mater. Chem.* **1995**, 5, 353.

Sun Y., Ma S., Du Y., Yuan L., Wang S., Yang J., Deng F., Xiao F.S. "Solvent-Free Preparation of Nanosized Sulfated Zirconia with Brønsted Acidic Sites from a Simple Calcination", *J. Phys. Chem. B* **2005**, 109, 2567.

CHAPTER 7:
ULTRASONIC SYNTHESIS AND CATALYTIC ACTIVITY OF SULPHATED ZrO_2-TiO_2 SYSTEMS

The work presented in this chapter was carried out at the Sonochemistry Laboratory of the University of Melbourne (School of Chemistry) headed by Prof. M. Ashokkumar. A special thank goes to him. I would also like to acknowledge to the DEEWR (Department of Education, Employment and Workplace) of the Australian Government for awarding the Australian Awards Endeavour Research Fellowship and make this work possible.

Abstract

Different samples of sulphated zirconia and mixed zirconia/ titania (SO_4^{2-}/ZrO_2 and $SO_4^{2-}/80\%ZrO_2$-$20\%TiO_2$), were prepared with traditional and ultrasound (US) assisted sol-gel synthesis and tested in the free fatty acids esterification. The catalysts were characterized through acid sites quantification by ion exchange, specific surface area and porosity measurements (N_2 adsorption at 77 K), XRD, XPS and FT-IR spectroscopy. SEM-EDX and TEM analyses were also used to investigate the morphology of the samples. The results of this study demonstrate the possibility of increasing the acidity and the surface area of sulphated zirconia through the addition of TiO_2 and tune the same properties with the continuous or pulsed US. It is also demonstrated that it is necessary to combine specific values of both acidity and surface area and which type of active sites are essential to obtain better catalytic performances in the free fatty acids esterification.

7.1 Introduction

Free fatty acids (FFA) esterification reaction can be performed using both homogeneous (Aranda et al., 2008; Marchetti et al., 2008) and heterogeneous catalysis (Di Serio et al., 2007; Marchetti et al., 2007). For liquid phase reactions, the latter approach is preferred as it brings benefits such as the easier separation of the catalyst from the products, thus facilitating catalyst recovery and re-use. Much attention has been focused on the use of ion exchange acid resins as catalysts for the FFA esterification reaction (Bianchi et al., 2010, 2012; Pirola et al., 2010, 2011; Boffito et al., 2012). A significant outcome of these studies lies in the correlation between the catalytic activity of the tested catalysts with the acidity present on the catalyst outer surface regardless of the nature of adopted catalysts (Boffito et al., 2012).

As an alternative to the ion exchange resins inorganic acid catalysts, such as zirconium sulphate and sulphated zirconia, can be used. These materials are active because of the presence at the surface of both Brønsted acidic centres and Lewis acid sites (i.e. coordinatively unsaturated (cus) Zr^{4+} cations), as evidenced by Morterra et al. (Morterra et al, 2001). Zirconium sulphate has been widely studied for the FFA esterification reaction (Boffito et al., 2012; Juan et al., 2007) due to its high activity. Sulphated zirconia is widely studied for other different kinds of reactions, such as isomerizations, alkylations and esterification of other carboxylic acids (Ardizzone et al., 2004), but its use for FFA esterification directly performed in the oil is reported in few studies (Dijs et al., 2003).

In the present work, mixed zirconium and titanium sulphated oxides (SO_4^{2-}/80%ZrO_2-20%TiO_2) are reported as potential catalysts

for the FFA esterification reaction to be performed directly in the crude oil to be used for biodiesel production. The results of this study demonstrate the possibility of increasing the surface acidity of the catalysts with the addition of TiO_2 to the ZrO_2 and the use of US during the catalysts synthesis. The effect of different power intensities and the use of pulsed US are also investigated. The beneficial effects of acoustic cavitation on catalysts properties are already clearly reported in some recent papers (Neppolian et al., 2007; Pirola et al., 2020; Suslick and Doktycz, 1990). It has also been shown in the current study how it is possible to modulate catalysts features, such as the acidity and the surface area, employing different experimental conditions during the US-assisted synthesis.

7.2 Materials and Methods

7.2.1 Catalysts preparation

All the catalysts were synthesized using the sol-gel method. SO_4^{2-}/ZrO_2 (hereafter referred to as SZ) was synthesized using traditional sol-gel method, while $SO_4^{2-}/80\%ZrO_2$-$20\%TiO_2$ (hereafter referred to as SZT) was synthesized using both traditional and US-assisted sol-gel techniques. Zirconium tetra-n-propoxide (ZTNP) and titanium tetra-iso-propoxide (TTIP) were used as precursors in all the cases. i-PrOH was used as a solvent in all the synthesis with a molar ratio to the precursors (ZTNP+TTIP) equal to 15 (Ardizzone et al., 2004; Neppolian et al., 2007). Molar ratio between water and the alkoxides (ZTNP+TTIP) was kept constant at 30 as already reported elsewhere (Ardizzone et al., 2004) in the traditional syntheses and varied in the

ones with US. $(NH_4)_2SO_4$ was used as sulphating agent, keeping the molar ratio SO_4/Zr or SO_4/Zr+Ti constant at 0.15 in all the cases (Ardizzone et al., 2004).

Nitric acid was used to promote the hydrolysis of the precursors, as already reported in other works from the authors (Ardizzone et al., 2004; Neppolian et al., 2004). The molar ratio HNO_3/Zr or HNO_3/Zr+Ti was kept constant at 0.21 (Ardizzone et al., 2004).

A list of all the samples along with different synthesis parameters is provided in Tab. 7.1.

Entry	Sample		US power (%)[1]	Pulses (on/off)	H_2O: prec. mol ratio	Synthesis time	Sonication time
1	SZ	SO_4^{2-}/ZrO_2	-	-	30	123'0"	0"
2	SZT		-	-		123'0"	0"
2a	SZT_ 773_6h		-	-		123'0"	0"
3	USZT_20_1_30		20	1		43'0"	43'0"
4	USZT_40_0.1 _30	SO_4^{2-}/80%ZrO_2-20%TiO_2	40	0.1/0.9		43'0"	4'18"
5	USZT_40_0.3_30			0.3/0.7		43'0"	12'54"
6	USZT_40_0.5_7.5			0.5/0.5	7.5	17'30"	8'45"
7	USZT_40_0.5_15				15	26'0"	13'0"
8	USZT_40_0.5_30				30	43'0"	21'30"
9	USZT_40_0.5_60				60	77'0"	38'30"
10	USZT_40_0.7_30			0.7/0.3	30	43'0"	30'6"
11	USZT_40_1_15			1	15	26'0"	26'0"
12	USZT_40_1_30				30	43'0"	43'0"

[1] % of the maximum power.

Tab. 7.1. List of all samples and of employed synthesis parameters (max. power = 450 W).

Samples termed USZT refer to US-obtained sulphated 80%ZrO_2-20%TiO_2. The name is followed by the US power, by the length of US pulses and by the molar ratio of water over precursors, as reported in Table 1. For example, USZT_40_0.1 _30 indicates a sample SO_4^{2-}/80%ZrO_2-20%TiO_2 obtained with US, using the 40% of the

maximum power, with US on for 0.1 seconds (pulse length) and off for 0.9 seconds, using a water/ZTNP+TTIP molar ratio equal to 30.

ZTNP 70% in 1-PrOH, TTIP 98%, i-PrOH, HNO_3 69.5% wt and $(NH4)_2SO_4$ were used and are all Fluka products.

In the case of traditional sol-gel method, the starting solution was prepared by mixing 1.23 ml of TTIP and 5.52 ml of ZTNP with 25 mL of the solvent (i-PrOH) for 30 minutes in a bath thermostated at 298 K, stirring at 300 rpm through a mechanical stirrer. The aqueous solution containing the sulphating agent and HNO_3 was then added to the mixture at the rate of 0.25 ml/min. After finishing the addition, the gel was left aging for additional 90 minutes under stirring.

In the case of US synthesis, a 20 kHz horn sonicator was used. The tip of the horn was placed inside the sol-gel mixture in a 100-mL water-jacketed reactor. The power was varied at 20 and 40% of amplitude of the maximum power (450 W). Also US pulses were adopted for some syntheses.

For what concerns the US syntheses, as in the case of the traditional synthesis, the starting solutions were prepared by mixing the precursors with the solvent and stirring them for 30 minutes. After the mixing, the solutions were thermostated at 298 K and the aqueous solution containing the sulphating agent and HNO_3 was added at the rate of 0.25 ml/min. After finishing the addition of the aqueous solution, the gel was left aging for additional 10 minutes under US irradiation.

The total synthesis time reported in Tab. 7.1 indicates the time required to perform the whole sol-gel process, while the sonication time indicates the fraction of the total synthesis time while US were functioning. As an example, consider entry 4 in Tab. 7.1. The total synthesis time is 43'0", which is the sum of the time required for the

addition of the aqueous solution to one of the precursors at a rate of 0.25 ml/min and 10 minutes for the aging. Since the US was powered in pulse mode with on/off ratio 9:1, the actual sonication time is given by (1/10) • 43”0’, i.e. 4’18”.

The temperature was monitored during the course of the ultrasonic synthetic experiments. The temperature increased up to 313 K during the first few minutes of the reaction, then remained constant till the end of the experiments.

All the samples were calcined in static air atmosphere at 773 K for 3 hours with a heating rate of 2.5 K/min. The choice of such a temperature, along with the choice of both slow heating rate and duration of the treatment, was dictated by the need to preserve the largest number of sulphate groups after the calcination, as suggested by Dijs et al. (Dijs et al., 2003).

In order to demonstrate that the choice of specific calcination conditions is fundamental to avoid the loss of a too large fraction of surface sulphates groups, thereby affecting the catalytic activity, the sample SZT was also calcined at 773 K for 6 hours, employing the same heating rate. This sample is reported as SZT_773_6h in entry 2a, Tab. 7.1.

7.2.2. Catalysts characterization

Nitrogen adsorption – desorption isotherms were measured at 77 K using a Micromeritics Tristar 3000 system. All samples were degassed at 433 K overnight on a vacuum line. The standard multi-points Brunauer–Emmett–Teller (BET) method was utilized to calculate the specific surface area (SSA). The pores size distributions of the materials were derived from the adsorption branches of the

isotherms based on the Barett–Joyner–Halenda (BJH) model (Gregg and Sing, 1982).

XPS analyses were obtained using an M-probe apparatus (Surface Science Instruments). XP spectra were collected using a VG ESCALAB 220i-XL spectrometer equipped with a monochromatic Al Kα X-ray source which emitted a photon energy of 1486.6 eV at 10 kV and 12 mA. The measurements were processed at a step size either 1 eV (wide scans) or 0.1 eV (region scans). Film samples were screwed down to Al holders. Precursor samples were adhered to the surface of In metal and then mounted on Al holder. Charging of catalyst samples was corrected by setting the binding energy of adventitious carbon (C 1s) at 284.6 eV. Curve fitting and quantification of XP spectra were performed using Eclipse and Casa XPS programs.

FTIR spectra were run at 4 cm^{-1} resolution with a Bruker IFS 113v spectrophotometer equipped with MCT detector. The powder samples were investigated in the form of thin layer depositions (~ 10 mg cm^{-2}) on a pure Si wafer, starting from aqueous suspensions of the powders. After drying, all samples were activated in controlled atmosphere at 623 K in a homemade IR quartz cell, equipped with KBr windows, connected to a conventional vacuum glass line capable of a residual pressure $<1 \times 10^{-5}$ Torr, which allowed to perform strictly in situ adsorption/desorption experiments of molecular probes. The study of surface acidity was performed using as probe 2,6-dimethylpyridine (2,6-DMP; Lu). The standard IR experiment of 2,6-DMP adsorption/desorption on the various samples, was carried out as follows: (i) admission in the IR cell of an excess dose of 2,6-DMP vapour (~ 2 Torr), and equilibration at beam temperature (hereafter BT), i.e., the temperature reached by samples in the IR beam, for 5 minutes; (ii) evacuation of the base excess at

BT for 15 minutes; (iii) desorption of the strongly bonded 2,6-DMP fraction was eventually carried out at 423 K for 15 minutes.

The quantification of the Brønsted acidity was carried out through ion exchange with a NaCl saturated solution, leaving it in contact with the catalysts for 30 hours (López et al., 2007). The evaluation of H^+ concentration was carried out using a pH-meter. The number of H^+ milliequivalents released per gram of catalyst was then calculated.

The crystalline nature of the samples was investigated by X-ray diffraction (XRD) using a PW3050/60 X'Pert PRO MPD diffractometer from PANalytical working Bragg-Brentano, using as source the high power ceramic tube PW3373/10 LFF with a Cu anode equipped with Ni filter to attenuate Kβ. Scattered photons have been collected by a RTMS (Real Time Multiple Strip) X'celerator detector.

The morphology of the catalysts was inspected by means of high resolution electron transmission microscopy (HR-TEM) and scanning electron microscopy (SEM). SEM-EDX (Energy-dispersive X-ray spectroscopy) was used to determine the amount of Zr, Ti and S in the samples.

TEM images were recorded using a JEOL 3010-UHR instrument (acceleration potential: 300kV; LaB6 filament). Samples were "dry" dispersed on lacey carbon Cu grids. Philips XL-30CP with RBS detector of back scattered electrons was used for SEM-EDX analyses.

Sulphates amount of both SZT and SZT_773_6h samples was determined by ion chromatography (Metrohm mod. 883 Basic IC Plus) so to assess the loss of sulphate groups generated by the different calcination procedures. The solutions injected in the ion chromatograph and containing the sulphates were obtained

suspending the catalysts in a NaOH solution 0.1 M at ambient temperature and then filtering the liquid through a 0.45 μm PTFE filter, as already reported elsewhere (Sarzanini et al., 1995).

7.2.3 Catalytic tests

All catalysts were tested in the FFA esterification reaction with methanol.

The selected feedstock was a commercial rapeseed oil (initial acidity 0.1% wt), acidified with oleic acid up to 7.5% wt, in order to obtain a high initial acidity. The stoichiometric alcohol/acid ratio for the esterification reaction is 1:1, but it is advisable to use a higher amount of alcohol to shift the reaction towards the desired products. For this reason, the added amount of methanol was calculated taking into account the oil mass to treat and not the reaction stoichiometry. Consequently, the methanol/oil weight ratio was 16:100, corresponding to about 4.5:1 MeOH:oil molar ratio. All catalytic tests were performed with the catalyst suspended in the reaction medium, using 25-mL magnetically stirred vials as esterification reactors. Therefore, the composition of each vial was: 17 g of oil at 7.5% wt of acidity, 2.7 g of methanol and ~0.064 g of catalyst, corresponding to the 5% of catalyst over FFA by weight.

The reactors were thermostated before starting the activity tests using an oil bath at 336 ± 2 K. The mechanical stirring was maintained at 300 rpm. All the activity tests were carried out for 6 hours.

Oil acidity was determined through titration analyses with KOH 0.1 M in ethanol. Since oil and KOH are not soluble, each sample was dissolved before titration in a mixture of diethylether: ethanol 9:1 per volume, in order to obtain a homogeneous mixture.

Phenolphthalein was used as indicator. The percentage of FFA content per weight was calculated as in Eq.7.1 (Bianchi et al., 2010; Pirola et al., 2010; Boffito et al., 2012; Russbueldt and Hoelderich, 2009; Pasias et al., 2006):

$$FFA=\frac{V\times MW\times C}{W}\times 100 \qquad 7.1$$

where V is the volume of KOH solution employed for titration (mL), MW is the molecular weight of oleic acid (282.46 mg $mmol^{-1}$), C is the concentration of KOH (mmol mL^{-1}) and W is the weight of the analysed sample (mg).

FFA conversions, i.e. the percentage of oleic acid converted in oleic methylester were determined as in Eq. 7.2.

$$FFA\ conversion\ (\%)=\frac{FFA_{t=0}-FFA_t}{FFA_{t=0}}\times 100 \qquad 7.2$$

where a_i is the initial acid concentration by weight and a_f is the acid concentration after 6 hours of reaction.

As already evidenced in previous studies of the authors (Bianchi et al., 2010; Pirola et al., 2010), the experiment carried out in absence of the catalyst showed no FFA conversion.

All the products used for catalytic tests are Fluka products of high purity.

7.3 Results and Discussion

7.3.1 Catalysts characterization

7.3.1.1 Structural and morphological features

Brønsted acidity (measured through ion exchange), specific surface area and porosity features of all samples are reported in Tab. 7.2.

It can be noticed that the simple addition of TiO_2 to the sulphated ZrO_2 increases the acidity of the catalyst more than 2.5 times (compare entries 1 and 2 in Tab. 2). It is reported in the literature that the addition of TiO_2 to ZrO_2 can increase the surface concentration of –OH groups (Neppolian et al., 2007; Das et al., 2002).

Entry	Catalyst	Acid capacity (meq H^+/g)	SSA (m^2g^{-1})	V_p (cm^3g^{-1})	Ave. BJH D_p (nm)	Zr:Ti weight ratio	S/(Zr+Ti) atomic ratio
1	SZ	0.30	107	0.20	6.0	100	0.090
2	SZT	0.79	152	0.19	5.0	79:21	0.085
2a	SZT_773_6h	0.21	131	0.20	5.0	n.d.[1]	n.d
3	USZT_20_1_30	0.92	41.7	0.12	12.5	80:20	0.095
4	USZT_40_0.1_30	1.03	47.9	0.11	9.5	81:19	0.067
5	USZT_40_0.3_30	1.99	232	0.27	4.5	81:19	0.11
6	USZT_40_0.5_7.5	1.70	210	0.20	5.0	78:22	0.086
7	USZT_40_0.5_15	2.02	220	0.20	5.0	80:20	0.13
8	USZT_40_0.5_30	2.17	153	0.20	5.0	78:22	0.12
9	USZT_40_0.5_60	0.36	28.1	0.10	10	79:21	0.092
10	USZT_40_0.7_30	1.86	151	0.16	5.0	78:22	0.11
11	USZT_40_1_15	3.06	211	0.09	7.0	80:20	0.15
12	USZT_40_1_30	1.56	44.1	0.09	7.0	80:20	0.17

[1] not determined

Tab. 7.2.. Acid capacities (ion exchange), specific surface areas (BET) and porosity features (Pores volume V_p and average diameter D_p), elemental composition (EDX) of all catalysts.

This behaviour is generally observed for mixed oxides and it is probably due to the charge imbalance resulting from the heteroatoms linkage for the generation of acid centres (Kataota and Dumesic, 1988). The addition of TiO_2 to ZrO_2 is also reported to decrease the particle size and increase the surface area (Fu et al., 1996) as observed for the samples synthesized in the current study.

It has been observed that with the use of US during the synthesis a further increase in acidity occurred, as well as the surface area (compare entries 1 and 2 with entries from 3 to 12 in Tab. 7.2).

The improvement in the properties of the catalysts is probably due to the effects generated by acoustic cavitation. Acoustic cavitation is the growth of bubble nuclei followed by the implosive collapse of bubbles in solution as a consequence of the applied sound field. This collapse generates transient hot-spots with local temperatures and pressures of several thousand K and hundreds of atmospheres, respectively (Sehgal et al., 1979). Very high speed jets (up to 100 m/s) are also formed. As documented by Suslick and Doktycz (Suslick and Doktycz, 1990), in the presence of an extended surface, such as the surface of a catalyst, the formation of the bubbles occurs at the liquid-solid interface and, as a consequence of their implosion, the high speed jets are directed towards the surface. The use of sonication in the synthesis of catalysts can therefore result in the enhancement of the distribution of the active phase on the support (Pirola et al, 2010), increasing the rates of intercalation by a variety of species into a range of chalcogenides solids, improving the nucleation production rate (i.e. sol-gel reaction production rate) and the production of surface defects and deformations with the formation of brittle powders (Suslick and Doktycz, 1990).

At equal water/precursors molar ratios, the acidity of the catalysts increases further when pulse-on time of higher than 0.3 are adopted (compare entries 5, 8, 10 with entry 12 in Tab. 7.2). For these catalysts an increase in the SSA, as well as in the acidity is observed if compared to the sample obtained with continuous US.

An attempt was made to explain the effect of various pulse lengths and on/off ratios in terms of two times, τ1 and τ2 characteristics of each cavitation system (Suslick and Doktycz, 1990; Hengelein et al., 1989)). τ1 is the time required to produce and then grow chemically active gas bubbles, τ2 is the time taken by all the gas bubbles generated during the previous US pulse to dissolve away. If τ1 is shorter than the US pulse length, the system activates. If τ2 is longer than the interval time from one US pulse to the following one, gas bubbles still present in the system can generate bubble nuclei able to grown within the following US pulse. Hence, the active bubbles population is high at short τ1 with long τ2. This condition is more easily achieved when long pulse lengths and short intervals between one US pulses to the other are adopted. During the US pulse bubbles also coalesce leading to “degassing effect”. Moreover, at long US pulses with short intervals, including continuous sonication, degassing may result in a lower number of active bubbles: it can be stated that there is an optimal on/off ratio for US pulse times for which maximum cavitation efficiency (maximum number of active bubbles) can be achieved.

Considering the effect of different water/precursors ratios, a general observation can be done: the SSA decreases when higher water amounts are used (compare entries from 6 to 9 and 11 to 12 in Tab. 7.2). This may be ascribed to a decrease of US power per unit volume inside the sol-gel reactor. Increasing and decreasing the water amount can be seen in fact as increasing and decreasing,

respectively, the reactor size (Neppolian et al., 2007). When the ultrasonic power per unit volume is increased as a consequence of the diminishment of the reactor size, higher energy is supplied to the system. That is the reason why a lower water amount might lead to a higher surface damage and, as a consequence, to the formation of extra surface area under the effect of US. The effect of the increase of water amount on the SSA is particularly evident for the sample USZT_40_0.5_60, i.e., the one obtained with the highest H_2O/precursors ratio (entry 9 in Tab. 7.2). For this catalyst, the SSA is in fact significantly lower than the ones of the samples obtained with lower H_2O/ZTNP+TTIP ratios. From the BJH adsorption data (data not provided for the sake of brevity), it is evident that all the samples are characterized by similar pore size distribution. In particular, the distribution resulted to be rather narrow and mainly located in the lower region of the mesopores. In Tab. 7.2 the average pore diameter and the volume of the pores are reported for all the catalysts. No significant differences in the pores dimensions were observed among the samples.

For what concerns how the water/precursors ratio affects the catalysts acidity, it appears that increasing it up to a certain amount brings to an increase in the H^+ concentration (compare entries from 6 to 9 and 11 to 12 in Tab. 7.2). In fact, the rate of the hydrolysis, i.e., the rate of the sol-gel process, is enhanced when using higher water amounts. Moreover, the higher the water amount in the sol-gel medium, the higher the probability that H_2O molecules can be chemically bounded producing extra $–OH^+$ Brønsted acidity. Nevertheless, increasing the water/precursors ratio over a certain amount (30 for pulsed and 15 for continuous US, entries 8 and 11 in Tab. 2, respectively), seems to have a negative effect on the acidity concentration. In fact, the risk of the extraction of acid groups by

the excess of water increases as well. In addition, a role might have been also played by the different power densities, which lead to a more or less effective surface damage, as already explained for the differences in the specific surface areas.

For the same reason, the increase of the water amount produces a lowering of the overall Brønsted acidity and not just the decrease of the SSA for the sample USZT_40_0.5_60, (entry 9 in Tab. 7.2). As a consequence, these results may be considered due to the same phenomenon.

The XRD analysis highlights the total absence of crystalline structure in all materials. Curve (1) in Fig. 7.1. (SZT sample) is typical of an amorphous system. For the sake of brevity, we reported only this diffractogram, as all the others are almost perfectly coincident. The XRD pattern of SZT_773_6h is also reported in Fig. 7.1. [see curve (2)]. In this case, the material exhibits a net crystalline structure, revealing a series of reflections consistent with the presence of both ZrO_2 and TiO_2, in tetragonal and anatase phase, respectively. This result highlights the effects of the different calcination times (3 vs. 6 hours) at the same temperature (773 K): it is evident that these conditions deeply affect the nature of the above materials.

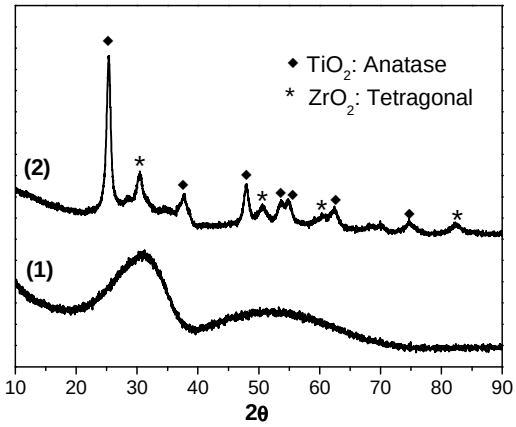

Fig.7.1. XRD patterns of SZT (1) and SZT_773_6h (2).

HR-TEM and SEM investigations of all samples further confirm what XRD analysis indicated. HR-TEM images (reported in Fig. 7.2) show the almost total amorphous nature of the particles in all cases: for the sake of brevity, we decided to report the features of SZT as this is typical of all systems (see the left hand image). On the contrary, crystalline particles with irregular shape (average diameter in the 4-7 nm range and exhibiting net fringe patterns) are easily observable in the case of the SZT_773_6h material (see the right hand image). SEM images are not reported here as the useful information about the morphology of the samples are already given in Fig. 7.2. for the HR-TEM survey.

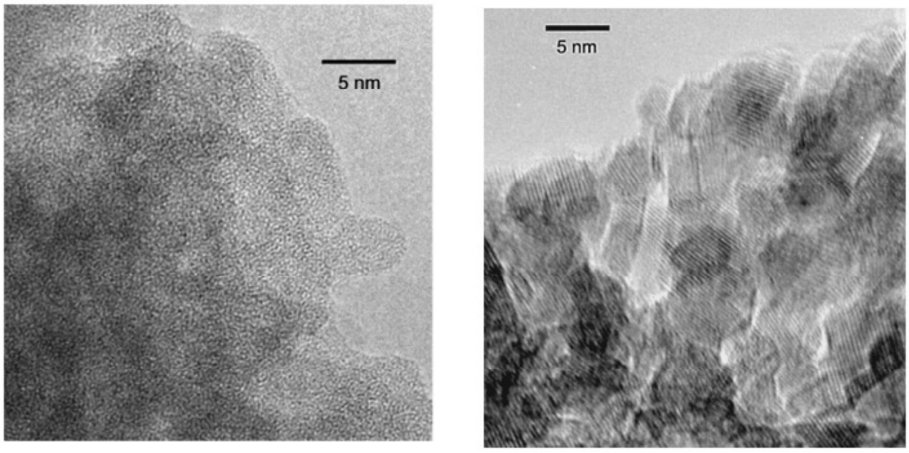

Figure 7.2. HR-TEM images of SZT (left hand) and SZT_773_6h (right hand).

The amount of sulphates concentration evaluated by ion chromatography for the samples SZT and SZT_773_6h was 1.4 and 1,1 mg SO_4^{2-}/mg (ZrO_2-TiO_2), respectively. This indicates that the sample calcined for long time (SZT_773_6h) significantly loses part of its surface sulphates groups, thus resulting in SO_4^{2-} content that is 20% less than SZT.

After all these preliminary characterization measurements, it can be stated that the choice of the calcination conditions reported in the catalysts preparation section (3 hours at 773 K) allows to obtain materials that still possess a good amount of surface sulphate groups. In fact, though the increase of the calcination time and/or the employment of a higher calcination temperature, would permit to generate crystalline materials, the subsequent consistent loss of surface sulphates might produce a drastic decrease of the catalytic activity.

7.3.1.2 Spectroscopic measurements

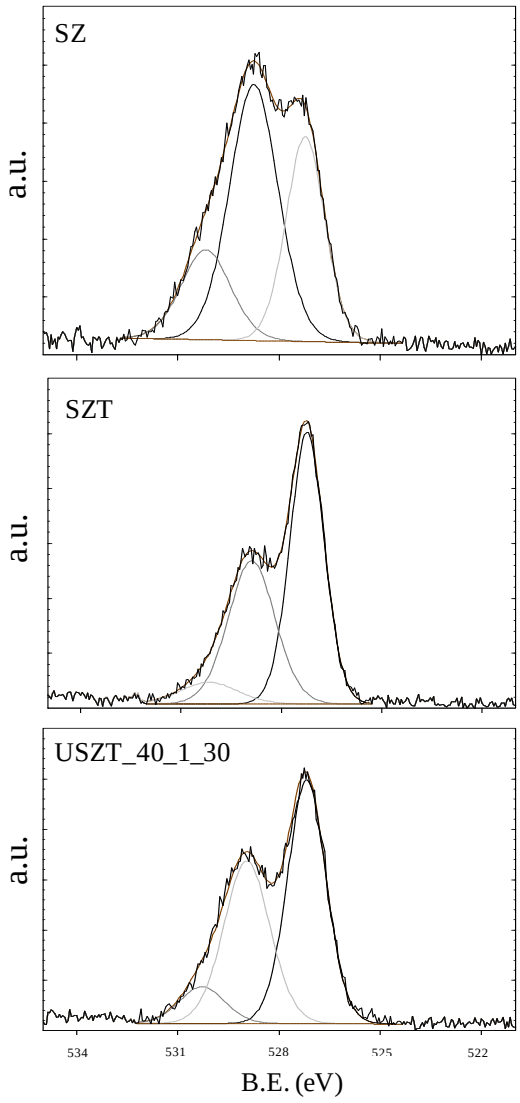

Fig. 7. 3. O 1s region of the samples SZ, SZT and USZT_40_1_30.

The region O 1s of the XP spectra are reported in Figure 7.3. for the samples SZ, SZT and USZT_40_1_30. XP spectra of the other samples obtained with US are not reported, being these almost perfectly coincident with the one reported for USZT_40_1_30.

In the XP spectra no significant amount of impurities was observed except for the ubiquitous carbon contaminant. In the case of the latter element, only the C 1s peak at 284.6 eV (due to –CH– species) was present. The spectrum of S 2p (not reported for the sake of brevity) was never intense, due to the low intrinsic sensitivity factor of this element, and could be fitted for all the samples by a single component at BE = 169.3 eV, in agreement with that expected for sulphur in sulphates (Moulder et al., 1992) and consistent with previous results relative to other SZ samples (Ardizzone et al., 2004; 2000; Ardizzone and Bianchi, 1999; Morterra et al., 2002). No appreciable presence of S-containing

species with valence different from S(+6) was ever observed. As for the S/(Zr+Ti) atomic ratios, they are reported in the Tab. 7.3. as well as the other atomic ratios between the elements. For the sample USZT_40_1_30 the calculated ratio of S/Zr+Ti is higher than the two samples obtained without ultrasound, i.e. 0.54 (USZT_40_1_30) vs. 0.40 (SZT) and 0.32 (SZ). The higher content of S in SZT than SZ can be explained considering that Ti is more electronegative than Zr. Therefore, the formation of mixed Zr and Ti species might have increased the electropositive character of Zr, thereby stabilizing sulphate groups, as also reported by Das et al. (Das et al., 2002). A higher amount of superficial sulphur indicates a higher surface functionalization. This may more likely result in a higher catalytic activity.

Sample	O 1s B.E. (eV)	Ti $2p_{3/2}$ B.E. (eV)	Zr $3d_{5/2}$ B.E. (eV)	S 2p B.E. (eV)	O/(Zr+Ti)	S/(Zr+Ti)	O/S
SZ	531.3	-	182.2	168.3	5.56	0.32	17.6
SZT	530.4	458.4	182.2	168.3	4.58	0.40	11.5
USZT_40_1_30	530.3	458.3	182.2	169.3	4.41	0.54	8.18

Tab. 7.3. XPS binding energies (B.E.) and elemental atomic ratios of the samples SZ, SZT and USZT_40_1_30.

The data obtained by XPS are in all cases far larger than those obtained by EDX (reported in Tab. 7.2). This is in agreement with the prevalent surface localization of sulphates introduced by impregnation (Morterra et al., 2002). The sulphation of zirconia samples, yielding strong acidic properties, has been reported to modify the spectral features of both O 1s and Zr 3d XPS signals (Ardizzone and Bianchi, 1999; Ardizzone et al., 2000; Morterra et al., 2002). But, unlike what has been tried by other authors (Paal et al., 1999; Bucholz et al., 1999) the intrinsic complexity of the O 1s

spectral region, brought about by the presence of several O-containing components, does not favour meaningful quantitative analytical use of the XPS O 1s peak. The peak of the Zr 3d doublet was found to be in any case regular with BE values (182.2–184.6 eV) for all the samples (spectra not reported for the sake of brevity), consistent with literature data relative to Zr(IV) species in the oxide phase (Moulder et al., 1992, Ardizzone and Bianchi, 1999; Ardizzone et al., 2002; Paal).

The FTIR spectra, in the 4000-800 cm^{-1} range, were collected for all samples after activation at 623 K in O_2 atmosphere. They showed the typical spectral features of sulphate-modified zirconia. These systems have been widely studied in recent years by means of FTIR spectroscopy (Bensitel et al., 1987; Chen et al., 1993; Comelli et al., 1995; Morterra et al., 1996; 1994; 1998; 2003) and, therefore, these spectra have not been presented.

IR spectroscopic investigation of 2,6-DMP (Lu) adsorption/desorption is a useful analytical tool in surface chemistry because: (i) the strong base can interact, in a molecular form, with both weak and strong Lewis acid site (Morterra et al., 2001; 2003). The presence of methyl groups in the two α-positions of the heteroaromatic ring renders labile and reversible at BT, or just above that, the species adsorbed on weaker Lewis sites, whereas the species adsorbed on strong Lewis sites are much less labile and can thus be resolved; (ii) the interaction with acid protonic sites (Brønsted acid centres) yields lutidinium ions (LuH^+), whose spectral features can be easily recognized and differentiated from those of all other 2,6-DMP adsorbed species (Morterra et al., 2001; 2003).

Fig. 7.4. reports, for some of the systems of interest, the main analytical spectral features in the region of the 8a–8b ring vibrational modes of adsorbed (solid lines) and desorbed (broken

lines) 2,6-DMP at BT. When a large dose of 2,6-DMP is adsorbed, a band doublet at ν > 1615 cm^{-1} (namely, ~ 1645 and ~ 1627 cm^{-1}) appears for all systems. This spectral feature clearly reveals the presence of abundant and strongly held LuH^+ species (Morterra et al., 2001; 1998), indicative of the presence of surface Brønsted acid centres.

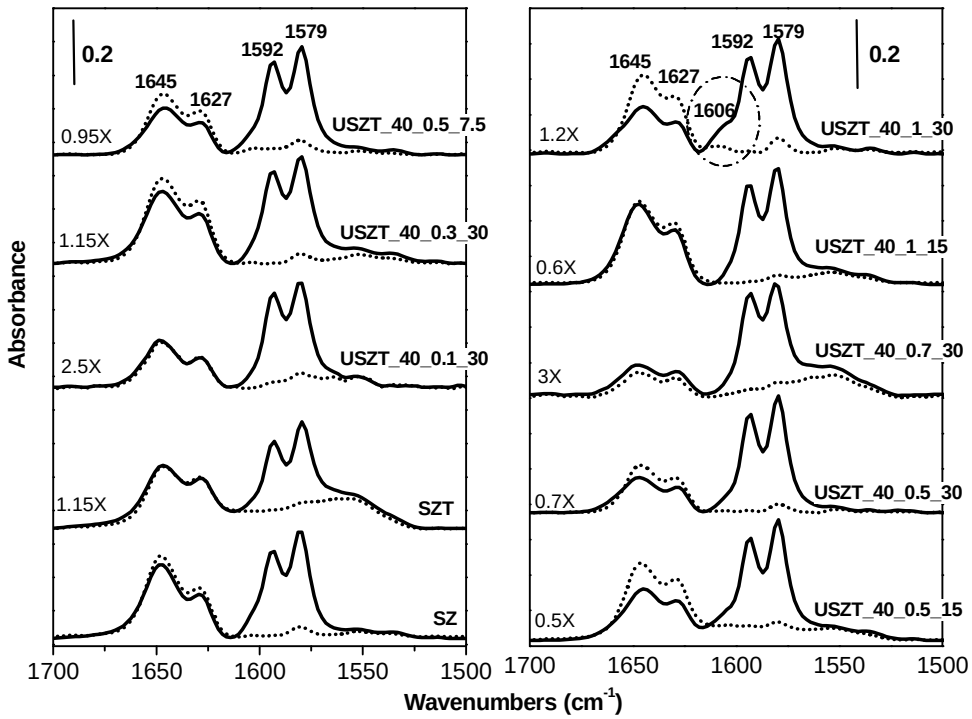

Fig. 7.4. Differential absorbance spectra, normalized against the background spectrum of the starting sample activated at 623 K, relative to the adsorption/desorption of 2,6-DMP on some samples, as obtained in the vibrational region of 2,6-DMP 8a and 8b modes after contact at BT with the vapour pressure of 2,6-DMP (~2 Torr) [solid curves], and after BT evacuation of the 2,6-DMP excess [broken curves]. For a better comparison among spectra of the different systems, the different spectral sets have been ordinate-magnified, as indicated on the curves.

As for the signals observed in the range below 1615 cm^{-1}, on the basis of literature data (Morterra et al., 2001; 1998), they can be ascribed as follows:

(i) A strong band at 1580 cm^{-1} is due to the 8b mode of all 2,6-DMP species adsorbed in a molecular form (liquidlike physisorbed species and H-bonded species).

(ii) A second strong component located at 1592 cm^{-1} is ascribed to the partner 8a mode of 2,6-DMP H-bonded to surface OH groups.

(iii) A third higher-υ band, present as a weak shoulder at 1606 cm^{-1} only in the case of the USZT_40_1_30 sample, can be ascribed to 2,6-DMP interacting with medium-strong Lewis acid sites [coordinatively unsaturated (cus) Zr^{4+} or Ti^{4+} cations]. The presence of this component in one single sample indicates that, only specific synthesis conditions (i.e., using 40% of the US maximum power, continuous US, and a water/precursors molar ratio equal to 30) are able to generate at the surface of the material the above mentioned sites.

When excess base is removed by vacuum at BT (see dotted lines in Figure 4), the bands due to protonated 2,6-DMP either remain virtually unchanged or slightly increase (meaning that the Brønsted-bound species are strongly adsorbed). On the contrary, the overall intensity of the envelope at $\upsilon < 1610$ cm^{-1} decreases drastically, as expected of H-bonded and/or physisorbed species. Within this envelope, only in the case of the USZT_40_1_30 sample, part of the 8a band of Lewis-coordinated 2,6_DMP remains at 1608 cm^{-1}, together with a residual fraction of the 8b band at 1580 cm^{-1}, indicating the presence of a stronger fraction of Lewis acid sites. After evacuation at 423 K (these spectra are not shown in order to not overload the figure) only the signals at $\upsilon > 1610$ cm^{-1} remain with virtually unchanged intensity (confirming that Brønsted-bound species are very strongly held), whereas no spectral components are

present at lower frequencies yet, meaning that all the other species are desorbed during this mild treatment.

The results of the elemental analysis obtained by the SEM-EDX analysis are displayed in Tab. 7.2. It can be observed that the ratio between Zr and Ti corresponds to that used in the synthesis mixtures. Differently, the amount of sulphur, indicated as S/(Zr+Ti) atomic ratio in Tab. 7.2, varies for the different samples and, in some cases, it is far from the adopted 0.15. Indeed, it can be noticed that some samples, i.e. USZT_40_0.5_15 (entry 7), USZT_40_1_15 (entry 11) and USZT_40_1_30 (entry 12) exhibit higher sulphur on the surface, mainly ascribable to the different synthesis conditions adopted.

7.3.2 Catalytic tests

The results of the catalytic tests are shown in Fig. 7.5. In Fig. 7.5a the FFA conversions (%) obtained at the end of the reaction (6 hours) are reported for the samples synthesized using the same H_2O/precursors ratio, whereas in Fig. 7.5b the conversions of the catalysts obtained using different H_2O/precursors ratio are shown. A typical trend of the FFA conversion over time is represented in Fig. 7.6 for the sample USZT_40_1_30 as way of example.

In Fig. 7.5a it can be observed that both the addition of TiO_2 to the SO_4^{2-}/ZrO_2 system and the use of US in specific conditions during the synthesis are able to improve the catalytic performances. As can be observed in Figure 7.5a, the addition of TiO_2 alone is able to improve the activity of the catalysts in the FFA esterification. The addition of TiO_2, in fact, as already highlighted in the discussion concerning the results of the characterization of the catalysts, is able

to increase the Brønsted acidity and, as a consequence, the catalytic activity (compare entries 1 and 2 in Tab. 7.2).

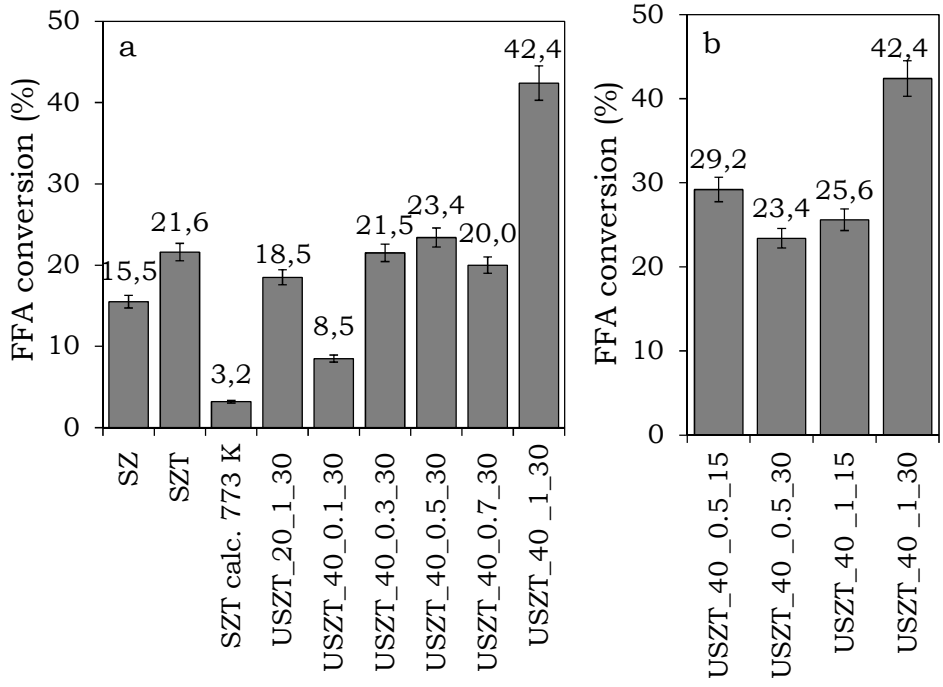

Fig. 7.5. Conversions obtained for some of the samples synthesized using a) the same or b) different H_2O/precursors ratio in the FFA esterification reaction after 6 hour of reaction, 336 ± 2 K, slurry reactor, initial acidity: 7.5% wt (oleic acid), MeOH: oil=16:100_{wt}, catalyst: oleic acid=5:100_{wt}.

Moreover, the SZT sample calcined for long time (SZT_773_6h) exhibits almost no catalytic activity (results not reported for the sake of brevity). This catalytic behaviour might be ascribable to the loss of part of the sulphates occurred during the calcinations step. This hypothesis is also confirmed by the sulphates concentration evaluated by ion chromatography. The SZT_773_6h sample is characterized by a lower sulphates concentration and, as a consequence, by a lower acid capacity (see Tab. 7.2) than the "plain" SZT sample (calcined for only 3 hours). Considering the samples obtained with the US pulses with on/off ratio from 0.3/0.7 on, the

conversion does not increase much more if compared to the one achieved with the sample obtained via traditional sol-gel synthesis . Their conversions are in fact comparable (see samples USZ_40_0.3_30, USZ_40_0.5_30, USZ_40_0.7_30 and SZT in Fig. 7.5). The similarity in the catalytic performance of these catalysts may be ascribable to the fact that they are characterized by comparable values of SSA (entries 2, 5, 8, 10 in Tab. 7.2) and, in the case of the catalysts obtained with pulses, also by comparable acidities (entries 5, 8, 10 in Tab. 7.2). A high SSA may in fact be disadvantageous for the catalysis of the reaction here studied. FFA are highly sterically hindered molecules, which might not be able to penetrate inside the pores as narrow as those of the catalysts here synthesized. The importance of the location of the active sites on the outer surface of the catalyst has already been evidenced by the authors in a previous work for other kinds of materials (Pirola et al., 2010). Therefore, it is possible to assume that, in the present case, the active sites located on the catalyst's outer surface are the most responsible for the reaction to occur. For high SSA, it is more likely that most part of the active sites is located inside the catalyst particles and, therefore, is not exploited in the catalytic process. As a consequence, for these samples, the high surface area results in a low catalytic performance.

The best catalytic performance is reached by the sample USZT_40_1_30, i.e. the one obtained using continuous US at higher power. This catalyst results in fact in a doubled catalytic activity with respect to the samples prepared either with the traditional synthesis or with the use of pulsed US. In spite the acidity of this catalyst is lower than that of the samples obtained with the US pulses, it is characterized by a rather low surface area (entry 12 in Tab. 7.2) that can be associated with a localization of the active sites

mainly on its outer surface. This feature results in many active sites immediately available for an efficient catalysis. As previously evidenced by the FTIR measurements, it is also important to highlight, that only in the case of the USZT_40_1_30 sample, a not negligible number of medium-strong Lewis acid sites is present at the surface, together with a high number of strong Brønsted acid centres. The good catalytic performances of this catalyst show that the presence of both these active sites is a necessary condition in order to obtain reasonably high values of conversion. As already evidenced by some of the authors, the acid-catalyzed esterification reaction may occur at the surface of catalyst on both Brønsted acidic centres and Lewis acid sites (i.e. coordinatively unsaturated (cus) Zr^{4+} cations) (Ardizzone et al., 2004).

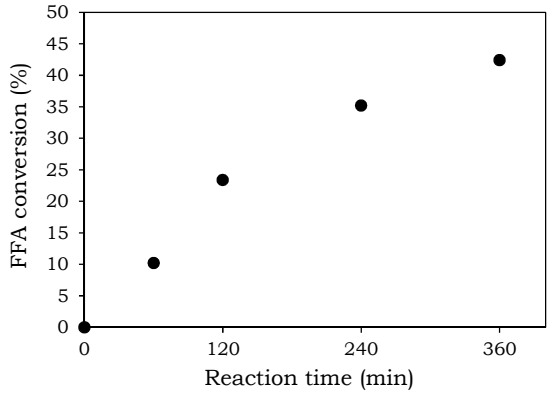

Fig. 7.6. Example of a typical trend of FFA conversion, catalyst: USZT_40_1_30, 336 ± 2 K, slurry reactor, initial acidity: 7.5% wt (oleic acid), MeOH: oil=16:100_{wt}, catalyst: oleic acid=5:100_{wt}.

The low catalytic activity of the sample USZT_20_1_30 may be ascribable to the US power, probably not sufficient to activate the sol-gel reaction under the effect of the cavitation. In the case of the sample USZT_40_0.1_30, the unsatisfactory catalytic activity might be due to the too low on/off pulses ratio. Too short pulse times may in fact not be sufficient to initiate the acoustic cavitation in the

medium, as previously explained and as evidenced in literature (Suslick and Doktycz, 1990; Henglein et al, 1989).

In Fig. 7.5b, a comparison among the catalytic activity of the samples obtained with continuous US and with the use of 0.5 on/off pulses are displayed for different water/precursors ratios.

As it can be noticed, there is a remarkable difference between the samples USZT_40_1_15 and USZT_40_1_30, i.e. obtained using continuous US. On the contrary, the same difference is not evident in the case of the corresponding catalysts obtained with pulsed US, i.e. USZT_40_0.5_15 and USZT_40_0.5_30. This catalytic behaviour can be explained considering that USZT_40_1_15 and USZT_40_1_30 possess distinct surface and morphological properties, resulting in different catalytic performances, whereas the samples, USZT_40_0.5_15 and USZT_40_0.5_30 are characterized by similar values of acidities and SSA, showing very close values of conversion. It can be noticed that the SSA of USZT_40_1_15 is considerably higher than the SSA of the catalyst obtained in the same conditions but doubling the amount of water (USZT_40_1_30). This latter catalyst, as reported above, results to be the best catalyst in the FFA esterification reaction.

In Fig. 7.7 the FFA conversions as a function of the concentration of the acid sites normalized to the surface area are reported for the most significative samples. It can be observed that the best catalyst, i.e. USZT_40_1_30, possesses the highest ratio of acid sites over surface area. This catalyst results in the highest FFA conversion among all the other samples, in spite it is not characterized by the highest acidity. This confirms that FFA esterification occurs mainly on the active sites located on the outer surface of the catalyst. The sample SZT_773_6h exhibits almost no conversion and shows the lowest content of acid sites/m^2. Samples SZT, USZT_40_0.3_30,

USZT_40_0.5_30, USZT_40_0.7_30 exhibit very similar FFA conversion as well as similar concentration of meqH^+/m^2. The sample SZ is characterized by a lower meqH^+/m^2 ratio and shows a lower catalytic activity than the above cited samples, with the exception of SZT_773_6h. This result confirms the importance of the localization of a high number of active acid sites on the outer surface of the catalyst for the reaction here studied. In the present work a high number of active acid sites on the outer surface of the catalyst was achieved adopting continuous ultrasound in the sol-gel synthesis of the sulphated ZrO_2-TiO_2 systems.

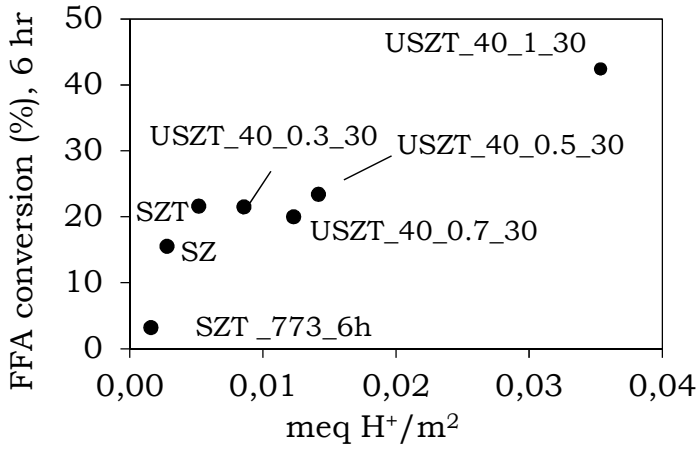

Fig. 7.7. FFA conversion obtained for the different catalysts as a function of the concentration of the acid sites normalized to the surface area.

FFA conversion results may appear discouraging from a first approach, in particular if compared to the other results reported in literature for similar catalysts (Das et al., 2002). Nevertheless, it has to be taken into account that these catalysts are normally tested for the esterification of shorter chain carboxylic acids (Ardizzone et al., 2004; 2009); Juan et al., 2007) and that, also in the case of the FFA esterification, they are usually experimented in the pure substrate,

i.e. as pure fatty acid (Das et al., 2002), and not directly in the acid oil. Taking into account these considerations, the FFA conversions obtained in this work appear encouraging.

Moreover, the outcome of this study is particularly important for what concerns the possibility of tuning the properties of acid catalysts based on mixed oxides by means of US (continuous or pulsed). This might be interesting also in view of the application of sulphated zirconias in other kinds of reactions, such as isomerizations, alkylations and esterifications of other kinds of carboxylic acids.

7.4 Conclusions

This study demonstrates how the surface acidity and specific surface area of sulphated zirconia can be increased by both adding TiO_2 and using ultrasound (US) in precise experimental conditions to assist the sol-gel synthesis of the catalysts.

The beneficial effects of the use of US in the sol-gel synthesis of the SO_4^{2-}/ZrO_2-TiO_2 systems are ascribable to the occurrence of acoustic cavitation, which causes faster hydrolysis (sol-gel reaction) rates and surface damage. This effect is particularly evident for the catalysts obtained with the use of pulses longer than 0.3 seconds. For these catalysts the acidity significantly increases along with the specific surface area if compared to the ones obtained with shorter pulses.

The more efficient catalyst in the FFA esterification reaction resulted to be the one obtained with continuous US and higher powers. For this sample, in fact, the lower surface area allows the location of the active acid sites mainly on the outer surface of the

catalysts. In this way, the FFA molecules can undergo a faster catalytic transformation. Moreover, it has been demonstrated that this catalyst is the only one that possesses both Lewis and Brønsted acidity. Therefore, its good catalytic performances can be ascribed to the presence of both these active sites, together with a low value of SSA.

References

Aranda D.A.G., Santos R.T.P., Tapanes N.C.O., Ramos A.L.D., Antunes, O.A.C., "Acid-catalyzed homogeneous esterification reaction for biodiesel production from palm fatty acids", *Catal. Lett.*, **2008**, 122, 20.

Ardizzone S., Bianchi C.L., Cappelletti G., Porta F., "Liquid-phase catalytic activity of sulfated zirconia from sol–gel precursors: the role of the surface features", *J. Catal.*, **2004**, 227, 470.

Ardizzone S., Bianchi C.L., "Acidity, sulphur coverage and XPS analyses of ZrO_2-SO_4 powders by different procedures, *Appl. Surf. Sci.*, **1999**, 152, 63.

Ardizzone S., Bianchi C.L., "XPS characterization of sulphated zirconia catalysts: the role of iron", *Surf. Interface Anal.*, **2000**, 30, 77.

Ardizzone S., Bianchi C.L., Cappelletti G., Annunziata R., Cerrato G., Morterra C., Scardi P., "Fe- and Mn-promoted sulphated ZrO_2 as liquid phase catalysts", *Appl. Catal. A: Gen.*, **2009**, 360, 137.

Bensitel M., Saur O., Lavalley J.C., Mabilon G., "Acidity of zirconium oxide and sulfated zirconia samples", *Mat. Chem. Phys.*, **1987**, 17, 249.

Bianchi C.L., Boffito D.C., Pirola C., Ragaini V., "Low temperature de-acidification process of animal fat as a pre-step to biodiesel production", *Catal. Lett.*, **2010**, 134, 179.

Bianchi C.L., Pirola C., Boffito D.C., Di Fronzo A., Carvoli G., Barnabè D., A. Rispoli, R. Bucchi, "Non edible oils: raw materials for sustainable biodiesel", in: Stoytcheva M., Montero G. (Eds.): *Biodiesel Feedstocks and Processing Technologies*, Intech, **2011**, pp. 3-22.

Boffito D.C., Pirola C., Bianchi C.L., "Heterogeneous catalysis for free fatty acids esterification rea.ction as a first step towards biodiesel production", *Chem, Today***, 2012**, 30, 14.

Buchholz T., Wild U., Muhler M., Resofski G., Paal Z., "Hydroisomerization of n-hexane over Pt/sulfated zirconia: activity, reversible deactivation, and surface analysis", *Appl. Catal. A*, **1999**, 189, 225.

Chen F.R., Coudurier G., Joly J.F., Vedrine J.C., "Superacid and catalytic properties of sulfated zirconia", *J. Catal.*, **1993**, 143, 616.

Comelli R.A., Vera C.R., Parera J.M., "Influence of ZrO_2 crystalline structure and sulfate ion concentration on the catalytic activity of SO_4^{2-}-ZrO_2", *J. Catal.*, **1995**, 151, 961.

Das D., Mishra H.K., Pradhan N.C., Dalai A.K., Parida K.M., "Studies on structural properties, surface acidity and benzene isopropylation activity of sulphated ZrO2-TiO2 mixed oxide catalysts", *Microp. Mesop. Mat.*, **2002**, 80, 327.

Di Serio M., Cozzolino M., Giordano M., Tesser R., Patrono, P. "From Homogeneous to Heterogeneous Catalysts in Biodiesel Production"., *Ind. End. Chem. Res.*, **2007**, 46(20), 6379.

Dijs I.J., Geus J.W., Jenneskens L.W., "Effect of Size and Extent of Sulfation of Bulk and Silica-Supported ZrO_2 on Catalytic Activity in Gas- and Liquid-Phase Reactions", *J. Phys. Chem. B*, **2003**, 107, 2003, 13403.

Fu X., Clark L.A., Yang Q., Anderson M.A., "The Enhanced Photocatalytic Performance of Titania-Based Binary Metal Oxides: TiO_2/SiO_2, TiO_2/ZrO_2", *Environ. Sci. Technol.*, **1996**, 30, 647.

Gregg S.J., Sing K.S.W., *Adsorption, Surface Area and Porosity*, Acad. Press, London, **1982**.

Henglein A., Ulrich R., Lilie J., "Luminescence and chemical action by pulsed ultrasound", *J. Am. Chem. Soc.*, **1989**, 111, 1974.

Juan J.C., Zhang J., Yarmo M.A., "Structure and reactivity of silica-supported zirconium sulfate for esterification of fatty acid under solvent-free condition", *Appl. Cat. A*, **200**7, 332, 209.

Juan J.C., Jiang Y., Meng X., Cao W., Yarmo M.A., Zhang J., "Supported zirconium sulfate on carbon nanotubes as water-tolerant solid acid catalyst", **2007**, *Mat. Res. Bullettin*, 42.

Kataoka T., Dumesic J.A., "Acidity of unsupported and silica-supported vanadia, molybdena, and titania as studied by pyridine adsorption", *J. Catal.*, **1988**, 112, 66.

López D.E., Goodwin Jr. J.G., Bruce D.A., "Transesterification of triacetin with methanol on Nafion acid resins", *J. Catal.*, **2007**, 345, 381.

Marchetti J.M., Errazu A.F., "Esterification of free fatty acid using sulfuric acid as catalyst in the presence of triglycerides", *Biomass. Bioener.*, **2008**, 32, 892.

Marchetti J.M., Miguel V.U., Errazu A.F., "Heterogeneous esterification of oil with high amount of free fatty acid", *Fuel*, **2007**, 86, 906.

Moulder J.F., Stickle W.F., Sobol P.E., Bomben K.D., "andbook of X-ray Photoelectron Spectroscopy, Perkin-Elmer Corp, Eden Praire, **1992**.

Morterra C., Cerrato G., Meligrana G., "6-dimethylpyridine as an analytical tool to test the surface acidic properties of oxidic systems", *Langmuir*, **2001**, 17, 70532.

Morterra C., Cerrato G., Ardizzone S., Bianchi C.L., Signoretto M., Pinna F., "Surface features and catalytic activity of sulfated zirconia catalysts from hydrothermal precursors", *Phys. Chem. Chem. Phys.*, **2002**, 4, 3136.

Morterra C., Cerrato G., Di Ciero S., "IR study of the low temperature adsorption of CO on tetragonal zirconia and sulfated tetragonal zirconia", *Appl. Surf. Sci.*,**1998**, 126, 107.

Morterra C.,Cerrato G., Pinna F., Signoretto M., "BrØnsted Acidity of a Superacid Sulfate-Doped ZrO_2 System". *J. Phys. Chem.*, **1994**, 98, 12373.

Morterra C., Meligrana G, Cerrato G., Solinas V., Rombi E., Sini M.F., "2,6-Dimethylpiridine adsorption on zirconia and sulfated zirconia systems. An FTIR and microcalorimetric study", *Langmuir*, **2003**, 19, 5344.

Neppolian B., Wang Q., Yamashita H., Choi H., "Synthesis and characterization of ZrO_2–TiO_2 binary oxide semiconductor nanoparticles: Application and interparticle electron transfer process" *Appl. Catal. A*, **2007**, 333, 264.

Neppolian B., Wang Q., Jung H., Choi H., "Ultrasonic-assisted sol-gel method of preparation of TiO_2 nano-particles: Characterization, properties and 4-chlorophenol removal application", *Ultrason. Sonochem.*, **2009**, 15, 649.

Paal Z., Wild U., Muhler M., ManoliJ.-M., Potvin C., Buchholz T., Sprenger S., Resofski G., "The possible reasons of irreversible deactivation of Pt/sulfated zirconia catalysts: structural and surface analysis", *Appl. Catal. A*, **1999**, 188, 257.

Pasias S., Barakos N., Alexopoulos C., "Heterogeneously catalyzed esterification of FFAs in vegetable oils", **2006**, *Chem. Eng. Technol.*, 29, 1365.

Pirola C., Bianchi C.L., Boffito D.C., Carvoli G., Ragaini V., "Vegetable oil deacidification by Amberlyst : study of catalyst lifetime and a suitable reactor configuration", *Ind. Eng. Chem. Res.*, **2010a**, 49, 4601.

Pirola C., Bianchi C.L., Di Michele A., Diodati P., Boffito D., Ragaini V., "Ultrasound and microwave assisted synthesis of high loading Fe-supported Fischer–Tropsch catalysts", *Ultrason. Sonochem.*, **2010b**, 17, 610.

Pirola C., Boffito D.C., Carvoli G., Di Fronzo A., Ragaini V., Bianchi C.L., "Soybean oil deacidification as a first step towards biodiesel production", in D. Krezhova (Ed.): Recent Trends for Enhancing the Diversity and Quality of Soybean Products, Intech, **2011**, pp. 321-44.

Russbueldt B.M.E., Hoelderich W.F., "New sulfonic acid ion-exchange resins for the preesterification of different oils and fats with high content of free fatty acids", *Appl. Catal. A*, **2009**, 362, 47.

Sarzanini C., Sacchero G., Pinna F., Cerrato G., Morterra C., "Amount and nature of sulfates at the surface of sulfate-doped zirconia catalysts", *J. Mater. Chem.*, **1995**, 5, 353.

Sehgal C., Steer R.P., Sutherland R.G., Verrall R.E., "Sonoluminescence of argon saturated alkali metal salt solutions as a probe of acoustic cavitation", *J. Chem. Phys.*, **1979**, 70, 2242.

Suslick K. S., Doktycz, S. J., "The Effects of Ultrasound on Solids" in Mason, T.J.: *Advances in Sonochemistry*, JAI Press: New York, **1990**, vol.1, pp. 197-230.

CHAPTER 8:
ULTRASOUND-ASSISTED BIODIESEL PRODUCTION

The work presented in this chapter was carried out at the Laboratory of Molecular Chemistry and Environment of the University of Savoy, in collaboration with Dr. Jean-Marc Leveque. A special thank goes to him.

Abstract

Present technologies to produce biodiesel are based on the use of multi-stages reactors and are dampened by mass transfer limitations that characterise the transesterification reaction.

Biodiesel process intensification using ultrasound horns in batch reactors (traditional vessel and Rosett cell reactor) and continuous flow reactors was studied in this work and compared with the conventional mechanically stirred method. The effect of pulses, power and temperatures was also investigated. Most of the ultrasound-assisted methods allowed obtaining the complete conversion into biodiesel within a single 30 minutes step, whereas the mechanically stirred transesterification requires two steps for a total duration of 150 minutes, in between which the separation of the products is necessary. Moreover, the ultrasound-assisted methods utilise much lower reagents and catalyst amounts than the traditional method. The use of the Rosett cell reactor, which combines hydrodynamic and acoustic cavitation, gave biodiesel yields higher than 90% after a reaction time of 5 minutes.

The most significative result of this work is the attainment of biodiesel yields higher than 90% after just one passage of the reagents in the continuous flow reactor in presence of pulsed ultrasound, corresponding to a reaction time of 18 seconds. In this case the reaction rate of the ultrasound-assisted process resulted to be 300 times faster than the conventional synthesis.

8.1 Introduction

Nowadays most biodiesel (BD) is produced through triglycerides transesterification of edible oils with methanol, in the presence of an alkaline catalyst (Bianchi et al., 2011; Antolin et al., 2012; Velijković et al., 212). Transesterification reaction, displayed in Fig. 1.4, is a sequence of three consecutive and reversible reactions, in which di- and monoglycerides are formed as intermediates.

Present technologies to produce BD involve multi-stage reactors processes with homogeneous basic catalysts such as NaOH, KOH or CH_3ONa, that after the reaction are neutralized and then disposed. Other limitations of the present technologies include: large equipment, long reaction times, use of excess of methanol (health hazard – not entirely contained) and high cost of the raw materials (up to 80% of the cost of the entire process) (Siddique et al., 2011). The major obstacle to an even larger-commercialization on greater scales of biodiesel production lies in fact in its high cost (Canakci et al., 2001). Therefore, much recent research has been focused on developing methods to reduce the biodiesel production cost. Homogeneous base-catalyzed transesterification is preferred over acid-catalyzed transesterification, due to the remarkably higher reaction rates (Freedman et al., 1984). However, homogeneously base-catalyzed transesterification is known to suffer from the mass transfer limitation in the initial period (Stamenković et al., 2007). Different intensification methods such as ultrasonic and microwave irradiation, hydrodynamic cavitation, addition of co-solvents or mass transfer catalysts and application of supercritical synthesis conditions have been tried out to eliminate or minimize the mass transfer limitation in order to improve the biodiesel production process Veljkovićt et al., 2012).

Recent developments in sonochemistry have dealt with the use of ultrasonic irradiation as a new, more efficient mixing tool in BD production. US biodiesel production from various feedstocks is the focus of many research groups all over the world in the last decade. Veljkovi´c (Veljkovićt al., 2012) reviews in detail the state of art and perspectives of the BD production by ultrasound-assisted transesterification and affirm that the use of low-frequency ultrasound (LFU) in BD production has several advantages over the classical synthesis.

In the present work we study in deep the BD production intensification with the use of US in both batch and continuous flow reactors. The novelty of the present work is based on the comparison between two different kinds of batch reactors: a traditional reaction vessel and a Rosett cell reactor. In Rosett cell reactor the combined approach exploiting acoustic cavitation along with hydrodynamic cavitation is presented. Hydrodynamic cavitation can simply be generated by the passage of the liquid through a constriction such as an orifice plate, as in the case of the characteristic loops of the Rosett cell reactor (Mason and Lorimer, 1988). In hydrodynamic cavitation, the cavitation is produced by pressure variations, which is obtained using geometry of the system creating velocity variation (Gogate and Pandit, 2001). Hydrodinamic cavitation is therefore able to generate flow energy at an intensity that is suitable for physical and chemical processing (Gogate and Pandit, 2001; Gogate, 2008).

The results of this work suggest that the combination of the two different kinds of cavitation, acoustic and hydrodynamic, is beneficial to the BD production yield. The effect of US pulses, different powers and temperature in the two different reactors is also investigated and discussed in detail.

The study of BD production in continuous flow reactors with the use of US is also object of the present work. The effect of the US power was investigated. Using pulsed US (2 seconds on and 2 seconds off), conversions into BD higher than 90% were obtained after just one passage in the continuous flow reactor, corresponding to a reaction time of 18 seconds and to a reaction rate 300X faster than the conventional process.

8.2 Materials and Methods

8.2.2 Description of the sonochemical equipment

In Tab. 8.1 and 8.2 a summary of all the transesterification experiments in batch and continuous modality, respectively, is reported.

Both a classical reaction vessel and a Rosett cell reactor were used for the ultrasound (US) assisted batch experiments. Reaction vessel consists of a classical cylindrical reaction tank. Rosett cell reactor consists of a tank equipped with four loops at the bottom, designed to originate hydrodynamic cavitation inside the reaction medium. A picture of the used Rosett cell reactor is provided in Fig. 8.1.

Both Rosett cell reactor and reaction vessel had a capacity of 0.068 L capacity. Experiments were carried out using two US tips with different diameters and maximal nominal power emissions: 13 mm (500 W) and 20 mm (400 W), respectively. Amplitude was varied at 60 and 80% of the maximum nominal power emissions for both the reactors. Within this manuscript, in the tables and figures, 60% of amplitude will be referred to as “low power” and 80% as to “high

power" for both the reactors. Standard calorimetric method (Mason and Lorimer, 1988) measurements resulted in the emitted powers reported in Tab.8.1 (correlation factors $R^2 > 0.99$).

	Reactor	D_{tip} (mm)	Power	Emitted power (W)	Mode	Temp. (K)
1	Vessel	13	low	17.6	continuous	313
1a					pulsed	313
2					continuous	333
3			high	21.7	continuous	313
4						333
5		20	low	19.0	continuous	313
6						333
7			high	27.1	continuous	313
8						333
9	Rosett cell	13	low	16.9	continuous	313
9a					pulsed	313
10					continuous	333
11			high	20.3	continuous	313
12						333
13		20	low	17.6	continuous	313
14						333
15			high	24.4	continuous	313
16						333

Tab. 8.1: Batch ultrasound-assisted transesterification experiments.

	Reactor volume (L)	Mode	Freq. (kHz)	Emitted power (W)	treated volume (L)	τ (sec)	Reaction time (sec)	US time (sec)	Power density (Wcm^{-3})
1	0.700	continuous US	20	68.2	2.4	19	66	66	0.28
2	0.070		35	19.3	2.4	19	66	66	0.081
3	0.070				0.68	1.9	18	18	0.28
4	0.070	pulsed US			0.68	1.9	18	9	0.28

Tab. 8.2: Continuous ultrasound assisted transesterification experiments,τ= residence time, T = 338 K.

Fig. 8.1. Rosett cell reactor.

For the continuous experiments two continuous tubular reactors of different volumes, 0.700 L (20 kHz) and 0.070 L (35 kHz), respectively were used. Both the reactors are Sonitube® reactors, designed and kindly provided by the Synetude Company (Chambery, France).

Both the sonicators were operated at the 85% of their nominal maximum power emission, corresponding to 1500 W and 400 W, for the 0.700 and the 0.070 L reactor, respectively. Standard calorimetric method (Mason and Lorimer, 1988) measurements resulted in the emitted powers reported in Tab. 8.2 (correlation factors $R^2 > 0.99$).

The experiments in the continuous reactors were carried out first using the same volume of the regents (entries 1 and 2 in Tab. 8.2) and then keeping constant the power/volume ratio for both the small and big reactor (entries 1 and 3 in Tab. 8.2). The experiments

conducted in the small reactor at high power/volume ratio were also carried out using pulsed US (2 seconds on and 2) seconds off (entry 4 in Tab. 8.2). The scheme of the two reactor set-ups is similar and is represented in Fig. 8.2, while in Fig. 8.3 the picture of the bigger Sonitube® reactor is displayed.

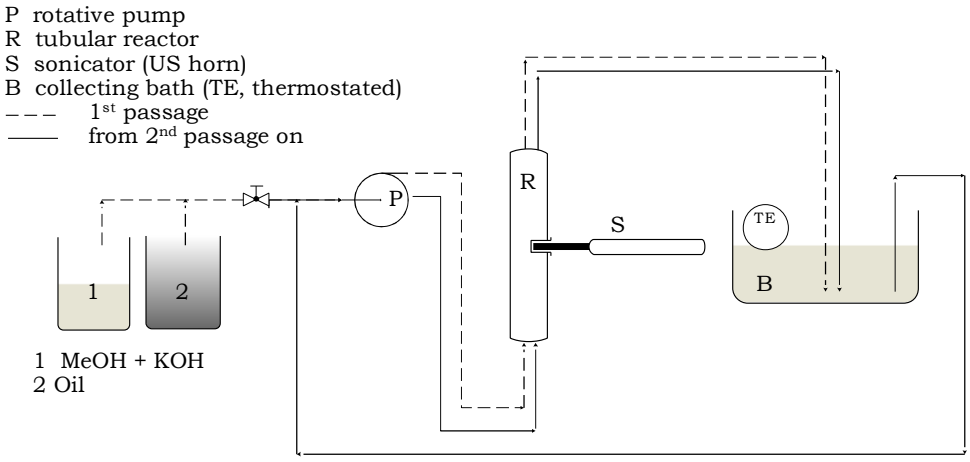

Fig. 8.2. Scheme of the continuous reactors.

For the first passage in the reactor (dotted line in Fig. 8.2) oil (a) and methanol containing the dissolved catalyst (b) were first fed together to the bottom of the reactors by a rotative pump (c) operating at 200 rpm and at a flow of ~38 $mLsec^{-1}$. The reagents and the catalyst passed through the tubular reactor (d) up to the top and then sent to an open thermostated collecting bath, where the temperature of the reaction mixture was measured. From the second passage in the reactor on (solid line in Fig. 8.2), the reaction mixture was recycled from the collecting thermostated bath to the rotative pump and then sent again to the bottom of the reactor. In Tab. 8.2, the residence time τ (equal to the ratio between US reactor volume and the total flow of reagents) is reported together with the "reaction

time", i.e. the time required by the whole treated volume of the reagents (2.40 or 0.68 L) to perform one passage in the tubular reactor.

It was necessary to cool the collecting bath when using the big and the small reactors, respectively, so as to keep the temperature of the reaction mixture below 338 K, i.e. the boiling temperature of methanol.

All the US horns, as well as the Sonitube® continuous reactors used in this work, were kindly provided by the Synetude Company (Chambery, France).

Fig. 8.3. Continuous reactor Sonitube® (Synetude Company – Chambery, France): V= 0.700 L.

8.2.3 Transesterification reaction

Commercial rapeseed oil was used as a feedstock for all the experiments. The oil was analysed by acid-base titrations in order to quantify the amount of free fatty acids (FFA). The procedure to determine the acidity has already been reported by the authors elsewhere (Boffito et al., 2012a; 2012b; Pirola et al., 2010; Bianchi et al., 2010; Canakci and Sanli, 2008). The acidity of the oil resulted 0.1%$_{wt}$. FFA react with the transesterification catalyst (KOH) and form soaps. Soaps can affect reaction yields and the quality of the finished products as already extensively documented (Boffito et al., 2012a; 2012b; Pirola et al., 2010; Bianchi et al., 2010). Nevertheless, a FFA concentration higher than 0.5%$_{wt}$ is reported to affect the reaction yields (Canakci and Sanli, 2008) and this was not the case. Potassium hydroxide (KOH) was used as transesterification catalyst.

Traditional transesterification experiments were performed in a classical batch reactor of 0.250 L capacity and stirred by mechanical agitation, while ultrasound batch experiments were carried out in 0.068 L vessels (traditional and Rosett reactor). The experimental conditions for both the methods are reported in Tab. 8.3.

Method	Reactor	Step	g_{MeOH}/100 g_{oil}	g_{KOH}/100 g_{oil}	Temp. (°C)	Time (min)
traditional	batch	1	20	1.0	333	90
		2	5.0	0.50		60
Ultrasound-assisted	batch	1	20	1.0	313, 333	30
Ultrasound-assisted	continuos	1	20	1.0	338	30

Tab. 8.3. Reaction conditions

Traditional transesterification was performed in two reaction steps as described in previous works (Bianchi et al., 2011). For this purpose, 100 g of oil and 20 g of MeOH containing 1 g of catalyst were charged into the reactor and made react for 90 minutes at 333 K (1st step). Afterwards, the mixture was transferred into a separating funnel and left stand for 30 minutes. Two phases were present: the bottom phase, composed by methanol, KOH and glycerol and the top phase, composed by biodiesel and unreacted mono-, di and triglycerides. The bottom phase (~95 g) was transferred again into the reactor. 5 g of MeOH containing 0.5 g of KOH were added and made react for 60 minutes at 333 K (2nd step). Afterwards the mixture was separated again and the bottom BD phase analysed.

In the US experiments just one reaction step was performed. In this case, after the reaction, the mixture was left stand for ~ 10 minutes and the biodiesel phase was withdrawn directly from the reactor.

All the BD samples were centrifuged before the analysis of biodiesel.

The yield in BD, corresponding to the FAME concentration, was determined by gaschromatografic analysis according to the normative UNI EN 14103. About 250 mg of the sample were dissolved in 2.50 mL of a standard solution 0.1 M of methylnonadecanoate. Methylnonadecanoate (>99%, Fluka product) was used as internal standard and heptane as a solvent. The capillary GC column OmegaWax (Sigma Aldrich) was used in a GC PerkinElmer Instruments AutoSystem XLGas Chromatograph, adopting an isotherm at 483 K. He was used as a carrier at 70 kPa. The biodiesel yield, i.e. the FAME content, expressed as a mass fraction in %, was calculated using the following equation (8.1):

$$BD\ yield = C_{FAME} = \frac{(\sum A) - A_{C19}}{A_{C19}} \times \frac{C_{C19} \times V_{C19}}{W} \times 100 \qquad 8.1$$

where ΣA is the total peak area of the methyl esters, A_{C19} is the peak area corresponding to methylnonanadecanoate; C_{C19} is the concentration, in milligrams per millilitre, of the methylnonadecanoate solution being used; V_{C19} is the volume, in millilitres, of the methylheptadecanoate solution being used; W is the mass, in milligrams, of the sample.

8.3 Results and Discussion

8.3.1 Comparison between traditional and ultrasound-assisted batch transesterification

In Fig. 8.4, the biodiesel (FAME- Fatty Acid Methyl Esters) yield in function of the reaction time is reported for all the batch experiments. For the sake of clarity only the results obtained using the low powers for both the Rosett cell and the vessel are reported (compare with actual emitted powers reported in Tab. 8.1).

BD yields obtained with the traditional mechanically- stirred method within 30 minutes of the first reaction step are also shown for the sake of comparison. The ultrasound (US)-assisted method performs much better than the traditional method. The transesterification reaction is known to be an equilibrium-limited reaction and it is therefore usually performed in two steps, as described in the experimental part. A second step is necessary to convert the unreacted mono- and di-glycerides to glycerol and methyl esters. BD yields around 90% were obtained in this work at

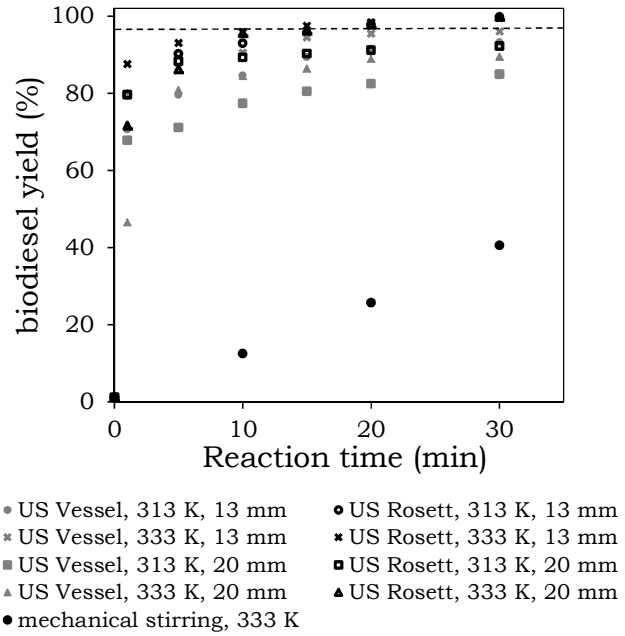

Fig. 8.4. Results of the transeterification batch experiments: triglycerides conversions into FAME vs. reaction time. Experimental conditions reported in Tab. 8.3.

the end of the first step (90 minutes) using the traditional method (results non reported in Fig. 8.4). This result is in agreement with what also Gole (Gole and Gogate, 2012) and Çaylı (Çaylı and Küsefoğlu, 2008) found in the same experimental conditions adopted in this work. After the first step, the separation of glycerol and the addition of fresh catalyst and methanol were required to shift the reaction equilibrium toward the products, as reported in Tab. 8.3. The second step was then carried out for an additional hour to obtain BD yields higher than 96.5%, which is the minimum FAME concentration required by the European normative on biodiesel.

The use of US allows achieving within 30 minutes the same conversion that with the traditional method is usually achieved in two steps for a total time of 150 minutes. Moreover, less methanol and catalyst are required to achieve yields higher than 96.5%. A comparison between the adopted conditions is displayed in Tab 4.3.

As shown in a paper of Kelkae on transesterification of virgin vegetable oil (sunflower oil and palm oil) (Kelkae et al., 2008), the

conventional approach of stirring is about 10 times slower as compared to acoustic and hydrodynamic cavitation.

The positive effect of US on BD production from vegetable oils via transesterification may be ascribable to different phenomena connected with the occurrence of the acoustic cavitation inside the reaction medium. Veljković and co-authors (Veljković et al., 2008) give an extensive explanation of the effects caused by the acoustic cavitation occurring during the transesterification reaction.

US can have physical and chemical effect on heterogeneous reaction systems through cavitation bubbles (Verzie et al., 2009). The physical effects are connected with the formation of emulsions between liquid reactants that are usually not miscible, as well as triglycerides and methanol. The micro turbulences generated by the collapse of the cavitation bubbles would be able to disrupt the phase boundary leading to the formation of the microemulsion. The increased interfacial area of exchange between the micro-phases of triglycerides and methanol enhances the reaction rates as well as a very vigorously mechanically agitated reactor. These emulsions are reported to have drops smaller in size and be more stable than those obtained using conventional techniques, which is very beneficial for liquid-liquid reaction systems (Georgianni et al., 2008a). The positive effect of oil-MeOH emulsions to yield FAME has already been reported by the authors in a recent work (Pirola et al., 2010). In this case stable emulsions were obtained with an emulsificator endowed with five coaxial rotating-ring gears that were able to break the biphasic mixture into very small drops.

The chemical effects are due to the radicals formation caused by the collapse of the transient cavitation bubbles. The transesterification reaction may be governed by the in situ generation of methoxy radicals, provided that the temperature

generated by the collapse of the cavitation bubbles is high enough to allow their formation (Georgianni et al., 2008b). Ultrasonically generated radicals increase reaction rate in bulk mixture. Few researchers also reported that ultrasonic cavitation can also provide the activation energy required for initiating the transesterification reaction (Siatis et al., 2006).

The role of the temperature in the US-assisted experiments cannot be assessed easily. Transesterification reaction is an exothermic reaction, but temperatures up to 333 K are usually adopted to favour the kinetic and also to favour the solubility of methanol in the oil (Gole and Gogate, 2012). Moreover, as reported by Mahamuni (Mahamuni and Adewuyi, 2009), increasing the temperature decreases the viscosity of the reaction medium, which makes cavitation easier. From the other side, it is well known that high temperatures dampen acoustic cavitation effects due to the lower amount of dissolved gases. Colucci et al. (Colucci et al., 2005) observed the maximum FAME formation at 313 K. Also Gole (Gole and Gogate, 2012) observed that above 313 K, no significant improvement of the BD yield is observed for the US assisted methods compared to the traditional methods, while in this work, US methods perform much better than the conventional method at all the adopted conditions.

The BD yields obtained at different temperatures in this work have to be interpreted taking into account of all the aspects above mentioned.

8.3.2 Ultrasound batch experiments: comparison between Rosett cell and vessel

In Fig. 8.5a and 8.5b the BD yields obtained with the 20 mm US horn after 1 minute and 30 minutes, respectively, are reported. At the same way, in Fig. 8.5c and 8.5d the biodiesel (FAME) yields obtained with the 13 mm US horn after 1 minute and 30 minute, respectively, are shown.

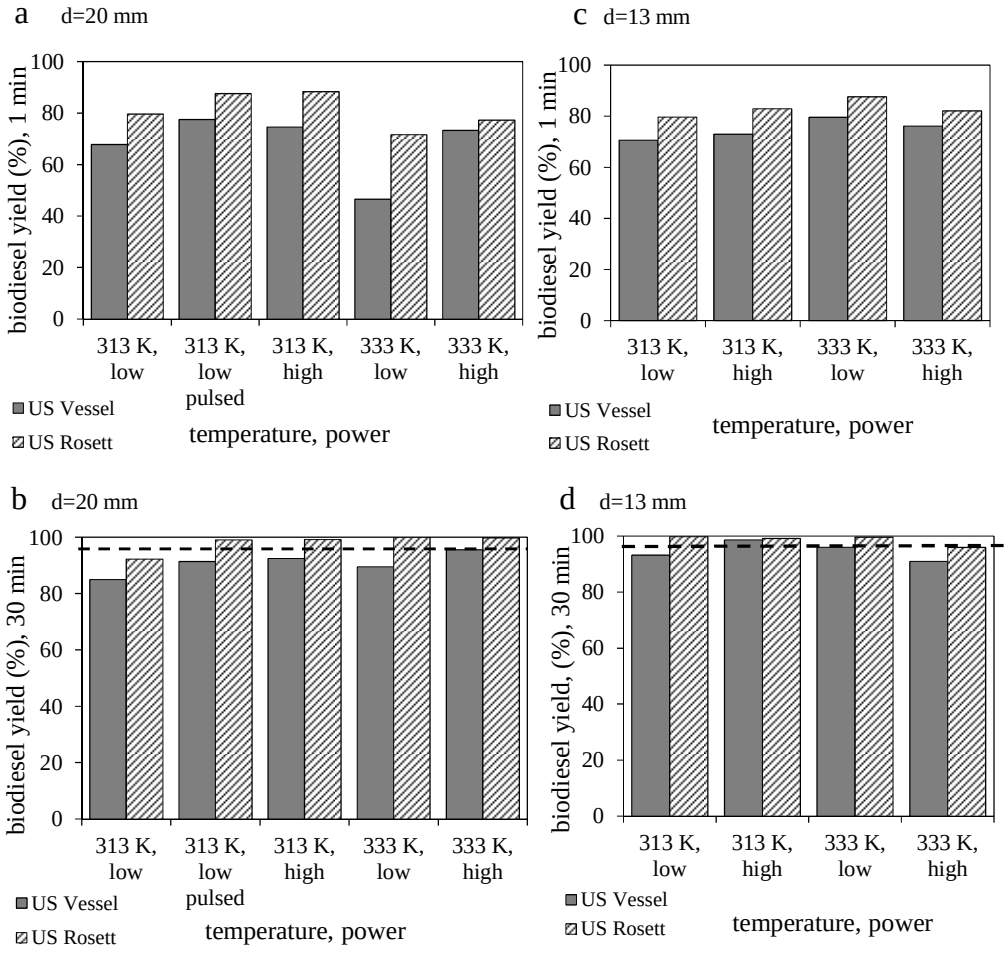

Fig. 8.5. Results of the transeterification batch experiments: biodiesel conversions at different powersand temperatures: a) after 1 minute and b) after 30 minutes of reaction for the 20 diameter tip (400W); c) after 1 minute and b) after 30 minutes of reaction for the 13 diamter tip (500 W).

Conversions after 1 minute (Fig. 8.5a and 8.5c) resulted particularly useful for the sake of comparison. In Fig. 8.5b and 8.5d the dotted lines represent a FAME concentration corresponding to 96.5%, i.e. the minimum limit required by the European Normative on BD EN 14214.

In all the adopted conditions, the Rosett cell reactor always exhibits higher conversions into BD than the traditional vessel. The design of the cell allows the irradiated reaction mixture to be sonically propelled from the end of a probe around the loops of the vessel. The sudden increase of the pressure at the entrance of the loops, which propagates throughout all their length, causes hydrodynamic cavitation, which provides a very efficient mixing. Rosett cell reactor is therefore able to provide both optimal temperature control within the reactor and enhanced mass transfer.

The higher yields provided by the Rosett cell reactor are attributable to the combined effect of the acoustic and hydrodynamic cavitation. Hydrodynamic cavitation is already reported to highly contribute in process intensification of BD production (Kelkar et al., 2008). Kelkar reviews the separate use of ultrasonic and hydrodynamic cavitation for methyl esters productions.

As already mentioned in the introduction, hydrodynamic cavitation consists of pressure variations, which are generated using geometry of the system that creates velocity variation (Gogate and Pandit, 2001). Hydrodynamic cavitation is therefore able to generate flow energy at an intensity that is suitable for physical and chemical processing (Gogate, 2008; Gogate and Pandit, 2001).

Fig. 8.5b and 8.5c show that the use of US in the Rosett cell reactor allows to obtain BD yields, i.e. FAME concentrations higher

than 96.5% in all the adopted conditions, with the exception of the low temperature (313 K) and the US tip of d=20 mm at low power.

Trying to rationalize the extent of the beneficial effects brought by the use of the Rosett cell reactor compared to the traditional vessel, the biodiesel yields were plotted against the power density expressed as power intensity over treated volume of the reagents (power intensity=emitted power/irradiation area). The results obtained from this study are displayed in Fig. 8.6a and 8.6b for the two different working temperatures.

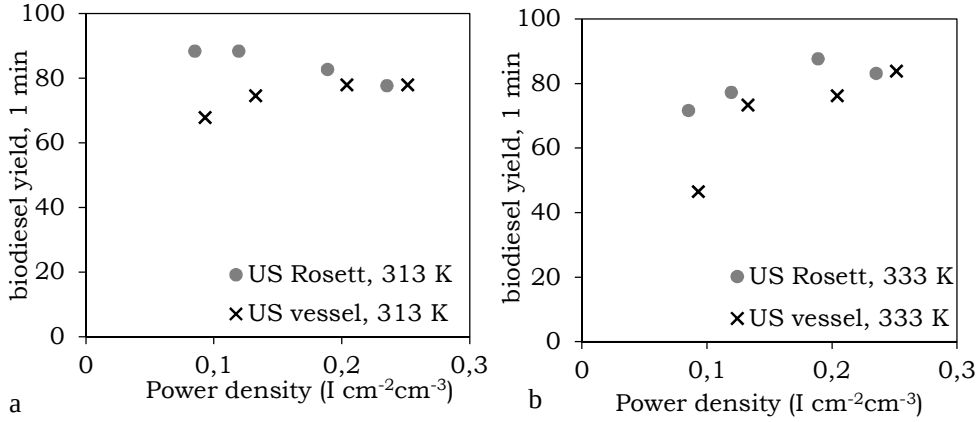

Fig. 8.6. Biodiesel conversions in function of the power density at a) 313 K and b) 333 K.

When low power intensities are delivered to the system, much higher conversions are obtained with the Rosett cell than with the traditional vessel. Moreover, the difference between FAME conversions obtained at lower power intensities and higher power intensities is much more remarkable for the traditional vessel, while in the case of the Rosett cell a significative difference cannot be recognized, meaning that this reactor is optimized also to work at lower power intensities. This effect, as already described above, is ascribable to the benefits brought by the hydrodynamic cavitation.

8.3.3 Ultrasound batch experiments: effect of pulses

In Fig. 8.5a and 8.5b is shown how the effect of pulses is beneficial in both the cases of the reaction vessel and in the Rosett cell reactor. The beneficial effect of pulses for the reactivity of the transesterification has been extensively reported (Chand et al., 2010; Kumar et al., 2010a; 2010b). In particular, as reported by Chand et al. (Chand et al., 2010) when pulses are adopted, excessive heating of the reaction medium is not promoted. Excessive heating during the transesterification reaction might lead to the evaporation followed or not by pyrolysis of methanol and its subsequent removal from the reaction environment. The removal of one of the reagents results of course in slowing down the reaction rate. The beneficial effects of the pulses were found to be to the same extent in both the traditional reaction vessel and in the Rosett cell reactor. In the Rosett cell reactor, in particular, the transesterification reaction rate resulted to be 15X faster than the conventional process.

Moreover, the use of pulses is particularly interesting in the case of electrical energy saving considerations.

8.3.4 Ultrasound batch experiments: effect of tip diameter and power

As it can be observed clearly in Fig. 8.5a and 8.5c, other conditions being equal, an increase in the power brings generally to the enhancement of the conversion into FAME at both the temperatures of 313 K 313 K and with both the horns. Experiments performed at high powers exhibit in fact higher conversions than the corresponding experiments carried out at low powers.

The increase in the FAME yields as the power increases has already been reported at different frequencies (Mahamuni and Adewuyi, 2009). When the intensity (i.e., ultrasonic power/irradiation area) is increased, the acoustic amplitude increases and a more violent collapse of the cavitation bubble will occur (Mahamuni and Adewuyi, 2009). Nevertheless this does not happen for experiments performed with the 13 mm US horn at 333 K and high powers. The result is consistent with the general view that there is an optimum power density (or acoustic intensity) that can be applied in an ultrasonic process to obtain maximum reaction rates before a point of diminishing return is reached (Mahamuni and Adewuyi, 2009; Sivakumar and Pandit; 2001). Singh et al. (Singh et al., 2007) have also observed an optimum energy input for BD formation from soybean oil in the presence of US. However, the authors of the present paper also hypothesized that the too high temperatures generated inside the reaction medium at the 80% of amplitude using the 13 mm diameter tip (500W) might have led to

the methanol removal from the system, so diminishing transesterification reaction rate.

The comparison between the two different horns, i.e. the 13 mm (500 W) and the 20 mm (400 W) horn may be made matching Fig. 8.5a with 8.5c and 8.5b with 8.5d. It can be observed a general trend: usually, conditions being equal yield achieved with the small tip are higher than the big one. In particular, using the 13 mm tip, FAME conversions higher than 96.5% are achieved within 30 minutes also using the classical reaction vessel, as displayed in Fig. 8.5d. This is not worthy in the case of the 20 mm tip, as shown in Fig. 8.5b, where the maximum yield obtained in the case of the traditional vessel is 95.5%, achieved at 333 K and high powers.

8.3.5 Ultrasound continuous experiments

The continuous experiments were performed using two different continuous tubular reactors, of different volumes, equipped with two different horns working at different powers as displayed in Tab. 8.2. First the same total volume of reagents, corresponding to 2.40 L was fed to both the 0.700 and 0.070 L reactors (entries 1 and 2 in Tab. 8.2). Afterwards, for the sake of comparison, a lower amount of reagents, corresponding to 0.68 L was fed to the smaller reactor, in order to have the same power density in the 0.700 L as well in the 0.070 L reactor. This last experiment was performed using both continuous and pulsed ultrasound in the smaller reactor (entries 3 and 4 in Tab. 8.2).

The results of all the continuous experiments are displayed in Fig. 8.7, where the conversions into BD (FAME) are reported in function of the time of the experiment, as defined in the experimental part. The dotted lines represent a FAME concentration corresponding to

96.5%, i.e. the minimum limit required by the European Normative on biodiesel EN 14214.

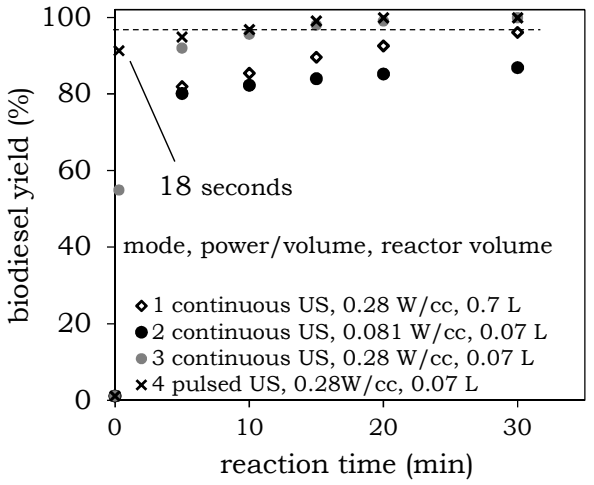

Fig. 8.7. Results of the transesterification continuous experiments: biodiesel yield vs. time of the experiment. Experimental conditions reported in Tab. 8.3.

At equal volume of the reagents (2.40 L), biodiesel conversions achieved in the bigger reactor are higher than the ones achieved in the smaller reactor (compare series 1 and 2 in Fig. 8.7). This may be ascribable to the higher powers delivered by the US horn operating in bigger reactor against the one used in the smaller reactor, as indicated in Tab. 8.2. Experiments carried out in the smaller volume reactor, lowering the total volume of treated reagents are indicated as series 3 and 4 in Fig. 8.7. It can be observed that very high yields are achieved within very short times. In particular, in the case of pulsed ultrasound biodiesel yields higher than 90% are achieved after just 18 seconds, corresponding to a single passage in the reactor, i.e. to the residence time of the reactor. It has to be noted that since pulses are adopted, the total time of sonication during one passage in the reactor is 9 seconds. BD yields higher than 96.5% are achieved within 10 minutes (sonication time: 5 minutes). To the best of the authors' knowledge, this result has never been achieved previously and no evidence in literature was found.

The positive effect of pulses was already discussed in the section 8.3.3. In the continuous experiments the use of US pulses resulted

particularly beneficial to the reaction due to the difficulty in controlling the temperature below 338 K. The use of pulses might have prevented the removal of methanol from the reacting system. Moreover, the lower heating generated in the reacting system compared the continuous US, might have prevented the formation of too high temperatures dampening the acoustic cavitation effects due to the removal of the gases dissolved in the system.

8.4 Conclusions

The use of ultrasound horns in the transesterification reaction of triglycerides to produce biodiesel tremendously increases the final yield in fatty acids methyl esters (FAME) with respect to the traditional method. In order to achieved a biodiesel yield higher than 96.5% complying with the European Normative on biodiesel EN14124, the ultrasound assisted method required just one 30 minutes step, differently from the traditional methods that is usually performed in two steps for a total duration of 150 minutes with separation of the products in between the two steps. Moreover, ultrasound assisted techniques required lower reagents and catalysts amount and lower temperatures than the traditional method to achieve the desired FAME content.

Other condition being equal, the Rosett cell reactor always exhibited higher conversions into FAME than the traditional vessel. This result is ascribable to the combined effect of the acoustic cavitation and the hydrodynamic cavitation achieved thanks to the loops of the Rosett cell.

Optimal conditions for the ultrasound-assisted batch esterification were found to be 313 K using the 20 mm diameter tip

(emitted power: 17.6 W) in the Rosett cell reactor. Too high temperatures, together with too high powers were found to be detrimental for the transesterification reaction, probably due to the removal of methanol from the system.

The effect of pulses resulted beneficial in all the experimented reactor configurations. The positive effect of pulses may be ascribable to the less heating generated within the reaction medium, that prevents the removal of methanol as a consequence of its evaporation or pyrolysis and keep the gases dissolved in the reaction system.

In particular, a very remarkable result was achieved in the case of continuous reactor when pulses were adopted: a BD yield higher than 90% was achieved after just one passage in the reactor, equivalent to 18 seconds. In this case the reaction rate resulted to be well 300X with respect to the conventional process.

References

Antolin G., Tinaut F.V., Briceno Y., "Optimization of biodiesel production by sunflower oil transesterification", *Bioresour. Technol.* **2002,** 83, 111.

Bianchi C.L., Boffito D.C., Pirola C., Ragaini V., "Low temperature de-acidification process of animal fat as a pre-step to biodiesel production", *Catal. Lett.* **2010,** 134, 179.

Bianchi C.L., Pirola C., Boffito D.C., Di Fronzo A., Carvoli G., Barnabè D., Bucchi R., Rispoli A., Non edible oils: raw materials for sustainable biodiesel, in: Feedstocks and Processing Technologies, M. Stoytcheva (Ed.), ISBN: 978-953-307-713-0, InTech 2011, pp. 3-22.

Boffito D.C., Pirola C., Bianchi C.L., "Heterogeneous catalysis for free fatty acids esterification reaction as a first step towards biodiesel production", *Chim. Oggi - Chem Today* **2012a,** 30(1), 42.

Boffito D.C., Crocellà V., Pirola C., Neppolian B., Cerrato G., Ashokkumar M., et al., Ultrasonic enhancement of the acidity, surface area and free fatty acids esterification catalytic activity of sulphated ZrO_2-TiO_2 systems, *J. Catal.* 2012, accepted on September **2012b**., DOI: 10.1016/j.jcat.2012.09.013.

Canakci M., Sanli H., "Biodiesel production from various feedstocks and their effects on the fuel properties", *J. Ind. Microbiol. Biotechnol.* **2008,** 35, 431.

Canakci M., Van Gerpen J., "Biodiesel production from oils and fats with high free fatty acids", *Trans. Am. Soc. Agric. Eng.* **2001,** 44, 1429.

Çaylı G., Küsefoğlu S., "Increased yields in biodiesel production from used cooking oils by a two step process: Comparison with one step process by using TGA", *Fuel Process. Technol.* **2008,** 89, 118.

Chand P., Chintareddy V.R., Verkade J.G., Grewell D., "Enhancing biodiesel production from soybean oil using ultrasonics", *Energy Fuels* **2010,** 24, 2010.

Colucci J.A., Jose A., Borrero E.E., Alape F., "Biodiesel from an alkaline transesterification reaction of soybean oil using ultrasonic mixing", *J. Am. Oil Chem. Soc.* **2005,** 82(7), 525.

Freedman B., Pryde E.H., Mounts T.L., "Variables affecting the yields of fatty esters from transesterified vegetable oils", *J. Am. Oil Chem. Soc.* **1984,** 61, 1638.

Georgogianni K.G., Kontominas M.G., Pomonis P.J., Avlonitis D., Gergis V., "Conventional and in situ transesterification of sunflower seed oil for the production of biodiesel", *Fuel Process. Technol.* **2008a,** 89, 503.

Georgogianni K.G., Kontominas M.G., Pomonis P.J., Avlonitis D., Gergis V., "Alkaline conventional and in situ transesterification of cottonseed oil for the production of biodiesel", *Energy Fuels* **2008b,** 22, 2110.

Gogate, P.R., "Reactors for process intensification of chemical processing applications: A critical review", *Chem. Eng. Proc.* **2008**, 47, 515.

Gogate, P.R., Pandit A.B., "Hydrodynamic cavitation: a state of the art review", *Rev. Chem. Eng.* **2001**, 17, 1.

Gole V.L., Gogate P.R., "Intensification of Synthesis of Biodiesel from Nonedible Oils Using Sonochemical Reactors", *Ind. Eng. Chem. Res.* **2012,** 51(37), 11866.

Kelkar M.A., Gogate P.R., Pandit A.B., "Intensification of esterification of acids for synthesis of biodiesel using acoustic and hydrodynamic cavitation", *Ultrason. Sonochem.* **2008,** 15, 188.

Kumar D., Kumar G., Poonam C.P., "Fast easy ethanolysis of coconut oil for biodiesel production assisted by ultrasonication", *Ultrason. Sonochem.* **2010a,** 17, 555.

Kumar D., Kumar G., Poonam C.P., "Ultrasonic-assisted transesterification of Jatropha curcus oil using solid catalyst, Na/SiO2", *Ultrason. Sonochem.* **2010b,** 17, 839.

Lang X., Dalai A.K., Bakhshi N.N., "Preparation and characterization of bio-diesels from various bio-oils", *Bioresour. Technol.* **2001,** 80, 53.

Leung D.Y.C., Wu X., Leung M.K.H., "A review on biodiesel production using catalyzed transesterification", *Appl. Energy* **2010,** 87, 1083.

Lotero E., Liu Y., Lopez D.E., Suwannakarn K., Bruce D.A., Goodwin J.G., "Synthesis of Biodiesel Via Acid Catalysis", *Ind. Eng. Chem. Res.* **2005,** 44(14), 5353.

Mahamuni N.N., Adewuyi Y., "Optimization of the Synthesis of Biodiesel via Ultrasound-EnhancedBase-Catalyzed Transesterification of Soybean Oil Using a Multifrequency Ultrasonic Reactor", *Energy Fuels* **2009,** 23, 2757.

Mason T.J., Lorimer J.P., Sonochemistry, Theory, Applications and Uses of Ultrasound in Chemistry, Efford, J. Wiley, New York, **1988**.

Pirola C., Bianchi C.L., Boffito D.C., Carvoli G., Ragaini V., "Vegetable oil deacidification by Amberlyst : study of catalyst lifetime and a suitable reactor configuration", *Ind. Eng. Chem. Res.* **2010,** 49(10), 4601.

Pirola C., Boffito D.C., Carvoli G., Di Fronzo A., Ragaini V., Bianchi C.L., "Recent Trends for Enhancing the Diversity and Quality of Soybean Products", *in: D. Krezhova (Eds.), Intech* **2011,** , 321.

Salvi B.L., Panwar N.L., "Biodiesel resources and production technologies - A review", *Renewable Sustainable Energy Rev.* **2012,** 16(6), 3680.

Siatis N.G., Kimbaris A.C., Pappas C.S., Tarantilis P.A., Polissiou M.G., "Improvement of biodiesel production based on the application of

ultrasound: monitoring of the procedure by FTIR spectroscopy", *J. Am. Oil Chem. Soc.* **2006,** 83, 53.

Siddique M.N., Rohani S., "Lipid extraction and biodiesel production from municipal sewage sludges : a review", *Renewable Sustainable Energy Rev.* **2011,** 15, 1067.

Singh A.K., Fernando S.D., Hernandez R., "Base-catalyzed fast transesterification of soybean oil using ultrasonication", *Energy Fuels* **2007,** 21, 1161.

Sivakumar M., Pandit A.B., "Ultrasound enhanced degradation of Rhodamine B: Optimization with power density", *Ultrason. Sonochem.* **2001,** 8(50), 233.

Stamenković O.S., Lazić M.L., Todorović Z.B., Veljković V.B., Skala D.U., "The effect of agitation intensity on alkali-catalyzed methanolysis of sunflower oil", *Bioresour. Technol.* **2007,** 98, 2688.

Veljković V.B., Avramović J.M., Stamenković O.S., "Biodiesel production by ultrasound-assisted tranesterification: State of art and the perspectives", *Renewable Sustainable Energy Rev.* **2012,** 16, 1193.

Verziu M., Florea M., Simon S., Simon V., Filip P., Parvulescu V., Hardacre C., "Transesterification of vegetable oils on basic large mesoporous alumina supported alkaline fluorides—evidences of the nature of the active site and catalytic performances", *J. Catal.* **2009,** 263, 56.

Final Remarks and Conclusions

Besides the conclusions reported at the end of each single chapter, as final remark it can be stated that the original objectives have been achieved. In particular:

- Feedstocks with a high potential for biodiesel (BD) production are *Brassica juncea* oilseed, which can be used as feedstock for B100, *Carthamus tinctorus*, tobacco, animal fat and waste cooking oil to be used in BD blends with other oils or in diesel blends. However, blending different oils or with diesel already during the free fatty acids (FFA) esterification reaction may increase the reaction rate due to the lowered viscosity.
- Free fatty acids esterification over acid ion exchange resins in slurry reactors remains the preferred method of deacidification due to the optimal contact between the reagents and the catalyst and the good durability over time.
- Surface acidity and specific surface area of sulphated inorganic systems can be increased by both adding TiO_2 and using ultrasound (US) in precise experimental conditions to assist the sol-gel synthesis of the catalysts. It was demonstrated that changing the experimental conditions of US during the sol-gel synthesis is also possible to tune the properties of the catalysts.
- Both US and microwaves (MW) enhanced the FFA esterification reaction rate at temperatures lower than the one used conventionally (336 K). The positive effects of US are attributable to the phenomena generated inside the reaction medium by the acoustic cavitation, while MW are able to generate hot-spots in the proximity of the catalyst surface and to create methanol-oil emulsions very efficiently.

- US-assisted transesterification reaction resulted to be much faster than the conventional process: BD yields higher than 96% were achieved in most of the cases within 10 minutes of reaction, whereas the conventional method requires 150 minutes, besides higher reagent concentrations and higher temperatures. In particular, BD yields higher than 90% were obtained using a continuous reactor with pulsed US after 18 seconds, corresponding to just one passage in the reactor. The US-assisted batch and continuous transesterification with US pulses resulted to be 15 and well 300X faster than the conventional process.

Suggestions for the continuations of the work concern the further study of the synthesis of sulphated inorganic systems such as SO_4^{2-}/ZrO_2 or SnO_2 or TiO_2 with US and MW.

Future work should also be devoted to the optimization of the experimental variables related to the use of MW and US to promote both in FFA esterification and transesterification reactions.

List of publications

Papers in peer-reviewed journals

D.C. Boffito, C. Pirola C., F. Galli, A. Di Michele A., "Free Fatty Acids Esterification of Waste Cooking Oil and its mixtures with Rapeseed Oil and Diesel", *Fuel*, 2012, http://dx.doi.org/10.1016/j.fuel.2012.10.069

D.C. Boffito, V. Crocellà, C. Pirola, B. Neppolian, G. Cerrato. M. Ashokkumar, C.L. Bianchi, "Ultrasonic enhancement of the acidity, surface area and free fatty acids esterification catalytic activity of sulphated ZrO_2-TiO_2 systems", *J. Catal.* 2013, 297, 17

D.C. Boffito, C. Pirola, C.L. Bianchi, Heterogeneous catalysis for free fatty acids esterification reaction as a first step towards biodiesel production, *Chem. Today*, 30 (2012) 14-18.

C. Pirola, **D.C. Boffito**, S. Vitali, Claudia L. Bianchi, Photocatalytic Coatings for Building Industry: Study of one year of activity in the NO_x degradation, *J. Coat. Technol. Res.* 2012, 9 (4), 453.

C. Pirola, C.L. Bianchi, **D.C. Boffito**, G. Carvoli, V. Ragaini, Vegetables Oils De-acidification by Amberlyst: Study of Catalyst Lifetime and Suitable Reactor Configuration, *Ind. Eng, Chem. Res.* 2010, 49(10), 4601.

C. Pirola, C.L. Bianchi, A. Di Michele, P. Diodati, **D.C. Boffito**, G. Carvoli, V. Ragaini, Ultrasound and microwave assisted synthesis of high loading Fe-supported Fischer–Tropsch catalysts, *Ultrason. Sonochem*. 2010, 17(3), 610.

C.L. Bianchi, C. Pirola, **D.C. Boffito**, V. Ragaini, Low Temperature De-acidification Process of Animal Fat as a Pre-Step to Biodiesel Production, *Catal. Lett.* 2010, 134, 179.

D.C. Boffito, S. Mansi, J.-M. Leveque, C. Pirola, C.L: Bianchi "Ultra-fast biodiesel production using ultrasound in batch and continuous reactors", submitted to Ultrason. Sonochem. on December 2012.

Book chapters

D.C. Boffito, C. Pirola, C. L. Bianchi, G. Cerrato, S. Morandi, M. Ashokkumar, "Sulphated inorganic oxides for methyl esters production: traditional and ultrasound-assisted techniques", in R. Luque and A.M. Balu (Eds), *Producing Fuels and Fine Chemicals from Biomass Using Nanomaterials*, CRC Press, July 2013.

D. Barnabè, R. Bucchi, A.Rispoli, C.L. Bianchi, G. Carvoli, C. Pirola, **D. C. Boffito**, C. Chiavetta, P. L. Porta, Land Use Change Impacts of Biofuels: a methodology to evaluate biofuel sustainability in: I. Simsic (Eds.) Biofuel / Book 2, Intech, ISBN 980-953-307-471-4, accepted on August 2012.

C.L. Bianchi, **D.C. Boffito**, C. Pirola, S. Vitali, G. Carvoli, D. Barnabè, A. Rispoli, "Non Edible Oils: Raw Materials For Sustainable Biodiesel" in: M. Stoytcheva and G. Montero (Eds.) *Biodiesel Feedstocks and Processing Technologies*, Intech, 2011, p. 3-22.

C. Pirola, **D.C. Boffito**, G. Carvoli, A. Di Fronzo, V. Ragaini, C.L. Bianchi, "Soybean Oil Deacidification as a First Step towards Biodiesel Production" in D. Krezhova (Eds.), *Recent Trends for Enhancing the Diversity and Quality of Soybean Products*, Intech, 2011, p. 321-344.

Publications in Conference Proceedings (peer reviewed)

D.C. Boffito, S. Mansi, C. Pirola, J-M. Leveque, G. Carvoli, S. Vitali, C.L. Bianchi, A.Rispoli, D. Barnabè, R. Bucchi, High Efficiency Esterification and Transesterification of Alternative Feedstock for Biodiesel Production, Proceedings of the DGMK Conference 2012, Reducing Carbon Footprint of Fuels and Petrochemicals, 8-10 October 2012, Berlin, Germany, ISBN 978-3-941721-26-5,.

C. Pirola, C.L. Bianchi, A. Di Fronzo, **D.C. Boffito**, A. Di Michele, Biosyngas Fischer-Tropsch Conversion by High Fe Loaded Supported Catalysts Prepared with Ultrasound and Microwave, Proceedings of the DGMK Conference 2012, Reducing Carbon Footprint of Fuels and Petrochemicals, 8-10 October 2012, Berlin, Germany, ISBN 978-3-941721-26-5.

C.L. Bianchi, C. Pirola, **D.C. Boffito**, A. Di Fronzo, A. Di Michele, R. Vivani, M. Nocchetti, M. Bastianini, S. Gatto, Co-Zn-Al based Hydrotalcites as catalysts for Fischer – Tropsch process, Proceedings of DGMK Conference 2011, Catalysis: Innovative Applications in Petrochemistry and Refining, 4-6 October 2011, Dresden, Germany ISBN 978-3-941721-17-3.

Communications at congresses

Sonochemical Production of Fatty Alkyl Methyl Esters from Raw Oils

Daria Camilla Boffito[1], Silvia Mansi[1], Jean-Marc Leveque[2], Carlo Pirola[1], Claudia Bianchi[1]

[1]Department of Physical Chemistry and Electrochemistry - University of Milan, via Golgi 19, 20133 Milano, Italy

[2] LCME/CISM- *Savoie University, 73376 Le Bourget du Lac cedex, France*

ESS13 Conference, 13th European Society of Sonochemistry Meeting, 1-5 July 2012, Lviv, Ukraine

Scalable free fatty acids esterification for methyl esters production

A. Di Fronzo[1], D.C. Boffito[1], C.Pirola[1], G. Carvoli[2], S. Vitali[1], C.L. Bianchi[1]

[1]Department of Physical Chemistry and Electrochemistry - University of Milan, via Golgi 19, 20133 Milano, Italy

[1]Khemistar s.r.l., P.le Lombardia 10, 28100 Novara, Italy

18th National Congress of the Industrial Chemistry Division of the Italian Chemistry Society, 11-14 June 2012, Firenze, Italy

Synthetic Hydrotalcites as suitable Co-based catalysts for Fischer-Tropsch Process

C.L. Bianchi[1], C. Pirola[1], A. Di Fronzo[1], D.C. Boffito[1], A. Di Michele[2], R. Vivani[3], M. Nocchetti[3], M. Bastianini[3]

[1]Department of Physical Chemistry and Electrochemistry - University of Milan, via Golgi 19, 20133 Milano, Italy

[2] Department of Physics- University of Perugia, Via Elce di Sotto – 06123 Perugia (Italy)

[3] Department of Chemistry- University of Perugia, Via Elce di Sotto – 06123 Perugia (Italy)

18th National Congress of the Industrial Chemistry Division of the Italian Chemistry Society, 11-14 June 2012, Firenze, Italy

Separation of water and acetic acid by distillation using p-xylene as entrainer: experimental data and computer simulation

C. Pirola[1], A. Di Fronzo[1], F. Galli[1], D.C. Boffito[1], G. Carvoli[2]

[1]Department of Physical Chemistry and Electrochemistry - University of Milan, via Golgi 19, 20133 Milano, Italy

[2] *[1]Khemistar s.r.l., P.le Lombardia 10, 28100 Novara, Italy*

18th National Congress of the Industrial Chemistry Division of the Italian Chemistry Society, 11-14 June 2012, Firenze, Italy

Catalytic conversion of non-food oilseeds into methyl esters: traditional and ultrasound assisted techniques

Daria.C.Boffito[1], Carlo Pirola[1], Stefania Vitali[1], Gianni Carvoli[1], Claudia L. Bianchi[1], Ada Rispoli[2], Davide Barnabè and Renzo Bucchi

[1]*Department of Physical Chemistry and Electrochemistry - University of Milan, via Golgi 19, 20133 Milano, Italy*
[2]*Agri2000 Soc. Coop., 40013 Castel Maggiore (BO), Italy*

Cat4Bio Conference, Advances in Catalysis for biomass valorisation, 8-11 July 2012, Thessaloniki, Greece

Synthetic Hydrotalcites as suitable Co-based catalysts for Fischer-Tropsch Process

C.L. Bianchi[1], C. Pirola[1], A. Di Fronzo[1], D.C. Boffito[1], A. Di Michele[2], R. Vivani[3], M. Nocchetti[3], M. Bastianini[3]
[1]*Department of Physical Chemistry and Electrochemistry - University of Milan, via Golgi 19, 20133 Milano, Italy*
[2] *Department of Physics- University of Perugia, Via Elce di Sotto – 06123 Perugia (Italy)*
[3] *Department of Chemistry- University of Perugia, Via Elce di Sotto – 06123 Perugia (Italy)*

Cat4Bio Conference, Advances in Catalysis for biomass valorisation, 8-11 July 2012, Thessaloniki, Greece

Ultrasound assisted catalysis for biodiesel production

D.C. Boffito[1], G. Carvoli[1], S. Mansi[1], C. Pirola[1], S. Vitali[1], J.M. Leveque[2], C.L. Bianchi[1]

[1]*Department of Physical Chemistry and Electrochemistry - University of Milan, via Golgi 19, 20133 Milano, Italy*

[2] LCME/CISM- *Savoie University, 73376 Le Bourget du Lac cedex, France*

ICEC Conference, 7th International Conference on Environmental Catalysis, 2-6 September 2012, Lyon, France

Synthetic Hydrotalcites as suitable Co-based catalysts for Fischer-Tropsch Process

C.L. Bianchi[1], C. Pirola[1], A. Di Fronzo[1], D.C. Boffito[1], A. Di Michele[2], R. Vivani[3], M. Nocchetti[3], M. Bastianini[3]

[1]*Department of Physical Chemistry and Electrochemistry - University of Milan, via Golgi 19, 20133 Milano, Italy*

[2] *Department of Physics- University of Perugia, Via Elce di Sotto – 06123 Perugia (Italy)*

[3] *Department of Chemistry- University of Perugia, Via Elce di Sotto – 06123 Perugia (Italy)*

ICEC Conference, 7th International Conference on Environmental Catalysis, 2-6 September 2012, Lyon, France

Raw glycerol transformation: the role of different matrixes selectivity and durability of the catalytic system

Claudia L. Bianchi[1], Daria C. Boffito[1], Carlo Pirola[1], Alberto Villa[2], Marco Schiavone[2], Laura Prati[2]

[1]*Department of Physical Chemistry and Electrochemistry - University of Milan, via Golgi 19, 20133 Milano, Italy*

[2]*Dipartment of Inorganic, Metallorganic and Analytical Chemistry - University of Milan, via Venezian 21, 20133 Milano, Italy*

CatBior, 1st International Congress on Catalysis for Biorefineries, 2-5 October 2012, Torremolinos, Spain

High loaded supported Fe catalysts for biosyngas conversion: effect of support, diluting materials and preparation procedures

C. Pirola[1], A. Di Fronzo[1], D. Boffito[1], C.L. Bianchi[1], S. Vitali[1], A. Di Michele[2]

[1]*Department of Physical Chemistry and Electrochemistry - University of Milan, via Golgi 19, 20133 Milano, Italy*
[2] *Department of Physics- University of Perugia, Via Elce di Sotto – 06123 Perugia, Italy*

CatBior, 1st International Congress on Catalysis for Biorefineries, 2-5 October 2012, Torremolinos, Spain

Acid Heterogeneous Catalysis for Free Fatty Acids Esterification

D.C. Boffito[1], C.L. Bianchi[1], G. Carvoli[1], C. Pirola[1], S. Vitali[1], D. Barnabé[2], R. Bucchi[2], A. Rispoli[2]

[1]*Department of Physical Chemistry and Electrochemistry - University of Milan, via Golgi 19, 20133 Milano, Italy*
[2]*Agri2000 Soc. Coop., 40013 Castel Maggiore (BO), Italy*

CatBior, 1st International Congress on Catalysis for Biorefineries, 2-5 October 2012, Torremolinos, Spain

Sustainable Biodiesel Production from Alternative Oils

Daria C. Boffito[1], Carlo Pirola[1], Stefania Vitali[1], Claudia L. Bianchi[1]

[1]Department of Physical Chemistry and Electrochemistry - University of Milan, via Golgi 19, 20133 Milano, Italy

EuroBioRef Summer School, 18-24 September 2011, Lecce, Italy

Innovative agronomic solutions to rescue marginal soil and to produce sustainable biodiesel

D. Barnabè[1], R. Bucchi[1], C. Nunzi[1], A. Rispoli[1], G. Carvoli[2], C.L. Bianchi[2], D. Boffito[2], C. Pirola[2], V. Ragaini[2], A. Rossi[3]

[1]Agri2000 Soc. Coop., 40013 Castel Maggiore (BO), Italy
[2]Department of Physical Chemistry and Electrochemistry - University of Milan, via Golgi 19, 20133 Milano, Italy
[3]CRPA S.p.A (Research Center for Animal Productions)- C.so Garibaldi, 42, 42121 Reggio Emilia, Italy

XXIV CIOSTA CIGR V Conference 2011 "Efficient and safe production processes in sustainable agriculture and forestry", 29 June – 1 July 2011, Wien, Austria

High Loading Fe-based Catalysts for Fischer Tropsch Synthesis: Optimization of Synthesis Procedure

D.C. Boffito[1], C.Pirola[1], C.L. Bianchi[1], E. Moretti[1], V. Ragaini[1]

[1]Department of Physical Chemistry and Electrochemistry - University of Milan, via Golgi 19, 20133 Milano, Italy

Summer School of Catalysis of the Italian Chemistry Society – Interdivisional Group of Industrial Chemistry, 15-18 September 2010, Palermo, Italy

Vegetable oils deacidification by heterogeneous catalysis: a comparison of different types of catalysts and batch reactors

D.C. Boffito[1]

[1]Department of Physical Chemistry and Electrochemistry - University of Milan, via Golgi 19, 20133 Milano, Italy

Summer School of Catalysis of the Italian Chemistry Society – Interdivisional Group of Industrial Chemistry, 15-18 September 2010, Palermo, Italy

Biodiesel Production from Non Edible Oils: Standardization and Synthesis

D.C. Boffito[1], C.Pirola[1], C.L. Bianchi[1], G. Carvoli, D. Barnabè[2], V. Ragaini[1]

[1]Department of Physical Chemistry and Electrochemistry - University of Milan, via Golgi 19, 20133 Milano, Italy
[2]Agri2000 Soc. Coop., 40013 Castel Maggiore (BO), Italy

XXIV National Congress of Catalysis of the Italian Chemistry Society – Interdivisional Group of Industrial Chemistry, 18-23 September 2010, Palermo, Italy

Ultrasound and Microwave Prepared Fe-supported Catalysts for Biosyngas Conversion by Fischer Tropsch

C.Pirola[1], C.L. Bianchi[1], D. Boffito[1], E. Moretti[1], A. Di Michele[2], P. Diodati[2]

[1]Department of Physical Chemistry and Electrochemistry - University of Milan, via Golgi 19, 20133 Milano, Italy
[2] Department of Physics- University of Perugia, Via Elce di Sotto – 06123 Perugia (Italy)

ESS12 Conference, 12th European Society of Sonochemistry Meeting, 30 May-3 June 2010, Crete, Greece

Feasibility Study for the Production of Biofuels from Brassicaceae spp. and Nicotiana Tabacum Oilseeds and from By-products or Waste Materials

C. Pirola[1], G. Carvoli[1], V. Ragaini[1], D.C. Boffito[1], D. Barnabè[2], R. Bucchi[2], C. Nunzi[2], A. Rispoli[2], A. Rossi[3]

[1]Department of Physical Chemistry and Electrochemistry - University of Milan, via Golgi 19, 20133 Milano, Italy
[2]Agri2000 Soc. Coop., 40013 Castel Maggiore (BO), Italy
[3]CRPA S.p.A (Research Center for Animal Productions)- C.so Garibaldi, 42, 42121 Reggio Emilia, Italy

14th IBS (International Biotechnology Symposium and Exhibition), 14-18 September 2010, Rimini, Italy

Deacidification of Vegetable Oils for Biodiesel Production by Heterogeneous Catalysis Using Low Temperature and Pressure

Carlo Pirola[1], Claudia L. Bianchi[1], Stefano Pinetti[1], Daria C. Boffito[1], V. Ragaini[1]

[1]*Department of Physical Chemistry and Electrochemistry - University of Milan, via Golgi 19, 20133 Milano, Italy*

XXIV National Congress of Catalysis of the Italian Chemistry Society, 5-10 July, 2009, Sorrento, Italy